NUCLEAR MAGNETIC RESONANCE AND ELECTROCHEMICAL STUDIES OF BORON HYDRIDE DERIVATIVES

by

MARISA ARUNCHAIYA, BSc.

Thesis submitted to the Department of Pure and Applied Chemistry, University of Strathclyde, in part fulfilment of the requirements for the Degree of Doctor of Philosophy.

June, 1984.

ACKNOWLEDGEMENTS

I am extremely grateful to my supervisor, Dr. J.H. Morris, for his constant enthusiastic help, guidance and encouragement throughout the course of this work. I would also like to express my gratitude to Dr. D. Reed, of the University of Edinburgh, for running n.m.r. spectra and for valuable discussions.

Thanks are also due to Miss A. Drummond for assistance, discussions and encouragement, and also to my colleagues, Dr. G.B. Jacobsen, Dr. P.C. Choi, Mr. D.G. Meina and Mr. C. Thompson for helpful discussions.

I am deeply indebted to Miss S.Y. Chauh, Miss Li-Li Koh and Mr. W.Y. Chang for their help and encouragement. Special appreciation for typing to Miss E. Robbie.

Financial support by the Thai Government and the high-field NMR service by the S.E.R.C. are acknowledged.

Praise and thanksgiving above all, to my Lord Jesus Christ who is the source of my inner strength and who makes all things possible in his Love.

ABSTRACT

The new monosubstituted octahydrotriborate anions $[B_3H_7(NCO)]^-$, $[\{B_3H_7(NC)\}_2Ag]^-$, $[B_3H_7(NCBH_2Cl)]^-$ and disubstituted octahydrotriborate anions $[B_3H_6(Cl)_2]^-$, $[B_3H_6(Cl)(NCS)]^-$, $[B_3H_6(Cl)(NCBH_3)]^-$, $[B_3H_6(Cl)(NCBH_2Cl)]^-$, $[\{B_3H_6(Cl)(NC)\}_2Ag]^-$ were prepared and their ^{11}B and ^1H n.m.r. spectra were studied. Cyclic and a.c. voltammetry and controlled potential electrolyses of $[B_3H_7(NCS)]^-$, $[B_3H_7(NCO)]^-$, $[B_3H_6(Cl)_2]^-$ and $[B_3H_6(Cl)(NCS)]^-$ in various solvents such as acetonitrile, 1,3-dioxalane, dichloromethane and benzonitrile were carried out and attempts to prepare metallaboranes at Cu or Ni anodes were described.

The ^{11}B and ^1H n.m.r. and electrochemistry of $[B_{10}H_{13}(PPh_3)]^-$ and $[B_{10}H_{13}(SMe_2)]^-$ were investigated. The ^{11}B and ^1H n.m.r. evidence confirmed that $[B_{10}H_{13}(PPh_3)]^-$ is isostructural to $[B_{10}H_{14}]^{2-}$ whereas that of $[B_{10}H_{13}(SMe_2)]^-$ suggested that it is similar to $[B_{10}H_{13}]^-$ anion. Cyclic and a.c. voltammetry of these anions were studied in acetonitrile, 1,3-dioxalane, dichloromethane and tetramethylurea. Exhaustive electrolysis of $[B_{10}H_{13}(PPh_3)]^-$ at Pt in acetonitrile led to $[B_{10}H_{12}(PPh_3)(CH_3CN)]$ whereas that of $[B_{10}H_{13}(SMe_2)]^-$ gave rise to $B_{10}H_{14}$ and $B_9H_{13}[CH_3CN]$. Anodic dissolution of Cu in acetonitrile solution of $[B_{10}H_{13}(PPh_3)]^-$ yielded a product which showed a weak interaction between Cu(I) and the BH_2 group at the

B(9) position of the starting anion. Similar dissolution of Cu in a solution of $[B_{10}H_{13}(SMe_2)]^-$ led to $[B_{10}H_{13}]^-$ and possibly $[B_{10}H_{15}]^-$. Anodic dissolution of Ni or Zn in acetonitrile solution of $[B_{10}H_{13}(PPh_3)]^-$ led to $[B_{10}H_{12}(PPh_3)(CH_3CN)]$. Chemical reaction of $[B_{10}H_{13}(PPh_3)]^-$ with Hg_2Cl_2 or HCl in acetonitrile also yielded $[B_{10}H_{12}(PPh_3)(CH_3CN)]$ whereas in dichloromethane, $B_9H_{13}[PPh_3]$ was obtained.

CONTENTS

		Page
Acknowledgements		i
Abstract		ii
List of Figures		vii
List of Tables		xi
CHAPTER 1	INTRODUCTORY SURVEY	
1.1	Introduction	1
1.2	Boron Hydride Chemistry	1
1.2.1	Historical Background	1
1.2.2	Bonding, Structure and Nomenclature in Boranes	2
1.2.3	Octahydrotriborate (-1), $[B_3H_8]^-$, and Derivatives	6
1.2.4	Closo-, Nido- and Arachno-Derivatives Containing Ten Boron Atoms	12
1.3	Electrochemistry of Boron Hydride Compounds	24
1.3.1	Overview of Electrochemical Techniques	24
1.3.2	Electrochemical Studies of Boron Hydrides	29
1.4	NMR Studies of Boron Hydrides	42
1.4.1	Introduction	42
1.4.2	Information from Boron NMR Data	43
1.4.3	NMR Spectra	46

		Page
CHAPTER 2	PREPARATION AND CHARACTERIZATION OF MONO-SUBSTITUTED AND DI-SUBSTITUTED OCTAHYDROTRIBORATE ANIONS	
2.1	Introduction	63
2.2	Results and Discussion	63
2.2.1	Preparation and Reactions	63
2.2.2	Characterization	70
2.3	Experimental	88
CHAPTER 3	ELECTROCHEMICAL STUDIES OF MONO-SUBSTITUTED and DI-SUBSTITUTED OCTAHYDROTRIBORATE ANIONS	
3.1	Introduction	98
3.2	Results and Discussion	99
3.2.1	Cyclic and A.c. Voltammetry	99
3.2.2	Anodic Behaviour of Transition Metals	117
3.2.3	Controlled Potential Electrolysis	120
3.2.4	Electrochemical Synthesis	129
3.2.5	Conclusion	130
3.3	Experimental	131
CHAPTER 4	HIGH FIELD ^{11}B AND ^{1}H N.M.R. STUDIES OF THE OCTAHYDROTRIBORATE ANION, AND ITS MONOSUBSTITUTED DERIVATIVES	
4.1	Introduction	141
4.2	Results and Discussion	142
4.2.1	^{11}B N.m.r.	142

		Page
4.2.2	^1H N.m.r.	151
4.2.3	Discussion	166
4.3	Experimental	172
CHAPTER 5	NMR AND ELECTROCHEMICAL STUDIES OF $[B_{10}H_{13}(L)]^-$ ANIONS	
5.1	Introduction	173
5.2	Results and Discussion	173
5.2.1	Preparations and NMR Studies of $[B_{10}H_{13}L]^-$	173
	(a) $[B_{10}H_{13}(PPh_3)]^-$	173
	(b) $[B_{10}H_{13}(NCS)]^{2-}$	178
	(c) $[B_{10}H_{13}]^-$	181
	(d) $[B_{10}H_{13}(SMe_2)]^-$	183
5.2.2	Electrochemical Studies of $[B_{10}H_{13}(PPh_3)]^-$	188
5.2.3	Chemical Oxidation of $[B_{10}H_{13}(PPh_3)]^-$	204
5.2.4	Electrochemical Studies of $[B_{10}H_{13}(SMe_2)]^-$	210
CHAPTER 6	EXPERIMENTAL TECHNIQUES	227
6.1	Experimental Techniques	227
6.2	Spectroscopic Techniques	228
6.3	Electrochemical Techniques	229
REFERENCES		233

FIGURES

		Page
1.3.1	Linear potential sweep and i-E curve.	24
1.3.2	Cyclic potential sweep and cyclic voltammogram.	25
1.3.3	A.c. voltammogram.	27
1.3.4	Cyclic d.c. and cyclic a.c. voltammograms for a a reversible system.	28
1.3.5	Cyclic voltammograms of $B_{10}H_{14}$.	34
1.4.1	^{11}B and ^{1}H n.m.r. spectra of B_2H_6.	48
1.4.2	Pseudorotation of $[B_3H_8]^-$.	50
1.4.3	Structure, ^{1}H n.m.r. spectra and pseudorotation of $[(C_6H_5)_3P]_2CuB_3H_8$.	51
1.4.4	Structure of $B_{10}H_{14}$.	54
1.4.5	^{11}B n.m.r. spectra of $B_{10}H_{14}$.	55
1.4.6	^{11}B n.m.r. spectra of $B_{10}H_{14}$ (line-narrowed)	56
1.4.7	^{11}B COSY spectrum of $B_{10}H_{14}$.	57
1.4.8	^{1}H and $^{1}H\{^{11}B\}$ n.m.r. spectra of $B_{10}H_{14}$.	59
1.4.9	Structure and ^{11}B n.m.r. spectrum of $[B_{10}H_{14}]^{2-}$.	62
2.1	115.5 MHz ^{11}B and $^{11}B\{^{1}H\}$ n.m.r. spectra of $[B_3H_7(NCO)]^-$ in $CDCl_3$.	72
2.2	115.5 MHz ^{11}B n.m.r. spectrum of $[B_3H_6(Cl)_2]^-$ in $CDCl_3$ at 303 K.	74
2.3	115.5 MHz ^{11}B n.m.r. spectrum of $[B_3H_6(Cl)(NCS)]^-$ in $CDCl_3$.	75
2.4	115.5 MHz ^{11}B n.m.r. spectrum of $[B_3H_6(Cl)(NCBH_3)]^-$ and $[B_3H_7(NCBH_3)]^-$ in $CDCl_3$.	77
2.5	115.5 MHz ^{11}B n.m.r. spectrum of $[\{B_3H_6(Cl)(NC)\}_2Ag]^-$ in $CDCl_3$.	78
2.6	80.2 MHz ^{11}B and $^{11}B\{^{1}H\}$ n.m.r. spectra of reaction product of $[B_3H_7(NCBH_3)]^-$ with HCl at 1:3 ratio.	79
2.7	80.2 MHz ^{11}B and $^{11}B\{^{1}H\}$ n.m.r. spectra of reaction product of $[B_3H_7(NCBH_3)]^-$ with HCl at 1:5 ratio.	80

2.8	Infrared spectra of $[B_3H_7(Cl)]^-$ $[B_3H_6(Cl)_2]^-$, $[B_3H_7(NCS)]^-$, $[B_3H_6(Cl)(NCS)]^-$, $[B_3H_7(NCO)]^-$ and $[\{B_3H_7(NC)\}_2Ag]^-$.	86
2.9	Structure of $[B_3H_6(Cl)_2]^-$.	89
2.10	Structure of $[B_3H_6(Cl)(NCS)]^-$.	90
3.1	Cyclic and a.c. voltammograms of $[B_3H_6(Cl)_2]^-$. in acetonitrile.	100
3.2	Cyclic voltammograms of $[B_3H_6(Cl)_2]^-$ in acetonitrile.	101
3.3	Cyclic voltammogram of $[B_3H_6(Cl)_2]^-$ in acetonitrile at scan rate $1.999\ ^2VS^{-1}$.	102
3.4	Cyclic voltammogram of $[B_3H_6(Cl)_2]^-$ in dichloromethane.	105
3.5	Cyclic voltammograms of $[B_3H_6(Cl)_2]^-$ in benzonitrile.	108
3.6	Cyclic and a.c. voltammograms of $[B_3H_6(Cl)(NCS)]^-$ in acetonitrile.	110
3.7	Cyclic and a.c. voltammograms of $[B_3H_6(Cl)(NCS)]^-$ in 1,3-dioxalane.	113
3.8	Cyclic voltammograms of $[B_3H_7(NCO)]^-$ in dichloromethane.	115
3.9	Cyclic voltammograms of $[B_3H_6(Cl)(NCS)]^-$. Illustrate type (a), (b), (c) and (d) behaviour.	121
4.1	80.2 MHz ^{11}B n.m.r. spectrum of $[B_3H_6(Cl)_2]^-$ in CD_3CN.	143
4.2	Simulated and experimental ^{11}B n.m.r. spectrum of $[B_3H_6(Cl)_2]^-$ in $CDCl_3$.	144
4.3	115.5 MHz $^{11}B\{^1H\}$ n.m.r. spectra of $[B_3H_6(Cl)_2]^-$ in $CDCl_3$ and in CD_3CN.	147
4.4	115.5 MHz ^{11}B n.m.r. spectrum of $[B_3H_6(Cl)(NCS)]^-$ in CD_3CN.	150
4.5	Experimental and simulated ^{11}B n.m.r. spectra of $[B_3H_7(NCO)]^-$ in $CDCl_3$ at 303K.	153
4.6	115.5 MHz $^{11}B\{^1H\}$ n.m.r. spectra of $[B_3H_7(NCO)]^-$ in $CDCl_3$ at 323K.	154
4.7	360 MHz ^1H n.m.r. spectrum of $[B_3H_8]^-$ in CD_3CN.	156

4.8	360 MHz $^{1}H\{^{11}B\}$ n.m.r. spectra of $[B_3H_7(Cl)]^-$ in CD_3CN.	158
4.9	360 MHz $^{1}H\{^{11}B\}$ n.m.r. spectra of $[B_3H_7(Cl)]^-$ in $CDCl_3$.	159
4.10	360 MHz $^{1}H\{^{11}B\}$ n.m.r. spectra of $[B_3H_7(NCBH_3)]^-$ in	162
4.11	360 MHz $^{1}H\{^{11}B\}$ n.m.r. spectra of $[B_3H_6(Cl)_2]^-$ in $CDCl_3$.	165
4.12	Correlation diagram of the ^{11}B chemical shifts of $[B_3H_8]^-$ and its mono- and disubstituted derivatives.	171
5.1	115.5 MHz ^{11}B n.m.r. spectrum of $[B_{10}H_{13}(PPh_3)]^-$ in CD_3CN.	175
5.2	360 MHz $^{1}H\{^{11}B\}$ n.m.r. spectra of $[B_{10}H_{13}(PPh_3)]^-$ in CD_3CN.	176
5.3	Structure of $[B_{10}H_{13}(PPh_3)]^-$.	177
5.4	Structures of $[B_{10}H_{13}]^-$ and $[B_{10}H_{13}(SMe_2)]^-$.	182
5.5	115.5 MHz ^{11}B n.m.r. spectrum of $[B_{10}H_{13}(SMe_2)]^-$.	184
5.6	Cyclic and a.c. voltammograms of $[B_{10}H_{13}(PPh_3)]^-$ in acetonitrile.	189
5.7	Cyclic voltammogram of $[B_{10}H_{13}(PPh_3)]^-$ in 1,3-dioxalane.	194
5.8	Cyclic voltammograms of $[B_{10}H_{13}(PPh_3)]^-$ in 1,3-dioxalane.	195
5.9	Cyclic voltammograms of $[B_{10}H_{13}(PPh_3)]^-$ in dichloromethane.	196
5.10	Cyclic anda.c. voltammograms of $[B_{10}H_{13}(PPh_3)]^-$ in tetramethylurea.	198
5.11	115.5 MHz ^{11}B n.m.r. spectrum of $[B_{10}H_{12}(PPh_3)(CH_3CN)]$ in CD_3CN.	201
5.12	360 MHz $^{1}H\{^{11}B\}$ n.m.r. spectra of $[B_{10}H_{12}(PPh_3)(CH_3CN)]$ in CD_3CN.	202
5.13	115.5 MHz ^{11}B n.m.r. spectrum of $B_9H_{13}[PPh_3]$.	206
5.14	Structure of $B_9H_{13}[PPh_3]$.	207
5.15	Cyclic and a.c. voltammograms of $[B_{10}H_{13}(SMe_2)]^-$ in acetonitrile.	211

5.16 Cyclic voltammograms of $[B_{10}H_{13}(SMe_2)]^-$ in acetonitrile. 212

5.17 Cyclic voltammograms of $[B_{10}H_{13}(SMe_2)]^-$ in acetonitrile. 213

5.18 Cyclic and a.c. voltammograms of $[B_{10}H_{13}(SMe_2)]^-$ in 1,3-dioxalane. 215

5.19 115.5 MHz ^{11}B and $^{11}B\{^1H\}$ n.m.r. spectra of electrolysis product of $[B_{10}H_{13}(SMe_2)]^-$ at Pt in acetonitrile. 217

5.20 115.5 MHz ^{11}B and $^{11}B\{^1H\}$ n.m.r. spectra of electrolysis product of $[B_{10}H_{13}(SMe_2)]^-$ at Cu in acetonitrile. 218

TABLES

		Page
2.1	Reaction Products from $[B_3H_7(NCBH_3)]^-$ and HCl	68
2.2	^{11}B n.m.r. Data for Substituted Anions $[B_3H_6(X)(X')]^-$ at 115.5 MHz in $CDCl_3$	81
2.3	^{11}B n.m.r. Data for substituted Anions $[B_3H_6(X)(X')]^-$ at 80 MHz in $CDCl_3$	82
2.4	^{11}B Chemical Shift Data for Ions $[B_3H_7(X)]^-$ at 80 MHz in $CDCl_3$	83
2.5	Infrared Absorptions of Octahydrotriborate Derivatives	85
3.1	Anodic Properties of Metals in solution of $[B_3H_6(Cl)_2]^-$ anion.	118
3.2	Anodic Properties of Metals in solution of $[B_3H_6(Cl)(NCS)]^-$ anion.	119
4.1	^{11}B n.m.r. Data for Octahydrotriborate Derivatives at 115.5 MHz	152
4.2	^{1}H n.m.r. Data for Octahydrotriborate Derivatives at 115.5 MHz	167
5.1	115.5 MHz ^{11}B n.m.r. Spectral Data for $[B_{10}H_{13}(L)]^-$ compounds in CD_3CN	179
5.2	360 MHz ^{1}H n.m.r. Spectral Data for $[B_{10}H_{13}(PPh_3)]^-$ and $[B_{10}H_{12}(PPh_3)(CH_3CN)]$ in CD_3CN	180
5.3	115.5 MHz ^{11}B n.m.r. Spectral Data for $[B_{10}H_{13}]^-$ and $[B_{10}H_{13}(SMe_2)]^-$ in CD_3CN	185
5.4	360 MHz ^{1}H n.m.r. Spectral Data for $[B_{10}H_{13}]^-$ and $[B_{10}H_{13}(SMe_2)]^-$ in CD_3CN	186
5.5	^{11}B and ^{1}H n.m.r. Spectral Data for $B_9H_{13}(PPh_3)$	209

CHAPTER ONE

INTRODUCTORY SURVEY

1.1 INTRODUCTION

In this chapter, the general chemistry of boron hydrides is briefly mentioned. Specific areas of the octahydrotriborate (-1) ion and its derivatives, and closo-, nido-, and arachno- boron hydride derivatives containing ten boron atoms are mentioned in this introduction, but also discussed in more detail in later chapters. The electrochemical and nuclear magnetic resonance (n.m.r.) studies of these derivatives are also reviewed. An overview of electrochemical techniques, cyclic voltammetry and a.c. voltammetry, employed to this work and a short discussion of ^{11}B and ^{1}H n.m.r. spectral features are included for general background.

1.2 BORON HYDRIDE CHEMISTRY

1.2.1 Historical Background

The existence of a hydride of boron was first reported by Sir H. Davy in 1810. F. Jones in 1879 investigated the product of the action of dilute acids on magnesium boride (MgB_2) and this reaction was also examined by Ramsay and Hatfield in 1901. The systematic investigation of the hydrides of boron is due to Alfred Stock and his co-workers, (1912 onwards).

Stock and his collaborators[1] developed vacuum line techniques to handle the volatile and air-sensitive gaseous product of the reaction between magnesium boride

and dilute hydrochloric acid and were able to isolate and identify these boranes as B_4H_{10}, B_5H_9, B_5H_{11}, B_6H_{10} and $B_{10}H_{14}$. Since there are now various improved methods for preparing boranes, Stock's original method is now used only for B_6H_{10}. Most syntheses now involve thermolysis of B_2H_6 under a variety of conditions, and often in the presence of H_2 or other reagents[1,2,3].

1.2.2 Bonding, Structure and Nomenclature in Boranes

(a) Bonding.

The boron hydrides belong to a general class of compounds known as "electron deficient", that is, there are not enough electrons to allow the formation of conventional two-electron bonds (2c-2e bonds) between all adjacent pairs of atoms. It was to rationalise the structures of boranes that the various concepts of multicenter bonding were first developed. Longuet-Higgins[4] employed the three-center bonds (3c-2e bonds) which were formed by a combination of three atomic orbitals from one hydrogen atom and two boron atoms (BHB) for a rationalisation of the diborane (6) structure. Then, Eberhardt, Crawford, and Lipscomb[5] presented a generalization of the localized three-center concept for closed and open bonds involving three boron atoms and two boron atoms with one hydrogen atom. The structure/bonding elements in boron hydride compounds can be represented in the following way:

Terminal 2c-2e boron-hydrogen bond	B-H
3c-2e Hydrogen bridge bond	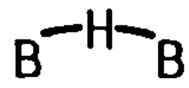
2c-2e Boron-boron bond	B-B
Open 3c-2e Boron bridge bond	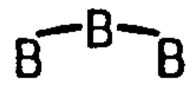
Closed 3c-2e boron bond	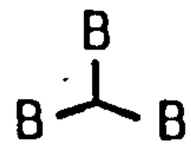

By using these five elements, Lipscomb and his collaborators were able to develop the "topological" treatment of boron hydrides[6,7,8]. This topological analysis was of empirical value for electron and connectivity count in not only rationalizing structural features of known boron hydrides but also in notable predictions about possible new structures.

(b) Structure.

The structures of the boranes are unlike those of other hydrides such as those of carbon and are unique. They can be classified as follows:

(i) Closo-boranes

These are molecules which have a complete closed polyhedron with triangular faces, such as closo-tetrahedron, closo-trigonalbipyramid, closo-octahedron, etc. The best known closo-molecules are the $[B_nH_n]^{2-}$ ions (n = 6-12), and the carbaboranes such as $B_{n-2}C_2H_n$ (n = 5-12), $[B_{10}CH_{11}]^{3-}$, which are

called quasi-closo-boranes.

(ii) Nido-boranes

These are molecules which have nonclosed structures and which encompass not just the B_nH_{n+4} hydrides but also heteroboranes in which one or more boron atoms are substituted by other atoms, most notably carbon, [to give nido-carbaborane, $C_mB_nH_{n+4}$ $(m = 1-4)$]. A nido-boron hydride of n framework atoms can be considered to arise by removing the highest connected vertex in a (n+1) closo-borane.

(iii) Arachno-boranes

These are molecules of B_nH_{n+6} and the carba-borane analogs of the type $C_mB_nH_{n+6}$. The arachno-boron hydrides are formally derived from the (n+2) closo-boranes by elision of two adjacent boron atoms of high framework connectivity and their exopolyhedral substit-uents.

In addition, the skeletal structures (closo, nido, or arachno) of boranes or carbaboranes are related to the number of skeletal bonding electron pairs. These are summarized as follows:

n framework atoms of closo-boranes relate to n+1 pairs of skeletal e^-.

n framework atoms of nido-boranes relate to n+2 pairs of skeletal e^-.

n framework atoms arachno-boranes relate to n+3 pairs of skeletal e^-.

Such relationships and the electron-counting method have

been discussed by Wade[9]. The idealized polyhedral boron frameworks for closo-, nido-, and arachno-boranes and heteroboranes have also been well presented by Rudolph[10].

(c) Nomenclature.

It is appropriate to outline briefly the nomenclature of the polyhedral boranes and related compounds. This has previously been described by a stoichiometric nomenclature[11] which provided information on the number and type of skeletal atoms and exopolyhedral hydrogen atoms, substituents, or ligands, e.g.

$2,4\text{-}C_2B_5H_7$ 2,4-dicarba-closo-heptaborane (7)

$2,3\text{-}C_2B_4H_8$ 2,3-dicarba-nido-hexaborane (8)

The skeletons of the various polyhedra were designated by the Greek terms closo (closed), nido (nestlike) and arachno (weblike); the order indicates increasing openness.

However, this method of nomenclature was found to be insufficient in an increasing number of cases, where structures could only be inferred by those with a knowledge of boron hydride chemistry. With the rapid advance of polyboron hydride chemistry, especially heteropolyboron hydride chemistry, there are polyboron hydride ions having the same stoichiometry but different geometry. Therefore a method for definitively describing structures of polyhedral compounds has been reported[12].

1.2.3 Octahydrotriborate (-1), $[B_3H_8]^-$, and Derivatives

The octahydrotriborate (-1) ion has been found to possess an intriguing chemistry. It is an important intermediate in the synthesis of higher boranes[13], polyhedral borane anions[14], and transition-metal complexes[15]. In this section, the preparations and the reactions of $[B_3H_8]^-$ and its derivatives are reviewed.

(a) Preparation of the $[B_3H_8]^-$ anion.

There have been numerous reports of preparation of several salts of the octahydrotriborate anion. A few methods are summarized as follows:

(1) $Na[B_3H_8]$ was originally prepared by the reaction between diborane and sodium amalgam in other media[16].

$$Na(Hg) + 2\ B_2H_6 \longrightarrow Na[B_3H_8] + NaBH_4 \qquad (1.2\text{-}1)$$

(2) The unsymmetrical cleavage of B_4H_{10} by ammonia[17] has led to the boronium salt.

$$B_4H_{10} + 2NH_3 \longrightarrow [(H_3N)_2\ BH_2][B_3H_8] \qquad (1.2\text{-}2)$$

(3) $[N(CH_3)_4][B_3H_8]$ was prepared from methanolysis of $B_{10}H_{12}[S(C_2H_5)_2]_2$[18] (1.2-3 to 1.2-5) or B_5H_9 (1.2-6).

$$B_{10}H_{12}[S(C_2H_5)_2]_2 + 3\ CH_3OH \longrightarrow B_9H_{13}[S(C_2H_5)_2] + B(OCH_3)_3 + S(C_2H_5)_2 + H_2 \qquad (1.2\text{-}3)$$

$$B_9H_{13}[S(C_2H_5)_2] + [N(CH_3)_4][OH] \longrightarrow [N(CH_3)_4][B_9H_{12}]^+$$

$$S(C_2H_5)_2 + H_2O \qquad (1.2\text{-}4)$$

$$[N(CH_3)_4][B_9H_{12}] + 18CH_3OH \longrightarrow [N(CH_3)_4][B_3H_8] +$$

$$6B(OCH_3)_3 + 11H_2 \qquad (1.2\text{-}5)$$

$$B_5H_9 + 6CH_3OH + [N(CH_3)_4][OH] \longrightarrow [N(CH_3)_4][B_3H_8]+$$

$$2B(OCH_3)_3 + 3H_2 + H_2O \qquad (1.2\text{-}6)$$

(4) A convenient large-scale preparation of $Na[B_3H_8]$ has been developed [20] from the following reaction in diglyme at about 100°C.

$$3NaBH_4 + I_2 \longrightarrow Na[B_3H_8] + 2H_2 + 2NaI \qquad (1.2\text{-}7)$$

(5) The reaction of B_2H_6 with $NaBH_4$ in diglyme at 100°C[21,22] (1.2-8) and the following sequence of reactions in diglyme[21,23] (1.2-9 to 1.2-10) have also been used for large-scale preparations.

$$NaBH_4 + B_2H_6 \longrightarrow Na[B_3H_8] + H_2 \qquad (1.2\text{-}8)$$

$$7NaBH_4 + 4BF_3 \longrightarrow 3NaBF_4 + 4NaB_2H_7 \qquad (1.2\text{-}9)$$

$$2NaB_2H_7 \xrightarrow{100°C} NaBH_4 + Na[B_3H_8] + H_2 \quad (1.2\text{-}10)$$

(b) Preparation of octahydrotriborate (-1) derivatives.

There had been relatively few reports of substituted octahydrotriborate anions in comparison to those of triborane (7) adducts. The $[B_3H_7(X)]^-$ anions (X = Cl, Br, I) were prepared[24] by the reactions between $[NBu_4^n][B_3H_8]$ and the appropriate hydrogen halide in the non-coordinating solvent, CH_2Cl_2.

$$[NBu_4^n][B_3H_8] + HX \longrightarrow [NBu_4^n][B_3H_7(X)] + H_2 \quad (1.2\text{-}11)$$

The cyanide ion was reported[25] to cleave tetraborane (10) symmetrically to yield a substituted triborate anion.

$$B_4H_{10} + 2[CN]^- \longrightarrow [B_3H_7(CN)]^- + [BH_3(CN)]^- \quad (1.2\text{-}12)$$

The preparation of $[B_3H_7(OH)]^-$ was also reported[26] through the following reactions in methanol-water.

$$K[B_3H_8] + HCl + H_2O \longrightarrow B_3H_7OH_2 + H_2 + KCl \quad (1.2\text{-}13)$$

$$B_3H_7OH_2 + NaOH \longrightarrow Na[B_3H_7(OH)] + H_2O \quad (1.2\text{-}14)$$

Recently, the preparations of a series of monosubstituted and disubstituted octahydrotriborate anions have been reported[27,28] which provide a systematic study of triborate derivatives. The $[B_3H_7(X)]^-$ anions (X = F, Cl, Br)

can also be prepared[27] by the reactions of $[B_3H_8]^-$ with mercury (I) halide in CH_2Cl_2.

$$2[B_3H_8]^- + Hg_2X_2 \longrightarrow 2[B_3H_7(X)]^- + H_2 + 2Hg \qquad (1.2\text{-}15)$$

The disubstituted octahydrotriborate anion, $[B_3H_6(Cl)_2]^-$ was obtained as a byproduct in the preparation of $[B_3H_7(Cl)]^-$ and was produced exclusively by the reaction of $[B_3H_8]^-$ with one equivalents of Hg_2Cl_2.

$$[B_3H_8]^- + \tfrac{1}{2}Hg_2Cl_2 \longrightarrow [B_3H_7(Cl)]^- + \tfrac{1}{2}H_2 + Hg \qquad (1.2\text{-}16)$$

$$[B_3H_7(Cl)]^- + \tfrac{1}{2}Hg_2Cl_2 \longrightarrow [B_3H_6(Cl)_2]^- + \tfrac{1}{2}H_2 + Hg \qquad (1.2\text{-}17)$$

Furthermore, the chloride substituent of $[B_3H_7(Cl)]^-$ is labile and can be substituted by ions such as NCS^-, $NCBH_3^-$, NC^-, NCO^- and $NCSe^-$ to give a series of mono-substituted triborate derivatives,

$[B_3H_7(NCS)]^-$[27], $[B_3H_7(NCBH_3)]^-$[27], $[\{B_3H_7(NC)\}_2Ag]^-$[28], $[B_3H_7(NCO)]^-$[28] and $[B_3H_7(NCSe)]^-$[29] respectively.

(c) Reactions of $[B_3H_8]^-$ and its derivatives.

(i) Reactions of $[B_3H_8]^-$ with HCl or Hg_2Cl_2 or $HgCl_2$.

It had previously been shown that $[(H_3N)_2BH_2][B_3H_8]$ reacted at -78°C with HCl or HBr in diethylether to give $B_3H_7[O(C_2H_5)_2]$[17,30]. The reaction between $[N(CH_3)_4][B_3H_8]$ and HCl in acetonitrile yielded $B_3H_7[CH_3CN]$ and the reaction of $[NPr_4][B_3H_8]$with HCl in dimethylformamide gave $B_3H_7[DMF]$[31]. It was also found that treatment of $Na[B_3H_8]$ with HCl rapidly yielded a $[B_3H_7]$ intermediate[13a]. The reactions between $[N(CH_3)_4][B_3H_8]$ and mercury (I) or mercury (II) chlorides in tetrahydrofuran were reported[32] to yield $B_3H_7[THF]$. However, the reactions between $[NBu_4^n][B_3H_8]$ with HCl or Hg_2Cl_2[27] in dichloromethane yielded $[B_3H_7(Cl)]^-$ anion. Thus, these reactions had shown that the products were solvent dependent. When the reactions were carried out in coordinating solvents, the products were triborane (7) adducts whereas in non-coordinating solvents, chlorination reaction took place giving rise to the substituted triborate anion.

(ii) Reactions of triborate derivatives.

It has been mentioned in sect. 1.2.3(b) that the $[B_3H_7(Cl)]^-$ anion underwent substitution reaction in the presence of other ions such as NCS^- or $NCBH_3^-$, providing a series of monosubstituted triborate derivatives. It had also been shown that[24] pyrolysis of $[NBu_4^n][B_3H_7(Br)]$ at 95-100°C led to B_5H_9.

(iii) Synthesis of higher boranes from $[B_3H_8]^-$

It had been shown that[13a,b] the reaction of tetramethylammonium triborohydride (8) with polyphosphoric acid *in vacuo* resulted in products which comprised the higher boranes, $^{'}B_4H_{10}$, B_6H_{12} and B_8H_{18}. The reaction which was claimed to be the first synthesis of a boron hydride molecule containing a boron isotopic label in a specific position involved the reaction of the labelled octahydrotriborate with diborane and hydrogen chloride to give tetraborane (10). The reactions were suggested to proceed by the pathway[13c]

$$Na\left[^{10}B_3H_8\right] + HCl \longrightarrow NaCl + {}^{10}B_3H_9 \quad (1.2\text{-}18)$$

$$^{3}/_{2}\ {}^{10}B_2H_6 \longleftarrow {}^{10}B_3H_9 \longrightarrow {}^{10}B_3H_7 + H_2 \quad (1.2\text{-}19)$$

$${}^{10}B_3H_7 + {}^{11}B_2H_6 \longrightarrow {}^{10}B_3{}^{11}BH_{10} + {}^{11}BH_3 \quad (1.2\text{-}20)$$

(iv) Synthesis of polyhedral borane anions from $[B_3H_8]^-$.

Ellis, Gaines and Schaeffer had shown that[14a] pyrolysis of $[B_3H_8]^-$ at ~100-130°C in diethylene glycol dimethyl ether yielded $[B_{12}H_{12}]^{2-}$. Treatment of $Na[B_3H_8]$ (or $Na[B_3H_8]$ from B_2H_6 and $NaBH_4$) with $(CH_3)_4NHCl$[14a] or $(C_2H_5)_3N$[14b] also yielded $[B_{12}H_{12}]^{2-}$. The octahydrotriborate ion was reported[14c] to be an important intermediate in syntheses of $[B_{12}H_{12}]^{2-}$ and $[B_{11}H_{14}]^-$.

(v) Synthesis of metallaboranes from the $[B_3H_8]^-$ anion.

The preparations[15,33] of metal complexes containing the octahydrotriborate (1-) ion were achieved by simple displacement of coordinated ligands by $[B_3H_8]^-$.

$$M(CO)_6 + [B_3H_8]^- \longrightarrow [(CO)_4M\ B_3H_8]^- + 2CO \quad (1.2\text{-}21)$$

M = Cr, Mo, W[15b]

$$(CH_3)_2MCl + [B_3H_8]^- \longrightarrow [(CH_3)_2M\ B_3H_8] + Cl^- \quad (1.2\text{-}22)$$

M = Al, Ga[33]

$$[(C_6H_5)_3Y]_m\ CuCl + Cs[B_3H_8] \longrightarrow [(C_6H_5)_3Y]_n\ Cu[B_3H_8] \quad (1.2\text{-}23)$$

For Y = P (n = 2), As (n = 2) and Sb (n = 3)[15a].

1.2.4 Closo-, Nido-, and Arachno-Derivatives Containing Ten Boron Atoms

(a) Preparations of nido-decaborane (14), $B_{10}H_{14}$.

Decaborane (14) is an important starting material in the study of reaction chemistry of $B_{10}H_{14}$ and its derivatives such as the large carbaboranes[34], metallocarboranes[35], and boron hydrides[36]. Several methods of preparing decaborane (14) have been reported, and a few

synthetic routes which were claimed to give good yields of decaborane (14) are presented as follows:

(1) The pyrolysis of B_2H_6 at 150°C for 10 minutes in the presence of a Lewis base gave a 50% yield of $B_{10}H_{14}$. When B_5H_9 was present in a similar system, a 70% yield of $B_{10}H_{14}$, based upon the amount of B_2H_6 consumed, was obtained[37]. There is evidence that in the pyrolysis of B_2H_6 to form $B_{10}H_{14}$, B_5H_9 is an intermediate product[38].

(2) The pyrolysis of B_4H_{10} for 2.5 hours at 65°C under nitrogen pressure of 1750 psi[39], and the copyrolysis of a mixture of B_4H_{10} and B_5H_9 at 65°C under nitrogen pressure of 1300 psi[40] yielded $B_{10}H_{14}$.

(3) $B_{10}H_{14}$ from $NaBH_4$ via $[B_{11}H_{14}]^-$ ion.

It had been shown that [41] oxidation of the aqueous solution of $[B_{11}H_{14}]^-$ ion, which was prepared from the reaction of $NaBH_4$ with acids including $BF_3.O(C_2H_5)_2$, BCl_3, $SiCl_4$ and alkyl halides, produced $B_{10}H_{14}$. The reactions were summarized as follows:

$$17NaBH_4 + 20BF_3.O(C_2H_5)_2 \longrightarrow 2Na[B_{11}H_{14}] + 15NaBF_4 + 20H_2 + 20O(C_2H_5)_2 \qquad (1.2\text{-}24)$$

$$17NaBH_4 + 5BCl_3 \longrightarrow 2Na[B_{11}H_{14}] + 15NaCl + 20H_2 \qquad (1.2\text{-}25)$$

$$22NaBH_4 + 5SiCl_4 \longrightarrow 2Na[B_{11}H_{14}] + 5SiH_4 +$$

$$20NaCl + 20H_2 \qquad (1.2\text{-}26)$$

$$11NaBH_4 + 10RX \longrightarrow Na[B_{11}H_{14}] + 10RH + 10NaX + 10H_2 \qquad (1.2\text{-}27)$$

$$2[B_{11}H_{14}]^- + 36H_2O \longrightarrow B_{10}H_{14} + 12B(OH)_3\ 18H_2 +$$

$$14H^+ + 16e^- \qquad (1.2\text{-}28)$$

(4) $B_{10}H_{14}$ from B_5H_9 via $[B_9H_{14}]^-$ ion.

It was shown that[42] $B_{10}H_{14}$ could be readily prepared in yields up to 50% from $[B_9H_{14}]^-$ through the hydride ion abstraction reaction.

$$[M][B_9H_{14}] + BX_3 \longrightarrow B_{10}H_{14} + H_2 + [M][HBX_3] +$$

$$[\text{solid BH residue}] \qquad (1.2\text{-}29)$$

$$M = [N(CH_3)_4]^+,\ [NBu_4^n]^+;\quad BX_3 = BF_3,\ BCl_3,\ BBr_3$$

This method is of no practical consequence without the availability of a convenient high-yeild preparation of the $[B_9H_{14}]^-$ anion. The traditional synthesis has involved degradation of $B_{10}H_{14}$[43], a route which is of no use in this case. However, recently, the decomposition

of $[B_5H_8]^-$ to $[B_9H_{14}]^-$ in yields up to 60% has been recognized as a potential source of this anion[44], the $[B_5H_8]^-$ ion being generated through the deprotonation of B_5H_9.

(5) A potential source of $B_{10}H_{14}$ also came from the reaction of LiB_5H_8 with an equimolar quantity of B_2H_6 in an ethereal medium[45]. This reaction was used to prepare B_6H_{10} in 25% yields, and $B_{10}H_{14}$ was formed as a side product. (0.5 moles of LiB_5H_8 yielded 5 gm of $B_{10}H_{14}$).

(b) Reactions of <u>nido</u>-$B_{10}H_{14}$

(i) Bridge proton abstraction.

A commonly recognized property of the <u>nido</u>- and <u>arachno</u>- boron hydrides is the apparent negative (hydridic) character of their hydrogens. In contrast, decaborane (14) functions as a monoprotic Brönsted acid in titration studies[46,47]. The source of the proton is the hydrogen bridge system which has been shown to rapidly exchange protons with deuterons under mildly basic, ionizing conditions[48,49]. Examples of proton abstraction reactions are given below[46,47,50,51]:

$$B_{10}H_{14} + NaOH \longrightarrow Na[B_{10}H_{13}] + H_2O \quad (1.2\text{-}30)$$

$$B_{10}H_{14} + NaH \longrightarrow Na[B_{10}H_{13}] + H_2 \quad (1.2\text{-}31)$$

$$B_{10}H_{14} + P(C_6H_5)_3CH_2 \longrightarrow [P(C_6H_5)_3CH_3][B_{10}H_{13}] \quad (1.2\text{-}32)$$

$$B_{10}H_{14} + [N(CH_3)_4][OH] \longrightarrow [N(CH_3)_4][B_{10}H_{13}] + H_2O \qquad (1.2\text{-}33)$$

$$B_{10}H_{14} + CH_3MgI \longrightarrow B_{10}H_{13}MgI + CH_4 \qquad (1.2\text{-}34)$$

Over extended periods of time, alkali metal hydrides remove a second proton[52].

$$M[B_{10}H_{13}] + MH \longrightarrow M_2[B_{10}H_{12}] + H_2 \qquad (1.2\text{-}35)$$

where M = Li, Na.

(ii) Base adducts of decaborane (14).

The existence of molecular adducts of decaborane (14) has not been well-established. A monoligand compound $B_{10}H_{14}N(CH_3)_2H$ has been claimed to be molecular because it sublimes at relatively low temperature (33°C in vacuum with continuous pumping)[53]; however, a possible ionic product, $[N(CH_3)_2H_2][B_{10}H_{13}]$, cannot be ruled out. A second material which is thought to be molecular is $B_{10}H_{14}N(C_2H_5)_2H$. It was prepared by protonating $[B_{10}H_{13}N(C_2H_5)_2H]^-$ but was not isolated from solution[54].

(iii) Base adducts of fragments derived from <u>nido</u>-decaborane (14)

(1) <u>Arachno</u>-$[B_{10}H_{12}L_2]$, -$[B_{10}H_{12}(CN)L]^-$, $[B_{10}H_{12}LL']$

While strong bases readily deprotonate $B_{10}H_{14}$

[sect. 1.2.4(b)(i)], certain weaker bases such as acetonitrile[55], phosphines, diethylcyanamide[56], amines[57], sulphides, sulphoxides, phosphine oxides, amides and thioamides[58], react with $B_{10}H_{14}$ according to the following equation:

$$B_{10}H_{14} + 2L \longrightarrow B_{10}H_{12}L_2 + H_2 \qquad (1.2\text{-}36)$$

Mixed ligand adducts have been prepared in the following reaction with $B_{10}H_{14}$[58]:

$$B_{10}H_{14} + NaCN + L \longrightarrow Na\left[B_{10}H_{12}(CN)L\right] + H_2 \qquad (1.2\text{-}37)$$

where L = $S(CH_3)_2$, $S(CH_2)_4$

Ligand exchange reactions involving $B_{10}H_{12}$ $(ligand)_2$ led to many more derivatives of this type.

$$B_{10}H_{12}\ (ligand)_2 + 2\ Ligand \longrightarrow B_{10}H_{12}\ (Ligand)_2 + 2\ ligand \qquad (1.2\text{-}38)$$

It was first shown that[56] triphenylphosphine would displace both acetonitrile and diethylcyanamide ligands and that diethylcyanamide would displace acetonitrile ligand. Later work[59] expanded this displacement reaction series to include a much larger array of ligands which included dialkylsulphides, amides, amines, phosphite and

phosphinate esters, thiophosphite esters, and arsines. The general utility of the ligand-exchange reaction is thus well established on a qualitative basis in which dialkyl sulphides and alkyl nitriles act as weakly bound and easily displaced ligands, whereas amines, phosphines, etc., behave as tightly bonded ligands capable of displacing dialkyl sulphides and nitriles.

The neutral mixed ligand adducts, $B_{10}H_{12}LL'$, could be prepared by the reaction of $[B_{10}H_{13}L]^-$ [sect. 1.2.4(b)(iii)(2)] with amine hydrochlorides[54].

$$Na[B_{10}H_{13}L] + L'HCl \longrightarrow B_{10}H_{12}LL' + H_2 + NaCl \quad (1.2\text{-}39)$$

where L = $N(C_2H_5)_2H$, L' = pyridine, $N(CH_3)_3$, $N(C_2H_5)H_2$, $N(C_2H_5)_2H$ or L = pyridine, L' = pyridine.

The following reaction has also been used to prepare mixed ligand adducts[54].

$$[B_{10}H_{13}N(C_2H_5)_2H]^- + HCl + L \longrightarrow B_{10}H_{12}[N(C_2H_5)_2H][L] + H_2 + Cl^- \quad (1.2\text{-}40)$$

where L = CH_3CN, $S(CH_3)_2$

(2) Arachno-$[B_{10}H_{13}L]^-$, -$[B_{10}H_{13}L]^{2-}$

The $[B_{10}H_{13}]^-$ ion [sect. 1.2.4(b)(i)] reacted readily with a number of bases[54,58].

$$Na\left[B_{10}H_{13}\right] + L \longrightarrow Na\left[B_{10}H_{13}L\right] \qquad (1.2\text{-}41)$$

where L = $N(C_2H_5)H_2$[54], $N(C_2H_5)_2H$[47,54], $N(C_2H_5)_3$[54], $P(C_6H_5)_3$[54], pyridine[54,60], piperidine[54], $S(CH_3)_2$[58].

An isothiocyanate derivative, $\left[B_{10}H_{13}(NCS)\right]^{2-}$, was reported[61] to have been prepared from the reaction of thiocyanate with $\left[B_{10}H_{13}\right]^-$ in anhydrous ethereal media. On the other hand, these ions did not react with each other in aqueous media to give borane species containing the NCS group. Instead, $\left[B_{10}H_{13}\right]^-$ and $\left[B_9H_{14}\right]^-$ salts were obtained.

In aqueous media $\left[B_{10}H_{13}(CN)\right]^{2-}$ was prepared by adding CN^- to $\left[B_{10}H_{13}\right]^-$ [61] and also through the following reaction[58]:

$$2\ NaCN + B_{10}H_{14} \longrightarrow Na_2\left[B_{10}H_{13}(CN)\right] + HCN \qquad (1.2\text{-}42)$$

The salt $Cs_2\left[B_{10}H_{13}(OH)\right]$ had been isolated from aqueous solution containing $Cs\left[B_{10}H_{13}\right]$ and CsOH[62]. Less direct observations of $\left[B_{10}H_{13}(OH)\right]^{2-}$ in which the ion was not isolated had also been reported[43,63]. It was shown that[62] decaborane (14) reacted with aqueous ammonia in a 1:2 molar ratio to yield $\left[B_{10}H_{13}(NH_3)\right]^-$ which was isolated as the cesium salt. This anion was termed "labile" because, unlike typical $\left[B_{10}H_{13}L\right]^-$ species, it was easily hydrolyzed. However, upon recrystallization from a 50% KOH solution, a "stable" form of $\left[B_{10}H_{13}(NH_3)\right]^-$ was isolated which was resistant

to hydrolysis and believed to be of the same structural class as the $[B_{10}H_{13}L]^-$ species.

(3) Arachno-$[B_{10}H_{14}]^{2-}$

This dianion was first prepared[64] through the reaction of sodium with decaborane (14) in liquid ammonia and also in ethereal solvents.

$$2\ Na + B_{10}H_{14} \longrightarrow Na_2\ [B_{10}H_{14}] \qquad (1.2\text{-}43)$$

A convenient high yield (90%) synthesis of $[B_{10}H_{14}]^{2-}$ had been achieved[65] from the reaction of $B_{10}H_{14}$ with aqueous KBH_4 in a 1:4 molar ratio. The reactions were summarized as follows:

$$B_{10}H_{14} + H_2O \rightleftharpoons [B_{10}H_{13}]^- + H_3O^+ \qquad (1.2\text{-}44)$$

$$[B_{10}H_{13}]^- + [BH_4]^- \rightleftharpoons [B_{10}H_{14}]^{2-} + \{BH_3\} \qquad (1.2\text{-}45)$$

$$\{BH_3\} + 3H_2O \xrightarrow{\text{fast}} B(OH)_3 + 3H_2 \qquad (1.2\text{-}46)$$

Note from (1.2-45) that $[B_{10}H_{14}]^{2-}$ was believed to be formed essentially by transfer of H^- from $[BH_4]^-$ to $[B_{10}H_{13}]^-$.

(4) Closo-$[B_{10}H_{10}]^{2-}$

It had previously been reported[57a] that displacement of acetonitrile by triethylamine from

$B_{10}H_{12}[CH_3CN]_2$ yielded covalent and ionic displacement products.

$$B_{10}H_{12}[CH_3CN]_2 + N(C_2H_5)_3 \longrightarrow B_{10}H_{12}[N(C_2H_5)_3]_2 + 2\ CH_3CN \qquad (1.2\text{-}47)$$

$$B_{10}H_{12}[CH_3CN]_2 + N(C_2H_5)_3 \longrightarrow [N(C_2H_5)_3H]_2[B_{10}H_{10}] + 2\ CH_3CN \qquad (1.2\text{-}48)$$

It was also found[66] that a nearly quantitative conversion of <u>nido</u>- $B_{10}H_{14}$ to <u>closo</u>-$[B_{10}H_{10}]^{2-}$ took place as shown in (1.2-49).

$$2(C_2H_5)_3N + B_{10}H_{14} \longrightarrow [(C_2H_5)_3NH]_2[B_{10}H_{10}] + H_2 \qquad (1.2\text{-}49)$$

This is the only synthesis of a <u>closo</u>-boron hydride for which some mechanistic information is available[67]. The overall reaction (1.2-49) in refluxing toluene proceeded with kinetic behaviour consistent with the scheme:

$$B_{10}H_{14} + 2L \longrightarrow B_{10}H_{12}(L)_2 + H_2 \qquad (1.2\text{-}50)$$

$$B_{10}H_{12}[L]_2 \underset{k_{-1}}{\overset{k_1}{\rightleftharpoons}} B_{10}H_{12}(L) + L \qquad (1.2\text{-}51)$$

$$B_{10}H_{12}[L] + N(C_2H_5)_3 \xrightarrow{k_2} [B_{10}H_{11}]^- + [N(C_2H_5)_3H]^+ + L \qquad (1.2\text{-}52)$$

$$[B_{10}H_{11}]^- + N(C_2H_5)_3 \xrightarrow{\text{very fast}} [B_{10}H_{10}]^{2-} + [N(C_2H_5)_3H]^+ \qquad (1.2\text{-}53)$$

Interfering reactions were

$$B_{10}H_{12}[L] + N(C_2H_5)_3 \longrightarrow B_{10}H_{12}[L][N(C_2H_5)_3] \qquad (1.2\text{-}54)$$

$$B_{10}H_{12}[L] + L \longrightarrow \text{unidentified products} \qquad (1.2\text{-}55)$$

Eq. (1.2-55) applies if the ligand is a Lewis base other than $N(C_2H_5)_3$. The proposed intermediate $B_{10}H_{12}[L]$ is not the same as established compounds of the same formula such as $B_{10}H_{12}[S(CH_3)_2]$, since the latter is relatively unreactive toward $N(C_2H_5)_3$.

(5) <u>Nido</u>-$[B_{10}H_{13}L]$ and <u>arachno</u>-$[B_{10}H_{12}L]^-$

The neutral species $B_{10}H_{13}L$ has been prepared by the following reactions involving either $B_{10}H_{13}MgI$[68,69] or $Na[B_{10}H_{13}]$[70] as the starting material.

$$B_{10}H_{13}MgI + LCl \longrightarrow B_{10}H_{13}L + MgICl \qquad (1.2\text{-}56)$$

where L = $P(C_6H_5)_2$, $As(C_6H_5)_2$, $N(CH_3)_2$

$$Na[B_{10}H_{13}] + P(C_6H_5)_2Cl \longrightarrow B_{10}H_{13}[P(C_6H_5)_2]^+ NaCl \qquad (1.2\text{-}57)$$

The most extensively studied $B_{10}H_{13}L$ neutral species is $B_{10}H_{13}[P(C_6H_5)_2]$[68,70]. It shows little or no tendency to form $[B_{10}H_{14}]^{2-}$ type derivatives with neutral or anionic donors as in the case of $B_{10}H_{14}$[68]. It is, however, a strong monoprotic acid in aqueous media.

$$H_2O + B_{10}H_{13}[P(C_6H_5)_2] \longrightarrow H_3O^+ + [B_{10}H_{12}P(C_6H_5)_2]^- \quad (1.2\text{-}58)$$

Amines readily deprotonate $B_{10}H_{13}[P(C_2H_5)_2]$ to form quaternary ammonium salts of the $[B_{10}H_{12}\ P(C_6H_5)_2]^-$[68,70]

(6) $B_{10}H_{12}L$

A neutral monoligand adduct was produced in the following reaction[58]:

$$B_{10}H_{12}[S(CH_3)_2]_2 \xrightarrow[\text{mesitylene}]{110^\circ C}$$

$$B_{10}H_{12}[S(CH_3)_2] + S(CH_3)_2 \quad (1.2\text{-}59)$$

An improved synthesis of $B_{10}H_{12}[S(CH_3)_2]$ was claimed by heating $B_{10}H_{14}$ in $S(CH_3)_2$ at 120°C[71]. Ligand addition and ligand displacement had been observed[58].

$$B_{10}H_{12}[S(CH_3)_2] + NaCN \longrightarrow Na[B_{10}H_{12}\ S(CH_3)_2(CN)] \quad (1.2\text{-}60)$$

$$B_{10}H_{12}[S(CH_3)_2] + 2P(C_6H_5)_3 \longrightarrow B_{10}H_{12}[P(C_6H_5)_3]_2 + S(CH_3)_2 \quad (1.2\text{-}61)$$

1.3 ELECTROCHEMISTRY OF BORON HYDRIDE COMPOUNDS

1.3.1 Overview of Electrochemical Techniques

In this section, a brief report on linear potential sweep chronoamperometry, cyclic voltammetry, a.c. voltammetry and cyclic a.c. voltammetry is introduced to give an overview of the electrochemical techniques employed in studies of the electrochemical behaviour of boron hydride compounds. The details of these techniques can be found elsewhere in the literature[72].

Controlled Potential Techniques - Potential Sweep Methods

(i) Linear potential sweep chronoamperometry.

It is also called linear sweep voltammetry (LSV). In this experiment, the potential is swept linearly at v V/sec. as shown in Fig. 1.3.1(a). It is customary to record the current as a function of potential, which is obviously equivalent to recording current versus time. A typical LSV respond curve is shown in Fig. 1.3.1(b).

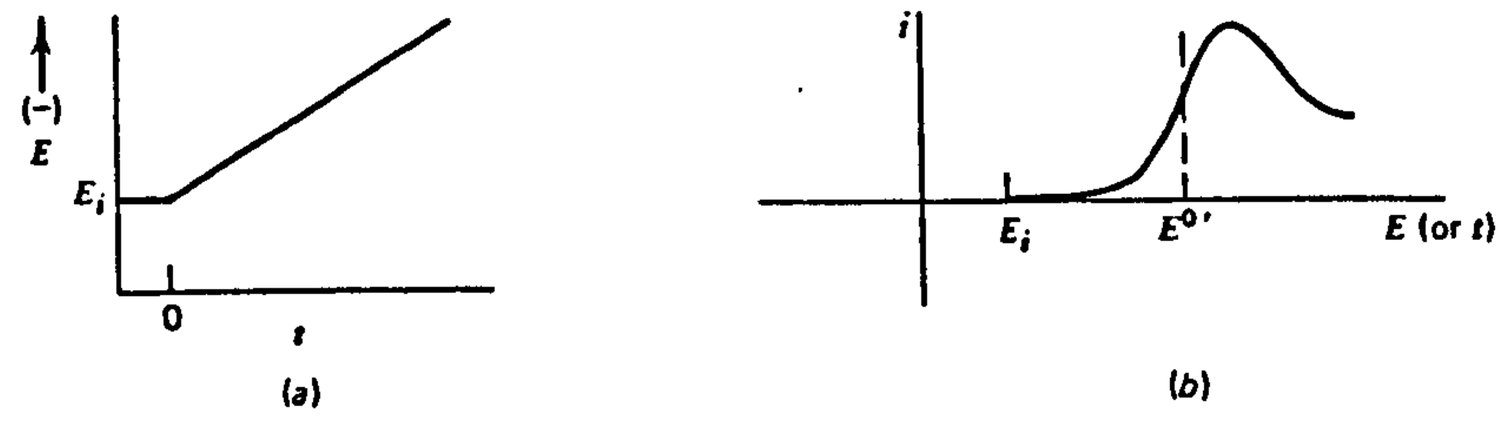

Fig. 1.3.1 (a) Linear potential sweep or ramp starting at E_i.
(b) Resulting i-E curve.

If the scan is begun at a potential well positive of $E^{\prime o}$ for the reduction, only nonfaradaic currents flow for a while. When the electrode potential reaches the vicinity of $E^{\prime o}$ the reduction begins and current starts to flow. As the potential continues to grow more negative, the surface concentration of oxidant must drop; hence the flux to the surface (and the current) increase. As the potential moves past $E^{\prime o}$, the surface concentration drops to near zero, mass transfer of the oxidant to the surface reaches a maximum rate, and then it declines as the depletion effect sets in. The observation is therefore a peak current-potential curve like that depicted.

(ii) Cyclic voltammetry.

In this experiment, the potential is swept linearly at v V/sec and the direction of the scan is reversed at a certain time, $t = \lambda$ (or at the switching potential, E_λ) as shown in Fig. 1.3.2(a).

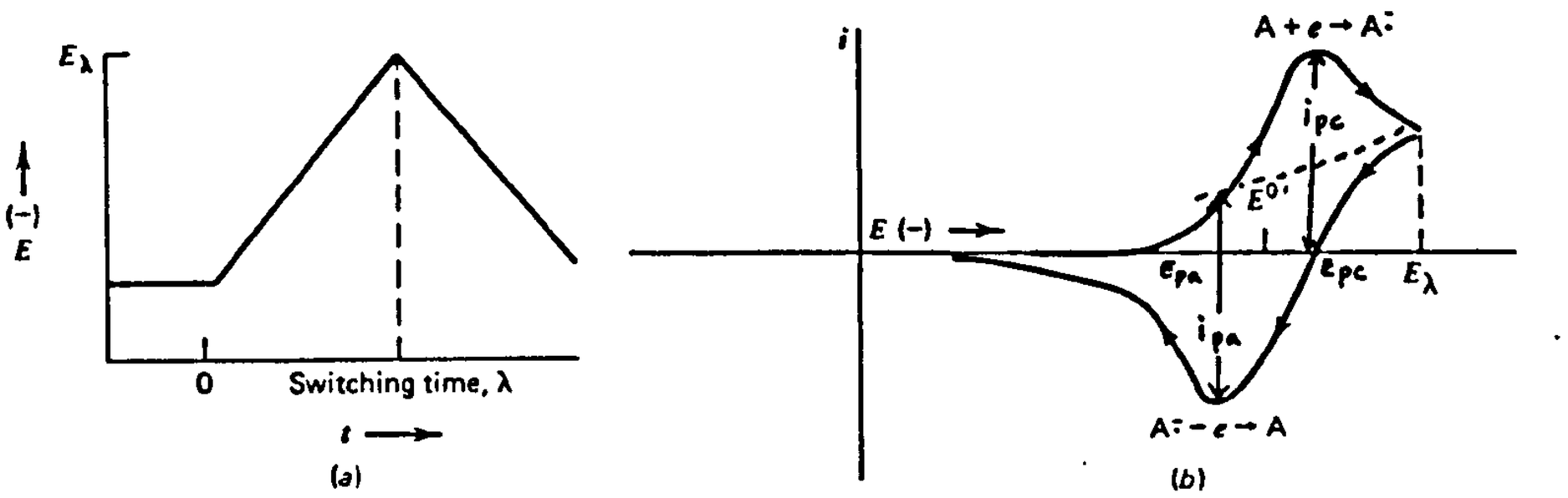

Fig. 1.3.2 (a) Cyclic potential sweep.

(b) Resulting cyclic voltammogram.

Consider the electrode reaction:

$$O + ne^- \underset{k_r}{\overset{k_f}{\rightleftharpoons}} R$$

where k_f is the forward rate constant and k_r is the reverse rate constant. If the electrode reaction is reversible, which means both forward and backward rate constants are fast enough [K^o (the standard rate constant > $0.3\ v^{\frac{1}{2}}$ cm/sec. v = scan rate in V/sec] to maintain [O] and [R] in equilibrium at the electrode surface, then the current-voltage curve obtained is as shown in Fig. 1.3.2(b). The curve obtained on forward scan is as that described in LSV respond curve. The shape of the curve on reversal depends on the switching potential, E_λ, or how far beyond the cathodic peak the scan is allowed to proceed before reversal. However, if E_λ is at least $\frac{35}{n}$ mV past the cathodic peak, the reversal peaks all have the same general shapes, basically consisting of a curve shaped like that of the forward current-potential plotted in the opposite direction on the current axis, with the decaying current of the cathodic wave used as a baseline and $i_{pa} = i_{pc}$. The average of forward and reverse peak potential corresponds to $E^{/o}$. The difference between E_{pa} and E_{pc} (ΔE_p) is a useful diagnostic test of a nernstian (reversible) reaction. Although ΔE_p is slightly a function of E_λ, it is always close to 2.3 RT/nF (or 59/n mV at 25°C). For an irreversible reaction, the charge transfer rate

constant, k^o, is $\leqslant 2 \times 10^{-5}\ v^{\frac{1}{2}}$ cm/sec and ΔEp is $\rangle 59/n$ mV at 25°C.

Techniques Based on Concepts of Impedance

(iii) A.C. voltammetry.

A.c. voltammetry is basically a faradaic impedance technique in which the d.c. potential (E_{dc}) is imposed potentiostatically at arbitrary values that usually differ from the equilibrium value. Ordinarily. it is varied systematically (e.g. linearly) on a long time scale compared to that of the superimposed AC potential ($E_{ac} \approx$ 10 mV peak to peak). The output is a plot of the magnitude of the a.c. component of the current vs. E_{dc}. The phase angle between the alternating current and E_{dc} is also of interest. The typical a.c. voltammogram is as shown in Fig. 1.3.3.

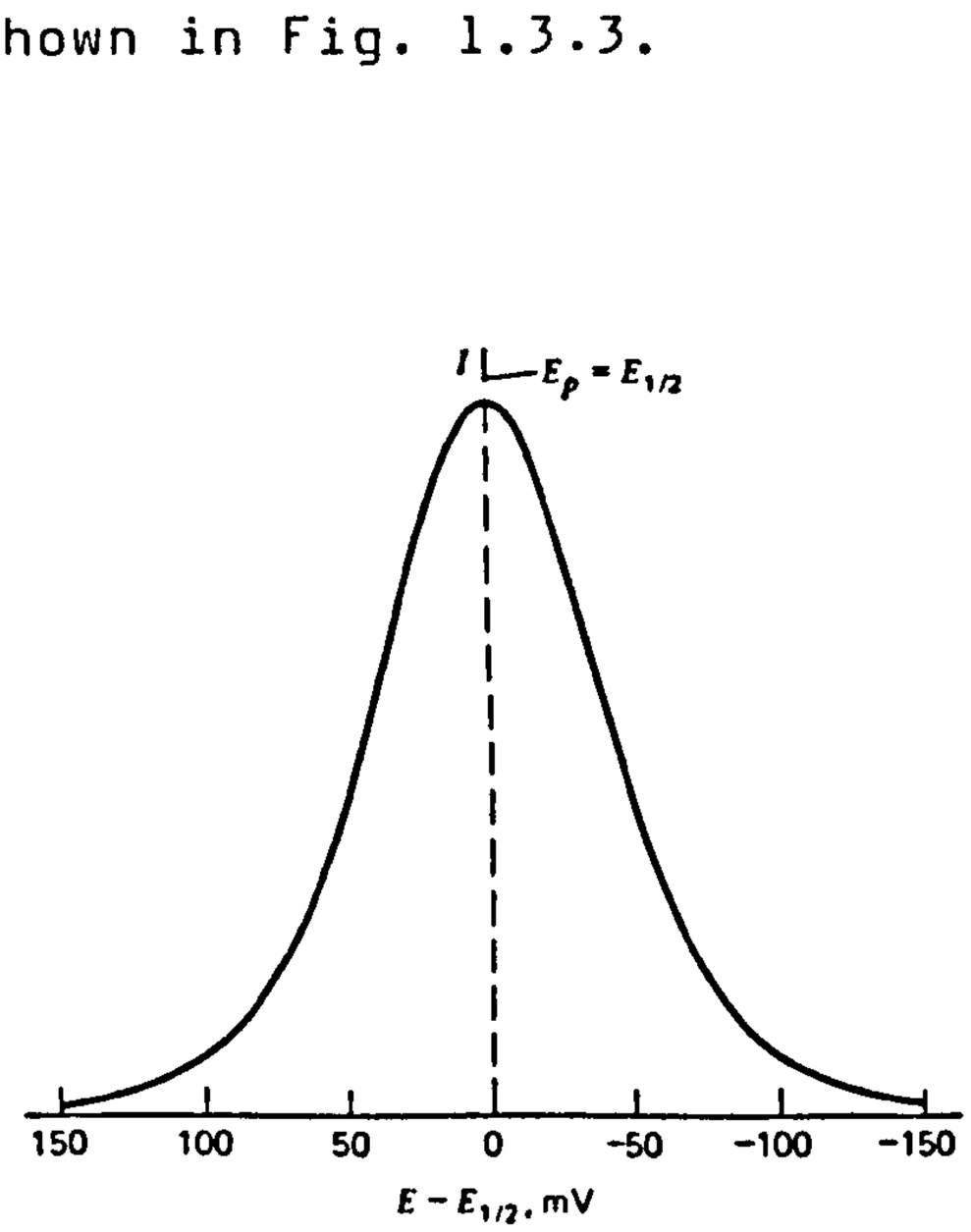

Fig. 1.3.3 Shape of a reversible a.c. voltammetric peak for n=1.

One of the important properties of the reversible a.c. voltammetry can be deduced from the peak width which is 90.4/n mV at 25°C (provided ΔE is $\leqslant$ 10/n mV peak to peak; ΔE = peak to peak potential/2).

(iv) Cyclic a.c. voltammetry.

Cyclic a.c. voltammetry is a simple extension of the linear sweep technique; one simply adds the reversal scan in E_{dc}. This technique is attractive because it retains the best features of two powerful complementary methodologies. Conventional cyclic voltammetry is especially informative about the qualitative aspects of an electrode process. However, the response waveforms lend themselves poorly to quantitative evaluations of parameters. Cyclic a.c. voltammetry retains the diagnostic utility of conventional cyclic measurements, but it does so with an improved response function that permits quantitative evaluations as precise as those obtainable with the usual a.c. approaches.

For a reversible system, the cyclic a.c. voltammogram shows superimposed forward and reverse traces of a.c. current amplitude vs. E_{dc}. Fig. 1.3.4 shows a comparison of response waveforms for cylic d.c. and cyclic a.c. voltammetry for a reversible system.

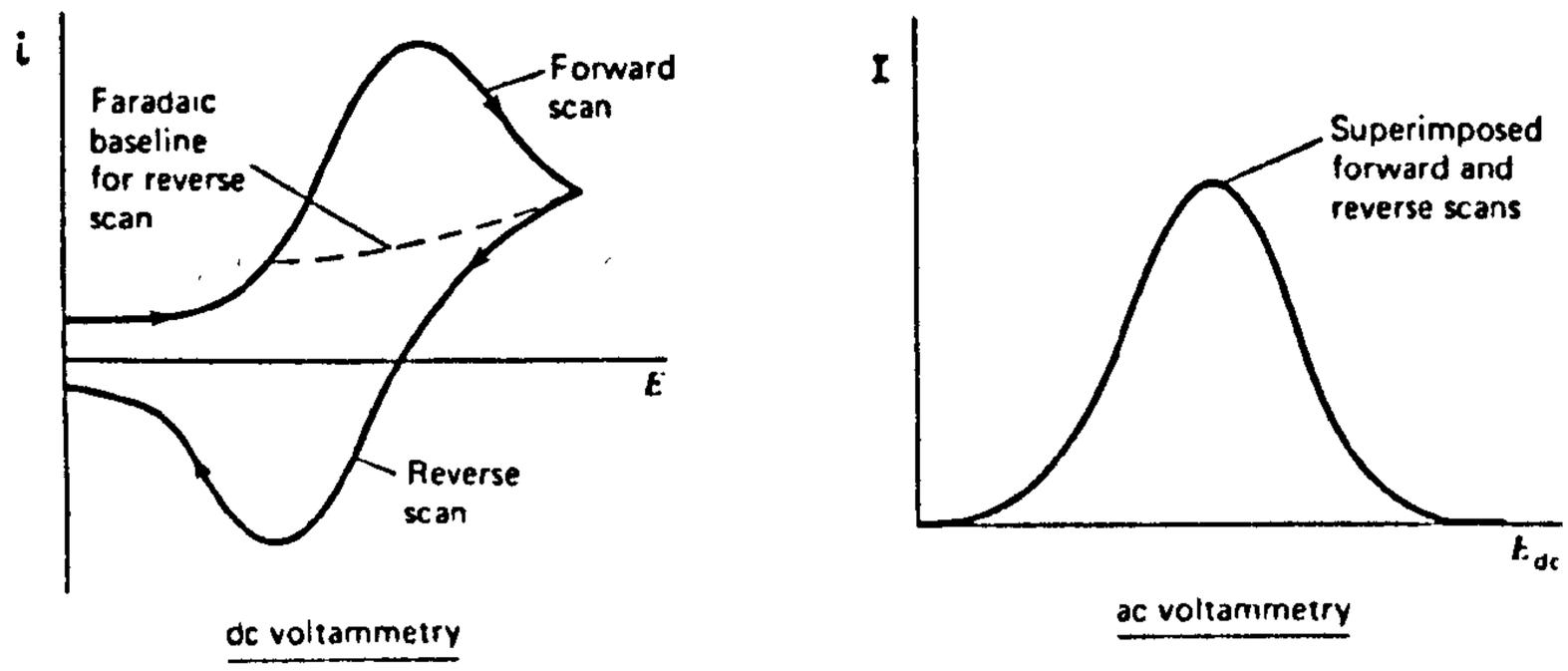

Fig. 1.3.4 Comparison of response waveforms for cyclic d.c. and cyclic a.c. voltammetry for a reversible system.

1.3.2 Electrochemical Studies of Boron Hydrides

Electrochemical methods are employed as tools in the study of chemical systems, in just the way spectroscopic methods are frequently applied. The application of electrochemical techniques to boron chemistry has recently received more attention and have proved to be quite encouraging. In this section, electrochemical behaviour of some boron hydrides is reviewed.

(i) $[BH_4]^-$.

Electrolysis of tetrahydroborate anion has previously been used as a method of preparing diborane. The reaction can be carried out in molten tetrahydroborate[73], because the mixed-alkali-metal tetrahydroborates have unusually low eutectic temperatures.

$$2[BH_4]^- \xrightarrow{\text{anode}} B_2H_6 + H_2 + 2e^- \qquad (1.3\text{-}1)$$

The electrolysis of $NaBH_4$ in polyethylene glycol dimethyl ethers with a mercury cathode gave diborane in good yield. The formation of sodium heptahydrodiborate is indicated by a time lag in the release of diborane[74].

$$2[BH_4]^- \longrightarrow [B_2H_7]^- + \tfrac{1}{2}H_2 + e^- \qquad (1.3\text{-}2)$$

$$[B_2H_7]^- \longrightarrow B_2H_6 + \tfrac{1}{2}H_2 + e^- \qquad (1.3\text{-}3)$$

Electrolysis of tetrahydroborate in DMF produces di-

borane[75] whereas such an electrolysis in dimethylamine yields dimethylamine borane[76]. A similar reaction has been used to prepare ethylamineborane[77].

The electrochemical studies of $NaBH_4$ [76,78,79,80] and KBH_4 [81,82] in aqueous solution have been reported. This system is complicated by the presence of a competitive chemical reaction (hydrolysis) that gives products that are themselves oxidizable at somewhat more negative potentials than the parent ion. A further complication is introduced by the pH dependence of the rate of formation of these hydrolysis products (i.e. $[BH_3OH]^-$, $[BH_2(OH)_2]^-$, $[BH(OH)_3]^-$). As a final complication, the composition of the electrode surface, by virtue of its role as a heterogeneous catalyst for the hydrolysis reaction, also influence the overall composition of a tetrahydroborate analyte and thus its voltammetry. These studies also clearly demonstrate the need for extreme care in purifying materials used in detailed electrochemical studies and the need for equally extreme caution in interpreting electrochemical data.

(ii) $[BH_3CN]^-$.

The cyclic voltammetry of $[BH_3CN]^-$ in acetonitrile has been examined[83,84,85] at various metal electrodes. No obvious oxidation or reduction waves were observed at an "inert" working electrode (e.g. Pt), whereas several reactive electrodes (e.g. Fe, Cu, Co, Ni) led to the formation of metallacyanoborane

derivatives. However, Mo or V electrodes resulted in oxidation of the $[BH_3CN]^-$ at $E_p \sim 0.9$ V to give the ion $[BH_3CNBH_2CN]^-$ by the process

$$[BH_3CN]^- \longrightarrow BH_2CN + H^{\cdot} + e^- \qquad (1.3\text{-}4)$$

$$BH_2CN + [BH_3CN]^- \longrightarrow [BH_3CNBH_2CN]^- \qquad (1.3\text{-}5)$$

$$H^{\cdot} \longrightarrow \tfrac{1}{2}H_2 \qquad (1.3\text{-}6)$$

The anodic dissolution of iron in an acetonitrile solution of $Na[BH_3CN]$ in the presence of $P(OMe)_3$ or $P(OEt)_3$ led to cis-trans mixture of $[Fe\{P(OR)_3\}_4\ (NCBH_3)_2]$[84]. Similarly, the anodic dissolution of cobalt or nickel in acetonitrile solutions of $Na[BH_3CN]$ yielded tetrahedral and octahedral neutral or anionic metallacyanoborane complexes, depending on the conditions[85].

(iii) $[B_3H_8]^-$.

Electrolysis of $[B_3H_8]^-$ at a platinum or gold anode in acetonitrile and dimethyl formamide resulted in a one-electron oxidation to yield $B_3H_7\cdot[CH_3CN]$ and $B_3H_7[DMF]$ respectively[86].

$$[B_3H_8]^- \xrightarrow{CH_3CN} B_3H_7\cdot[CH_3CN] + \tfrac{1}{2}H_2 + e^- \qquad (1.3\text{-}7)$$

The chronopotentiometric oxidation wave occurred near 0.4 V (Ag/AgCl/LiCl; 0.19 V vs. SCE).

The cyclic voltammogram of $[B_3H_8]^-$ in CH_3CN at a stationary Pt electrode was complex and highly irreversible, with an oxidation wave near 0.6 V ($Ag/AgNO_3$; 0.34 V vs. SCE)[87]. Anodic dissolution of acetonitrile solutions of $[B_3H_8]^-$ in the presence of PPh_3 at Cu or Ag anodes led to $[(Ph_3P)_2CuB_3H_8]$ and $[(Ph_3P)_3AgB_3H_8]$, whereas such electrolysis at Zn or Cd anodes, led to the isolation of $[Ph_3P]BH_3$ and $[Ph_3P]_2$ B_2H_4 [87]. Electrolysis of $[B_3H_8]^-$ at a Pt electrode in acetonitrile in the presence of PPh_3 led to $[Ph_3P]B_3H_7$ and its subsequent cleavage products $[Ph_3P]BH_3$ and $[Ph_3P]_2$ B_2H_4. Platinum dissolution was not detected[87]. Substitution of the $[B_3H_8]^-$ ion by NCS^- or $NCBH_3^-$ led to increased oxidative stability, with the first oxidation potential occurring near 1.32 V in $[B_3H_7(NCS)]^-$ and 1.2 V in $[B_3H_7(NCBH_3)]^-$. The first oxidation of $[B_3H_7(NCS)]^-$ involved four electrons[88].

(iv) $B_{10}H_{14}$.

The eletrochemical properties of decaborane have been studied most intensively. Detailed electrochemical studies in acetonitrile and glyme[89,90,91] have shown that the apparently simple reduction of $B_{10}H_{14}$ is in fact mechanistically complex. Decaborane in glyme solution (0.1 M $NBu^n_4ClO_4$) exhibits two polarographic reduction waves at $E_{\frac{1}{2}}$ = -1.54 V and -2.78 V ($Ag/AgNO_3$ satd) and no oxidation waves[89]. Under the conditions studied, at the first wave, plots of instantaneous limiting current vs. (mercury column

height)$^{\frac{1}{2}}$ were linear with intercepts at or near the origin, indicating a diffusion-controlled process. A linear plot was also observed for $\log[(i_d-i)/i]$ vs. potential with a slope of 0.06 V. These data strongly suggested a primary reduction step involving a one-electron reduction of $B_{10}H_{14}$.

$$B_{10}H_{14} + e^- \longrightarrow [B_{10}H_{14}]^- \qquad (1.3\text{-}8)$$

The diffusion-controlled character of the limiting-current first wave and total absence of kinetic character precluded the possibility of a chemical reaction preceding the charge-transfer step, such as

$$B_{10}H_{14} \underset{k_r}{\overset{k_f}{\rightleftharpoons}} [B_{10}H_{13}]^- + H^+ \qquad (1.3\text{-}9)$$

where the electroactive species is $[B_{10}H_{13}]^-$ or H^+. Fig. 1.3.5 shows the cyclic voltammograms for $B_{10}H_{14}$ in glyme after the application of several triangular wave cycles (i.e. approximately steady state) in a multicycle experiment in which the potential sweep did not encompass the second reduction wave. Wave B corresponded to the first reduction wave of $B_{10}H_{14}$. Wave A, C and D did not appear unless wave B was included in the potential sweep, indicating that these waves are associated with the products of the first reduction step (wave B). The decreasing magnitude of wave C with decreasing scan rate indicates that the

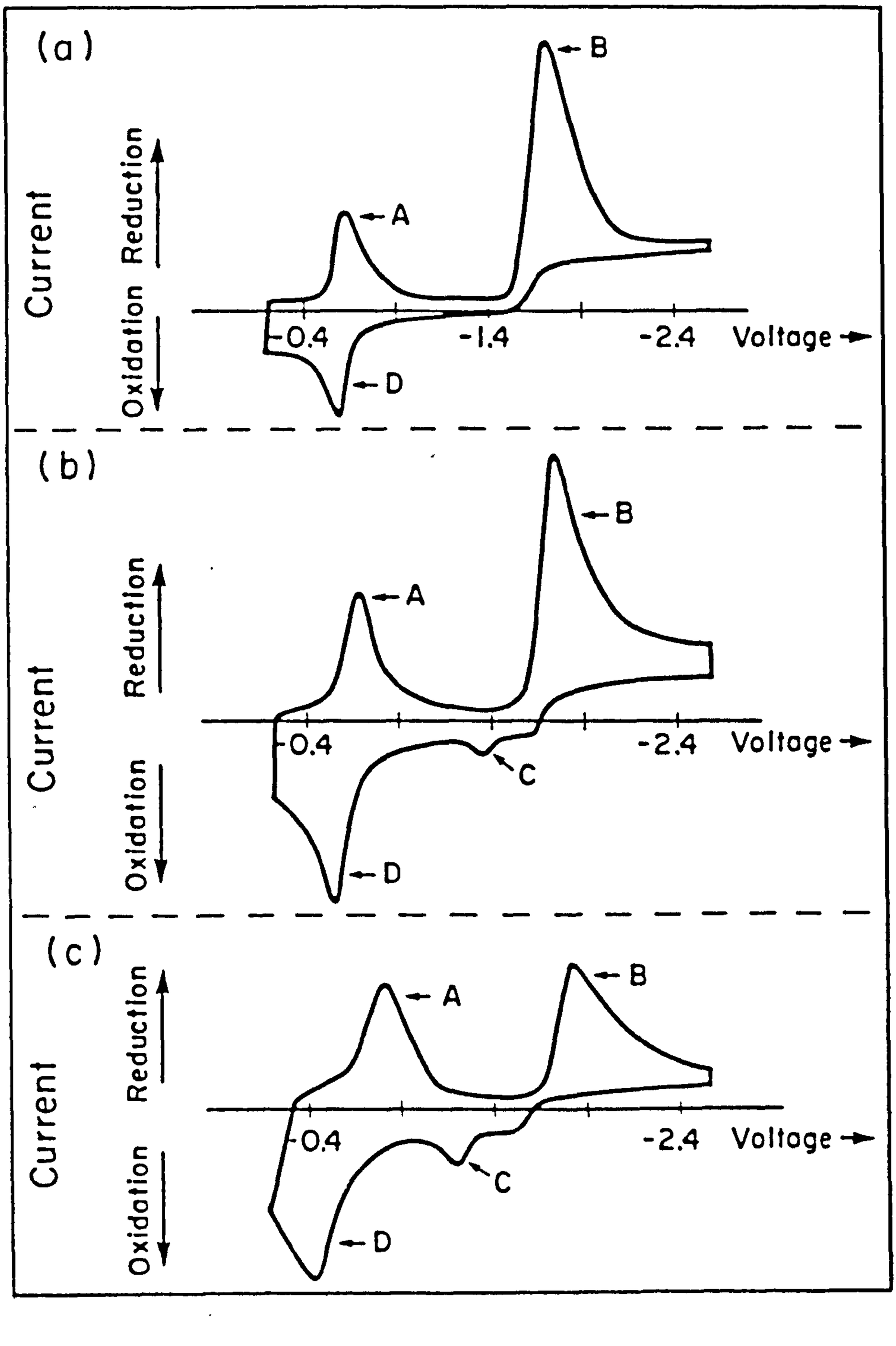

Fig.1.3.5. Cyclic voltammograms of $B_{10}H_{14}$(0.99×10^{-3} M; 0.1 M Bu_4NClO_4 in 1,2-dimethoxyethane) with scan rates (a) 0.88 VS^{-1}, (b) 1.9 VS^{-1}, and (c) 5.5 VS^{-1}.

species responsible for this oxidation wave is a transient intermediate. This is further confirmed by the fact that wave C decreases with increasing temperature. Increasing decaborane concentration also suppresses the magnitude of wave C, relative to the other waves, suggesting that this species decomposed by a second (or higher) order reaction. The magnitude and other characteristics of wave C were not significantly influenced by whether waves A and D were included in the sweep, showing that the electrode reaction associated with the reversible couple A and D neither served as the origin nor influenced the depletion of the species produced at wave C. On the basis of the above evidence, wave C was assigned to the oxidation of the $[B_{10}H_{14}]^{-}$ radical anion. However, the substantial overvoltage separating the reduction step (wave B) and the oxidation step(wave C) suggested that the species producing wave C was not the product of the initial electron-transfer step, $[B_{10}H_{14}]^{-}$, but was due to some species which resulted from a unimolecular transformation of the primary electrolysis product. Unlike wave C, the sweep-rate dependence of waves A and D suggested that they arose from a product of $B_{10}H_{14}$ reduction that was stable in the time scale of the cyclic voltammetric experiment. These waves were assigned to the redox processes of $[B_{10}H_{13}]^{-}$. The presence of $[B_{10}H_{15}]^{-}$ in the solution was deduced from the overall stoichiometry of the electrode reaction.

Constant-potential electrolysis at the first reduction wave (B) gave a solution whose UV spectrum and polarogram supported the presence of equimolar amounts of $[B_{10}H_{13}]^-$ and $[B_{10}H_{15}]^-$. These overall mechanisms proposed were[89]:

$$B_{10}H_{14} + e^- \rightleftharpoons \{[B_{10}H_{14}]^{\cdot -}\} \qquad (1.3\text{-}10)$$

$$\{[B_{10}H_{14}]^{\cdot -}\} \rightleftharpoons [B_{10}H_{14}]^{\cdot -} \qquad (1.3\text{-}11)$$

$$2\,[B_{10}H_{14}]^{\cdot -} \rightleftharpoons [B_{10}H_{13}]^- + [B_{10}H_{15}]^- \qquad (1.3\text{-}12)$$

$$2B_{10}H_{14} + 2e^- \longrightarrow [B_{10}H_{13}]^- + [B_{10}H_{15}]^- \qquad (1.3\text{-}13)$$

The oxidation wave due to the postulated $\{[B_{10}H_{14}]^{\cdot -}\}$ was not observed up to the limit of the instrumentation used, but polarographic data support such a unimolecular decomposition after the one-electron charge-transfer step. If the second-order decomposition (1.3-13) were directly coupled to a reversible one-electron charge-transfer step (wave B), a linear plot of log $[(i_d - i)/i^{2/3}]$ vs. E would have resulted. However, this was not the case.

The second reduction wave which has also been studied in detail[90] is assigned to a one-electron reduction of $[B_{10}H_{13}]^-$. The resulting radical dianion,

$[B_{10}H_{13}]^{2-}$, rapidly disproportionates to form $[B_{10}H_{14}]^{2-}$ and $[B_{10}H_{12}]^{2-}$ which react rapidly with bulk $B_{10}H_{14}$ to regenerate more electroactive $[B_{10}H_{13}]^{-}$. The overall reduction at the second reduction wave corresponds to:

$$4B_{10}H_{14} + 6e^{-} \rightleftharpoons [B_{10}H_{12}]^{2-} + [B_{10}H_{14}]^{2-} + 2[B_{10}H_{15}]^{-} \qquad (1.3\text{-}14)$$

A reaction between $[B_{10}H_{15}]^{-}$ and $[B_{10}H_{12}]^{2-}$, generating $[B_{10}H_{13}]^{-}$, appears to contribute to the electrode reaction over the longer times of constant-potential electrolysis experiments (1-2 hr.), so the net reaction under these conditions is

$$B_{10}H_{14} + 2e^{-} \rightleftharpoons [B_{10}H_{14}]^{2-} \qquad (1.3\text{-}15)$$

When $[B_{10}H_{13}]^{-}$ is reduced in absence of bulk $B_{10}H_{14}$, the reaction stops with the formation of $[B_{10}H_{14}]^{2-}$ and $[B_{10}H_{12}]^{2-}$.

The first reduction wave of $B_{10}H_{14}$ has also been studied in acetonitrile and dichloromethane solutions[91]. Constant-potential coulometry at this wave gave an n value of about one electron per $B_{10}H_{14}$ molecule, and ^{11}B n.m.r. showed that the electrolysis product was an equimolar mixture of $[B_{10}H_{13}]^{-}$ and $[B_{10}H_{15}]^{-}$. The reduction in these solvents, however, has been postulated as a two-electron irreversible step,

on the basis of detailed analysis of the cyclic voltammograms, the formal reduction potential for the $B_{10}H_{14}/B_{10}H_{14}^{2-}$ couple in acetonitrile being -0.78 ± 0.02 V (vs. SCE)

$$B_{10}H_{14} + 2e^- \longrightarrow [B_{10}H_{14}]^{2-} \qquad (1.3\text{-}16)$$

$$B_{10}H_{14} + [B_{10}H_{14}]^{2-} \underset{k_{-1}}{\overset{k_1}{\rightleftharpoons}} [B_{10}H_{13}]^- + \{[B_{10}H_{15}]^-\} \qquad (1.3\text{-}17)$$

$$\{[B_{10}H_{15}]^-\} \xrightarrow{k_2} [B_{10}H_{15}]^- \qquad (1.3\text{-}18)$$

The kinetically important reaction following charge transfer both in the reduction of $B_{10}H_{14}$ and in the oxidation of $[B_{10}H_{14}]^{2-}$ was a proton transfer between $B_{10}H_{14}$ and $[B_{10}H_{14}]^-$. The rate of this reaction is approximately 5×10^4 $M^{-1}S^{-1}$ at 24°C. Thus, on the short time scale of the polarographic experiment there is a considerable mechanistic difference in the redox characteristics of $B_{10}H_{14}$ in glyme[89] vs. acetonitrile[91] and dichloromethane[91]. However, in both cases, on the time scale of a constant-potential electrolysis, the reaction products were the same.

(v) $B_{10}H_{12}[CH_3CN]_2$.

The cyclic voltammogram of $B_{10}H_{12}[CH_3CN]_2$ in acetonitrile at platinum comprised two irreversible oxidation waves at E_p 0.75 V and 1.2 V ($Ag/AgNO_3$) with

no well-defined corresponding reduction wave[92]. However, a broad reduction wave at E_p -0.8 V, which appeared only after a scan to anodic potentials, is probably best interpreted as the reduction of H^+. Exhaustive oxidation of $B_{10}H_{12}[CH_3CN]_2$ at 0.9 V showed that the first oxidation involved two electrons. The minor products were identified as $B_9H_{13}[CH_3CN]$ and a species thought to be the nido-$B_{10}H_{10}[CH_3CN]_2$. The electrochemical oxidation was not simple, but at least part of the overall reaction may have proceeded as follows:

$$B_{10}H_{12}[CH_3CN]_2 \longrightarrow B_{10}H_{10}[CH_3CN]_2 + 2H^+ + 2e^- \quad (1.3\text{-}19)$$

The cyclic voltammograms of $B_{10}H_{12}[SMe_2]_2$ and $B_{10}H_{12}[CH_3C(NEt_2)NH]_2$ were very similar to that of $B_{10}H_{12}[CH_3CN]_2$, and thus imply similar electrochemical behaviour.

(vi) $[B_nH_n]^{2-}$ anions.

There have been several reports of polarographic data for $[B_nH_n]^{2-}$ polyhedral anions[93] and some halogenated derivatives of the B_{10} and B_{12} cages[94] as a criterion of their comparative oxidative stabilities. The order of oxidative stability was $B_7 < B_6 < B_9 < B_8 < B_{11}$ $B_{10} < B_{12}$. The halogenation of the B_n cage increased the oxidation stability, although the nature of the various oxidateion products was not studied in the original work[94]. Substitution with OH^- decreased

the oxidative stability of the anions.

(a) $[B_{10}H_{10}]^{2-}$.

Various electrochemical techniques have been employed to elucidate the mechanism and reaction products of the oxidation of $[B_{10}H_{10}]^{2-}$ at a platinum electrode in acetonitrile[95]. This work represented the first application to boron hydride systems of nonaqueous polarography utilizing operational amplifier circuitry with three-electrode system along with the methods of cyclic voltammetry and chronopotentiometry. The chemical oxidation of $[B_{10}H_{10}]^{2-}$ (by Fe^{3+} and Ce^{4+}) led to $[B_{20}H_{18}]^{2-}$ [96-100] and under milder conditions the one-electron oxidation product, $[B_{20}H_{19}]^{3-}$, was isolated[98-100]. The voltammogram of $[B_{10}H_{10}]^{2-}$ at a rotating platinum electrode exhibited two anodic waves. A variety of electrochemical techniques have been used to establish that the oxidation proceeded by an initial reversible one-electron transfer to form a free radical, which then underwent a second-order chemical reaction to form $[B_{20}H_{19}]^{3-}$, which was further oxidised to $[B_{20}H_{18}]^{2-}$ at a slightly greater potential than $[B_{10}H_{10}]^{2-}$ [95]. The overall reaction scheme was

$$[B_{10}H_{10}]^{2-} \longrightarrow [B_{10}H_{10}]^{\cdot-} + e^{-} \qquad (1.3\text{-}20)$$

$$2[B_{10}H_{10}]^{\cdot-} \longrightarrow [B_{20}H_{19}]^{3-} + H^{+} \qquad (1.3\text{-}21)$$

$$[B_{20}H_{19}]^{3-} \longrightarrow [B_{20}H_{18}]^{2-} + H^{+} + 2e^{-} \qquad (1.3\text{-}22)$$

Both $[B_{20}H_{19}]^{3-}$ and $[B_{20}H_{18}]^{2-}$ have been isolated by constant-potential electrolysis at a rotating platinum gauze electrode with 0.1 M $LiClO_4$ as the supporting electrolyte. The $[B_{10}H_{10}]^{\cdot-}$ radical anion was depleted too quickly by the bimolecular reaction (1.3-21) to be isolated, but fast-scan cyclic voltammetry has established the reversible nature of the oxidation.

Cyclic voltammogram of $[N(CH_3)_4]_3\ [B_{20}H_{19}]\cdot\frac{1}{2}H_2O$ showed an anodic wave near 0.7 V and a cathodic wave at -0.1 which increased on each cycle and was assumed to be due to the protons liberated by the oxidation of $[B_{20}H_{19}]^{3-}$ to $[B_{20}H_{18}]^{2-}$. The former wave corresponded to the second anodic wave of $[B_{10}H_{10}]^{2-}$. There was no evidence that the oxidation of $[B_{20}H_{19}]^{3-}$ was reversible within the scan rates and potential limits available.

At a DME, a solution of $[N(CH_3)_4]_2\ [B_{20}H_{18}]$ displayed a cathodic wave at 1.48 V (vs. SCE).

(b) $[B_{12}H_{12}]^{2-}$.

Voltammetry of $[NEt_4]_2\ [B_{12}H_{12}]$ at a rotating platinum electrode in acetonitrile solution (0.1 M Et_4NClO_4) showed an anodic one-electron wave at $E_{\frac{1}{2}}$ = 1.5 V (vs. SCE)[101,102]. Constant-potential electrolysis under nitrogen at 1.45 V with a graphite-cloth anode with no supporting electrolyte and precipitation of the oxidation product with CsF gave a product identified as $Cs_3[B_{24}H_{23}].3H_2O$ on the basis of elemental analysis, a conductivity measurement and ^{11}B n.m.r. spectroscopy. A graphite anode was necessary because the oxidation produced severe filming on a platinum electrode.

1.4 NMR STUDIES OF BORON HYDRIDES

1.4.1 Introduction

Nuclear magnetic resonance has become one of the major physical tools for chemists dealing with molecules, since it provides much information concerning the composition, structure, and dynamics of compounds and systems in a fairly short time. The utility of n.m.r. spectroscopy for the elucidation of molecular structures of boron hydrides was recognized early in the development of the technique[103,104]. The basic work of Ogg[103], for example, elegantly confirmed the hydrogen bridge structure of diborane (6) as opposed to the ethanelike model. While single crystal X-ray diffraction is superior to n.m.r. spectroscopy for structure determination , the speed and convenience of the n.m.r. method significantly augments its usefulness. For compounds which are difficult to crystallize or which show dynamic behaviour in solution such as intramolecular exchange, n.m.r. can be more informative than other structural tools.

In early n.m.r. studies, difficulties were encountered in extracting structural information from spectra of the more complex hydrides and their derivatives owing to overlapping resonances. In recent years, however, these difficulties have been greatly reduced by advances in instrumentation which include superconducting magnets for work at higher field strengths, the use of pulsed and Fourier transform

n.m.r. techniques. The situation will further improve as data from high-field spectrometers become available. These instruments are now designed so that spectroscopic techniques requiring sophisticated data manipulation have become practical, examples of which are two-dimensional correlated ^{1}H - ^{11}B n.m.r., multiple resonance experiments, line narrowing, measurement of T_1 and T_2, and specific frequency irradiation. An additional development which contributes much to the appreciation of ^{11}B n.m.r. data is the increasing availability of X-ray crystallographic data, which establishes solid state structural details beyond cavil, although it is not necessarily true that these details will persist in solution.

1.4.2 Information from Boron NMR Data

(i) Chemical shifts.

Empirical correlations are of value in assigning ^{11}B and ^{1}H resonances on the basis of chemical shifts, but such correlations must be used with caution in view of the fact that no generally satisfactory theoretical treatment is available[105]. ^{11}B chemical shifts are apparently dominated by paramagnetic shielding effects, and terminal proton chemical shifts usually parallel the ^{11}B shifts of the boron atoms to which they are bonded[105]. Neither ^{11}B nor ^{1}H shifts necessarily reflect the electron density on the atom in question. For example, bridge hydrogens usually resonate at higher

field than do terminal hydrogens, yet it is now clear that bridge hydrogens are in general chemically acidic, this implying relatively low electron density at least compared to terminal hydrogens.

(ii) Spin coupling and coupling constant.

A consideration of first-order spin coupling between ^{11}B and hydrogen nuclei which are directly bonded is almost always adequate to explain the major features of the ^{11}B or ^{1}H n.m.r. spectrum. Examples are presented in sect. 1.4.3.

Many coupling constants between directly bonded nuclei $^{1}J(^{11}BX)$ can be obtained from ^{11}B n.m.r. spectra. The accuracy is somewhat limited because of the line width of the resonance signals. In most cases it is also possible to observe $^{1}J(^{11}BX)$ by recording the n.m.r. spectra of X. Long-range couplings $^{n}J(^{11}BX)$ (n>1) have been observed so far only for compounds in which boron has a highly symmetric electronic environment.

The importance of coupling constants in discussing bonding has been established for many other nuclei. Coupling constants for terminal ^{11}B-^{1}H bonds are in the range 80-190 Hz and correlate reasonably well with the percent S character in the bond[106]. Outstanding efforts have been made to develop in deep theoretical understanding of ^{11}B chemical shifts and coupling constants[107].

(iii) Line width.

It has long been recognized that only nuclei with spin $I \geq 1$ possess electric quadrupole moments (e.g. ^{11}B, 80% natural abundance, $I = \frac{3}{2}$; and ^{10}B, 20% natural abundance, $I = 3$). The nonspherical electric charge distribution in the nuclei, which reflects the presence of the electric quadrupole moment, can interact with any electric field gradient present at the nuclei. This leads to a very efficient relaxation mechanism and thus results in broad resonances. The line width of the ^{11}B n.m.r. signal (at half height, $h_{\frac{1}{2}}$) depends on quadrupolar relaxation time, T_q:

$$h_{\frac{1}{2}} \sim \frac{1}{T_q}$$

The quadrupole relaxation of boron is also observable from the n.m.r. spectra of other nuclei X (preferably with $I = \frac{1}{2}$) in the same molecule. Spin-spin coupling of ^{11}B or ^{10}B to X is then clearly visible, partially or completely collapsed, or reduced to a single sharp line[108], depending on the magnitude of T_q.

(iv) Exchange Processes.

NMR has proved a very valuable tool in studying exchange processes of boron compounds[109]. The information can be obtained by observing at various temperatures either the resonances of ^{11}B or those of other nuclei showing coupling or partially relaxed coupling to ^{11}B (dynamic nuclear magnetic resonance,

DNMR)[109]. When coupling constants are involved, the investigations are particularly interesting because the magnitude of the coupling constant and the absence or appearance of coupling leads to the elucidation of the exchange mechanism[109]. The utility of double resonance experiments $^{1}H-\{^{11}B\}$ in the case of partially or almost completely relaxed couplings has been pointed out[100].

(v) Conventions.

Spectra recorded in the field sweep mode are conventionally displayed so that the magnetic field strength increases from left to right. Frequency swept spectra are displayed so that frequency decreases from left to right. The two methods are equivalent for all practical purposes. Chemical shifts are reported in parts per million relative to a designated standard ($BF_3.OEt_2$ as a reference standard for ^{11}B n.m.r. and $(CH_3)_4Si$ as a reference standard for ^{1}H n.m.r.) with values decreasing from left to right when the spectra are displayed as indicated above.

1.4.3 NMR Spectra

(i) Diborane (6), B_2H_6.

The ^{11}B and ^{1}H n.m.r. spectra of diborane (6) have been intensively studied at various temperatures, with several frequencies, and using various isotope ratios, early by Ogg[103] and Shoolery[104] and then with considerable refinement by Gaines and Schaeffer[111]. The most highly resolved ^{11}B and ^{1}H n.m.r. spectra are

those presented by Farrar[112] and are shown in Fig. 1.4.1. The ^{11}B n.m.r. spectrum of diborane (6) reveals a triplet of triplets. The major spin coupling is due to the two terminal hydrogens on each boron (^{11}B) which split the resonance into a 1:2:1 triplet. Each member of this triplet is further split into a 1:2:1 triplet by coupling of lesser magnitude to the two bridge hydrogens. The fine structure underlying the ^{11}B-^{1}H resonances are due to the ^{10}B-^{1}H coupling. The ^{1}H n.m.r. spectrum of diborane (6) further substantiates the bridge structure. It comprises a quartet which is attributed to the terminal hydrogens attached to ^{11}B atoms and a multiplet at higher field which is due to the bridging hydrogens. The complex fine structures observed in the quartet and the multiplet are due to long-range spin coupling $[^{2}J(H_t\text{-}H_b)]$ and consequent second order effects[112].

(ii) Octahydrotriborate (-1) and derivatives.

Phillips et al[113] published the ^{11}B spectrum of a diethyl ether solution of $Na[B_3H_8]$, interpreting it as a septet, and assigned a possible structure in which each of three equivalent boron atoms is bonded to six bridge hydrogen atoms. Lipscomb interpreted[114] the spectrum as the visible members of a nonet on the basis of peak intensities, and suggested a more plausible bond arrangement with equivalent coupling of all boron atoms to all hydrogen atoms attributed to intramolecular exchange (by pseudorotation). An X-ray crystallo-

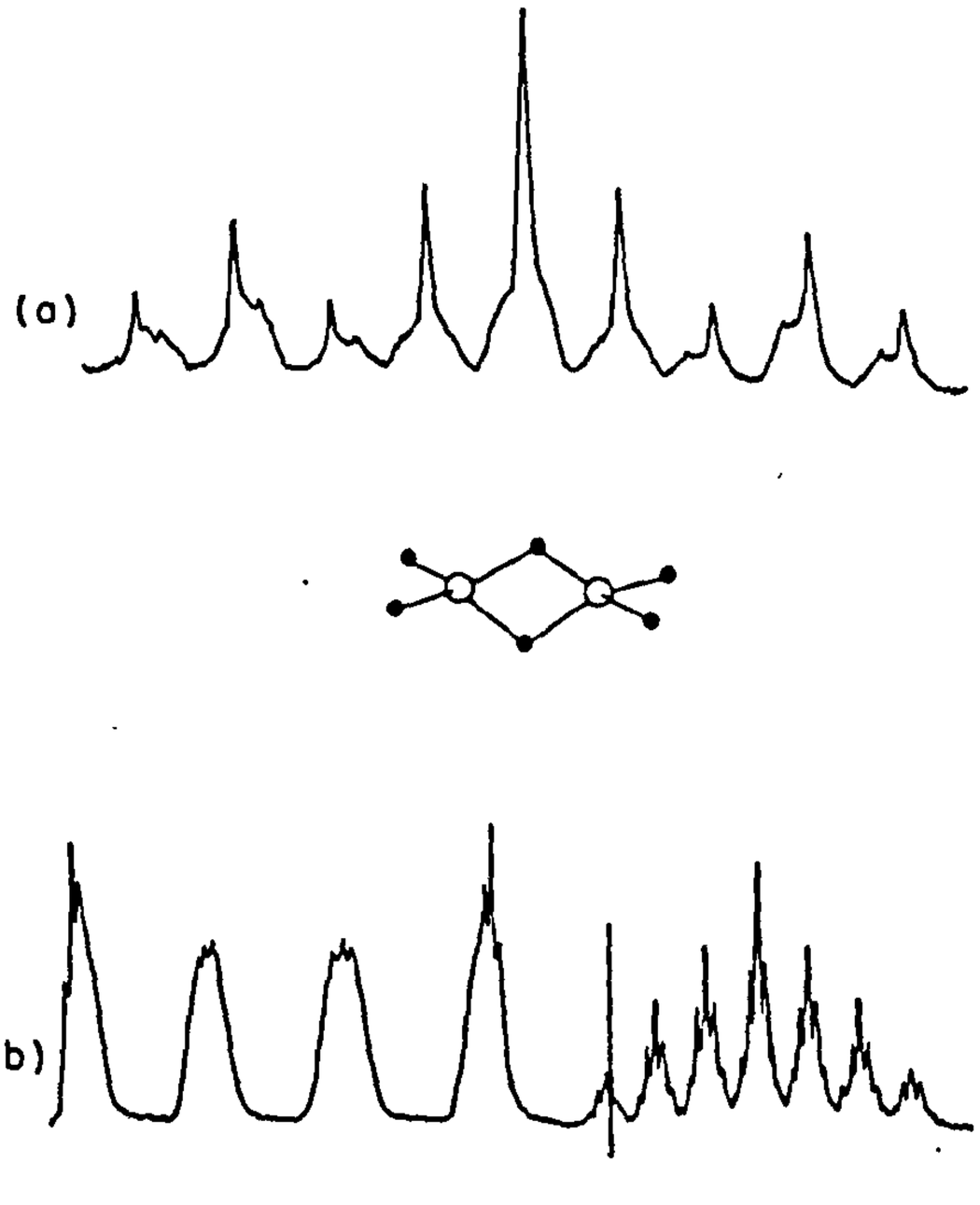

Fig.1.4.1. (a) ^{11}B (19.3 MHz) and ^{1}H (100 MHz) n.m.r. spectra of B_2H_6.

graphic study of $[(H_3N)_2BH_2][B_3H_8]$ revealed the "free" $[B_3H_8]^-$ ion to have the geometry as shown below (I)[115].

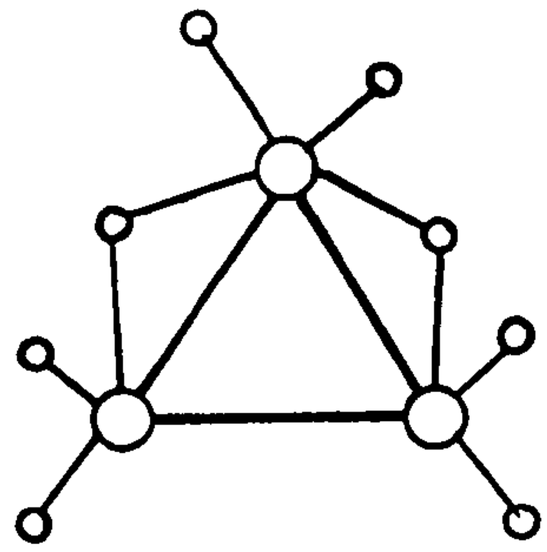

(I)

Several later n.m.r. studies of various $[B_3H_8]^-$ salts revealed changes in the ^1H n.m.r. spectrum at low temperatures consistent with both quadrupole-induced spin decoupling and variable rates of $[B_3H_8]^-$ internal exchange depending on structure. The ^1H n.m.r. spectrum of $Tl[B_3H_8]$ in 50% CD_3OD - 50% CD_3COCD_3 (V/V) at 33°C consisted of a ten-line multiplet (two outer peaks lost in noise) revealing coupling to three-equivalent ^{11}B nuclei ($I = {}^3/_2$; $J_{H-}{}^{11}B = 33$ Hz)[116] with smaller ^{10}B coupling in the background and consistent with rapid scrambling of $[B_3H_8]^-$ hydrogens. Upon lowering the temperature, the spin-spin coupling pattern coalesced and the ^1H n.m.r. spectrum sharpened into a singlet resonance at about -127°C. Essentially identical behaviour is observed for $[N(CH_3)_4][B_3H_8]$[116,117]. The loss of $^{10,11}B$ - ^1H spin-spin coupling in $Tl[B_3H_8]$ and $[N(CH_3)_4][B_3H_8]$ at lower temperatures is completely

consistent with more efficient boron quadrupole relaxation effectively decoupling boron from hydrogen. In addition, the observation of a singlet proton resonance at -137°C is best rationalized on the basis of fast $[B_3H_8]^-$ scrambling or "pseudorotation" (Fig. 1.4.2) at this very low temperature.

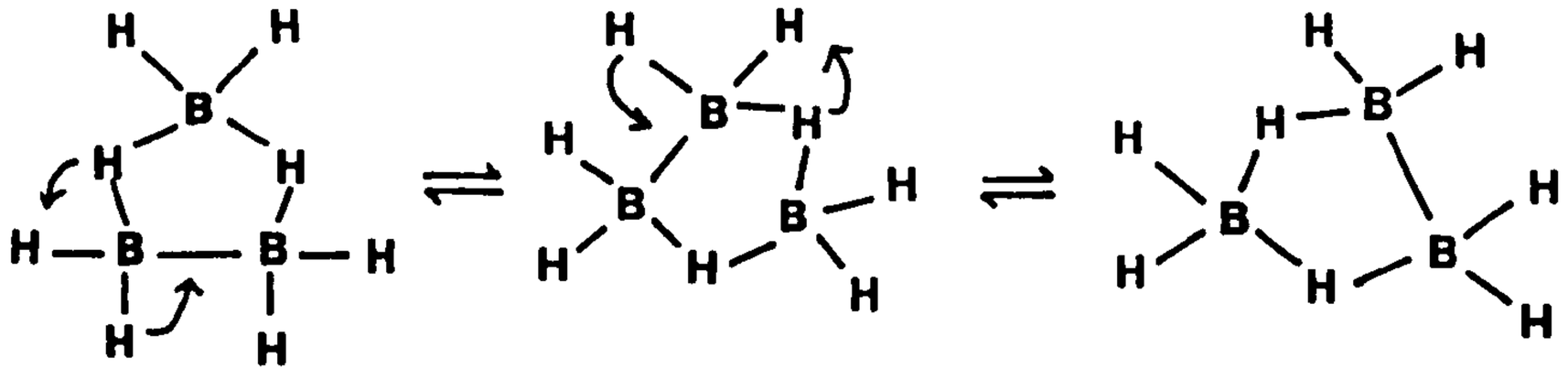

Fig. 1.4.2 Pseudorotation of $[B_3H_8]^-$.

In contrast to $Tl[B_3H_8]$ and $[N(CH_3)_4][B_3H_8]$, the ^1H n.m.r. spectrum of $[(C_6H_5)_3P]_2CuB_3H_8$ [118] [structure[119] as shown in Fig. 1.4.3(a)] in 50% $CDCl_3$ - 50% CD_2Cl_2 at 20°C is a broad singlet with no fine structure. Upon lowering the temperature, the B_3H_8 resonance sharpens to some extent (quadrupole-induced decoupling), then broadens in an asymmetric fashion and separates into several resonances at -90°C (Fig. 1.4.3(b). This behaviour is best rationalized in terms of slowing of the B_3H_8 moiety pseudorotation at low temperatures [Fig. 1.4.3(c)] and a static B_3H_8 system at -97°C.

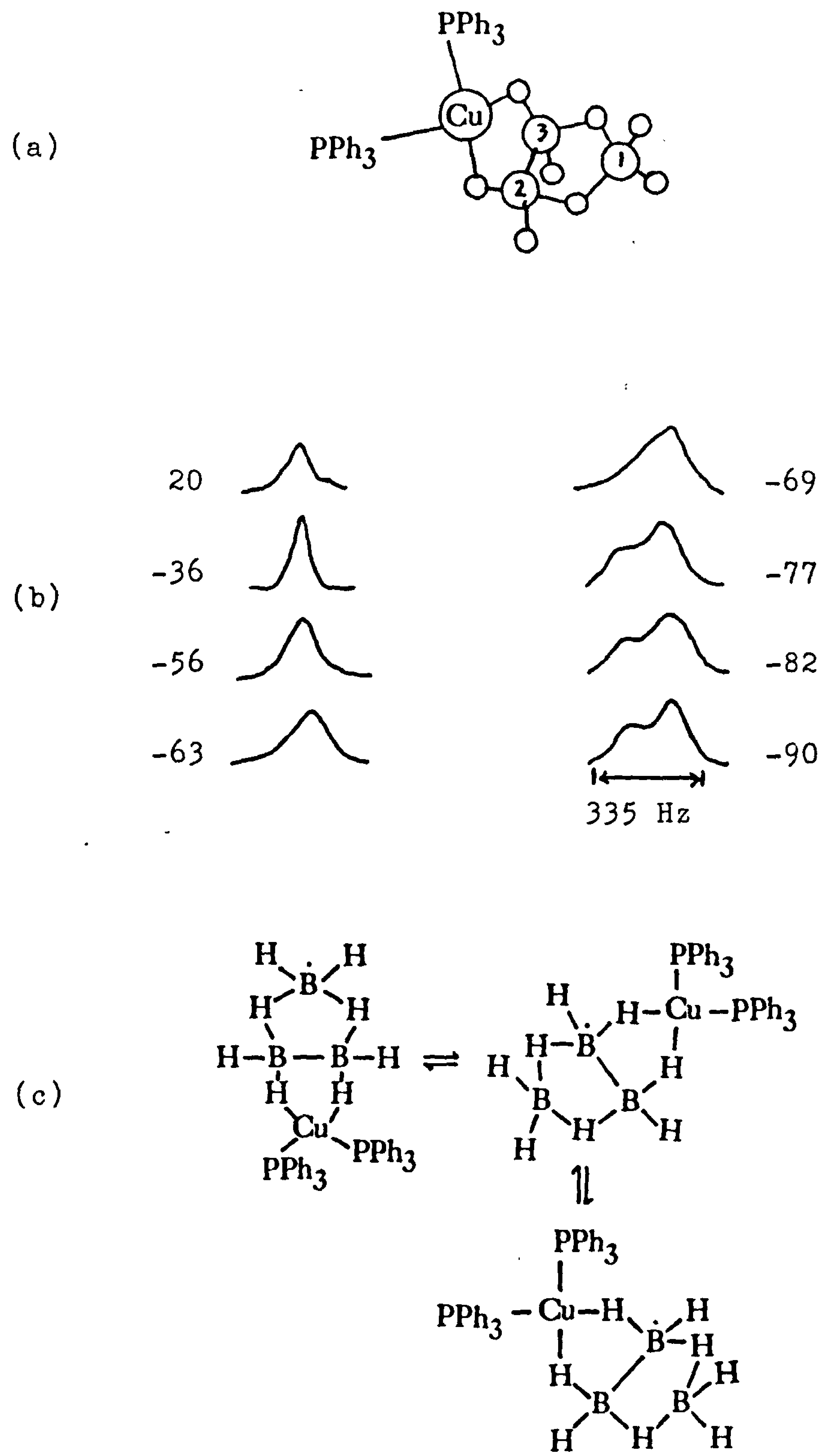

Fig.1.4.3. (a) Structure, (b) ^{1}H n.m.r. spectra, and (c) pseudorotation of $[PPh_3]_2CuB_3H_8$.

The ^{11}B n.m.r. spectra of $[(CO)_4MB_3H_8]^-$ ion[120] structure as shown below (II)[121], M = Cr, Co, W

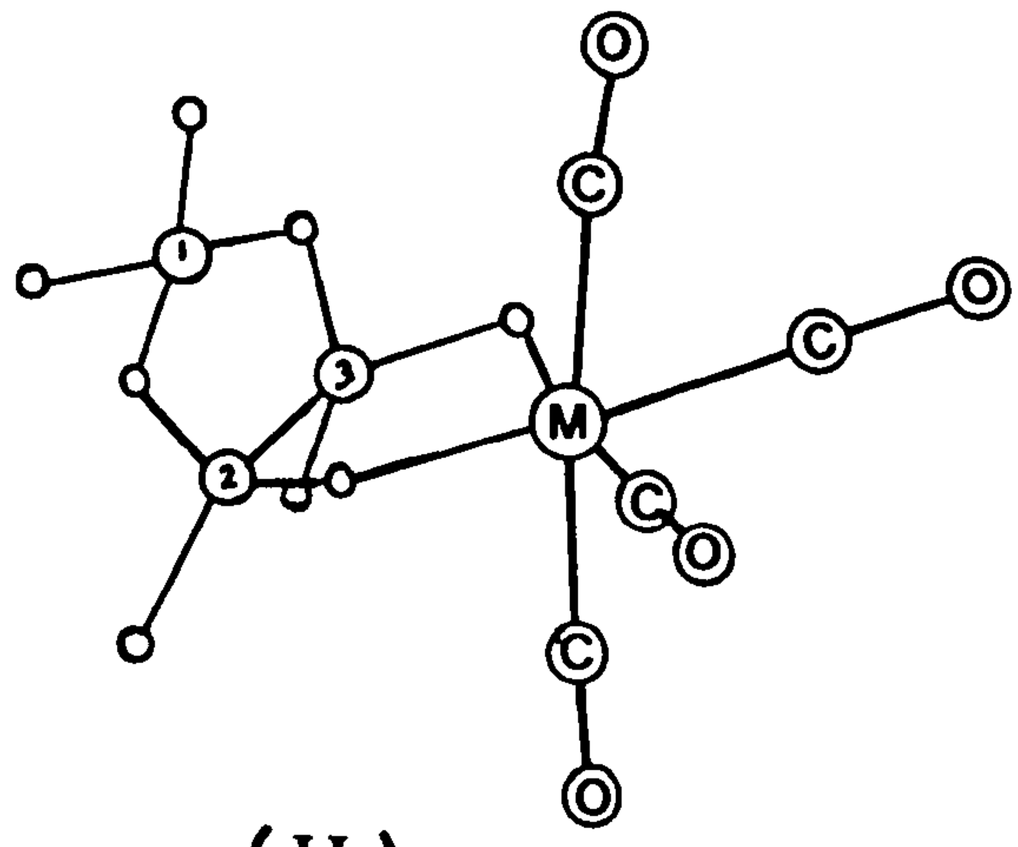

(II)

in CH_3CN at room temperature consist of two broadened signals at 23.0 and 61.3 ppm relative to $[B(OCH_3)_3]$ of relative intensity 1:2. These spectra are clearly consistent with slow B_3H_8 pseudorotation on the n.m.r. time scale at room temperature and represent a more static B_3H_8 system than in the $[(C_6H_5)_3P]_2CuB_3H_8$, Tl $[B_3H_8]$ or $[N(CH_3)_4][B_3H_8]$. However, it is clear that complexation of $[B_3H_8]^-$ by a metal via hydrogen bridge bonds slows the rate of B_3H_8 pseudorotation as compared with free $[B_3H_8]^-$; i.e. the complexed metal acts as a "lock" on the pseudorotatory process.

(iii) Nido-decaborane (14), $B_{10}H_{14}$.

Decaborane (14) and its derivatives have been more extensively studied by n.m.r. than any other boron hydrides. Following the initial study of the 12.3 MHz

^{11}B and 30 MHz ^{1}H spectra by Schoolery[122] there has been a progression of n.m.r. studies interacting with X-ray crystallographic studies and theoretical arguments for interpretation and assignment of the spectra.

Fig. 1.4.4 shows the known molecular structure and atom numbering for $B_{10}H_{14}$[123]. The ^{11}B n.m.r. spectrum of $B_{10}H_{14}$ consists of four sets of doublets of relative area 2:2:4:2 which have been assigned[124,125], (in order of increasing field strength) to B(1,3); B(6,9); B(5,7,8,10) and B(2,4) respectively. It has recently been shown[126] that the ^{11}B n.m.r. spectrum of $B_{10}H_{14}$ exhibits substantial solvent effects as illustrated in Fig. 1.4.5. The most dramatic solvent effects are associated with the B(1,3) and B(6,9) resonances at the lowest field positions. The spectral appearances can be grouped into three categories on the basis of the solvent polarities. The largest chemical shift differences, between the B(1,3) and B(6,9) resonances, occur in the least polar solvents, such as butane and n-pentane. Somewhat more polar solvents, such as benzene and dichloromethane give rise to intermediate shift differences, while in Lewis base solvents such as acetone and acetonitrile the B(1,3) and B(6,9) resonances are coincident.

In low polarity, low molecular weight solvents such as n-butane and n-pentane, the ^{11}B n.m.r. spectra of $B_{10}H_{14}$ display evidence of substantial fine structure in the B(6,9) resonance as shown in Fig. 1.4.6. Upon

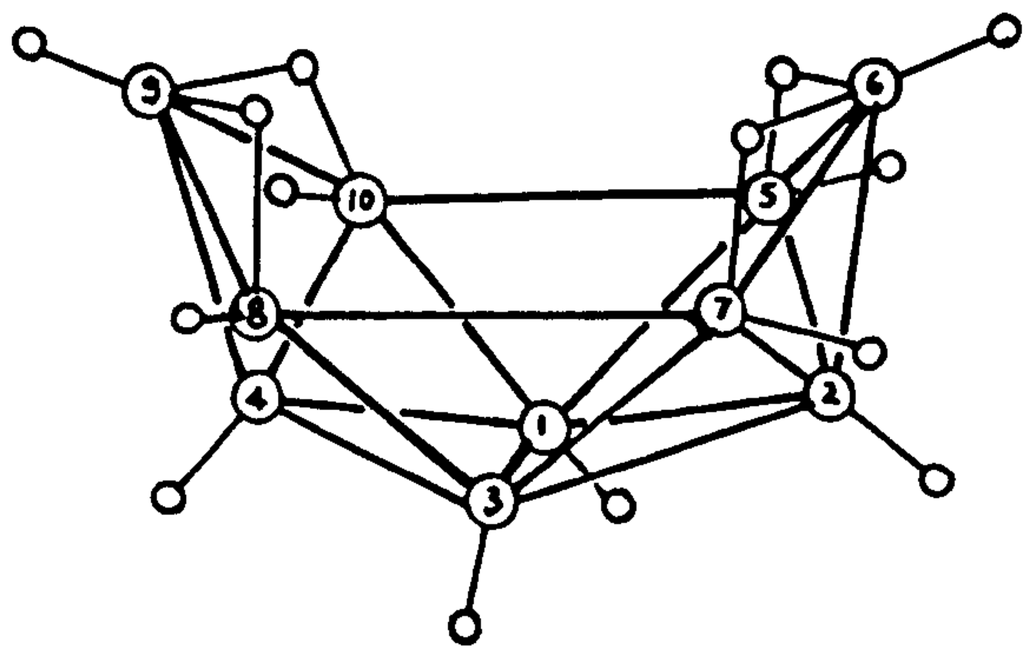

Fig.1.4.4. The structure of $B_{10}H_{14}$.

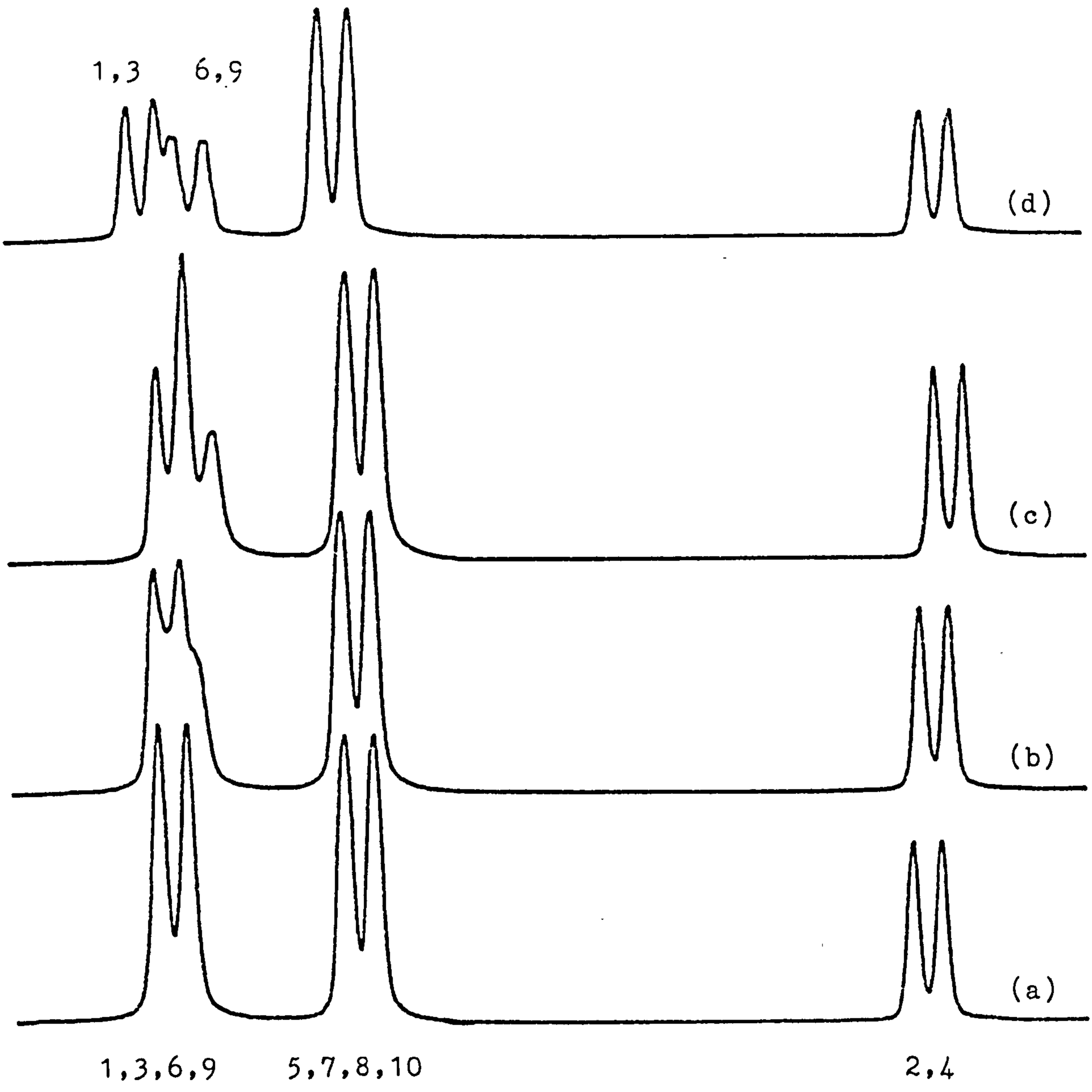

Fig.1.4.5. 86.6 MHz ^{11}B n.m.r. spectra of $B_{10}H_{14}$ in selected solvents (a) CH_3CN, (b) C_4H_8O, (c) C_6H_6, and (d) C_5H_{12}.

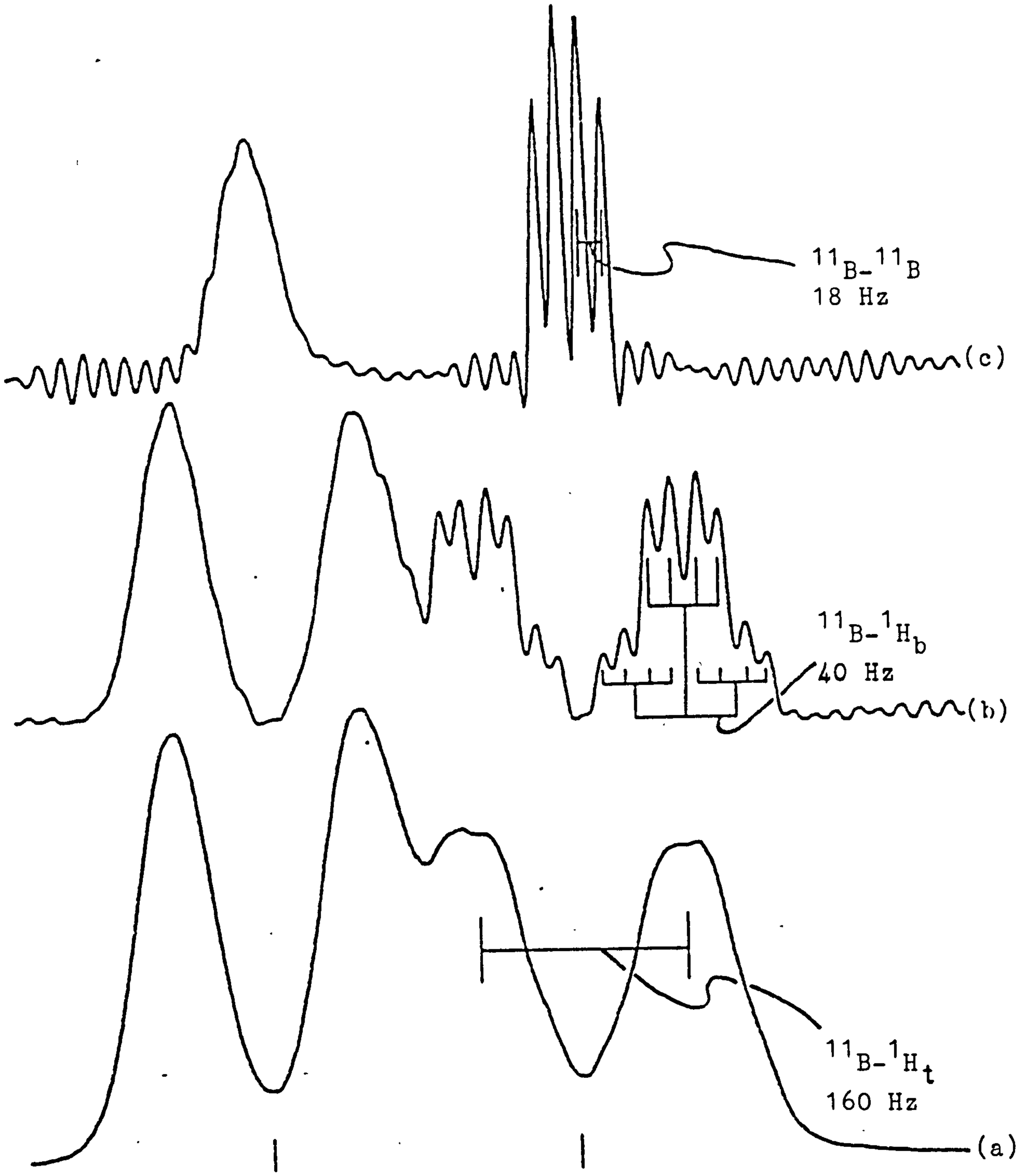

Fig.1.4.6. (a) 86.6 MHz ^{11}B n.m.r. spectra of $B_{10}H_{14}$ in Pentane (b) line-narrowed, and (c) $^{11}B\{^{1}H\}$ line-narrowed.

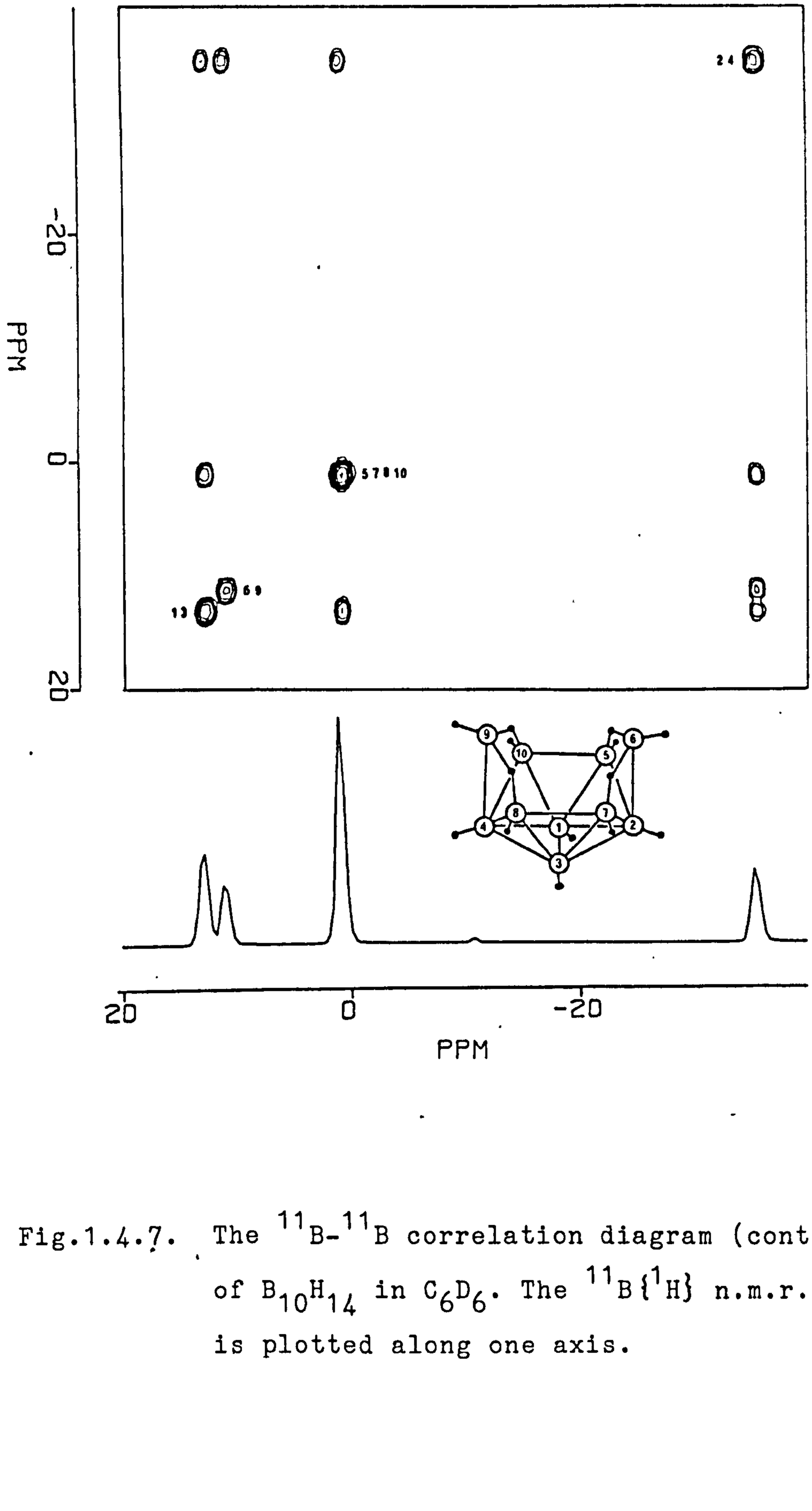

Fig.1.4.7. The ^{11}B-^{11}B correlation diagram (contour map) of $B_{10}H_{14}$ in C_6D_6. The $^{11}B\{^1H\}$ n.m.r. spectrum is plotted along one axis.

line narrowing, each half of the B(6,9) resonance exhibits eight lines of approximate intensities 1:1:3:3:3:3:1:1. In the line-narrowed $^{11}B\{^{1}H\}$ n.m.r. spectrum, the B(6,9) resonance is a 1:1:1:1 quartet with $J_{B(2,4)B(6,9)} = 18 \pm 2$ Hz. The B(6,9) resonance is then a doublet of triplets of quartets with coupling constants of 160 ± 2 (^{11}B-H_t), 40 ± 2 (^{11}B-H_b), 18 ± 2 (^{11}B-^{11}B), respectively.

Recently, the COSY spectrum of $B_{10}H_{14}$ which provides a comprehensive study of $^{11}B/^{11}B$ interactions has also been obtained[127]. The ^{11}B COSY plot for $B_{10}H_{14}$, together with a one dimensional ^{11}B-$\{^{1}H\}$ spectrum, is shown in Fig. 1.4-7. The diagonal from bottom left to top right follows the one dimensional spectrum. Coupled borons give rise to signals which occur off the diagonal at coordinates (X_a, Y_b) and ($X_b Y_a$). It can be seen that B(1,3) is coupled to B(5,7,8,10) and B(2,4); B(5,7,8,10) is coupled to B(2,4) and B(1,3). That the B(6,9) borons coupled to B(2,4) only is in agreement with the evidence from the line-narrowed ^{11}B-$\{^{1}H\}$ spectrum [Fig. 1.4-6(c)] discussed above. In both cases, there is no evidence for coupling between boron atoms linked by hydrogen bridges which has also been reported[128] by Grimes et al.

The ^{1}H n.m.r. spectrum of $B_{10}H_{14}$ was also shown to be substantially solvent dependent[126,129], although the chemical shift effects in ^{1}H spectra are less pronounced than those of the ^{11}B. The positions most

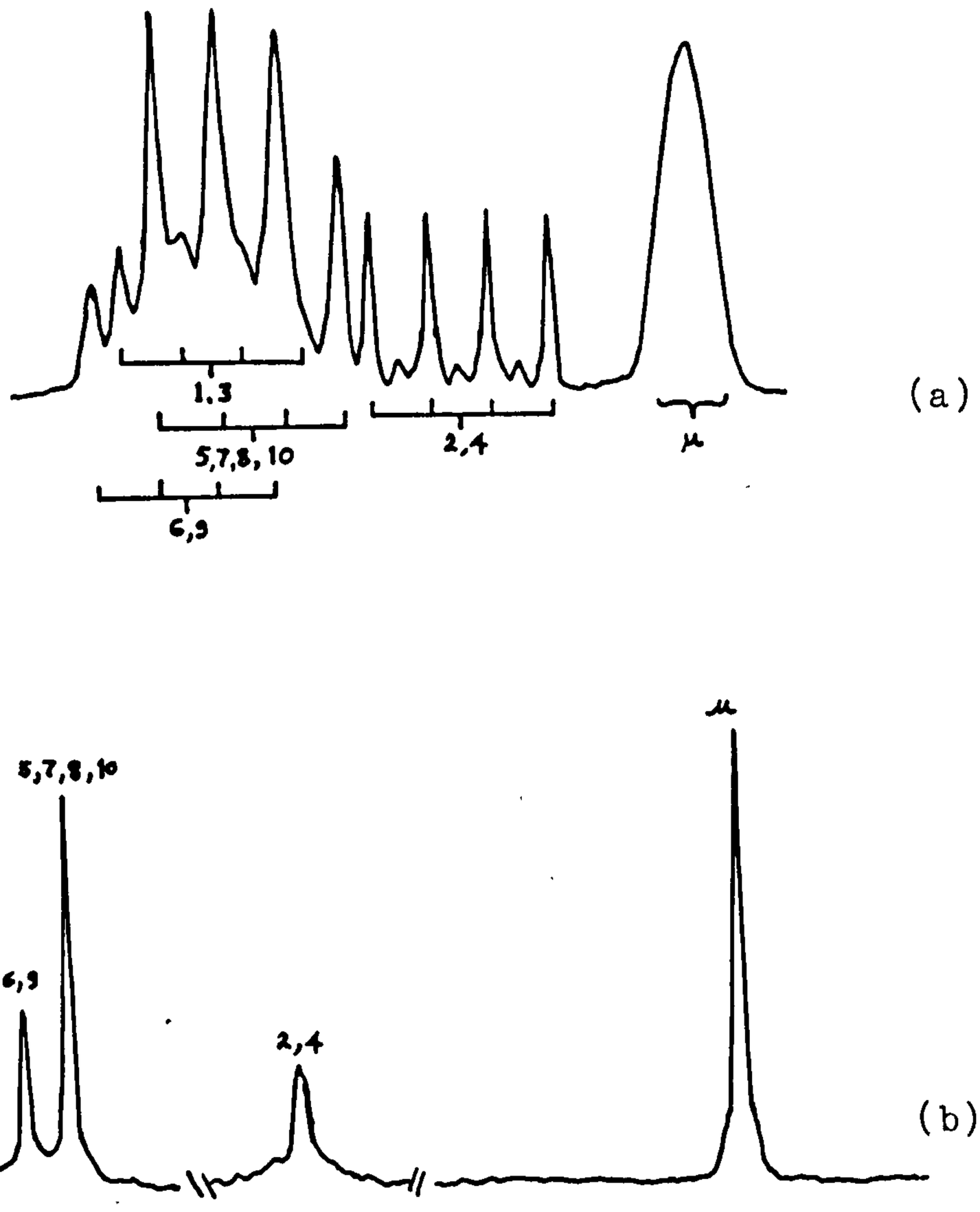

Fig.1.4.8. (a) 220 MHz ^{1}H n.m.r. spectrum of $B_{10}H_{14}$

(b) 250 MHz $^{1}H\{^{11}B\}$ n.m.r. spectrum of $B_{10}H_{14}$ in C_6D_6.

subject to solvent shifts were the bridge hydrogens which may be related to their acidic nature. Only minor changes were observed for all other positions, with exception of the spectra run in benzène, where chemical shifts of the B(6,9) and B(1,3) were noted. The $^{1}H^{129}$ and $^{1}H\{^{11}B\}^{126}$ n.m.r. spectra of $B_{10}H_{14}$ are presented in Fig. 1.4-8. The ^{1}H n.m.r. spectrum of $B_{10}H_{14}$ in CS_2 is composed of four overlapping quartets of intensity 2:2:4:2 and a broad upfield singlet of intensity four[129]. The spectrum has been assigned[129] as labelled in Fig. 1.4-8(a) where the order of chemical shifts in the ^{1}H n.m.r. parallels that of the ^{11}B n.m.r., with the exception of a small inversion of the 1,3 and 6,9 positions, and is in agreement with the order postulated by Williams, et al[130]. The assignments from the $^{1}H\{^{11}B\}$ data[126] agree, with the exception of the 1,3 and 6,9 positions.

(iv) <u>Arachno</u>-$[B_{10}H_{14}]^{2-}$.

The 19.2 MHz ^{11}B n.m.r. spectrum of $Rb_2[B_{10}H_{14}]$ in H_2O assigned by Muetterties[131] remained an uncertainty about the assignment of the B(1,3) and B(2,4). The subsequent study of the ^{11}B n.m.r. spectrum of $Rb_2[2\text{-}B_{10}H_{13}Br]$[132] indicated that the low-field doublet was associated with the B(2,4). The structure of $[B_{10}H_{14}]^{2-}$ has been assumed[133] to be similar to that of $B_{10}H_{12}(CH_3CN)_2$, with which it is isoelectronic in the sense that the ligand CH_3CN is replaced by H^-, rather than to be isostructural to

$B_{10}H_{14}$. In such case, there are two BH_2 groups at B(6) and B(9) [Fig. 1.4-9(a)] . The 80.5 MHz ^{11}B n.m.r. spectrum of $Rb_2[B_{10}H_{14}]$[134] in H_2O shown in Fig. 1.4-9(b) confirmed the existence of BH_2 group. This was further confirmed by the X-ray diffraction study of $[N(CH_3)_4][B_{10}H_{14}]$[135]. The structure is as shown in Fig. 1.4-9(a).

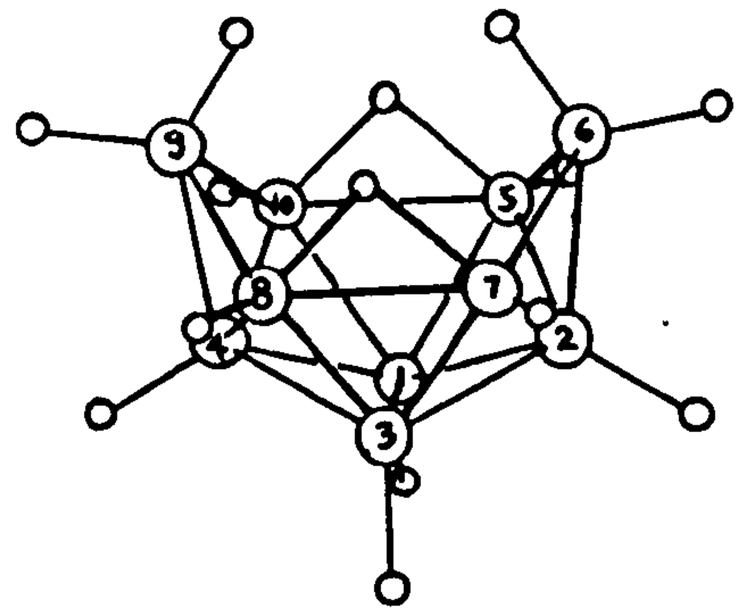

Fig.1.4.9(a) The structure of $[B_{10}H_{14}]^{2-}$ ion.

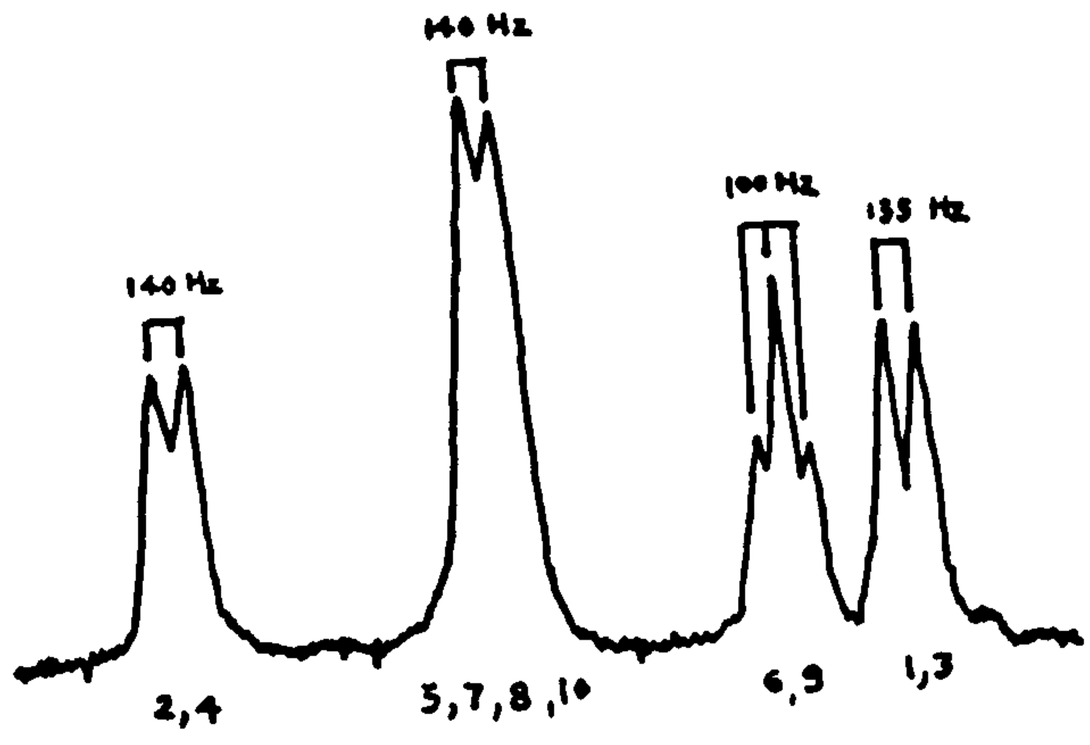

Fig.1.4.9(b) 80.5 MHz ^{11}B n.m.r. spectrum of $[B_{10}H_{14}]^{2-}$ in H_2O.

CHAPTER TWO

PREPARATION AND CHARACTERIZATION OF MONO-SUBSTITUTED AND DI-SUBSTITUTED OCTAHYDROTRIBORATE ANIONS

2.1 INTRODUCTION

Monosubstituted derivatives of octahydrotriborate (-1) ion $[B_3H_7(X)]^-$ (X = halogen, pseudohalogen) have been previously studied[24,27] but only some initial work on their stability and chemical behaviour has been described. A disubstituted derivative of octahydrotriborate (-1) ion, $[B_3H_6(Cl)_2]^-$ was known only as a byproduct in the preparation of monosubstituted species[27] and no systematic study of these derivatives had been reported. In this chapter, the preparation and chemical reactions of some compounds of these two types are further examined.

2.2 RESULTS AND DISCUSSION

2.2.1 Preparation and Reactions

(a) Preparation of monosubstituted triborate ions.

It has previously been shown[27] that the chloride substituent of $[B_3H_7(Cl)]^-$ is very labile and is readily substituted by ions such as NCS^- and $NCBH_3^-$ offering more interesting species. The preparation of a series of derivatives of this type was undertaken in order to investigate the effects of substituents on the chemical and electrochemical properties, and to study the n.m.r. spectroscopy of the triborate ions.

Treatment of $[B_3H_7(Cl)]^-$ with $[NCO]^-$ in dichloromethane yielded the desired product, $[B_3H_7(NCO)]^-$ by the simple substitution reaction, (2.1)

$$[B_3H_7(Cl)]^- + [NCO]^- \xrightarrow{CH_2Cl_2} [B_3H_7(NCO)]^- + [Cl]^- \quad (2.1)$$

In comparison with $[NCS]^-$ and $[NCBH_3]^-$, $[NCO]^-$ was found to be a weaker ligand in that the substitutions reaction took place much more slowly, and in the presence of acetonitrile in a dichloromethane solution of $[B_3H_7(NCO)]^-$, $[NCO]^-$ was replaced by CH_3CN to give $B_3H_7[CH_3CN]$ while $[B_3H_7(NCS)]^-$ and $[B_3H_7(NCBH_3)]^-$ as $[N(PPh_3)_2]^+$ salts in dichloromethane or acetonitrile decomposed slowly (several hours) depositing insoluble materials. However, a solution of $[B_3H_7(NCO)]^-$ in dichloromethane appeared to be stable for several days.

The reaction of $[B_3H_7(Cl)]^-$ with AgCN, which originally had been thought to produce $[B_3H_7(CN)]^-$ [27] has recently been shown, by X-ray diffraction[136], to yield the substituted silver anion $[\{B_3H_7(NC)\}_2Ag]^-$. The reaction is summarized in (2.2)

$$2[B_3H_7(Cl)]^- + 3AgCN \xrightarrow{CH_2Cl_2} [\{B_3H_7(NC)\}_2Ag]^- + [CN]^- + 2AgCl \quad (2.2)$$

The reactions of $[B_3H_7(Cl)]^-$ with $Hg(C \equiv CMe)_2$ or $(Me_2N)_2C = N$ Li did not give the desired products $[B_3H_7(C \equiv CMe)]^-$ or $[B_3H_7\ CN(NMe_2)]^-$, since $[B_3H_7(Cl)]^-$ remained unreacted but $Hg(C \equiv CMe)_2$ and $(Me_2N)_2CNLi$ decomposed.

(b) Deuteration.

It was known[137] that when $NaBH_3CN$ was treated

with CH_3COD-DCl in D_2O, $NaBD_3CN$ was obtained. It was found that when similar deuteration experiments were carried out in D_2O/CH_3CN media and the cations changed from Na^+ to $[NBu^n_4]^+$ or $[N(PPh_3)_2]^+$, deuterations of $[BH_3CN]^-$ were also successful. However, when this reagent mixture was introduced to $[N(PPh_3)_2][B_3H_7(NCBH_3)]$ very little exchange of D for H occurred at the $NCBH_3$ moiety and no exchange at all at the B_3 moiety occurred within 4-5 hr; a long time of reaction (15 hr) led to decomposition of $[B_3H_7(NCBH_3)]^-$.

Further investigation in chemical behaviour of $[B_3H_7(X)]^-$ helped to understand why this did not take place while deuteration of triborane (7) adducts[138] was possible. In later experiments, reactions of $[B_3H_7(NCBH_3)]^-$ with HCl [discussed in sect. 2.2.1(c)] led to chlorination initially at the $NCBH_3$ moiety, and then later at the B_3 moiety when a greater molar ratio of HCl was used, to give $[B_3H_7(NCBH_2Cl)]^-$, $[B_3H_6(Cl)(NCBH_3)]^-$ and $[B_3H_6(Cl)(NCBH_2Cl)]^-$. It should also be noted that Nelson and Kodama[139] prepared $Na[B_3D_8]$, $Na[B_3D_7H]$ and $Na[B_3H_7D]$ via B_3D_7[THF] and NaD.

(c) Chlorination.

$[NBu^n_4][B_3H_8]$ was shown[24] to react with hydrogen halides in the non-coordinating solvent, dichloromethane, to give the monosubstituted anions $[B_3H_7(X)]^-$ (X = Cl, Br, I), and these compounds could also be prepared[27] by treating $[NBu^n_4]^+$ or $[N(PPh_3)_2]^+$ salts of $[B_3H_8]^-$ with mercurous halides (X = F, Cl, Br).

$[B_3H_6(Cl)_2]^-$ was present as a small impurity in the products of the reaction between $[B_3H_8]^-$ and Hg_2Cl_2, but in the $[B_3H_8]^-$ and HCl reactions, an appreciable amount (about 25%) was obtained; furthermore this ion was produced exclusively by the reaction between $[NBu^n_4][B_3H_8]$ and two equivalents of Hg_2Cl_2.

In this work, $[B_3H_6(Cl)_2]^-$ was prepared as its $[N(PPh_3)_2]^+$ salt by treating the corresponding salt of $[B_3H_8]^-$ with HCl, according to reaction (2.3)

$$[B_3H_8]^- + 2HCl \longrightarrow [B_3H_6(Cl)_2]^- + 2H_2 \quad (2.3)$$

$[B_3H_6(Cl)(NCS)]^-$ was similarly obtained from $[B_3H_7(NCS)]^-$ and HCl as in reaction (2.4), and each of these reactions gave

$$[B_3H_7(NCS)]^- + HCl \longrightarrow [B_3H_6(Cl)(NCS)]^- + H_2 \quad (2.4)$$

the desired product cleanly. In contrast, although $[B_3H_7(NCBH_3)]^-$ also reacted with HCl to produce the di-substituted derivative $[B_3H_6(Cl)(NCBH_3)]^-$, the reaction was less clean and other products were also obtained.

A series of reactions of $[B_3H_7(NCBH_3)]^-$ with HCl at different molar ratios yielded these products in proportions which were dependent on the experimental conditions; from comparison of these reaction mixtures with others obtained from substitution reactions involv-

ing $[B_3H_6(Cl)_2]^-$ and $[BH_3CN]^-$ in which similar species were obtained, the products were identified as $[B_3H_7(NCBH_2Cl)]^-$ and traces of $[B_3H_6(Cl)(NCBH_2Cl)]^-$. The products characterized from each reaction are presented in Table 2.1.

When $[B_3H_7(NCO)]^-$ was treated with HCl, the reaction gave a mixture of products, the major component of which was a disubstituted triborate from its ^{11}B n.m.r. spectra. Although it has not been isolated in the pure state, it is likely that a similar chlorination reaction took place to give $[B_3H_6(Cl)(NCO)]^-$.

Attempts to synthesize $[B_3H_6(Cl)(CN)]^-$ from $[\{B_3H_7(NC)\}_2Ag]^-$ and HCl did not lead to the expected product, but instead a more complex reaction took place, the products of which have not yet been fully identified.

When $[B_3H_7(NCS)]^-$ and $[B_3H_7(NCBH_3)]^-$ were treated with Hg_2Cl_2 in several solvents, they failed to yield di-substituted derivatives and remained unreacted, although $[B_3H_7(NCO)]^-$ reacted to give a similar product mixture to that obtained from reactions with HCl.

(d) Substitution reaction.

As mentioned in sect. 2.2.1(a), the chloride substituent of $[B_3H_7(Cl)]^-$ is very labile and is readily substituted by ions such as $[NCS]^-$ and $[NCBH_3]^-$. It was thought that similarly, substitution of the two chlorine atoms in $[B_3H_6(Cl)_2]^-$ for other pseudohalogens would easily take place and thus provides another preparative route for disubstituted derivatives of octahydrotriborate

Table 2.1. Reaction Products from $[B_3H_7(NCBH_3)]^-$ and HCl

$[B_3H_7(NCBH_3)]^-$:HCl	Products (in order of decreasing quantity)
1 : 1	$[B_3H_7(NCBH_3)]^-$
1 : 2	$[B_3H_7(NCBH_3)]^-$ $[B_3H_7(NCBH_2Cl)]^-$
1 : 3	$[B_3H_7(NCBH_3)]^-$ $[B_3H_7(NCBH_2Cl)]^-$ $[B_3H_6(Cl)(NCBH_3)]^-$
1 : 4	$[B_3H_7(NCBH_2Cl)]^-$ $[B_3H_7(NCBH_3)]^-$ $[B_3H_6(Cl)(NCBH_3)]^-$ $[B_3H_6(Cl)(NCBH_2Cl)]^-$
1 : 5	$[B_3H_7(NCBH_2Cl)]^-$ $[B_3H_6(Cl)(NCBH_3)]^-$ $[B_3H_6(Cl)(NCBH_2Cl)]^-$

(-1) ion. However, only one of the chloride substituents in $[B_3H_6(Cl)_2]^-$ was replaced by a pseudohalide substituent and the rate of substitution was slow compared with that of $[B_3H_7(Cl)]^-$. Thus, when $[B_3H_6(Cl)_2]^-$ was treated with AgNCS, the product was $[B_3H_6(Cl)(NCS)]^-$ as shown in reaction (2.5),

$$[B_3H_6(Cl)_2]^- + AgNCS \xrightarrow{CH_2Cl_2} [B_3H_6(Cl)(NCS)]^- + AgCl \qquad (2.5)$$

but the reaction was less satisfactory as a preparative route than that of $[B_3H_7(NCS)]^-$ with HCl.

The reaction of $[B_3H_6(Cl)_2]^-$ with $[N(PPh_3)_2]^+$ $[BH_3CN]^-$ also gave $[B_3H_6(Cl)(NCBH_3)]^-$ but the product was contaminated with $[B_3H_7(NCBH_3)]^-$. As such, it is another example of the dual chemical character of $[BH_3CN]^-$ in which the ion can act either as a donor ligand or as a hydride transfer reagent[140].

The reaction of $[B_3H_6(Cl)_2]^-$ with AgCN also yielded a cyanide-substituted triborane derivative, which had properties similar to $[\{B_3H_7(NC)\}_2Ag]^-$ and it is believed to be the anion $[\{B_3H_6(Cl)(NC)\}_2Ag]^-$, and the proposed reaction is summarized in reaction (2.6)

$$2[B_3H_6(Cl)_2]^- + 3AgCN \xrightarrow{CH_2Cl_2} [\{B_3H_6(Cl)(NC)\}_2Ag]^- + CN^- + 2AgCl \qquad (2.6)$$

Solutions of $[\{B_3H_7(NC)\}_2Ag]^-$ and $[\{B_3H_6(Cl)(NC)\}_2Ag]^-$ decomposed on standing at room temperature, depositing silver.

Attempts to substitute $[B_3H_6(Cl)_2]^-$ with $[N(PPh_3)_2][NCO]$ were unsuccessful although $[B_3H_7(NCO)]^-$ has been prepared from $[B_3H_7(Cl)]^-$.

Attempts were made to substitute the second chlorine by treating $[B_3H_6(Cl)(NCS)]^-$ with AgNCS, however, the only species identified were unreacted starting materials along with some decomposition products.

2.2.2 Characterization

(a) Nuclear magnetic resonance (n.m.r.).

Characterization of the monosubstituted and disubstituted derivatives of octahydrotriborate anions was achieved principally on ^{11}B n.m.r. spectral evidence. It has been well substantiated that the ^{11}B n.m.r. spectra of monosubstituted triborate ions, $[B_3H_7X]^-$ [27,141] ($X = Cl, Br, NCS, NCBH_3$) and triborane (7) adducts, B_3H_7L [142,143,144,141] ($L = THF, OEt_2, NR_3, PR_3$ ($R_3 = H_3, H_2(CH_3), H(CH_3)_2, (CH_3)_3$) consist of a downfield resonance of area two due to the two unsubstituted boron atoms B(2) and B(3), structure I, II, and a resonance at higher field of area one due to the unique substituted boron atom B(1). The n.m.r. spectra are consistent with these expected structures (I and II). Since the seven hydrogens in the molecule were fluxional on the n.m.r. time

scale, I, II represent only two possible structures; others can be derived by placing X or L at other borons. The X-ray crystallographic studies have revealed the solid state structures of some of these compounds which are discussed in 2.2.2(c).

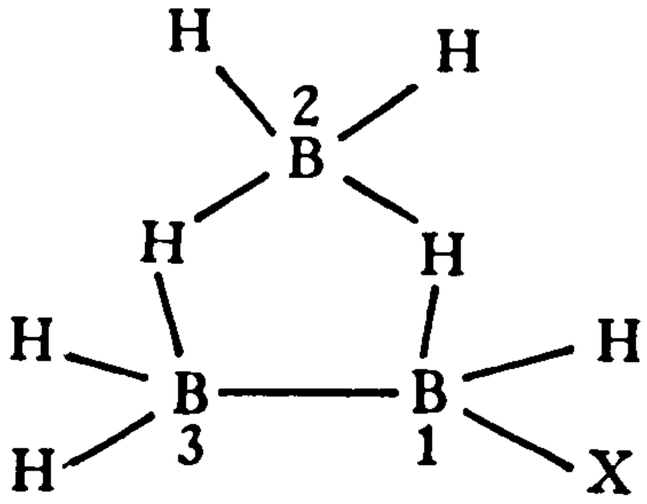

I

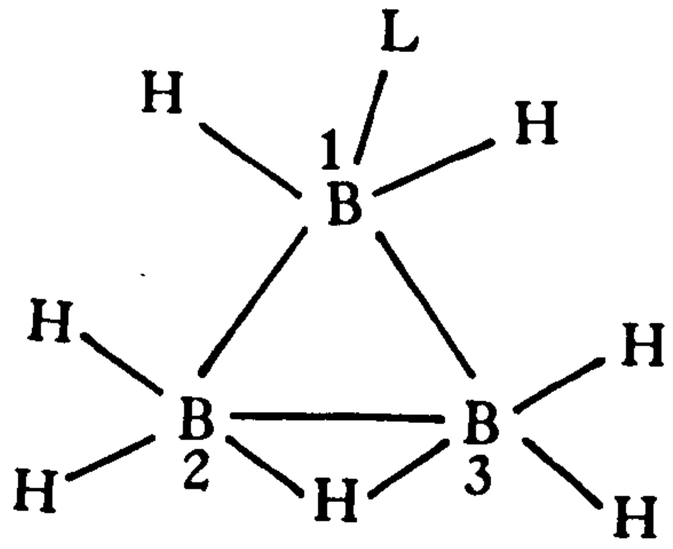

II

The ^{11}B n.m.r. spectrum of $[B_3H_7(NCO)]^-$ shown in Fig. 2.1 was slightly different to those of $[B_3H_7X]^-$ derivatives previously reported. It comprised an apparent multiplet of seven lines, the relative intensities of which suggested that the resonance of B(1) which appeared to be a "sextet" (however the intensities correspond to the six most intense lines of an "octet", i.e. intensities 7 21 35 35 21 7, the two outermost lines being lost in the noise) superimposed on the resonance of B(2) and B(3) which also appeared to be a "sextet" ("Octet" that lost the two outermost lines in the noise), with the chemical shift difference between the two resonances of similar magnitude to the B-H

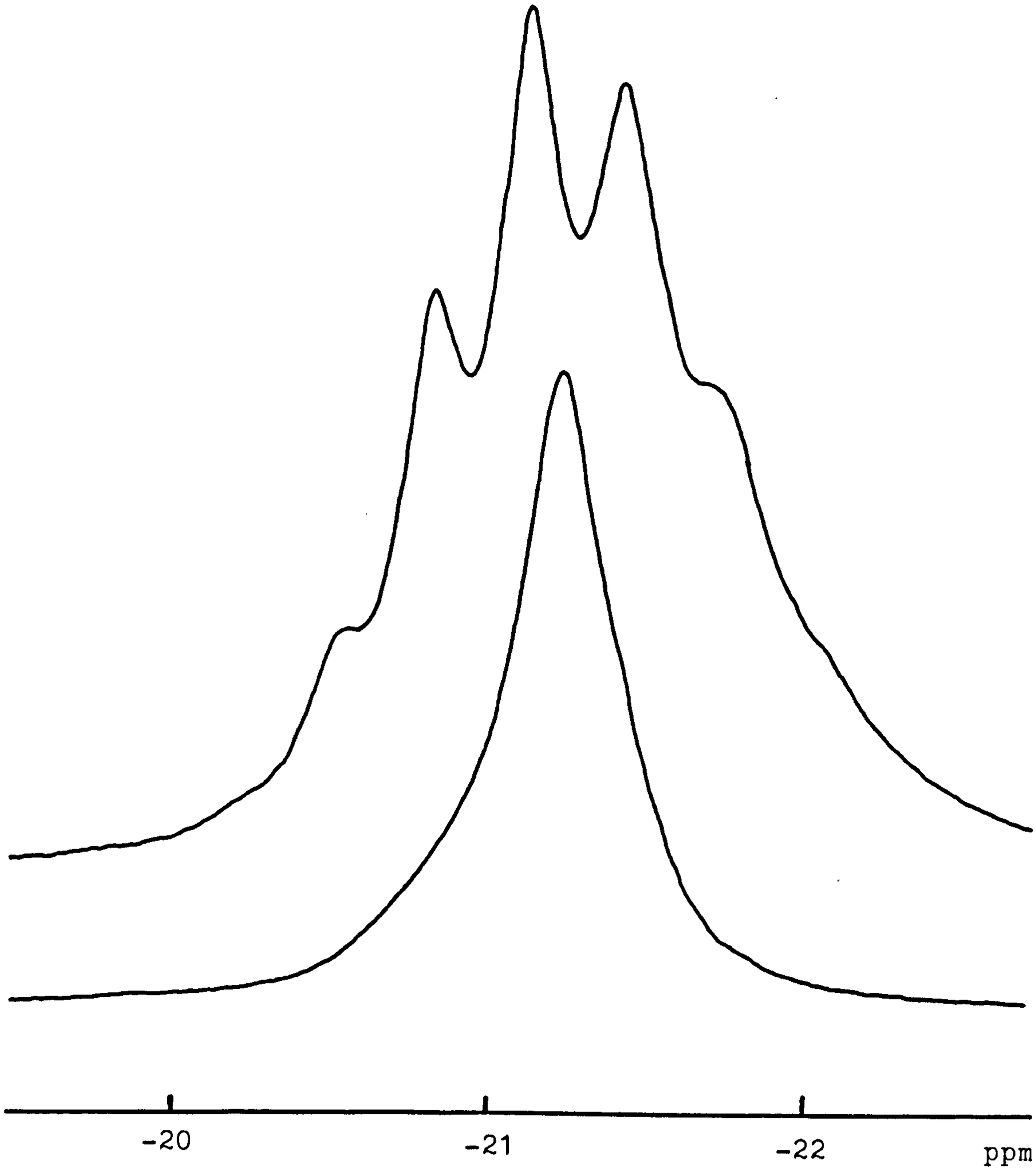

Fig.2.1. 115.5 MHz ^{11}B and $^{11}B\{^{1}H\}$ n.m.r. spectra of $[B_3H_7(NCO)]^-$ in $CDCl_3$

coupling constant. The $^{11}B\{^{1}H\}$ n.m.r. spectrum showed only a single peak. This is discussed again in Chapter 4.

The ^{11}B n.m.r. spectrum of $[B_3H_6(Cl)_2]^-$ shown in Fig. 2.2 consisted of resonance of area one at lower field and resonance of area two at higher field. The high field resonance exhibited a multiplet of seven lines, (intensities 1 7 21 35 35 21 7 1, two outermost lines being just lost in noise) indicating the fluxional behaviour of hydrogens with respect to borons. The ^{11}B n.m.r. evidence suggested two possible structure : (a) with chloride substituents attached to the

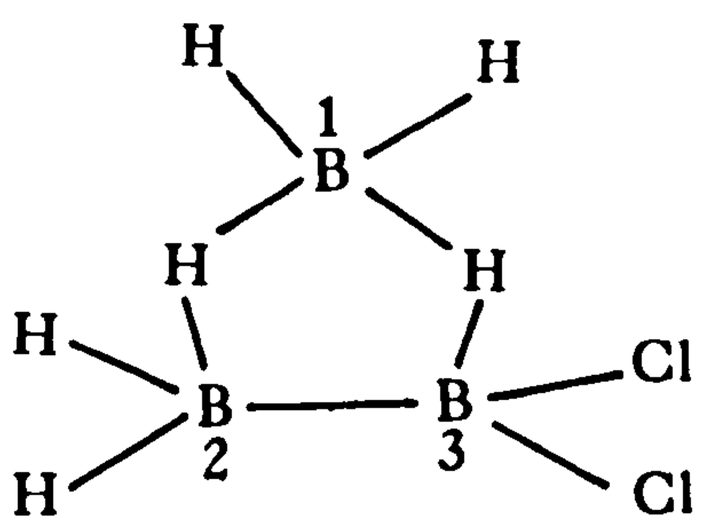

(a)

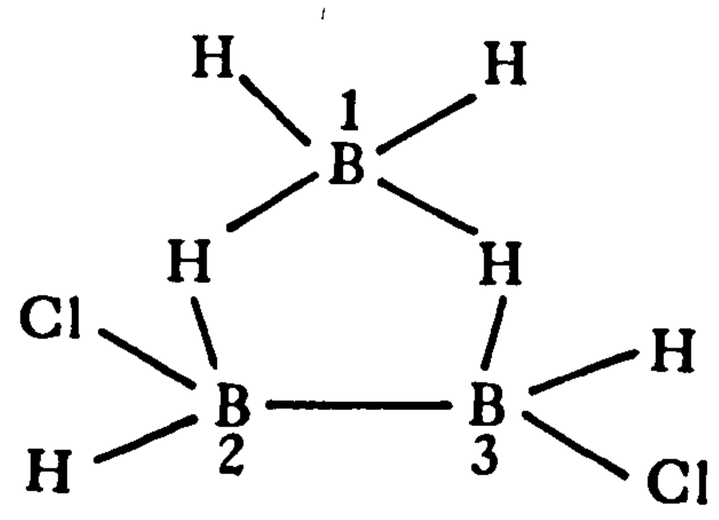

(b)

same boron; thus the low field resonance is B(3) that carried both chlorine atoms, or (b), substitutions occurred at different borons, thus the low field resonance is B(1) that carried both hydrogen atoms.

The ^{11}B n.m.r. spectrum of the reaction product of $[B_3H_7(NCS)]^-$ with HCl (Fig. 2.3) showed three

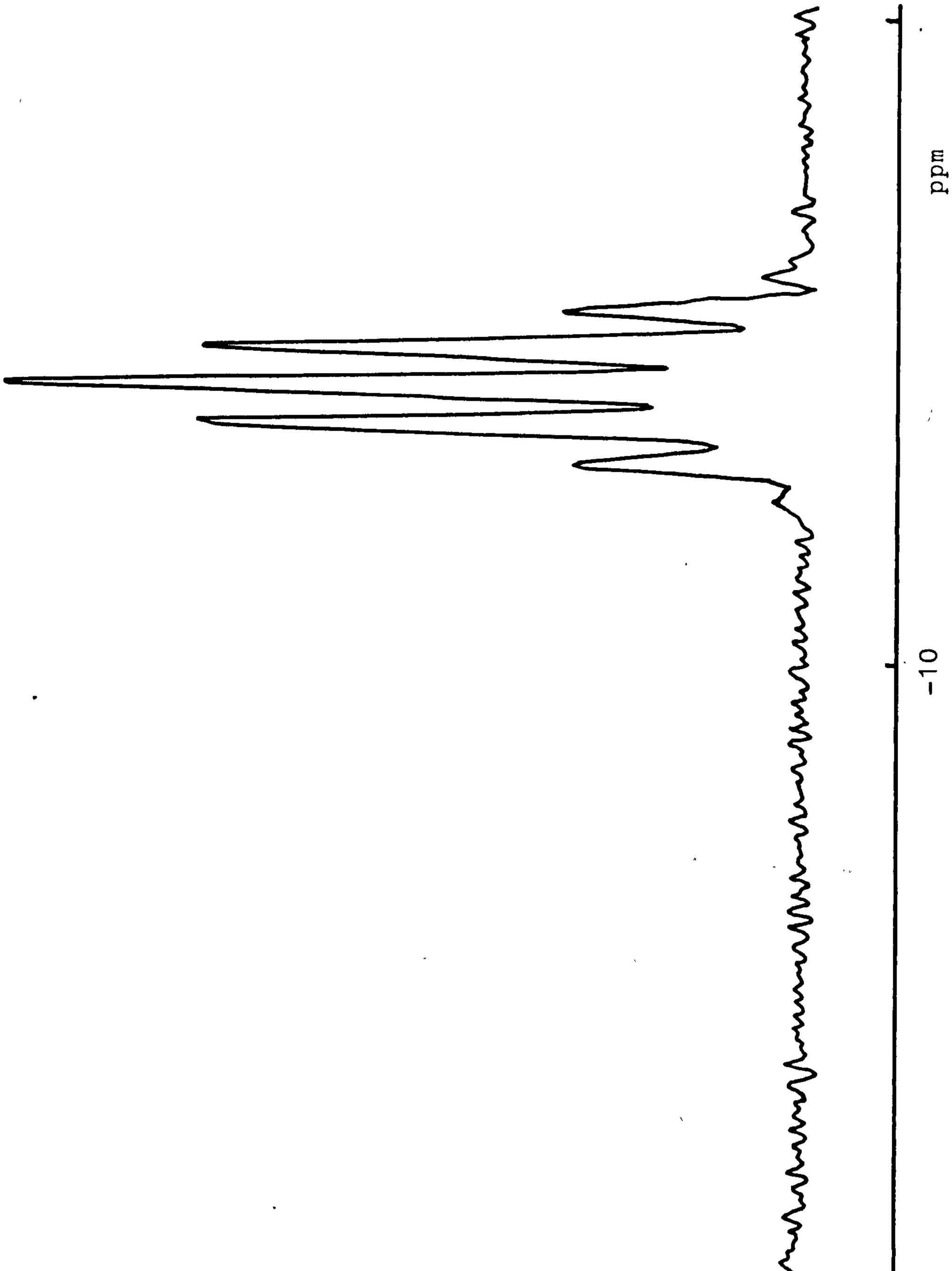

Fig.2.2. 115.5 MHz ^{11}B n.m.r. spectrum of $[B_3H_6(Cl)_2]^-$ in $CDCl_3$ at 303 K
(line-narrowed)

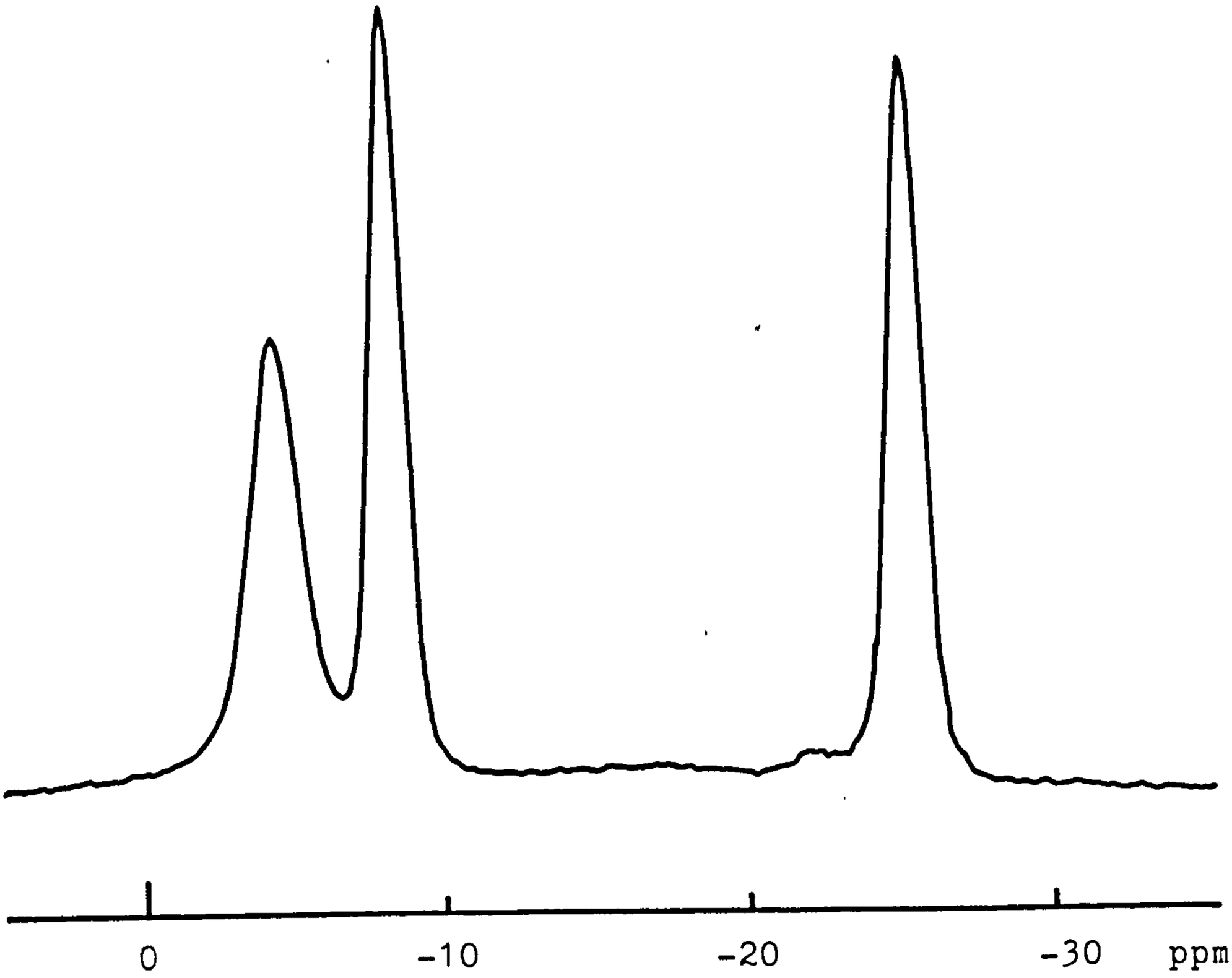

Fig.2.3. 115.5 MHz ^{11}B n.m.r. spectrum of $[B_3H_6(Cl)(NCS)]^-$ in $CDCl_3$.

unique borons with relative area of 1:1:1 which suggested chlorination took place at different borons. Substitution reaction of $[B_3H_6(Cl)_2]^-$ with AgNCS gave the same product, $[B_3H_6(Cl)(NCS)]^-$, (by its ^{11}B n.m.r. spectral evidence).

The ^{11}B n.m.r. spectra of $[B_3H_6(Cl)(NCBH_3)]^-$ and $[\{B_3H_6(Cl)(NC)\}_2Ag]^-$ prepared by substitution reactions of $[B_3H_6(Cl)_2]^-$ with $[N(PPh_3)_2][BH_3CN]$ or AgCN also showed three unique peaks with relative area of 1:1:1 as shown in Fig. 2.4 and Fig. 2.5. Thus it can be deduced that the structures of $[B_3H_6(X)_2]^-$ and $[B_3H_6(X)(X')]^-$ (X = Cl, X' = NCS, $NCBH_3$ $CN^{(a)}$) are as structure (b).

The ^{11}B n.m.r. spectra of reaction products of $[B_3H_7(NCBH_3)]^-$ with HCl at different molar ratio of HCl (from 1:1 to 1:5) showed that as the ratio of HCl was increased, the recovered $[B_3H_7(NCBH_3)]^-$ was decreased while the yields of the products $[B_3H_7(NCBH_2Cl)]^-$, $[B_3H_6(Cl)(NCBH_3)]^-$ and $[B_3H_6(Cl)(NCBH_2Cl)]^-$ built up. The n.m.r. spectra of these products at ratios 1:3 and 1:5 are shown in Fig. 2.6 and Fig. 2.7.

The assignments of the ^{11}B chemical shift to specific boron atoms in Table 2.2 and Table 2.3 are based on a comparison of the downfield shifts caused by the substituents in the monosubstituted derivatives with those in the unambiguous disubstituted derivatives. Additional support for the assignments came from the

---

Footnote (a) in the complex $[\{B_3H_6(Cl)(NC)\}_2Ag]^-$

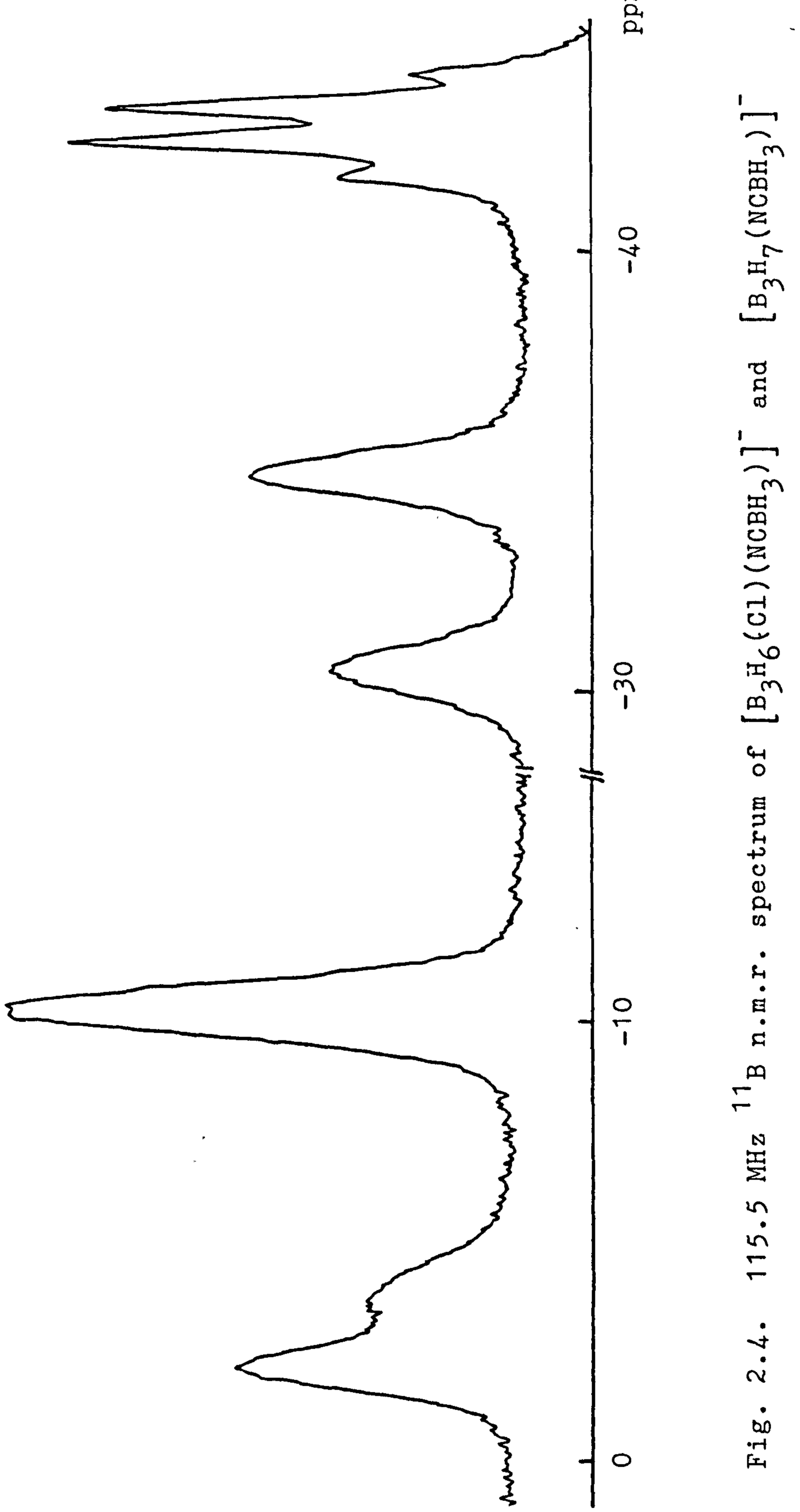

Fig. 2.4. 115.5 MHz ^{11}B n.m.r. spectrum of $[B_3H_6(Cl)(NCBH_3)]^-$ and $[B_3H_7(NCBH_3)]^-$ in $CDCl_3$

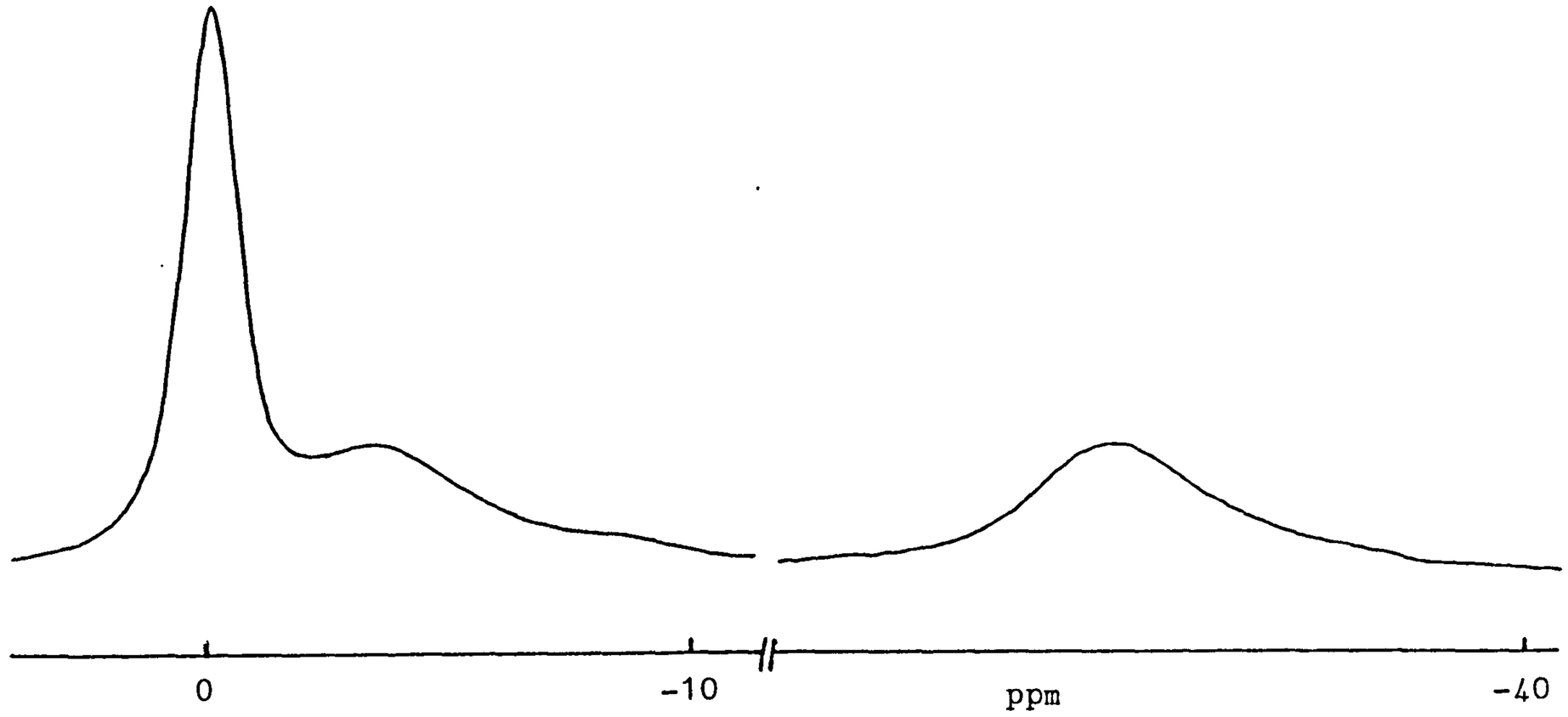

Fig 2.5. 115.5 MHz ^{11}B n.m.r. spectrum of $[\{B_3H_6(Cl)(NC)\}_2Ag]^-$ in $CDCl_3$

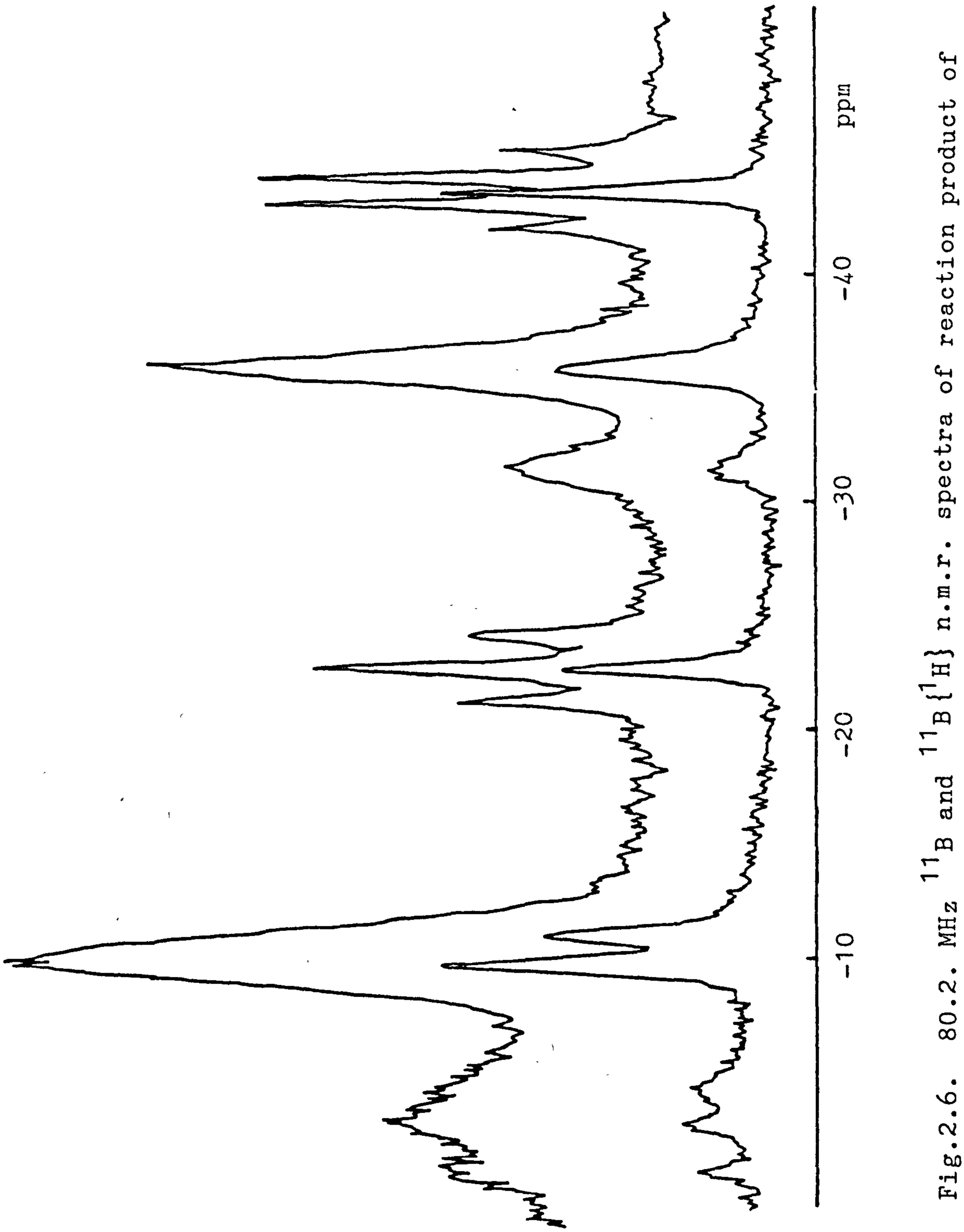

Fig.2.6. 80.2. MHz ^{11}B and $^{11}B\{^1H\}$ n.m.r. spectra of reaction product of $[B_3H_7(NCBH_3)]^-$ with HCl at 1:3 ratio.

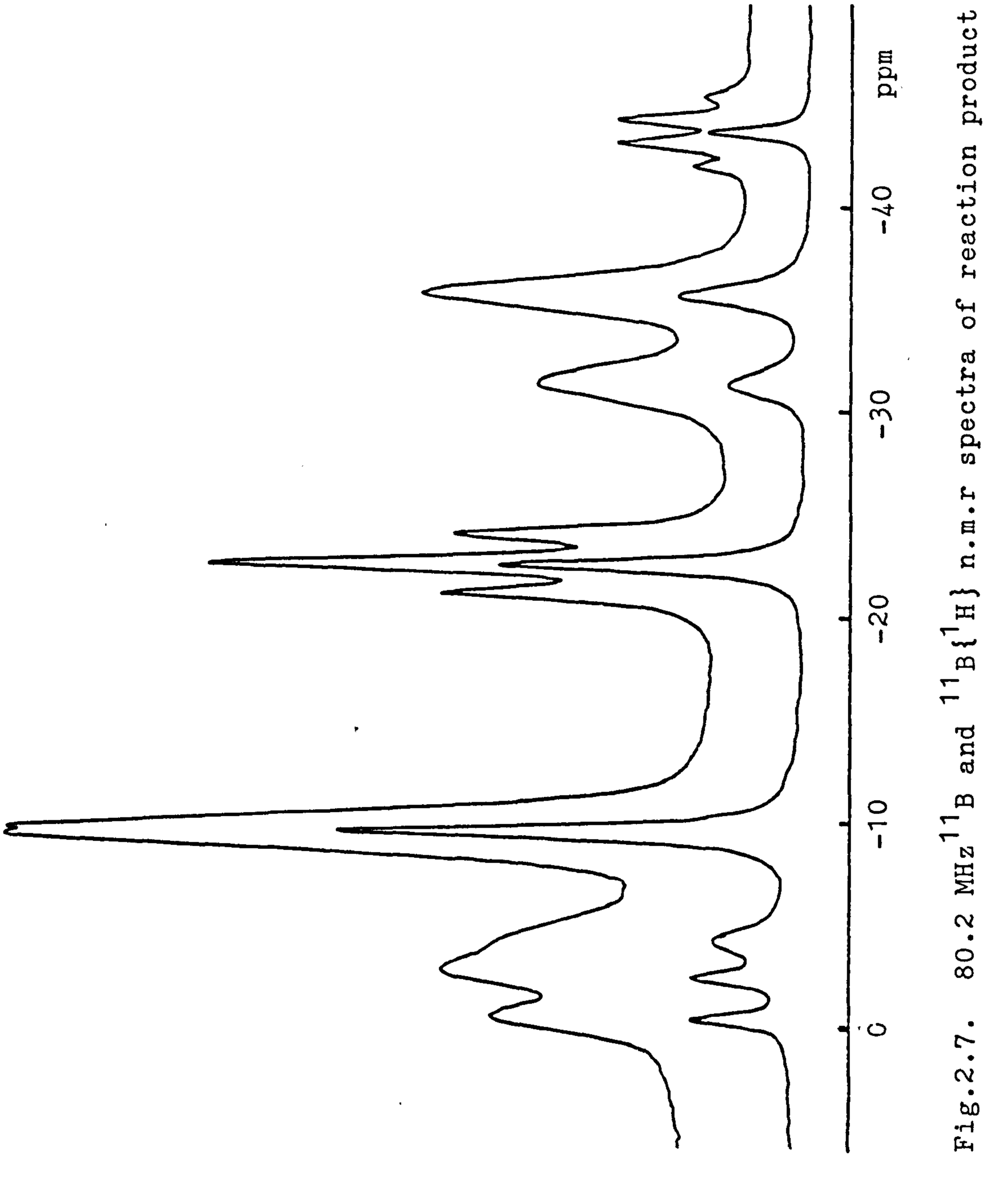

Fig.2.7. 80.2 MHz ^{11}B and $^{11}B\{^1H\}$ n.m.r spectra of reaction product of $[B_3H_7(NCBH_3)]^-$ with HCl at 1:5 ratio.

Table 2.2. ^{11}B n.m.r. Data for Substituted Anions $[B_3H_6(X)(X')]^-$ at 115.5 MHz $CDCl_3$

Substituents			Boron Chemical Shift (ppm)				
	X	X'	B	B(X)	B(X')	Other	Weighted average shift
(a)	Cl	Cl	-4.3		-11.9(S)		-9.4
(b)	Cl	Cl	-4.8		-11.8(S)		-9.5
(c)	Cl	CN	-0.09	-3.41	-31.45		-11.65
	Cl	NCS	-8.3	-4.2	-25.1		-12.5
	Cl	NCO	-8.0	-6.9	-13.1		-9.3
	Cl	$NCBH_3$	-2.09	-3.64	-30.5	-42.9(q)	-12.1
	H	$NCBH_3$	-10.35		-34.94	-42.9(q)	

Footnotes:
(a) 303K; (b) 323K; (q) quartet: (s) septet

(c) In the complex $[\{B_3H_6(Cl)(NC)\}_2Ag]^-$

Table 2.3 ^{11}B n.m.r. Data for Substituted Anions

$[B_3H_6(X)(X')]^-$ at 80 MHz in $CDCl_3$

Substituents		Boron Chemical Shift (ppm)				
X	X'	B	(BX)	B(X')	Other	Weighted average shift
Cl	NCS	-8.85	-5.14	-25.9		-13.3
Cl	NCO	-8.8	-7.4	-14.0		-10.1
Cl	$NCBH_3$	-2.54	-4.27	-31.34	-43.6(q)	-12.7
Cl	$NCBH_2Cl$	-0.53		-31.34	-22.54(t)	-10.8
H	$NCBH_3$	-10.86		-35.48	-43.69(q)	
H	$NCBH_2Cl$	-9.60		-35.66	-22.54(t)	

Table 2.4 ^{11}B Chemical Shift Data for Ions $[B_3H_7(X)]^-$ at 80 MHz in $CDCl_3$.

Substituents X		Chemical Shift B_2	B(X)	Other	Weighted average
H		-29.8			-29.8
	NCO	-21.3	-21.0		-21.2
	NCS	-14.6	-33.9		-21.0
(b)	NCSe	-10.0	-33.1		-17.7
	$NCBH_3$	-10.8	-35.5	-43.7(q)	-19.3
	$NCBH_2Cl$	-9.6	-35.6	-22.5(t)	-18.3
(b)	$NCBPh_3$	-9.2	-34.7		-17.7
(a)	CN	-10.2	-36.8		-19.1
	Cl	-16.9	-21.8		-18.5
	Br	-12.2	-28.4		-17.8
	F	-17.6	-15.4		-16.9

Footnote: (a) in the complex $[\{B_3H_7(NC)\}_2Ag]^-$

(b) data from D.G. Meina

observation that the weighted average chemical shift of the boron atoms in the B_3 unit is shifted downfield from -29.8 ppm in unsubstituted $[B_3H_8]^-$ to values in the range -17 to -21 ppm in monosubstituted compounds $[B_3H_7(X)]^-$, Table 2.4, and to values in the range -9 to -14 ppm for the disubstituted derivatives $[B_3H_7(X)(X')]^-$.

(b) Infrared spectra.

The relevant i.r. absorption frequencies of substituted octahydrotriborate ions are listed in Table 2.5. The B-H stretching modes shifted to higher and higher frequencies in going from the unsubstituted $[B_3H_8]^-$ to mono- and disubstituted derivatives. The frequencies of the B-H stretching modes increased in the order (a) $[B_3H_8]^- < [B_3H_7(Cl)]^- < [B_3H_6(Cl)_2]^-$ which is in agreement with the results previously reported[2]; (b) $[B_3H_7(NCS)]^- < [B_3H_6(Cl)(NCS)]^-$; (c) $[\{B_3H_7(NC)\}_2Ag]^- < [\{B_3H_6(Cl)(NC)\}_2Ag]^-$.

Comparisons of the i.r. spectra of $[B_3H_7(Cl)]^-$ with $[B_3H_6(Cl)_2]^-$ and $[B_3H_7(NCS)]^-$ with $[B_3H_6(Cl)(NCS)]^-$ are presented in Fig. 2.8. Also shown are the i.r. spectra of $[B_3H_7(NCO)]^-$ and $[\{B_3H_7(NC)\}_2Ag]^-$.

The i.r. spectra of $[B_3H_7(NCS)]^-$ and $[B_3H_6(Cl)(NCS)]^-$ [Fig. 2.8(c), (d)] showed, along with B-H stretching modes, strong bands at 2150 and 2155 cm^{-1} respectively which had been assigned to the NCS asymmetric stretch of nitrogen coordinated isothiocyanates as shown by X-ray studies[145,146,28].

Table 2.5. Infrared Absorptions of Octahydrotriborate Derivatives

Compounds		2600-1900 cm^{-1}
	$[B_3H_8]^-$	2435(s), 2380(s), 2105(m), 2060(m)
	$[B_3H_7(Cl)]^-$	2470(S), 2415(S), 2350(sh)
	$[B_3H_6(Cl)_2]^-$	2500(s), 2440(s), 2395(sh)
	$[B_3H_7(NCS)]^-$	2480(s), 2420(s), 2320(sh, 2150(s)
	$[B_3H_6(Cl)(NCS)]^-$	2510(s), 2440(s), 2415(sh), 2155(s), 2105(sh)
	$[B_3H_7(NCBH_3)]^-$	2500(s), 2430(s), 2340(s), 2250(s)
(A)	$[B_3H_6(Cl)(NCBH_3)]^-$	2500(s), 2430(s), 2400(s), 2340(sh), 2270(m), 2245(m)
	$[B_3H_7(NCO)]^-$	2480(s), 2490(s),. 2300(s)
	$[\{B_3H_7(NC)\}_2Ag]^-$	2480(s), 2445(sh), 2420(s), 2400(sh), 2350(sh), 2200(s)
(B)	$[\{B_3H_6(Cl)(NC)\}_2Ag]^-$	2510(b), 2450(b), 2340(b), 2290(b), 2180(s)

Footnotes: (s) strong; (m) medium; (sh) shoulder; (b) broad

(A) products of $[B_3H_7(NCBH_3)]^-$/HCl (1:5)

(B) crude products of $[B_3H_6(Cl)_2]^-$/AgCN reaction.

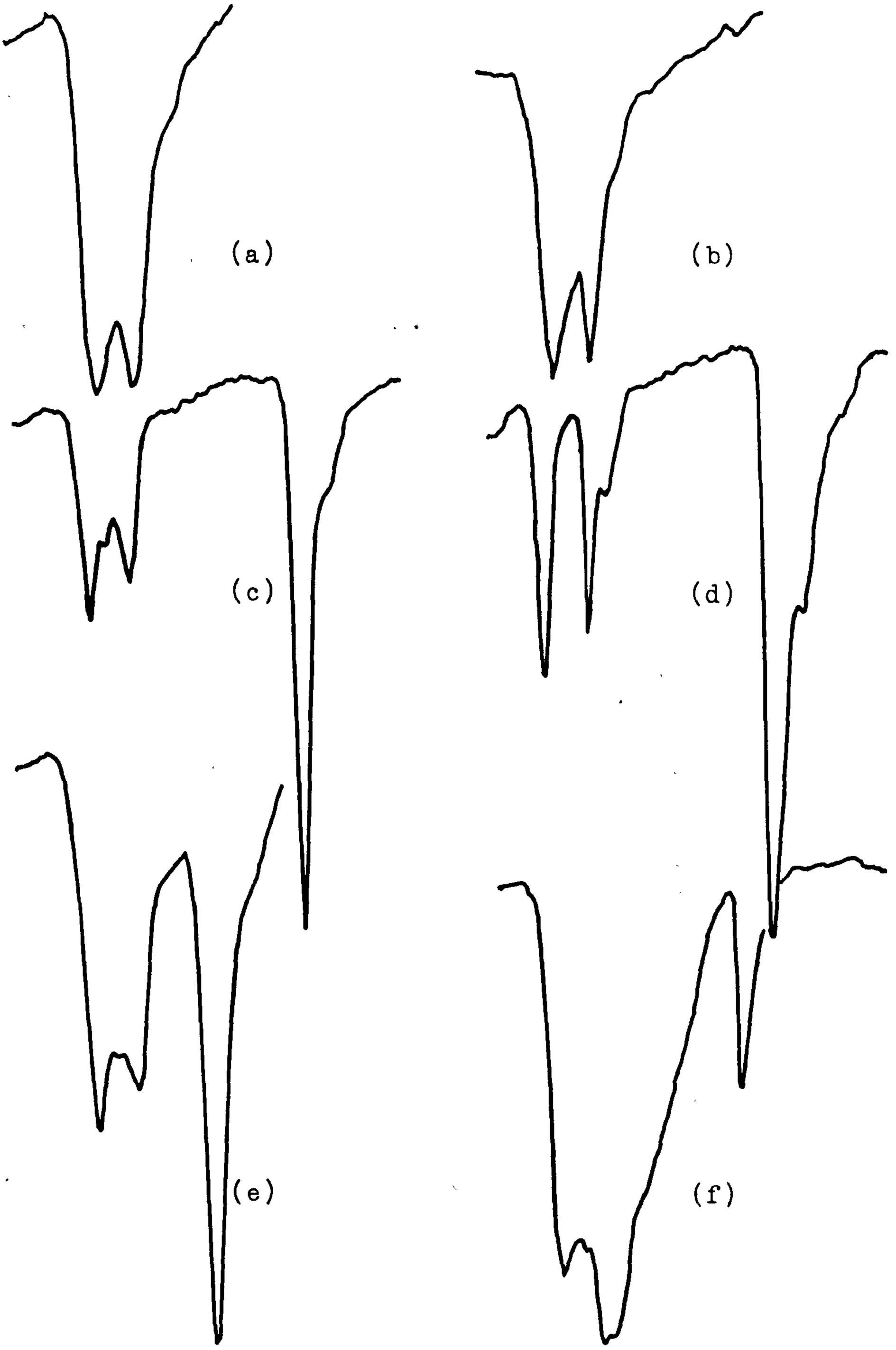

Fig.2.8. Infrared spectra of (a) $[B_3H_7(Cl)]^-$, (b) $[B_3H_6(Cl)_2]^-$, (c) $[B_3H_7(NCS)]^-$, (d) $[B_3H_6(Cl)(NCS)]^-$, (e) $[B_3H_7(NCO)]^-$ and (f) $[\{B_3H_7(NC)\}_2Ag]^-$.

The i.r. spectrum of $[B_3H_7(NCO)]^-$ [Fig. 2.8(e)] showed, along with B-H stretching mode, a strong band at 2300 cm^{-1} assigned to the asymmetric stretch of NCO (isocyanate).

The i.r. spectra of $[\{B_3H_7(NC)\}_2Ag]^-$ [Fig. 2.8(f)] and $[\{B_3H_6(Cl)(NC)\}_2Ag]^-$ showed, along with B-H stretching modes, strong bands at 2200 and 2180 cm^{-1} respectively assigned to be the asymmetric stretch of isocyanide.

(c) X-ray crystallography.

X-ray crystallographic studies of triborane (7) adducts and triborate ions have revealed interesting structural variations which are shown below:

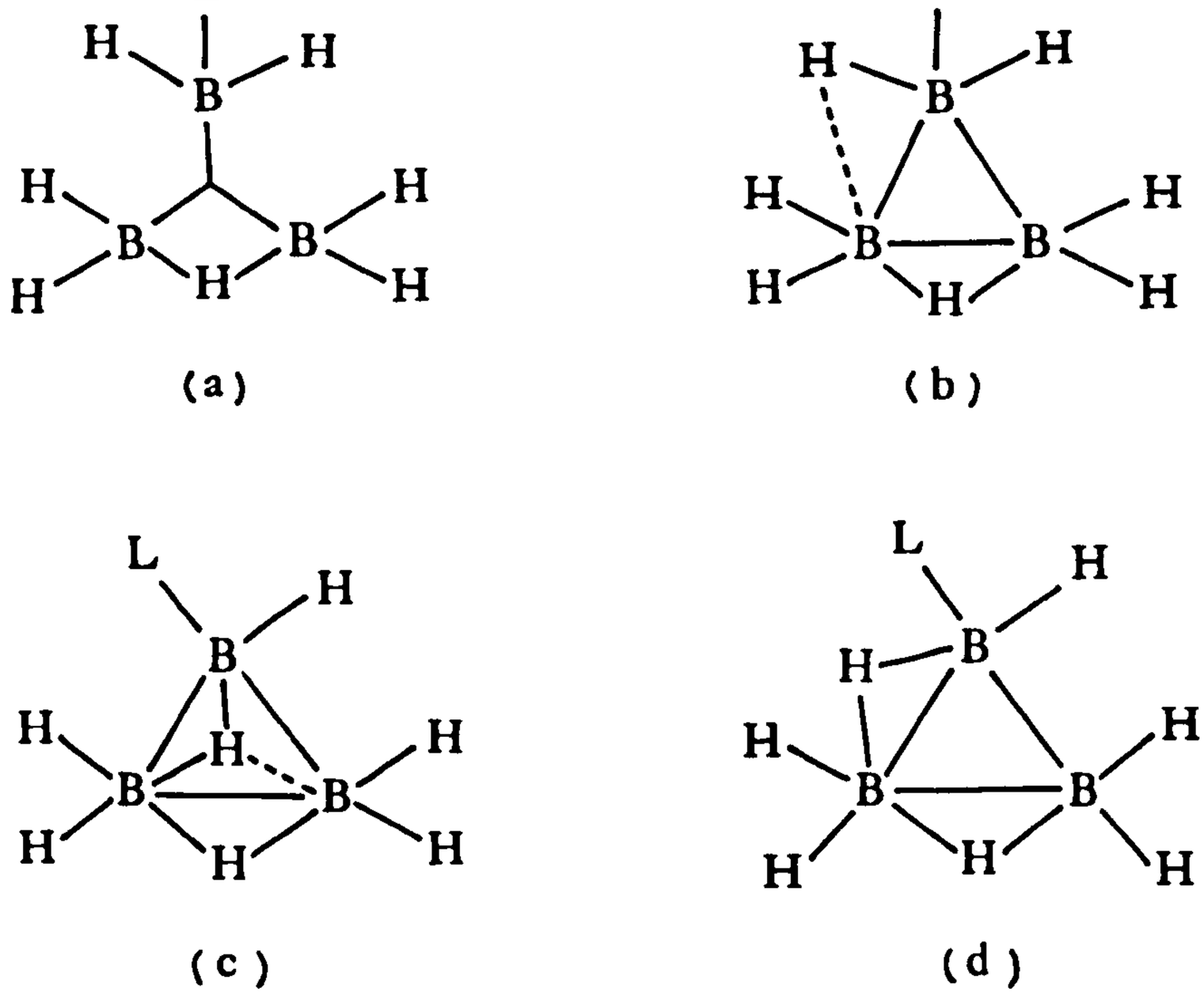

In B_3H_7CO[147] and the low temperature forms of $B_3H_7PR_3$[11] ($R_3 = H_3$, MeH_2 Me_2H), structure (a) is found,

whereas in $[B_3H_8]^-$ [115] structure (d) is known. Recently, structure (c) was found at room temperature in $[B_3H_7(NCS)]^-$ [145] in which a bridging hydrogen is located above the triboron face; however, in low temperature studies[146], it was found to exist as structure (b) where one of the hydrogen atoms of the BH_2L fragment semi-bridges between B(1) and B(2) leading to intermediate structure between structure (a) and structure (d). Studies of $[B_3H_7(NCSe)]^-$ [146] at RT and LT give similar results to those of $[B_3H_7(NCS)]^-$. Structure (b) is also found in $B_3H_7NH_3$[148].

Crystal structures of $[B_3H_6(Cl)_2]^-$ and $[B_3H_6(Cl)(NCS)]^-$ [28] shown in Fig. 2.9 and Fig. 2.10 relate to that of $[B_3H_8]^-$ [structure (d)] with trans substituents and is consistent with the n.m.r. evidence that the substituents are at different boron atoms.

2.3 EXPERIMENTAL

2.3.1 General

$[NMe_4][B_3H_8]$ was purchased from Callery Chemical Company and recrystallized from acetonitrile-diethylether before use. $[N(PPh_3)_2][B_3H_8]$ was prepared by a metathetical reaction from $[N(PPh_3)_2][Cl]$ in ethanol and $[NMe_4][B_3H_8]$ in water and recrystallized from dichloromethane-diethylether. $Na[BH_3CN]$ was a gift from Dr. R. Wade, Ventron Corporation, and was recrystallized from acetonitrile before use. $[N(PPh_3)_2][BH_3CN]$ was prepared from $[N(PPh_3)_2][Cl]$ in ethanol and $Na[BH_3CN]$

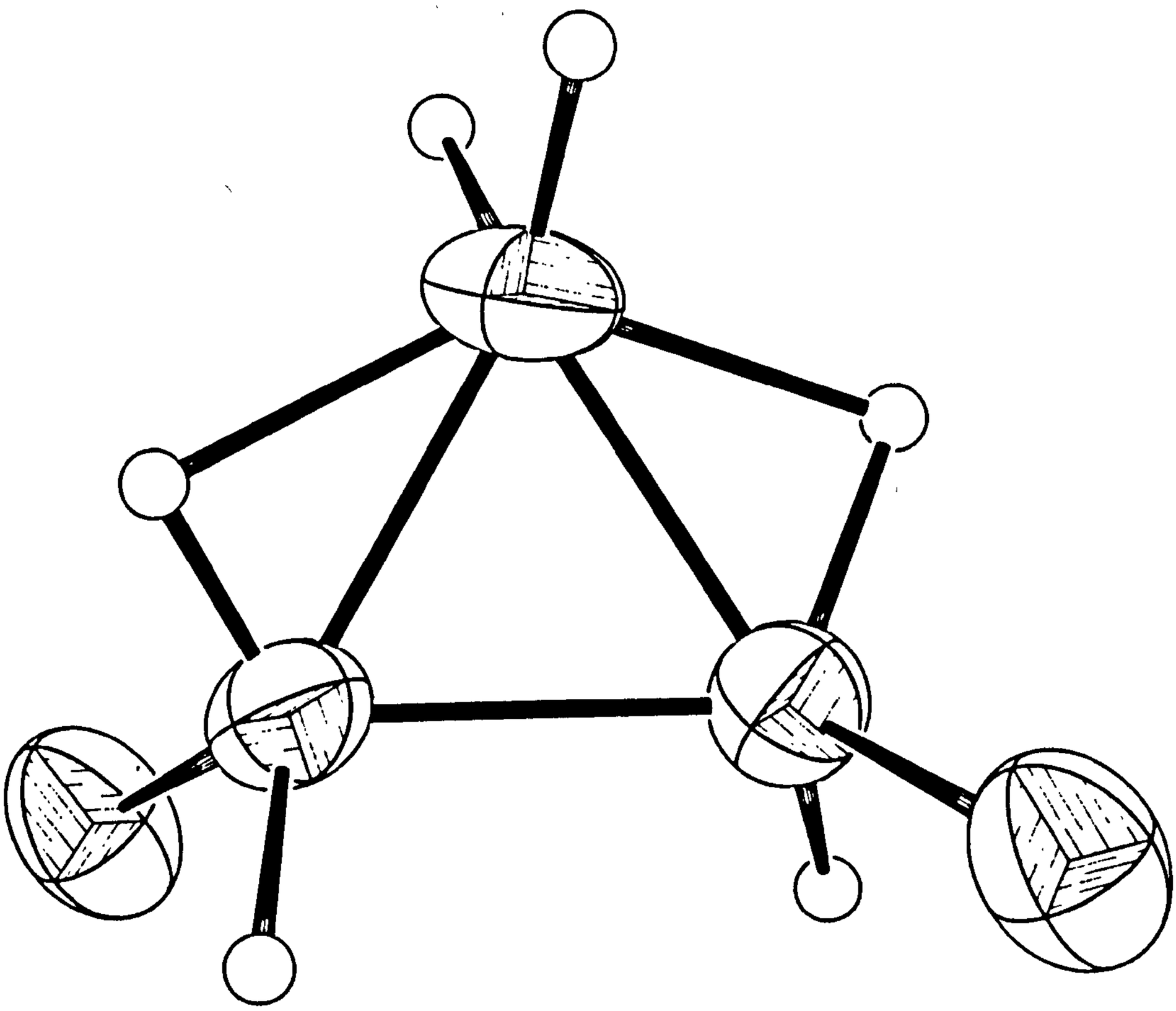

Fig.2.9. The structure of the $[B_3H_6(Cl)_2]^-$ ion.

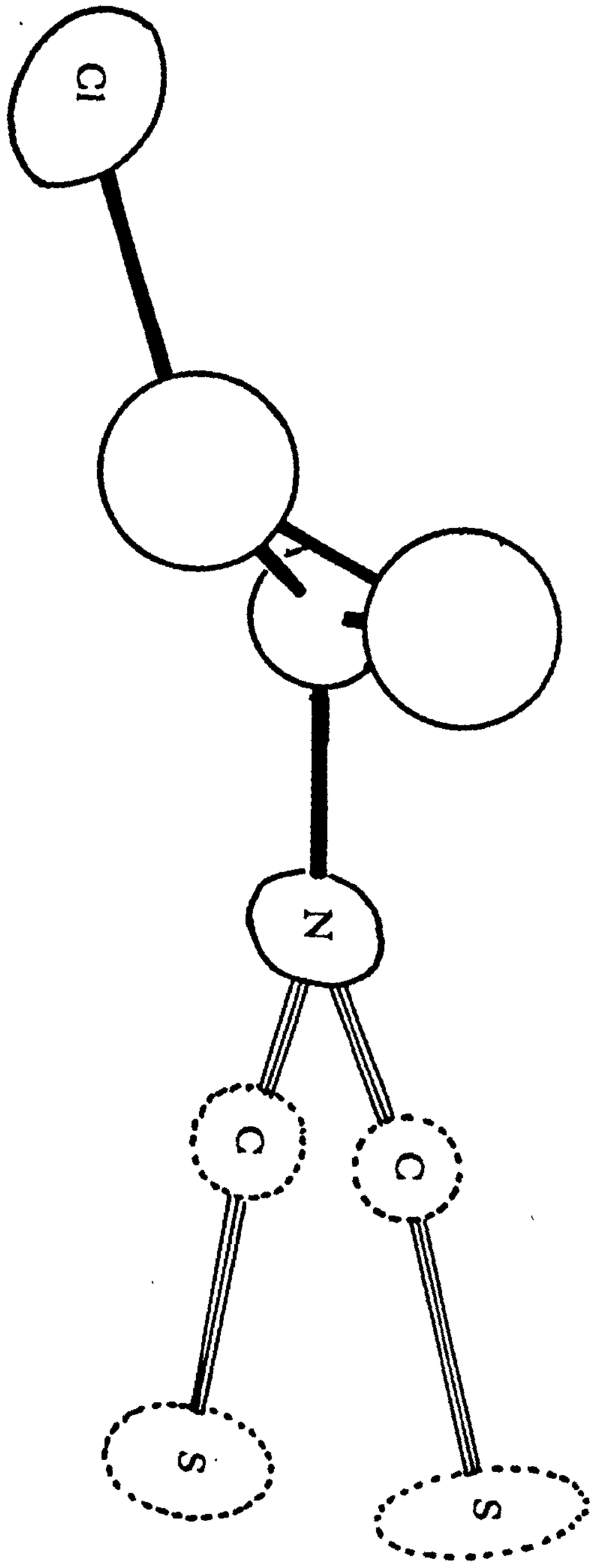

Fig.2.10. The structure of the $[B_3H_6(Cl)(NCS)]^-$ ion.

in water and recrystallized from dichloromethane-diethylether. AgNCS and AgCN were prepared from $AgNO_3$ and KNCS or NaCN in water. $[N(PPh_3)_2][B_3H_7(NCS)]$ and $[N(PPh_3)_2][B_3H_7(NCBH_3)]$ were prepared as previously described[27]. All other reagents were used as received.

2.3.2 Preparation of $[N(PPh_3)_2][B_3H_7(NCO)]$.

Dry CH_2Cl_2 (20 cm^3) was condensed onto the solid reagents $[N(PPh_3)_2][B_3H_8]$ (2.32g, 4.0 mmol) and Hg_2Cl_2 (0.94g, 2.0 mmol). The mixture was warmed to ca. 20°C and stirred for about 1 hr. until hydrogen evolution ceased. The solution of $[B_3H_7Cl]^-$ was filtered onto $[N(PPh_3)_2][OCN]$ (2.32g, 4.0 mmol), stirred for 4 hr., and solvent removed under vacuum. The white product was purified by chromatography over silica gel (200g) which had been treated with hexamethyldisilazane (16 cm^3 in hexane). The eluting solvent was CH_2Cl_2. Fractions collected (very weak in concentration) were monitored by thin layer chromatography (t.l.c.). The yield of colourless crystals was 0.23g, 10%. (Found: C, 71.7; H, 6.0; N, 4.4% $C_{37}H_{37}B_3N_2OP_2$ requires C, 71.7; H, 6.0; N, 4.5%).

2.3.3 Preparation of $[N(PPh_3)_2][\{B_3H_7(NC)\}_2Ag]$.

By a method similar to 2.3.2, $[N(PPh_3)_2][B_3H_8]$ (2.32g, 4.0 mmol) was treated with Hg_2Cl_2 (0.94g, 2.0 mmol) and the resulting solution was filtered onto AgCN (0.54g, 4.0 mmol). The mixture was stirred for ca. 3 hr.

and filtered. The brown filtrate was evaporated to dryness and the residue was purified by chromatography on silica gel using CH_2Cl_2:CH_3CN (25:1) as eluting solvent. After evaporating the solvent, the product was recrystallized from CH_2Cl_2-hexane. The colourless crystals deposited silver on prolonged standing, and decomposed more rapidly in solution. (Found : C, 58.8; H, 5.7; N, 5.1% $C_{38}H_{44}AgB_6N_3P_2$ requires C, 58.7; H, 5.7; N, 5.4%).

2.3.4 Deuteration of $[Na]^+$, $[NBu^n_4]^+$, $[N(PPh_3)_2]^+$ salts of $[BH_3CN]^-$ and $[N(PPh_3)_2][B_3H_7(NCBH_3)]$.

These were carried out by a method[6] similar to that of preparing $NaBD_3CN$ from $NaBH_3CN$ and CH_3COD-DCl except that in the deuteration of $NaBH_3CN$, CH_3CN (5 cm^3) was added; in the deuteration of $[NBu^n_4][BH_3CN]$, $[NBu^n_4][BH_3CN]$ (0.4 g) was dissolved in a mixture of CH_3CN (5 cm^3) and D_2O (3 cm^3); in the deuteration of $[N(PPh_3)_2][BH_3CN]$, $[N(PPh_3)_2][BH_3CN]$(1.11g) was dissolved in a mixture of CH_3CN (10 cm^3) and D_2O (6 cm^3); and in the deuteration of $[N(PPh_3)_2][B_3H_7(NCBH_3)]$, $[N(PPh_3)_2][B_3H_7(NCBH_3)]$ (0.14g) was treated with CH_3CN (9 cm^3) and D_2O (2 cm^3). The products were monitored by ^{11}B n.m.r. spectroscopy.

2.3.5 Preparation of $[N(PPh_3)_2][B_3H_6(Cl)_2]$.

In a 250 cm^3 flask fitted with a stopcock adaptor was placed $[N(PPh_3)_2][B_3H_8]$ (1.4g, 2.5 mmol), and 20 cm^3 of dried, degassed CH_2Cl_2 was condensed in under vacuum. Gaseous HCl (5 mmol) was introduced.

The mixture was warmed to ca.20°C and stirred for 30 min until hydrogen evolution ceased. Solvent was removed under vacuum and the dry solid was recrystallized from CH_2Cl_2-hexane to give colourless crystals, identical to those prepared earlier[24].

2.3.6 Preparation of $[N(PPh_3)_2][B_3H_6(Cl)(NCS)]$.

In a similar manner as sect. 2.3.5, $[N(PPh_3)_2][B_3H_7NCS]$ (0.318g, o.5 mmol) was placed in a 100 cm^3 flask, and treated with two successive aliquots (0.5 mmol) of HCl. The product, recrystallized from CH_2Cl_2-hexane, gave colourless crystals. (Found: C, 65.2; H, 5.2; Cl, 5.2; N, 3.9; S, 4.8% $C_{37}H_{36}B_3ClN_2P_2S$ requires C, 66.3; H, 5.4; Cl, 5.3; N, 4.2; S, 4.8%). The analytical data were obtained after the crystals had been pumped under high vacuum to remove dichloromethane from the solvate. Crystals for X-ray diffraction contained 1 mol of CH_2Cl_2 per mole of compound.

2.3.7 Preparation of $[N(PPh_3)_2][B_3H_6(Cl)(NCBH_3)]$

$[N(PPh_3)_2][B_3H_8]$(1.4, 2.5 mmol) was placed in a 250 cm^3 flask fitted with a stopcock adaptor and 20 cm^3 of dried, degassed CH_2Cl_2 was condensed in under vacuum. After the compound had dissolved, gaseous HCl (5 mmol) was condensed in, and the mixture was stirred for ca.30 min until hydrogen evolution ceased. Solvent was removed under vacuum. $[N(PPh_3)_2][BH_3CN]$ (2.44g, 2.5 mmol) was added and CH_2Cl_2 (20 cm^3) was condensed in.

The mixture was warmed to room temperature (ca. 20°C) and stirred for 4-5 hr and solvent was removed. The white product was purified by chromatography on treated silica gel as in sect. 2.3.2 using CH_2Cl_2 as eluting solvent. However, the product was still contaminated with $[N(PPh_3)_2][B_3H_7(NCBH_3)]$ since the R_f values of these two compounds were similar.

2.3.8. Preparation of $[N(PPh_3)_2][\{B_3H_6(Cl(NC)\}_2Ag]$

$[N(PPh_3)_2][B_3H_6(Cl)_2]$ (2.5 mmol) was freshly prepared as in sect. 2.3.7 and AgCN (0.34g, 2.5 mmol) was added, CH_2Cl_2 (20 cm^3) was condensed in and the mixture was stirred for 4-5 hr. After filtering, the filtrate was evaporated under vacuum to dryness yielding a brown solid. This was purified by chromatography on treated silica gel as in sect. 2.3.2 using CH_2Cl_2 as the eluting solvent. Evaporation of the solvent from the first product eluted yielded a colourless solid which turned brown on prolonged standing. The yield of product was small, although just enough for n.m.r. studies.

2.3.9 Reaction of $[N(PPh_3)_2][B_3H_7(NCBH_3)]$ with HCl.

A series of reactions of $[N(PPh_3)_2][B_3H_7(NCBH_3)]$ (0.309g, 0.5 mmol) with HCl (0.5, 1.0, 1.5, 2.0 and 2.5 mmol) were carried out. $[N(PPh_3)_2][B_3H_7(NCBH_3)]$ was placed in a 100 cm^3 flask and CH_2Cl_2 (15 cm^3) and HCl were introduced as described in sect. 2.3.5. The mixture was stirred for ca. 1 hr. and solvent was removed. The products were monitored by ^{11}B n.m.r. spectroscopy.

2.3.10. Reaction of $[N(PPh_3)_2][B_3H_7(NCO)]$ with HCl.

$[N(PPh_3)_2][B_3H_7(NCO)]$ (0.186g, 0.3 mmol) was treated with HCl (0.3 mmol) in the similar manner as described in sect. 2.3.5. The products were monitored by t.l.c. and ^{11}B n.m.r. spectroscopy. The chromatograms indicated at least three compounds.

2.3.11. Reaction of $[N(PPh_3)_2][\{B_3H_7(NC)\}_2Ag]$ with HCl.

Reactions of $[N(PPh_3)_2][\{B_3H_7(NC)\}_2Ag]$ (0.388g, 0.5 mmol) with HCl (0.5 mmol) were carried out as described in sect. 2.3.5. The products were monitored by ^{11}B n.m.r. spectroscopy.

2.3.12. Reaction of $[N(PPh_3)_2][B_3H_6(Cl_2)]$ with HCl.

Reactions of $[N(PPh_3)_2][B_3H_6(Cl)_2]$ (0.1944g, 0.3 mmol) with HCl (0.3, 0.6, 0.9, 1.2, 1.5 mmol) were carried out as described in sect. 2.3.9. No hydrogen evolutions were observed but the solutions deposited out more and more precipitate as HCl was increased. The filtrates were identified as $[B_3H_6(Cl)_2]^-$ by their n.m.r. spectra.

2.2.13. Reaction of $[N(PPh_3)_2][B_3H_6(Cl)_2]$ with AgNCS.

$[N(PPh_3)_2][B_3H_6(Cl)_2]$ (2.5 mmol) was freshly prepared from $[N(PPh_3)_2][B_3H_8]$ and HCl as in sect. 2.3.7 and AgNCS (0.41g, 2.5 mmol) was added. CH_2Cl_2 (20 cm^3) was condensed in and the mixture was stirred for 4-5 hr. After filtering, solvent was removed under vacuum.

The products identified by ~~its~~ their n.m.r. spectra were $[B_3H_6(Cl)_2]^-$ and $[B_3H_6(Cl)(NCS)]^-$ (50% substitution).

2.3.14 Reaction of $[N(PPh_3)_2][B_3H_6(Cl)(NCS)]$ with AgNCS.

About 15 cm^3 of dried, degassed CH_2Cl_2 was condensed onto the solid reagents $[N(PPh_3)_2][B_3H_6(Cl)(NCS)]$ (0.33g, 0.5 mmol) and AgNCS (0.09g, 0.5 mmol). The mixture was stirred at room temperature (ca.20°C) for 2 hr. and filtered. After removing the solvent, the products were monitored by ^{11}B n.m.r. spectroscopy.

2.3.15 Reaction of $[N(PPh_3)_2][B_3H_7(NCS)]$ with Hg_2Cl_2.

A series of reactions of $[N(PPh_3)_2][B_3H_7(NCS)]$ (0.159g, 0.25 mmol) with Hg_2Cl_2 (0.059g, 0.125 mmol) were carried out in 10 cm^3 of different solvents: CH_2Cl_2, THF, CH_3CN. The mixture was refluxed for 2 hr. under vacuum. After filtering, the filtrate was examined by the ^{11}B n.m.r. spectroscopy which indicated unreacted $[B_3H_7(NCS)]^-$.

2.3.16 Reaction of $[N(PPh_3)_2][B_3H_7(NCBH_3)]$ with Hg_2Cl_2.

Two sets of $[N(PPh_3)_2][B_3H_7(NCBH_3)]$ (0.154g, 0.25 mmol) and Hg_2Cl_2 (0.059g, 0.125 mmol) were refluxed in two different solvents, CH_2Cl_2 and $C_2H_4Cl_2$ under N_2 for 3.5 hr. The products were monitored by ^{11}B n.m.r. spectroscopy which indicated unreacted starting material.

2.3.17 Reaction of $[N(PPh_3)_2][B_3H_7(NCO)]$ with Hg_2Cl_2.

About 10 cm^3 of dried, degassed CH_2Cl_2 was condensed onto the solid reagents $[N(PPh_3)_2][B_3H_7(NCO)]$ (0.124g, 0.2 mmol) and Hg_2Cl_2 (0.047g, 0.1 mmol). The mixture was warmed up to ca. 20°C and stirred for ca. 6 hr. After filtering the droplets of mercury from the solution, solvent was removed under vacuum leaving behind white solid which was monitored by ^{11}B n.m.r. spectroscopy.

2.2.18 Hydrolysis of $[N(PPh_3)_2][B_3H_7(NCS)]$.

A series of solutions of $[N(PPh_3)_2][B_3H_7(NCS)]$ (0.06g) in 5 cm^3 of $CH_3CN:H_2O$ (4:1) were prepared at pH 5, 4, 3. the solutions were stirred at 50°C for 2 hr. and solvent was removed. The i.r. spectra of the products indicated that $[B_3H_7(NCS)]^-$ started to decompose slightly at pH 4 and more at pH 3 producing free NCS^-, which was monitored by the appearance of an absorption at 2040 cm^{-1}.

2.3.19 Hydrolysis of $[N(PPh_3)_2][B_3H_7(NCBH_3)]$.

A series of solutions of $[N(PPh_3)_2][B_3H_7(NCBH_3)]$ (0.03g) in 5 cm^3 of $CH_3CN:H_2O$ (4:1) were prepared at pH 5, 4, 3, 2, 1. The solutions were stirred at room temperature (ca. 20°C) for 1.5 hr. and solvent was removed. Their i.r. spectra indicated starting material.

CHAPTER THREE

ELECTROCHEMICAL STUDIES OF MONO-SUBSTITUTED AND DI-SUBSTITUTED OCTAHYDROTRIBORATE ANIONS

3.1 INTRODUCTION

Cyclic voltammetry, a.c. voltammetry and controlled potential electrolysis of salts of the anions $[B_3H_8]^-$ and $[B_3H_7(X)]^-$ (X = Cl, NCS, $NCBH_3$) had been studied. Anodic dissolutions of copper in acetonitrile solution of $[B_3H_8]^-$ [87] or $[B_3H_7(NCBH_3)]^-$ [88] in the presence of PPh_3 gave rise to $\{[PPh_3]_2\ Cu[B_3H_8]\}$ or $\{[PPh_3]_2\ Cu[(BH_3CN)B_3H_7]\}$ whereas those of $[B_3H_7(Cl)]^-$ and $[B_3H_7(NCS)]^-$ [88] led to removal of substituents ultimately leading to $B_3H_7[CH_3CN]$. It had also been shown[86] that electrochemical oxidation of $[B_3H_8]^-$ at platinum or gold anodes in acetonitrile or dimethylformamide yielded $B_3H_7[CH_3CN]$ or $B_3H_7[DMF]$.

In this work, the electrochemical properties of disubstituted octahydrotriborate derivatives, $[B_3H_6(Cl)_2]^-$ and $[B_3H_6(Cl)(NCS)]^-$ were studied in similar ways in acetonitrile and in other solvents such as 1,3-dioxalane, benzonitrile and dichloromethane for comparison in order to study the solvent effects, and to find a better solvent for this work. Attempts were also made to prepare metallaboranes by anodic dissolution of copper or nickel anodes in solutions of these anions.

3.2 RESULTS AND DISCUSSION

3.2.1 Cyclic and A.C. Voltammetry

(a) $[B_3H_6(Cl)_2]^-$

(i) In acetonitrile.

Cyclic and a.c. voltammograms of $[B_3H_6(Cl_2)]^-$ at Pt in acetonitrile containing $[NBu_4^n][BF_4]$(0.1 mol dm^{-3}) as supporting electrolyte are shown in Fig. 3.1. Irreversible oxidation waves were observed at +0.86 V and +1.1 V or +0.72 V and +1.2 V, and a reduction wave near -0.45 V or -1.0 V respectively. These indicate that the anion is more stable to oxidation than the monosubstituted derivative, $[B_3H_7(Cl)]^-$, where an irreversible oxidation wave at +0.6 V was observed.

The first oxidation wave at +0.86 V in the cyclic voltammogram of $[B_3H_6(Cl)_2]^-$ at a scan rate of 0.5 VS^{-1} was not well defined and the current was reduced as the scan rate was increased (0.5 $\longrightarrow$ 1.999 VS^{-1}) and the cathodic potential limit was decreased. Fig. 3.2 shows the cyclic voltammograms of $[B_3H_6(Cl)_2]^-$ run at different cathodic potential limits. It can be seen that the first oxidation wave was not observed when the cathodic potential limit was set at a potential more positive than the first reduction potential. This oxidation wave also decreased when the scan rate was increased and a discrete wave was not observed at scan rates faster than 1.5 VS^{-1} as shown in Fig. 3.3. It is likely that the electrochemical mechanism involved chemical processes following the electrochemical electron

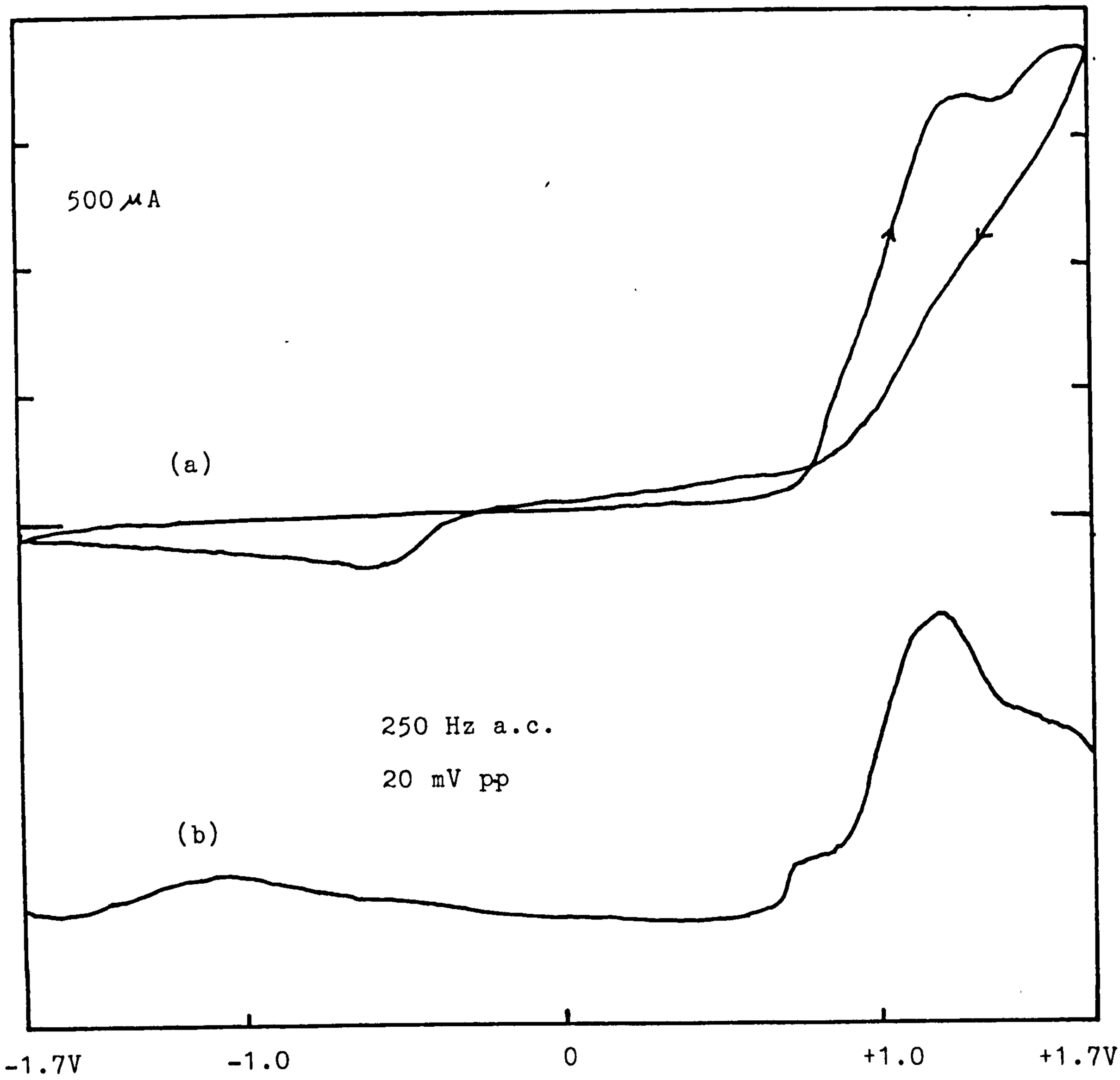

Fig. 3.1. (a) Cyclic voltammogram (scan rate 0.5 VS^{-1}) and (b) A.c. voltammogram (scan rate 0.05 VS^{-1}) of $[B_3H_6(Cl)_2]^-$ at Pt in 0.1 M Bu_4NBF_4/CH_3CN

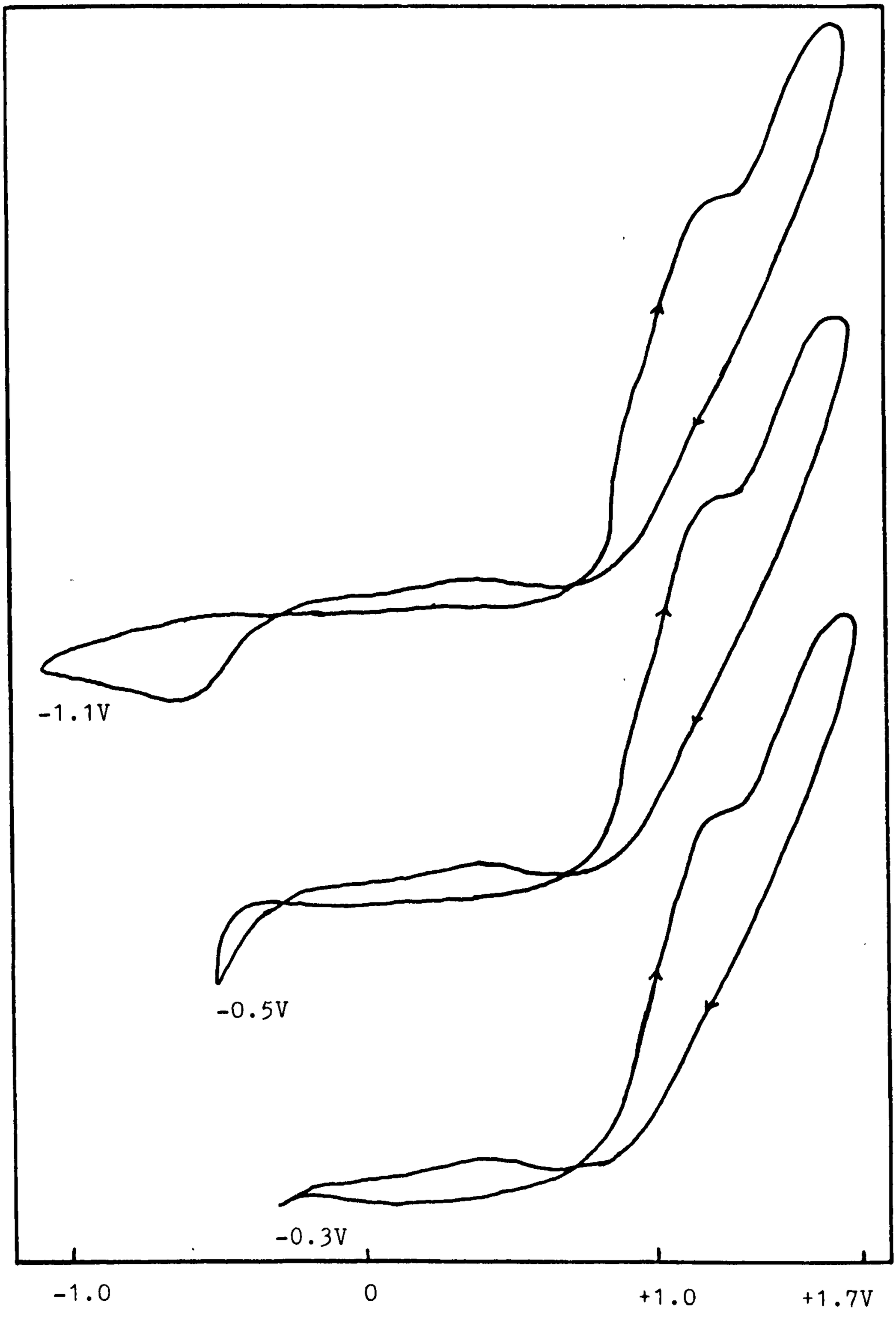

Fig. 3.2. Cyclic voltammograms (scan rate 0.5 VS^{-1}) of $[B_3H_6(Cl)_2]^-$ at Pt in 0.1 M Bu_4NBF_4/CH_3CN

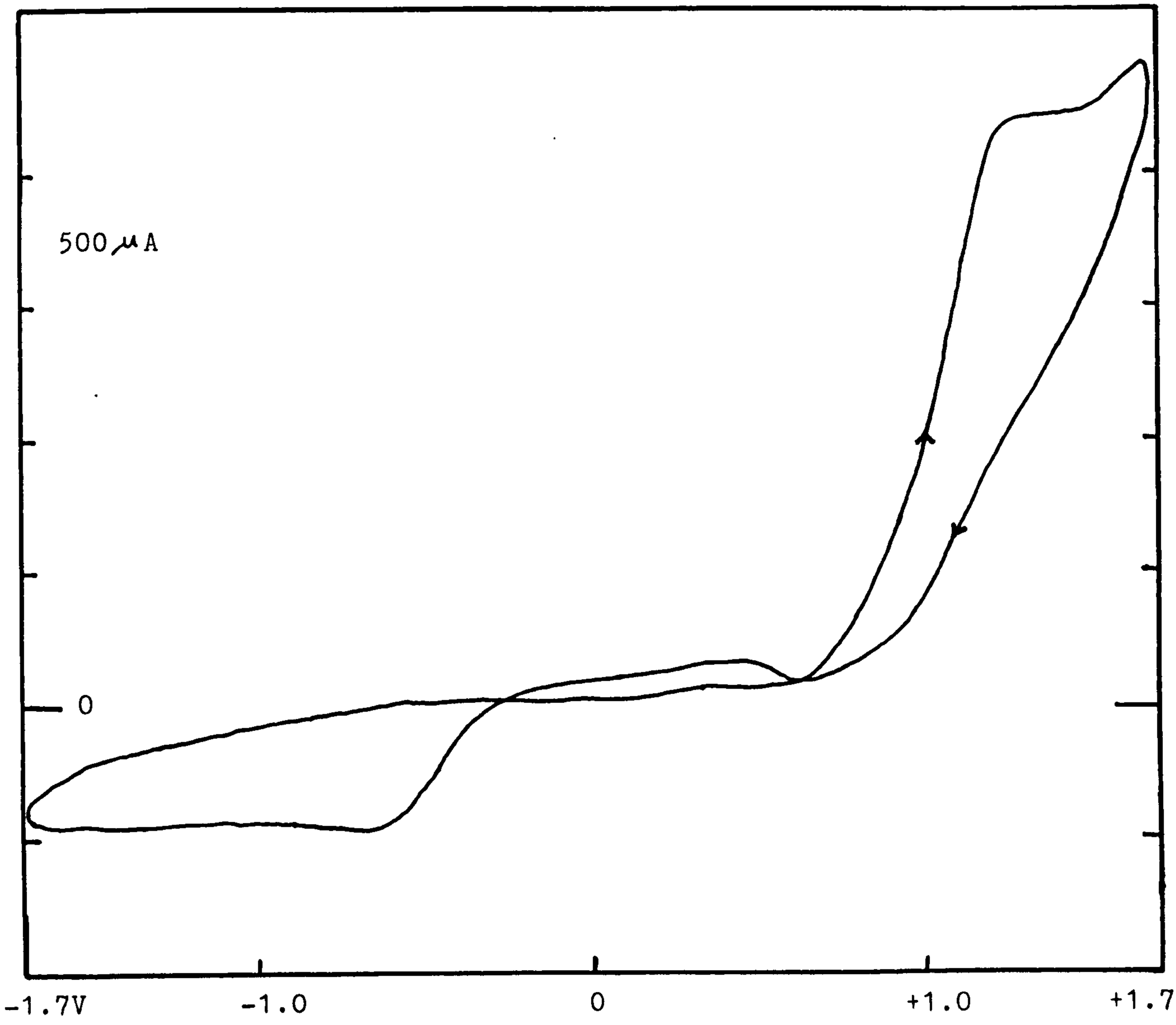

Fig.3.3. Cyclic voltammogram (scan rate 1.999 VS^{-1}) of $[B_3H_6(Cl)_2]^-$ at Pt in 0.1 M Bu_4NBF_4/CH_3CN

transfer steps; thus as the scan rate was increased, there probably was not enough time for a relatively slow chemical reaction to take place and therefore the oxidation wave of this chemical reaction product was not observed. When the potential was not scanned down to the reduction potential, there might not be the reduced species to undergo chemical reaction and therefore no chemical product to be oxidised. Possible processes can be written as follows,

$$[B_3H_6(Cl)_2]^- \longrightarrow [B_3H_6(Cl)_2]^{\cdot} + e^- \qquad (3.1)$$

$$[B_3H_6(Cl)_2]^{\cdot} \longrightarrow [B_3H_6(Cl)] + [Cl]^{\cdot} \qquad (3.2)$$

$$CH_3CN + [Cl]^{\cdot} \longrightarrow [CH_2CN]^{\cdot} + HCl \qquad (3.3)$$

$$[CH_2CN]^{\cdot} + e^- \longrightarrow [CH_2CN]^- \qquad (3.4)$$

$$[B_3H_6(Cl)] + [CH_2CN]^- \longrightarrow [B_3H_6(Cl)(CH_2CN)]^- \qquad (3.5)$$

$$[B_3H_6(Cl)(CH_2CN)]^- \longrightarrow [B_3H_6(Cl)(CH_2CN)]^{\cdot} + e^- \qquad (3.6)$$

The processes are divided into: (a) the first electrochemical oxidation step (eq. 3.1) which occurred at potential of 1.1 V followed by its subsequent chemical processes (eq. 3.2 and 3.3). It was found that[149] under the influence of strong bases (e.g. $NaNH_2$), acetonitrile is reduced to $\bar{C}H_2CN$, therefore eq. (3.3) and

eq. (3.4) are possible; and (b), the first reduction step (eq. 3.4) which took place near -0.45 V followed by a chemical process (eq. 3.5) yielding a disubstituted triborate which was oxidatively less stable than $[B_3H_6(Cl)_2]^-$ and was oxidised at 0.86 V (eq. 3.6).

Exhaustive electrolysis of acetonitrile solution of $[B_3H_6(Cl)_2]^-$ at Pt at +1.2 V [sect. 3.2.3(a)(i)] involved only one electron oxidation. The ^{11}B n.m.r. spectrum of the products indicated a minor component of disubstituted triborate which could possibly be $[B_3H_6(Cl)(CH_2CN)]^-$ and a major boron-containing component (δ = +21.4 ppm) which was probably resulted from further oxidation of $[B_3H_6(Cl)(CH_2CN)]^-$ following chemical processes. The ^1H n.m.r. spectrum, however, showed mixtures of products which probably arose from $[CH_2CN]^{\cdot}$, $[CH_2CN]^-$, CH_3CN, $[B_3H_6(Cl)(CH_2CN)]^{\cdot}$, etc. undergoing further chemical reactions.

(ii) In 1,3-dioxalane.

The cyclic voltammogram of $[B_3H_6(Cl)_2]^-$ at Pt in 1,3-dioxalane containing $[NBu_4^n][BF_4]$ (0.1 mol dm^{-3}) as supporting electrolyte showed an oxidation wave near +1.3 V. The voltammogram is similar to those of $[B_3H_6(Cl)(NCS)]^-$ and $[B_3H_7(NCS)]^-$ in 1,3-dioxalane shown in Fig. 3.7 and is discussed in sect. 3.2.1(c).

(iii) In dichloromethane.

The cyclic voltammogram of $[B_3H_6(Cl)_2]^-$ at Pt in dichloromethane containing $[NBu_4^n][BF_4]$ (0.1 mol dm^{-3}) as supporting electrolyte is shown in Fig. 3.4. This

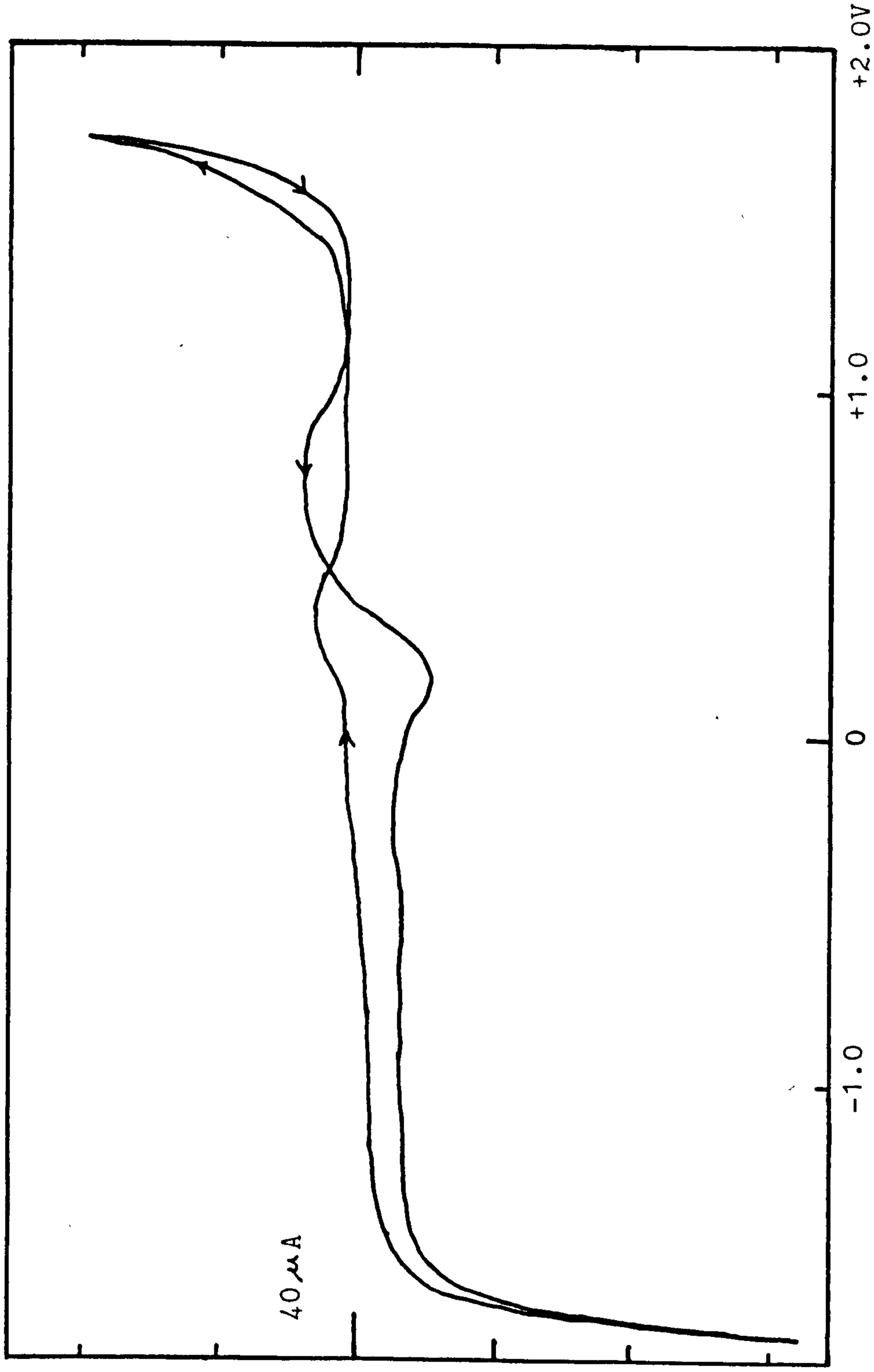

Fig.3.4. Cyclic voltammogram (scan rate 0.5 VS^{-1}) of $[B_3H_6(Cl)_2]^-$ at Pt in 0.1 M Bu_4NBF_4/CH_2Cl_2

shows only small oxidation waves near +0.3 V and +1.5 V and a relatively large oxidation current with trace crossing on the subsequent reduction scan. Reduction waves were observed near +0.2 V and -0.4 V and a further wave below - 1.4 V might be associated with the reduction of the solvent.

As the cathodic potential limits were adjusted to less negative potentials, the peak currents of both oxidation waves were reduced; when the cathodic potential limit was more positive than -1.0 V, the oxidation waves became featureless. When the anodic potential limit was decreased from +1.73 V to +1.3 V, the first oxidation wave at +0.3 V was not observed. This suggested that the $[B_3H_6(Cl)_2]^-$ anion itself was not oxidised at Pt in dichloromethane. The controlled potential electrolysis of $[B_3H_6(Cl)_2]^-$ in dichloromethane at +1.4 V confirmed this. Little current passed through the cell and the product was $[B_3H_6(Cl)_2]^-$.

(iv) In Benzonitrile.

The cyclic voltammogram of $[B_3H_6(Cl)_2]^-$ at Pt in benzonitrile containing $[NBu_4^n][BF_4]$ (0.1 mol dm^{-3}) as supporting electrolyte is shown in Fig. 3.5(a). This is similar to that in dichloromethane in that the oxidation waves near +0.3 V and +1.4 V and relatively large trace crossing were observed. However, as the cathodic potential limits were adjusted to less negative values, the oxidation waves were not affected. This indicated that different electrochemical processes

occurred in benzonitrile compared with dichloromethane. Furthermore, the extent of trace crossing was dependent on the anodic potential limit. Fig. 3.5(b) showed that as the anodic potential limit was decreased, trace crossing was reduced until at the limit of +1.0 V, it was not observed. This indicated that trace crossing was related to oxidation of species produced at the second oxidation wave.

(b) $[B_3H_6(Cl)(NCS)]^-$

(i) In acetonitrile.

Cyclic and a.c. voltammograms of $[B_3H_6(Cl)(NCS)]^-$ at Pt in acetonitrile containing $[NBu_4^n][BF_4]$(0.1 mol dm^{-3}) as supporting electrolyte are shown in Fig. 3.6. Irreversible oxidation waves near +0.4 V and +1.1 V and a reduction wave near -0.5 V were observed in the cyclic voltammogram. The a.c. voltammogram showed a better resolution of the electrochemical processes than the cyclic voltammogram and three oxidation waves at +0.3 V, +0.68 V and + 1.16 V and a reduction wave near -0.4 V were observed. These voltammograms are similar to those of $[B_3H_6(Cl)_2]^-$ in acetonitrile and the oxidation potentials are similar (+1.1 V). However, the electrode processes are different. Changes in scan rates (0.5 $\longrightarrow$ 1.999 VS^{-1}) did not affect the oxidation waves, which indicated that the subsequent chemical steps were probably very fast. When the cathodic potential limit was reduced to -0.5 V (before the reduction wave occurred), the first oxidation wave at +0.4 V (which resolved at

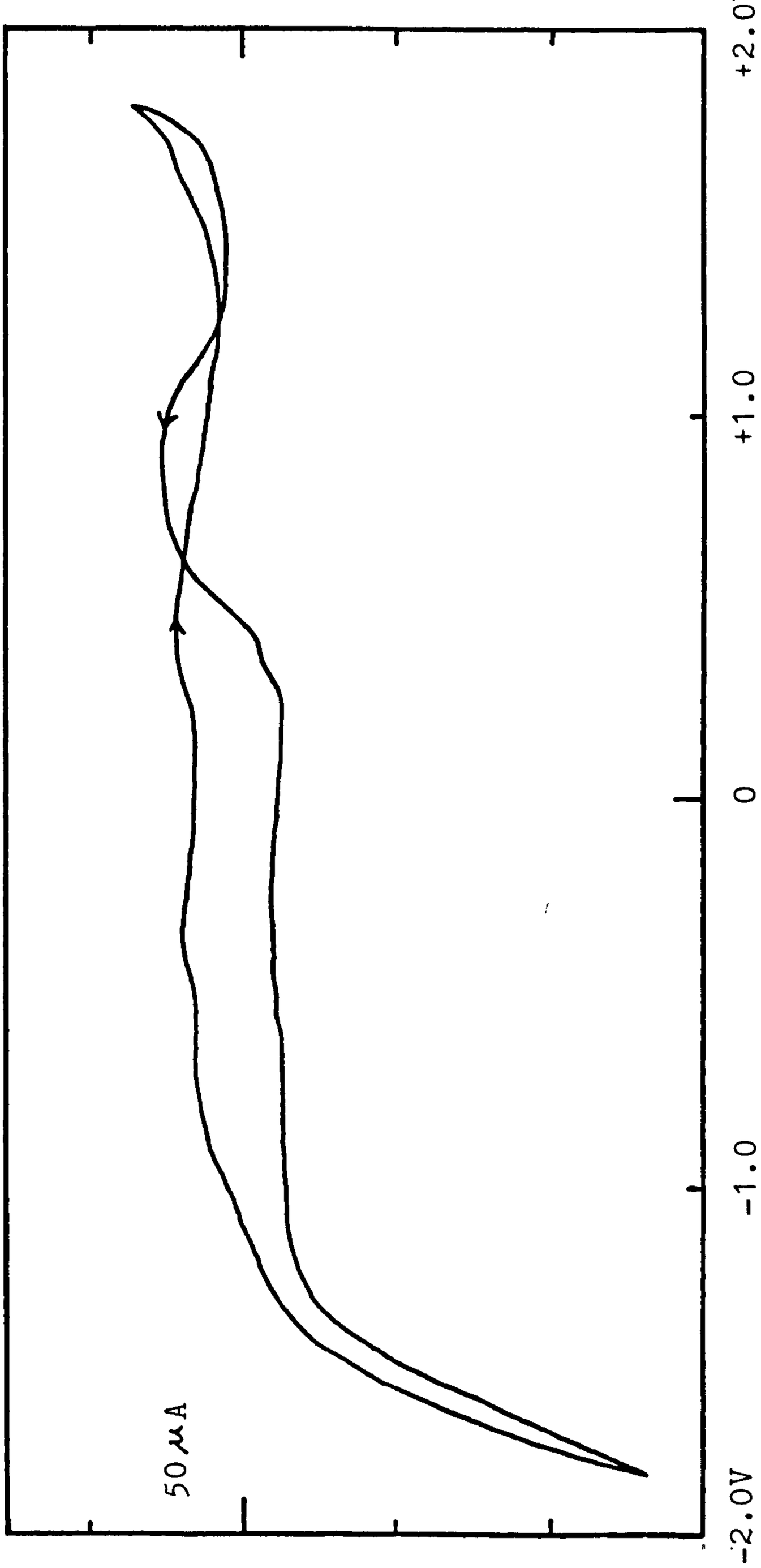

Cyclic voltammogram (scan rate 0.5 VS^{-1}) of $[B_3H_6(Cl)_2]^-$ at Pt in 0.1 M Bu_4NBF_4/PhCN

Fig. 3.5(a)

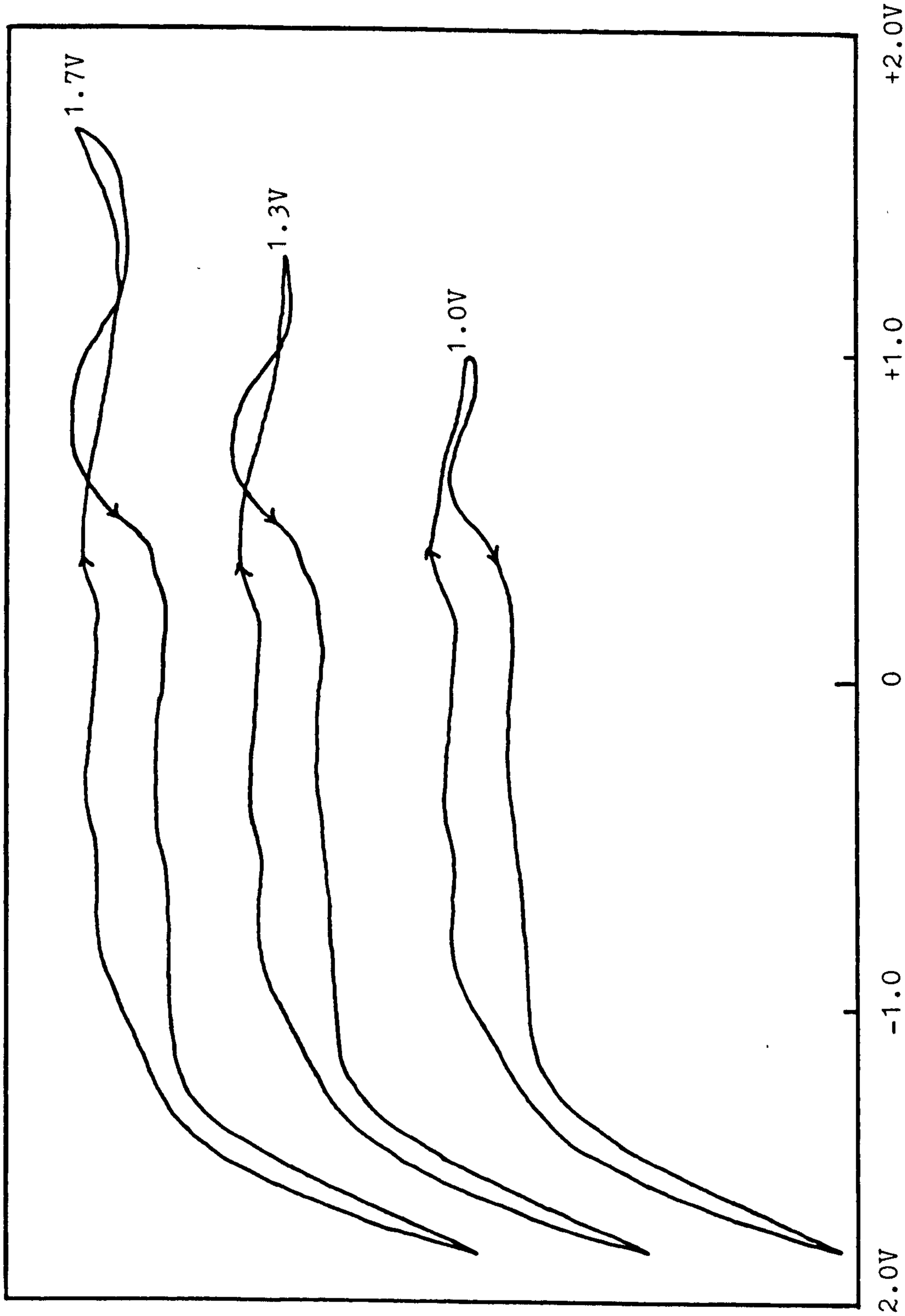

Fig.3.5(b) Cyclic voltammograms (scan rate 0.5 VS^{-1}) of $[B_3H_6(Cl)_2]^-$ at Pt in 0.1 M Bu_4NBF_4/PhCN

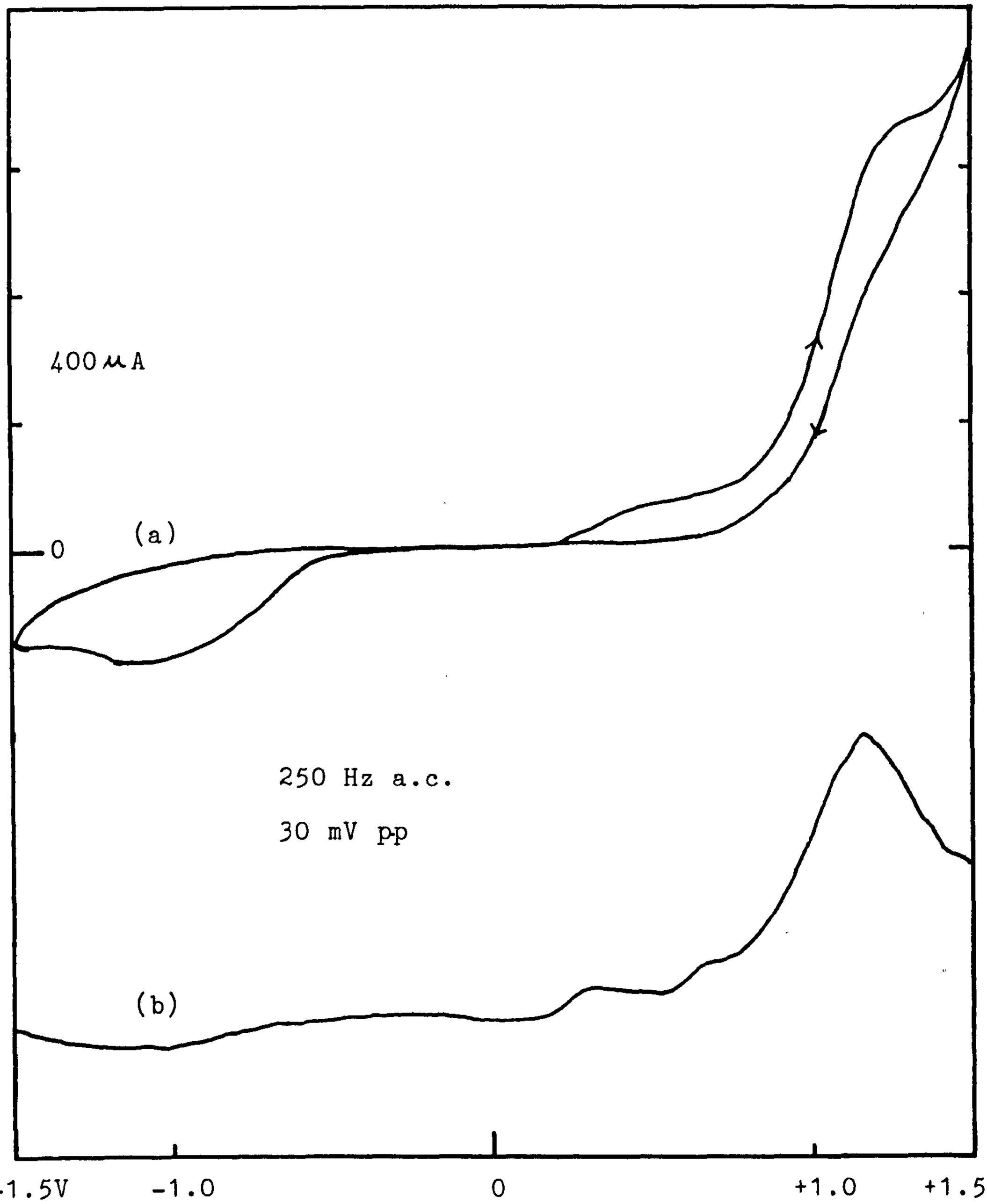

Fig.3.6. (a) Cyclic voltammogram (scan rate 0.5 VS^{-1}) and (b) A.c. voltammogram (scan rate 0.05 VS^{-1}) of $[B_3H_6(Cl)(NCS)]^-$ at Pt in 0.1 M Bu_4NBF_4/CH_3CN

+0.3 V and +0.68 V in a.c. voltammogram) was not observed; this probably resulted from the fact that no reduced species was produced to undergo chemical steps and therefore there were no products to be oxidised. Possible processes can be written as follows,

$$[B_3H_6(Cl)(NCS)]^- \longrightarrow [B_3H_6(Cl)(NCS)]^{\cdot} + e^- \quad (3.7)$$

$$[B_3H_6(Cl)(NCS)]^{\cdot} \longrightarrow [B_3H_6(Cl)] + [NCS]^{\cdot} \quad (3.8)$$

$$[NCS]^{\cdot} + e^- \longrightarrow [NCS]^- \quad (3.9)$$

$[B_3H_6(Cl)]$ and $[NCS]^-$ lead to unidentified decomposition products.

The processes can be divided into: (a) electrochemical oxidation of the $[B_3H_6(Cl)(NCS)]^-$ anion (eq. 3.7) followed by a chemical step (eq. 3.8), (b) electrochemical reduction of the product, $[NCS]^{\cdot}$, resulted from (a) yielding $[NCS]^-$ ion (eq. 3.9), (c) further chemical steps which led to unidentified decomposition products which were subsequently oxidised at +0.3 V and +0.68 V.

Exhaustive controlled-potential electrolyses of $[B_3H_6(Cl)(NCS)]^-$ in acetonitrile at Pt [sect. 3.2.3(b)(i)] which involved oxidation of about six electrons confirmed this. The ^{11}B n.m.r. spectrum indicated only a very small amount of boron-containing species which was not characterized.

(ii) In 1,3-dioxalane.

Cyclic and a.c. voltammograms of $[B_3H_6(Cl)(NCS)]^-$ at Pt in 1,3-dioxalane containing $[NBu_4^n][BF_4]$(0.1 mol dm^{-3}) as supporting electrolyte are shown in Fig. 3.7. The cyclic voltammogram showed an irreversible oxidation wave near +1.2 V and reduction waves near -0.3 V, -0.6 V and -0.9 V whereas the a.c. voltammogram showed an oxidation wave at +1.0 V and a reduction wave at -0.88 V. Changes in cathodic and anodic potential limits and scan rates (0.5 $\longrightarrow$1.999 VS^{-1}) did not affect the shape of the voltammogram.

(c) $[B_3H_7(NCS)]^-$

The cyclic and a.c. voltammograms of $[B_3H_7(NCS)]^-$ at Pt in acetonitrile had been studied previously[88]. The voltammograms showed an irreversible oxidation wave near +1.3 V and a reduction wave near -0.85 V.

In this work, cyclic and a.c. voltammograms of this anion were studied in 1,3-dioxalane for comparison with those of $[B_3H_6(Cl)_2]^-$ and $[B_3H_6(Cl)(NCS)]^-$ in 1,3-dioxalane. Since the voltammograms of $[B_3H_6(Cl)_2]^-$ and $[B_3H_6(Cl)(NCS)]^-$ in 1,3-dioxalane are very similar and exhaustive electrolyses of both anions yielded similar products in 1,3-dioxalane, it was suspected that this was due to either a solvent effect or that the two disubstituted triborate anions happened to undergo similar electrochemical and chemical processes. Thus a monosubstituted derivative, $[B_3H_7(NCS)]^-$, was chosen to study for comparison.

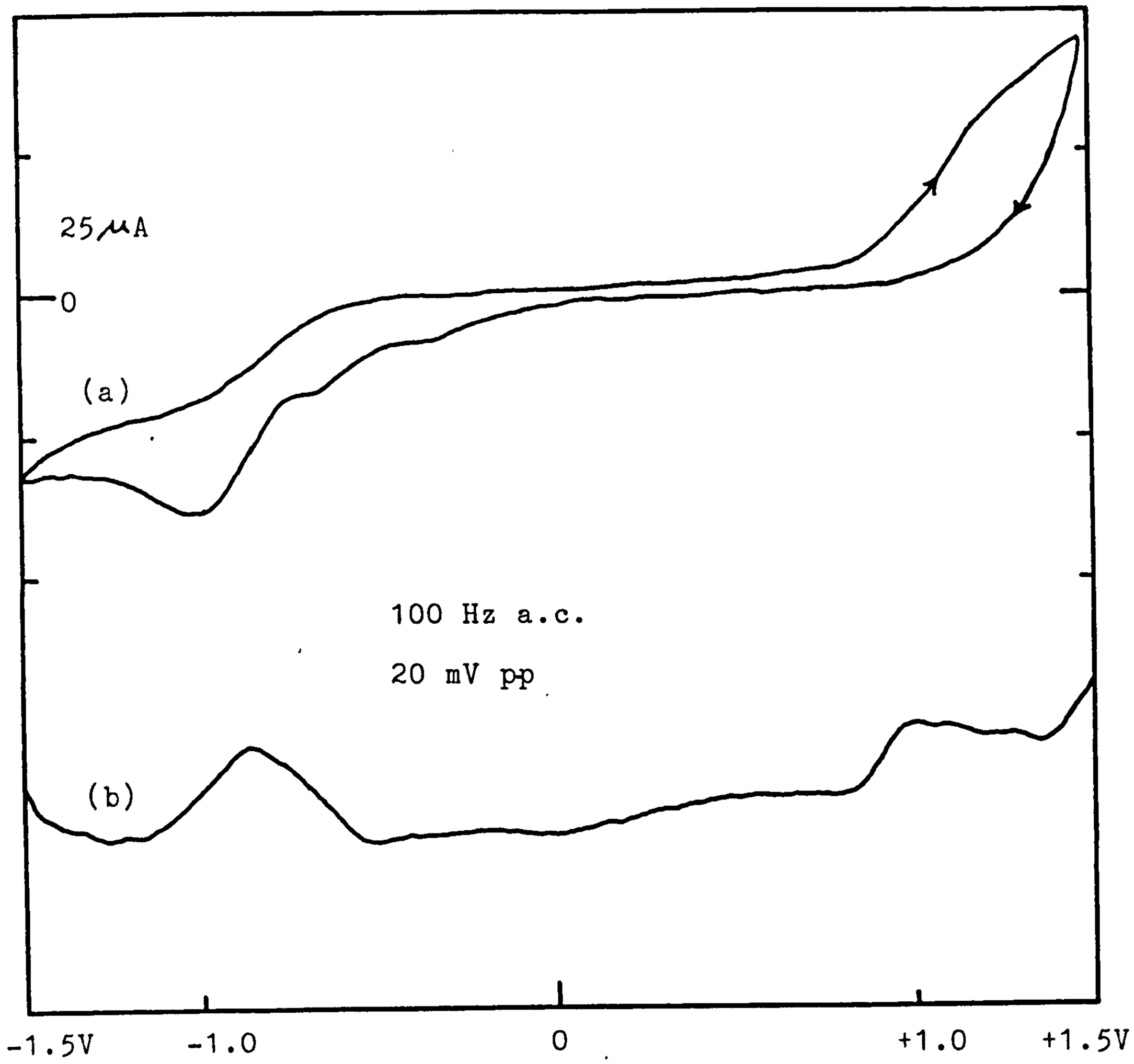

Fig.3.7. (a) Cyclic voltammogram (scan rate 0.5 VS^{-1}) and (b) A.c. voltammogram (scan rate 0.05 VS^{-1}) of $[B_3H_6(Cl)(NCS)]^-$ at Pt in 0.1 M Bu_4NBF_4/1,3-dioxalane

The cyclic voltammogram of $[B_3H_7(NCS)]^-$ at Pt in 1,3-dioxalane containing $[NBu_4^n][BF_4]$(0.1 mol dm^{-3}) as supporting electrolyte was again similar to that of $[B_3H_6(Cl)(NCS)]^-$ shown in Fig. 3.7. The irreversible oxidation wave near +1.3 V and reduction waves near -0.4 V, -0.8 V and -1.2 V were observed. The a.c. voltammogram of $[B_3H_7(NCS)]^-$ in 1,3-dioxalane was less well resolved than that of $[B_3H_6(Cl)(NCS)]^-$ in 1,3-dioxalane, and it showed a very weak oxidation wave at +1.3 V and a large broad reduction wave at -0.7 V.

Exhaustive controlled-potential (+1.3 V) electrolysis of $[B_3H_7(NCS)]^-$ at Pt in 1,3-dioxalane which involved one-electron oxidation again yielded similar products as those obtained from $[B_3H_6(Cl)_2]^-$ and $[B_3H_6(Cl)(NCS)]^-$. Thus it is likely that the solvent reacts with the compounds and undergoes further electrochemical and chemical steps in similar ways.

(d) $[B_3H_7(NCO)]^-$.

The cyclic voltammogram of $[B_3H_7(NCO)]^-$ at Pt in dichloromethane containing $[NBu_4^n][BF_4]$ (0.1 mol dm^{-3}) as supporting electrolyte is shown in Fig. 3.8(a). It consisted of an irreversible oxidation wave near +1.2 V and reduction waves near +0.2 V, -0.4 V and -0.9 V. Fig. 3.8(b), (c), (d) and (e) showed that as the cathodic potential limit was reduced to less negative values, the shape of the oxidation wave changed. It can be seen that the species being reduced near +0.2 V was related to the oxidation wave near +1.0 V and contributed to the

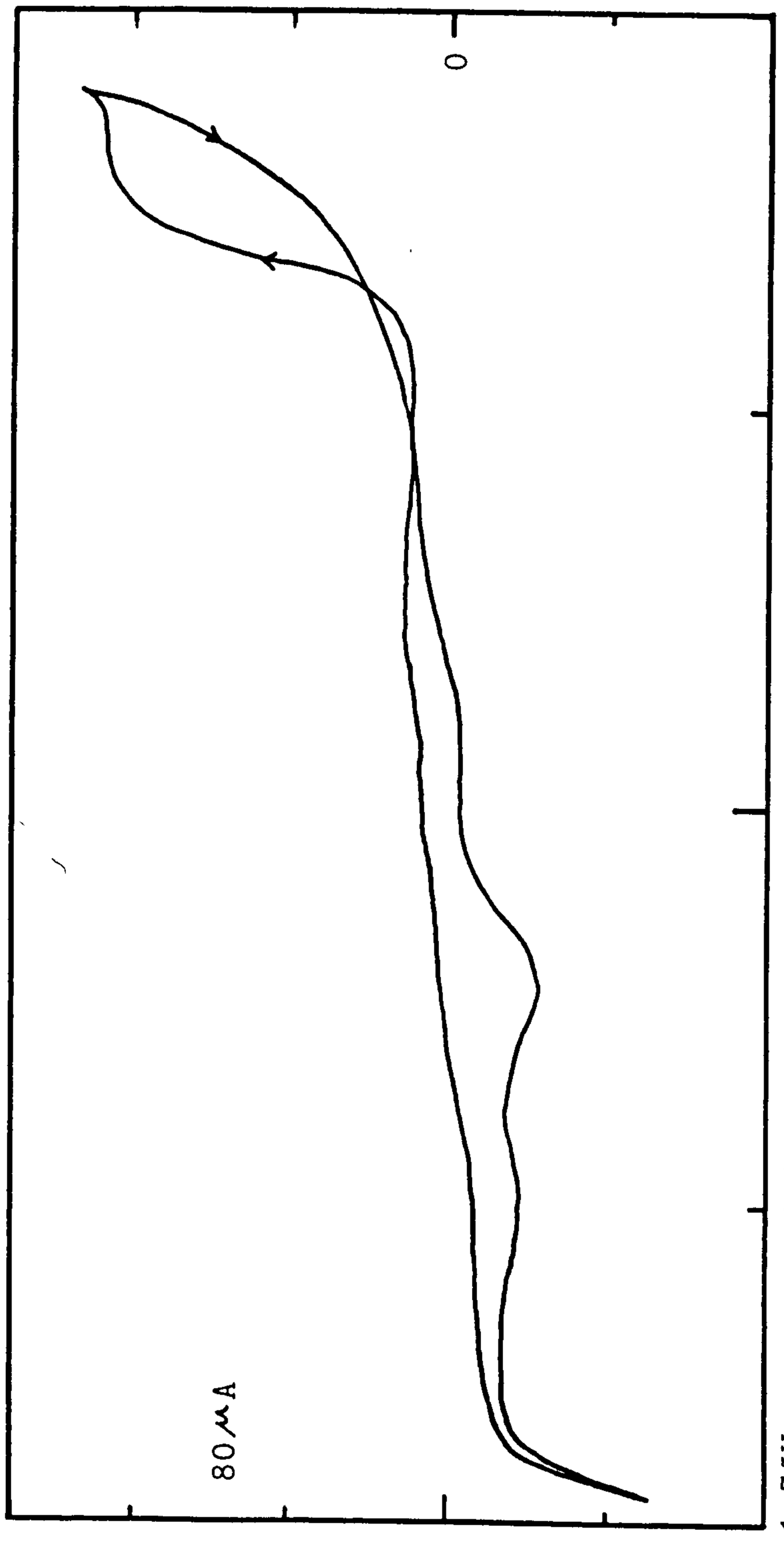

Cyclic voltammogram (scan rate 0.5 VS^{-1}) of $[B_3H_7(NCO)]^-$ at Pt in 0.1 M Bu_4NBF_4/CH_2Cl_2

Fig.3.8(a)

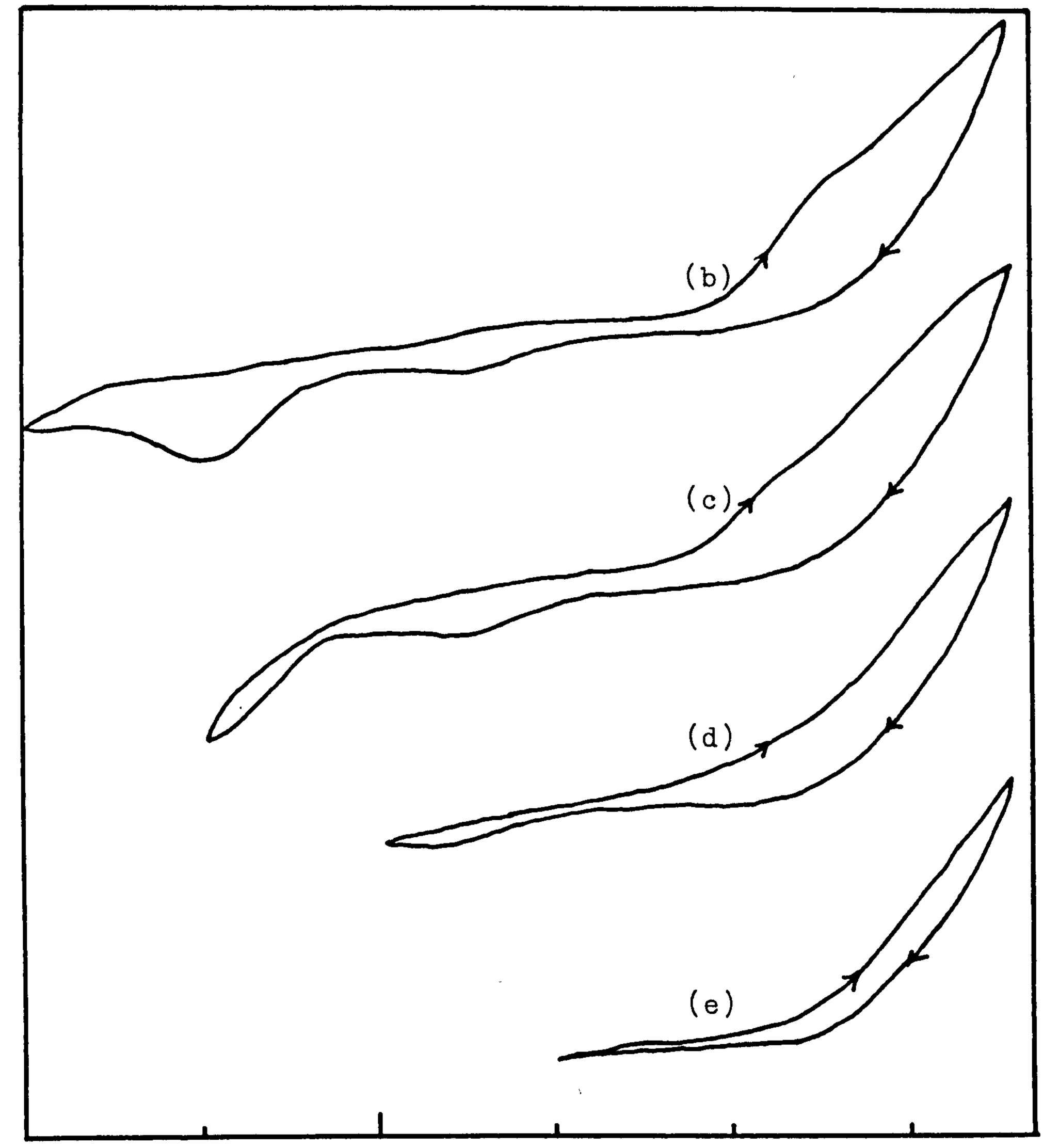

Fig.3.8. (b)(c)(d)(e) Cyclic voltammograms (scan rate 0.5 VS^{-1}) of $[B_3H_7(NCO)]^-$ at Pt in 0.1 M Bu_4NBF_4/CH_2Cl_2

oxidation processes which gave rise to a complex wave near +1.2 V. Thus the observed oxidation wave at +1.2 V in Fig. 3.8(a) did not arise from a simple oxidation of $[B_3H_7(NCO)]^-$ but rather it was complicated by oxidation of other species.

3.2.2 Anodic Behaviour of Transition Metals

It has previously been shown that transition metals exhibited three different types of behaviour in acetonitrile solution of $[BH_3CN]^-$ and $[BF_4]^-$ [83]. It is found that this behaviour also applies to solutions of $[B_3H_6(Cl)_2]^-$ and $[B_3H_6(Cl)(NCS)]^-$ in acetonitrile but there were differences in 1,3-dioxalane, dichloromethane or benzonitrile. In the latter solvents, some transition metals still exhibited behaviour which could be categorised in the three types described previously, whereas others showed no clear-cut type of behaviour. Nevertheless, the main purpose was to determine the stabilities toward oxidation of these anions and to find out which metals are suitable as anodes in each solvent for electrochemical preparation of metallaborane complexes.

The anodic behaviour of transition metals in solutions of $[B_3H_6(Cl)_2]^-$ and $[B_3H_6(Cl)(NCS)]^-$ in different solvents are presented in Tables 3.1 and 3.2. Type (a) represents metals that are themselves inert but allow anodic oxidation of the anions [Fig. 3.9(a)]. Type (b) represents metals that are inert, yielding no products from either anodic dissolution or anodic oxidation of

Table 3.1. Anodic Properties of Metals in Solution of $[B_3H_6(Cl)_2]^-$ Anion

Metals	Solvents							
	CH_3CN		1,3-dioxalane		CH_2Cl_2		PhCN	
	(1)	(2)	(1)	(2)	(1)	(2)	(1)	(2)
Ti	(a)	(0.80)	(d)	(-0.60)	(d)	(-0.5)	(b)	(-0.3)
Zr	(a)	(0.35)	(b)	(0.5)	(b)	(-0.5)	(b)	(0.6)
V	(a)	(0.40)	(d)	(-0.40)	(d)	(-0.5)	(d)	(-0.2)
Nb	(b)	(1.0)	(d)	(-0.40)	(d)	(-0.6)	(b)	(-0.3)
Ta	(a)	(0.5)	(b)	(1.20)	(b)	(-0.7)	(b)	(0.8)
Mo	(a)	(0.85	(d)	(-0.3)	(d)	(-0.4)	(d)	(-0.2)
W	(a)	(1.15)	(d)	(-0.4)	(d)	(-0.5)	(b)	(-0.4)
Co	(c)	(-0.30)	(c)	(-0.3)	(c)	(-0.3)	(c)	(0.0)
Ni	(c)	(-0.40)	(c)	(-0.4)	(e)	(-0.4)	(c)	(-0.4)
Pd			(d)	(0.0)	(d)	(-0.2)	(d)	(-0.2)
Pt	(a)	(0.85)	(a)	(1.05)	(a)	(0.4,1.0)	(a)	(1.3)
Cu	(c)	(-0.30)	(c)	(-0.3)	(c)	(-0.3)	(c)	(-0.3)
Cd	(c)	(-0.50)						

(1) Type of Behaviour (see discussion)

(2) Potential at which oxidation commenced [Type (a)]; potential at which oxidation apparently commenced [Type (b) and (d)]; dissolution potential [Type (c)]; [V vs $Ag-AgNO_3$ (0.1 mol dm^{-3})].

Table 3.2 Anodic Properties of Metals in Solution of $[B_3H_6(Cl)(NCS)]^-$ Anion.

Metals	Solvents			
	CH_3CN		1,3-dioxalane	
	(1)	(2)	(1)	(2)
Ti	(b)	(0.80)	(b)	(-0.60)
Zr			(b)	(0.20)
V			(d)	(-0.60)
Nb	(b)	(0.70)	(d)	(-0.70)
Ta			(b)	0.60)
Mo			(d)	(-0.50)
W			(d)	(-0.60)
Co	(c)	(-0.40)	(c)	(-0.30)
Ni	(c)	(-0.40)	(c)	(-0.50)
Pd			(d)	(-0.20)
Pt	(a)	(0.30)	(a)	(0.80)
Cu	(c)	(-0.60)	(c)	(-0.40)
Cd	(c)	(-0.60)		

the anions [(Fig. 3.9(b)]. Type (c) represents metals that undergo anodic dissolution [(Fig. 3.9(c)]. Type (d) represents metals that have no clear-cut behaviour of any type mentioned above [Fig. 3.9(d)].

It is found that Pt exhibits type (a) behaviour and Cu, Ni, Co exhibit type (c) behaviour in all the solvents investigated. Thus electrochemical oxidation of $[B_3H_6(Cl_2)]^-$ and $[B_3H_6(Cl)(NCS)]^-$ anions in each solvent were carried out at Pt electrodes and Cu or Ni were used as anodes for anodic dissolution in solutions of these anions.

3.2.3 Controlled Potential Electrolysis

Using the results obtained from cyclic voltammetry the anions were oxidised at Pt electrodes at suitable potentials in different solvents to investigate the electrochemical oxidation products. Attempts were also made to prepare metallaboranes from the anions studied using Cu or Ni as sacrificial anodes in the range of solvents investigated.

(a) $[B_3H_6(Cl)_2]^-$.

(i) In acetonitrile.

Controlled potential electrolysis at platinum of an acetonitrile solution of $[B_3H_6(Cl)_2]^-$ was carried out at potentials $+0.80 \longrightarrow +1.28$ V and overall one electron oxidation was involved. Gas evolution was observed in the anodic compartment. The 115.5 MHz ^{11}B n.m.r. spectrum of the product in CD_3CN indicated a major

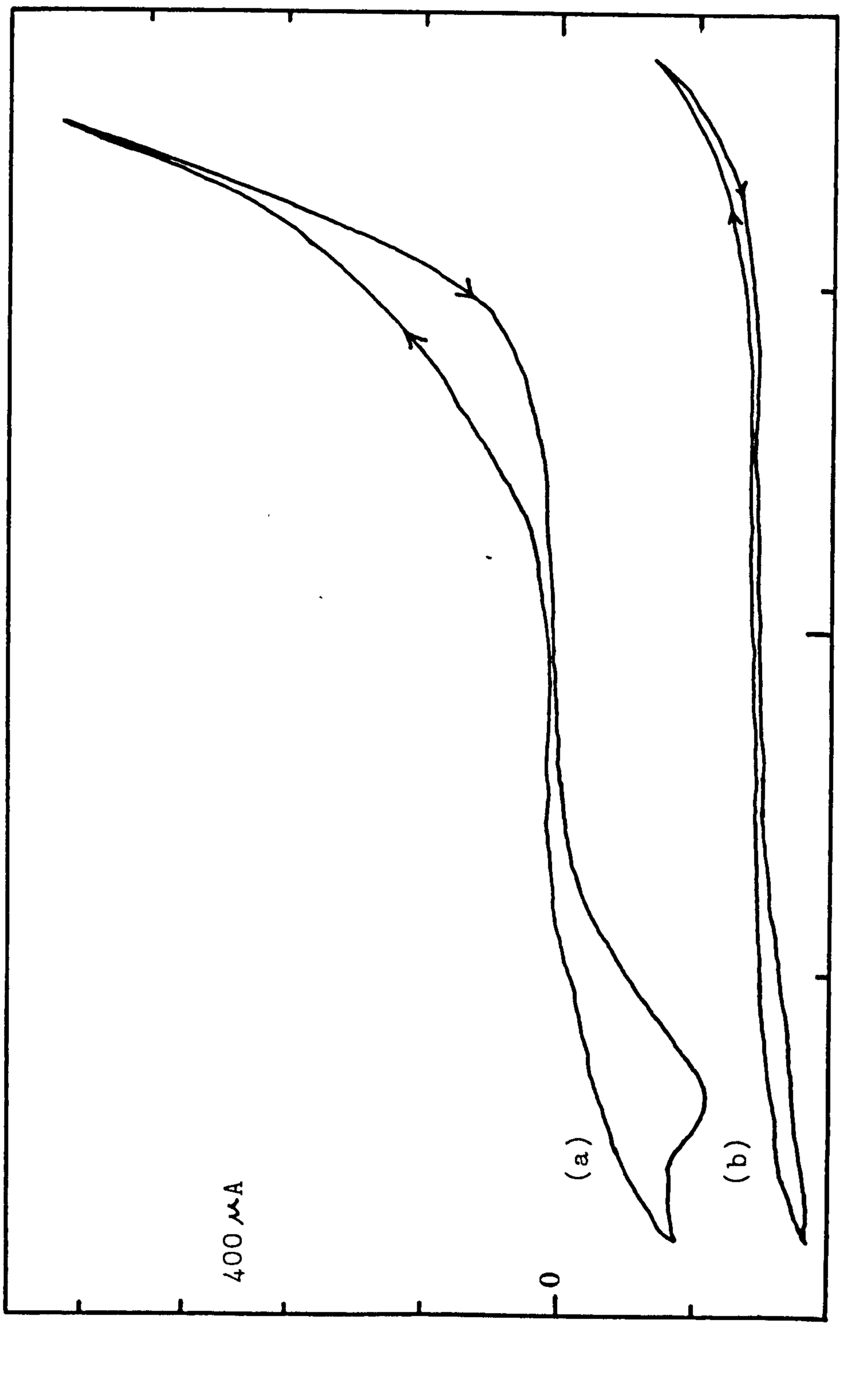

Fig.3.9. Cyclic voltammograms (scan rate 0.5 VS^{-1}) of 0.01 M $[B_3H_6(Cl)(NCS)]^-$ in CH_3CN
(a) at a Pt anode. Illustrate type (a) behaviour.
(b) at a Ti anode. Illustrate type (b) behaviour.

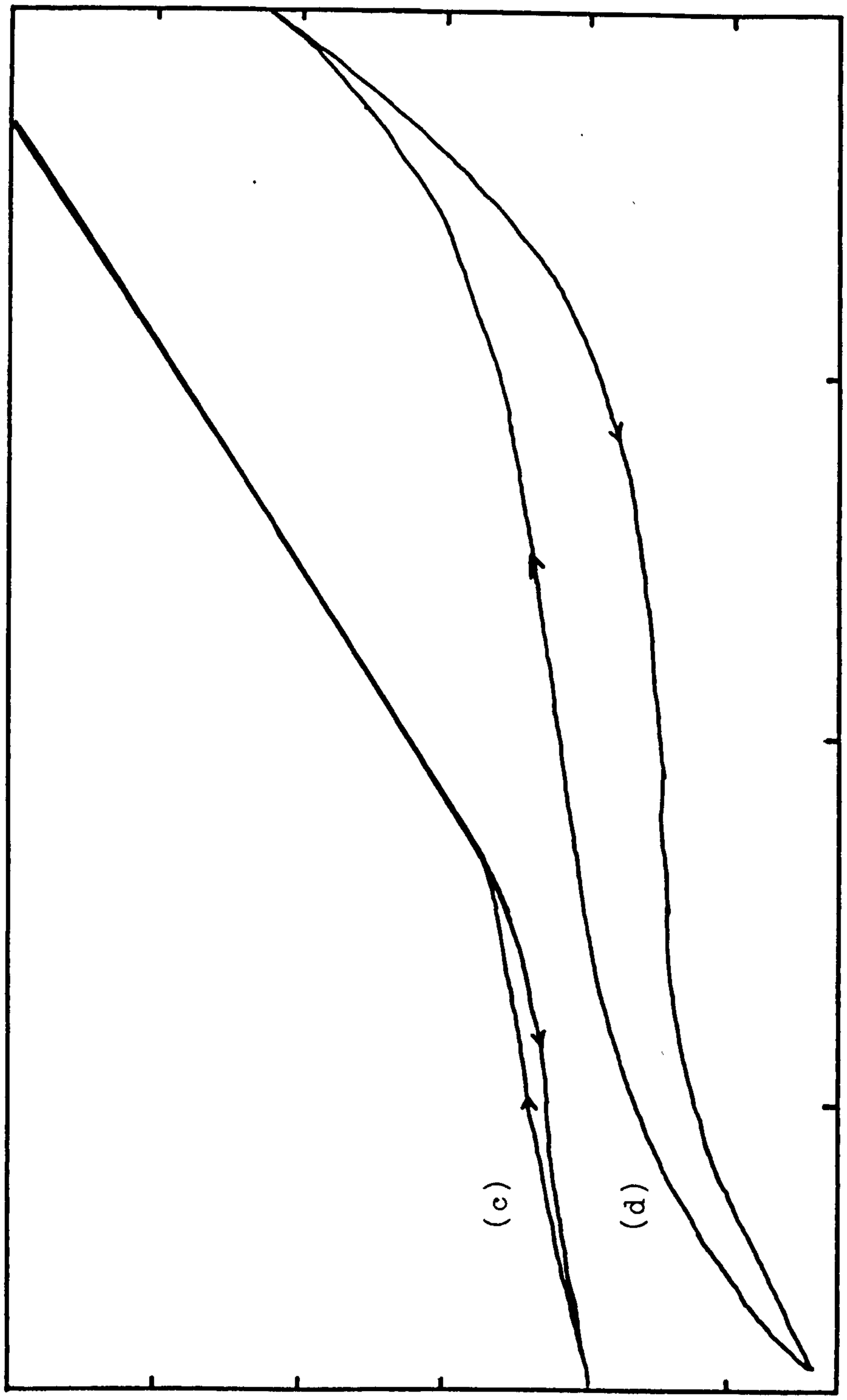

Fig.3.9. Cyclic voltammograms (scan rate 0.5 VS^{-1}) of $[B_3H_6(Cl)(NCS)]^-$ (c) at a Cu anode in CH_3CN. Illustrate type (c) behaviour. (d) at a Mo anode in 1,3-dioxalane. Illustrate type (d) behaviour.

component (90%) showing a singlet with a chemical shift of δ = +21.4 ppm (line width at half peak height = 137 Hz), a minor component showing chemical shifts at δ = +4.0, -2.8, -30.0 ppm with relative area 1:1:1, and a very small amount of starting material. A similar experiment was carried out with the addition of two equivalents of PPh_3 to the anodic compartment. The products obtained were the same with an additional small amount of $[PPh_3]BH_3$ (1:3:3:1 quartet of doublets, δ = -36.2 ppm, J_{BH} = 93 Hz)[150].

The electrolysis of an acetonitrile solution of $[B_3H_6(Cl)_2]^-$ at a copper anode proceeded at potentials -0.3 $\longrightarrow$ +0.3 V. Copper entered the solution as Cu(I). The products were identical to those obtained at Pt electrode except that no starting material was observed. The proton decoupled ^{11}B n.m.r. spectrum showed line sharpening at resonances +4.0, -2.8, -30.0 ppm whereas the boron resonance at δ = +21.4 ppm showed no significant line sharpening, this indicated that the former boron-containing product had hydrogens bonded to boron atoms.

The products obtained from electrolysis at the Cu anode were examined by ^1H n.m.r. spectroscopy. The ^1H n.m.r. spectrum revealed that the products consisted of several organic compounds. It showed resonances near +7.5 ppm which indicated the $[N(PPh_3)_2]^+$ cation, a broad peak at δ = +2.3 ppm which was probably assigned to protons in a disubstituted triborate and corresponded

to a minor component of the boron-containing products (δ = 4.0, -2.8, -30.0 ppm in ^{11}B n.m.r. spectrum), broad peaks at δ =+5.89 and +4.76 ppm which were possibly associated with the boron resonance at +21.4 ppm. Further peaks which appeared to be organic compounds were the resonances at δ = +0.9 ppm (a triplet of relative area three), δ = +1.35 ppm (a sextet of relative area two), and δ = +1.57 ppm (a poorly resolved quintet of relative area two), which looked to be related to each other and was probably an n-propyl group with the CH_2 group at the end of the chain additionally coupling to other nuclei. Other peaks appeared at δ = 3.14 ppm (quartet of ab pattern) and δ = 4.05 ppm quartet).

(ii) In 1,3-dioxalane.

The controlled potential electrolysis at platinum of $[B_3H_6(Cl)_2]^-$ in 1,3-dioxalane proceeded at a potential of +1.2 V and involved overall one electron oxidation. Gas evolution was observed in the anodic compartment and the anolyte became acidic (pHl). The ^{11}B n.m.r spectrum showed several intense resonances; at +24.0 ppm, a sharp peak (line width at half peak height = 104 Hz) with relative area one, and at +20.0 ppm, a broader peak (line width at half peak height = 500 Hz) with relative area two were major boron containing products; in addition very weak resonances were observed at -0.1 ppm (thought to be $[BF_4]^-$ passing through the membrane) and at +31.7 ppm (a trace of an

unidentified boron-containing impurity).

The electrolysis at a copper anode of $[B_3H_6(Cl)_2]^-$ in 1,3-dioxalane proceeded at a potential of +0.3 V. Copper entered the solution as Cu(I). The boron-containing products were similar to those obtained at the Pt electrode in 1,3-dioxalane. The ^{11}B n.m.r. spectrum showed resonances with chemical shifts at δ = +23.8 ppm with relative area one, δ = +19.5 ppm with relative area two as major products, and at δ = -0.3 ppm ($[BF_4]^-$) and δ = +31.5 ppm as trace impurities.

The proton-decoupled ^{11}B n.m.r. spectra of both products were very similar to those of the coupled ^{11}B n.m.r.; this indicated that the boron-containing products had no direct bond to hydrogens.

The 360 MHz ^1H n.m.r. spectrum in $CDCl_3$ of the products obtained from the Cu anode was complex. It comprised many peaks in the chemical shift range 3.2 - 4.8 ppm. Two intense peaks at δ = +3.65 ppm and +4.68 ppm with relative area 2:1 could be associated with coordinated 1,3-dioxalane (chemical shift of 1,3-dioxalane δ = 3.9 and 4.9 ppm with relative area 2:1), and other small peaks at 3.79, 4.1, 4.45, 4.75, 4.80, 4.83 ppm could be associated with products which resulted from ring opening of 1,3-dioxalane and further chemical reaction. The ring opening of 1,3-dioxalane may be due to hydrolysis, hydrogenation or chlorination yielding species such as $HOCH_2CH_2OH$, RCH_2-OR, R-CH_2Cl whose chemical shifts lie in this region. The resonances near +7.5 ppm which resulted from the $[N(PPh_3)_2]^+$ cation were

weak and this implied that the boron-containing products could be neutral compounds. Broad peaks at δ = 3.97 ppm and 4.25 ppm with some structure were also observed.

(iii) Dichloromethane.

The controlled potential electrolysis at platinum of $[B_3H_6(Cl)_2]^-$ in dichloromethane was carried out at potentials +1.2 $\longrightarrow$ +1.4 V but only a very small current passed through the cell. Thus dichloromethane is not a suitable solvent for this anion due to the low dielectric constant of the solvent.

(iv) In benzonitrile.

The controlled potential electrolysis at platinum of $[B_3H_6(Cl)_2]^-$ in benzonitrile proceeded at a potential of +1.2 V and involved overall one electron oxidation. The ^{11}B and $^{11}B\{^1H\}$ n.m.r. spectra in $PhCN/CD_3CN$ of the product were similar and each showed a broad peak (line width at half peak height ~ 230 Hz) at δ = +22 ppm and in addition a little starting material was left. The resonance with chemical shift of +22 ppm may be expected to occur at +23 ppm in CD_3CN with reference to starting material. Thus this boron-containing product is different to that obtained from electrolysis in acetonitrile. The ^{11}B n.m.r. spectrum in $CDCl_3$ of this product showed peaks at +20.5 ppm and +21.5 ppm (shoulder). This could be due to the solvent effect on resolution as shown in n.m.r. spectra of $[B_3H_6(Cl)(NCS)]^-$ in CD_3CN and $CDCl_3$. The ^1H n.m.r. spectrum showed weak resonances which indicated the $[N(PPh_3)_2]^+$ cation

near δ = 7.5 ppm, a singlet at δ = 1.26 ppm and a weak quartet at δ = 0.86 ppm.

The electrolysis of benzonitrile solution of $[B_3H_6(Cl)_2]^-$ at a copper anode proceeded at potentials $0.0 \longrightarrow +0.22$ V. Copper entered the solution as Cu(I). The yellowish product changed to a green solution during the course of monitoring it by n.m.r. spectroscopy. The ^{11}B n.m.r. spectrum showed only a single peak (line width at half peak height = 58 Hz) at δ = +0.7 ppm as the only boron-containing product.

(b) $[B_3H_6(Cl)(NCS)]^-$.

(i) In acetonitrile.

Controlled potential electrolysis in acetonitrile at platinum of $[B_3H_6(Cl)(NCS)]^-$ proceeded at potential +1.0 V and involved about six electrons oxidation. The ^{11}B n.m.r. spectrum of the products indicated only a small amount of boron-containing species present in the solution. The electrochemical oxidation might lead to an unstable intermediate which then degraded to insoluble precipitate or some volatile species.

The electrolysis of an acetonitrile solution of $[B_3H_6(Cl)(NCS)]^-$ at a copper anode proceeded at potentials $-0.4 \longrightarrow -0.2$ V. Copper entered the solution as Cu(I). The ^{11}B n.m.r. spectrum in CH_3CN/CD_3CN of the product indicated unchanged starting material as the major component (60%), and a product at δ = +20.0 ppm. The ^{11}B n.m.r. spectrum in $CDCl_3$ also indicated starting

material as the major component, and traces of unidentified decomposition products (δ = -14.75, -23.25, -32.5 ppm). The electrolysis at a copper anode of an acetonitrile solution of $[B_3H_6(Cl)(NCS)]^-$ with two equivalents of PPh_3 added was carried out in the same way. The products, identified by their ^{11}B n.m.r. spectra in $CDCl_3$, were $[PPh_3]BH_3$ (1:3:3:1 quartet of doublets δ = 38.2 ppm, J_{BP} = 53 Hz, J_{BH} = 92 Hz)[150] as a major component and other decomposition products (δ = -23.8, -22.8, +20.0 ppm). There was no starting material left.

The electrolysis at a nickel anode of an acetonitrile solution of $[B_3H_6(Cl)(NCS)]^-$ containing two equivalents of PPh_3 proceeded at potentials -0.35 $\longrightarrow$ -0.27 V. Nickel entered the solution as Ni(II), and therefore the electrolysis was stopped when only half equivalent of Ni(II) had dissolved. The products, identified by their 80 MHz ^{11}B n.m.r. spectra, were identified as starting material as the major component (50%), $[PPh_3]BH_3$ (δ = -36.8 ppm, J_{BP} = 53 Hz, J_{BH} = 92 Hz) and other unidentified products (δ = +20.5, +22.0 ppm).

(ii) In 1,3-dioxalane.

Controlled potential electrolysis at platinum of $[B_3H_6(Cl)(NCS)]^-$ in 1,3-dioxalane proceeded at potentials +1.2 $\longrightarrow$ +1.3 V and only one electron oxidation was involved. The 115.5 MHz ^{11}B and $^{11}B\{^1H\}$ n.m.r. spectra in $CDCl_3$ of the products were similar to those from electrolysis of $[B_3H_6(Cl)_2]^-$ in 1,3-dioxalane where

only peaks at δ = +23.7 ppm (relative area one) and at δ = +19.0 ppm (relative area two) were observed.

The electrolysis of 1,3-dioxalane solution of $[B_3H_6(Cl)(NCS)]^-$ at a copper anode proceeded at potentials 0.0 $\longrightarrow$ +1.0. There was no significant weight loss of the Cu electrode. The products were identical to those obtained at a Pt electrode.

(iii) In dichloromethane.

Controlled potential electrolysis at platinum of $[B_3H_6(Cl)(NCS)]^-$ in dichloromethane proceeded at potentials between +1.2 $\longrightarrow$ +1.3 V but only a very low current passed through the cell. The products were starting material (90%) and traces of decomposition products (δ = -14, -15.2, -22.4 ppm).

3.2.4 Electrochemical Synthesis

The $[B_3H_7(NCBH_3)]^-$ anion was prepared electrochemically by electrolysis in acetonitrile at Pt electrodes of $[N(PPh_3)_2][B_3H_8]$ in the presence of $[N(PPh_3)_2][BH_3CN]$. A potential of -0.3 V, which was high enough to oxidise $[B_3H_8]^-$ but not $[BH_3CN]^-$, was applied to the working electrode. The products consisted of $[B_3H_7(NCBH_3)]^-$ and $B_3H_7[CH_3CN]$ and were purified by chromatography.

Attempts to synthesize $[B_3H_7(NC)]^-$ in a similar method by electrolysis in dichloromethane at Pt electrodes of $[N(PPh_3)_2][B_3H_8]$ in the presence of $[PPh_4]CN$ were unsuccessful. $[B_3H_8]^-$ remained unoxidised at

potentials between -0.3 V $\longrightarrow$+0.10V whereas $[PPh_4]CN$ was oxidised to give a black-brown precipitate.

3.2.5 Conclusion.

The results showed that in acetonitrile, the oxidation potentials of $[B_3H_6(Cl)_2]^-$ and $[B_3H_6(Cl)(NCS]^-$ were near +1.1 V and their cyclic and a.c. voltammograms were similar; however their electrochemical processes were different. These were shown in cyclic voltammetry that the electrode mechanisms were different and electrolyses of the anions led to different products. Electrolyses of $[B_3H_6(Cl)(NCS)]^-$ in acetonitrile in most cases led to decomposition products, while electrolyses of $[B_3H_6(Cl)_2]^-$ in acetonitrile yielded some interesting minor products - including a disubstituted triborate, which was unstable and decomposed to other products. It was thought that acetonitrile might be a solvent which was too polar for the oxidation products or metallaborane complexes to survive; therefore cyclic voltammetry and electrolysis in other solvents were investigated.

It was found that 1,3-dioxalane is not a better solvent than acetonitrile for this work. It is likely that it reacted with the anions or intermediate species which underwent similar electrochemical or chemical processes yielding similar products. This was confirmed by electrolysis in 1,3-dioxalane at Pt electrodes of $[B_3H_7(NCS)]^-$, in which the ^{11}B and ^{1}H n.m.r. spectra of the products showed resonances of similar chemical shift

and appearance as those observed in the corresponding spectra of $[B_3H_6(Cl)_2]^-$.

Benzonitrile is not very convenient to use for electrolysis due to its high boiling point and is not suitable for this work because decomposition products of the anions precipitated on electrolysis.

Dichloromethane could not be used as a solvent for this work as its dielectric constant is too low to conduct the current through the electrolysis cell unless a suitable supporting electrolyte was introduced. In this work, addition of supporting electrolyte would lead to difficulties in separation since the disubstituted octahydrotriborate anions are readily hydrolyzed on the silica gel used in column chromatography.

3.3 EXPERIMENTAL

$[N(PPh_3)_2][B_3H_6(Cl)_2]$, $[N(PPh_3)_2][B_3H_6(Cl)(NCS)]$, $[N(PPh_3)_2][B_3H_7(NCS)]$ and $[N(PPh_3)_2][B_3H_8]$ were prepared as described in Chapter 2.

The details of general reagents and solvents for electrochemistry, cell designs and other electrochemical equipment are presented in Chapter 6.

3.3.1 Electrochemical Oxidation of $[N(PPh_3)_2][B_3H_6(Cl)_2]$

3.3.1(a) In acetonitrile.

(i) Without PPh_3

$[N(PPh_3)_2][B_3H_6(Cl)_2]$ (0.162g, 0.25 mmol) was dissolved in CH_3CN (15 cm^3) and placed in the anodic

compartment of the cell. The cathodic compartment contained a solution of $[NBu_4^n][BF_4]$ (0.1 mol dm^{-3}) in acetonitrile (15 cm^3). Both working and secondary electrodes were Pt foil, the reference electrode was $Ag/AgNO_3$ (0.1 mol dm^{-3}) in acetonitrile. A potential of $+0.80 \longrightarrow +1.28$ V was applied to the working electrode. The current rose to a maximum of 5 mA and decayed exponentially to 0.6 mA (ca. 3 hr.) after the passage of 24.98 C (this corresponded to 1.03 times that calculated for 1 e^- oxidation). Gas evolution was observed in both compartments. The clear, colourless anolyte was evaporated under vacuum to dryness and examined by 115.5 MHz n.m.r. spectroscopy.

(ii) With PPh_3.

The set-up was the same as that described above except that PPh_3 (0.131g, 0.50 mmol) was added. The product was examined by 80 MHz ^{11}B n.m.r. spectroscopy.

3.3.1(b) In 1,3-dioxalane.

The conditions were similar to those described in sect. 3.3.1(a) except that the solvent, 1,3-dioxalane was used and the reference electrode was $Ag/[N(PPh_3)_2]Cl$ (0.1 mol dm^{-3}) in 1,3-dioxalane. A potential of +1.2 V was applied to the working electrode. The current was 3 mA and fell exponentially to 0.1 mA after the passage of 28.9 C (corresponding to 1.2 times that calculated for 1 e^-). Gas evolution was observed in both compartments and the anolyte was found to be acidic (pH 1).

dryness and was examined by ^{11}B and ^{1}H n.m.r. spectroscopy.

3.3.2 Electrochemical Oxidation of $[N(PPh_3)_2][B_3H_6(Cl)(NCS)]$.

3.3.2(a) In acetonitrile.

The set-up was the same as that described in sect. 3.3.1(a) except that $[N(PPh_3)_2][B_3H_6(Cl)(NCS)]$ (0.213g, 0.318 mmol) was used. A potential of +1.0 V was applied to the working electrode. The current rose to a maximum of 20 mA and decayed exponentially to 0.5 mA after the passage of 175.9 C (compared with 184.1 C theoretically calculated for 6 e^- oxidation). The anolyte was evaporated under vacuum to dryness yielding a yellowish oil which was monitored by 80 MHz ^{11}B n.m.r. spectroscopy.

3.3.2(b) In 1,3-dioxalane.

$[N(PPh_3)_2][B_3H_6(Cl)(NCS)]$(0.134g, 0.2 mmol) was dissolved in 1,3-dioxalane (10 cm^3) in anodic compartment. The cathodic compartment contained solution of $[NBu^n_4][BF_4]$(0.1 mol dm^{-3}) in 1,3-dioxalane (10 cm^3). Both working and seconary electrodes were Pt foil, the reference electrode was Ag/$[N(PPh_3)_2]$Cl (0.1 mol dm^{-3}) in 1,3-dioxalane. A potential of +1.2 $\longrightarrow$ +1.3 V was applied to the working electrode. The current was 2.5 mA and dropped exponentially to 0.3 mA after the passage of 19.3 C which is equivalent to 1 e^- oxidation.

The clear colourless anolyte was evaporated under vacuum to dryness and was examined by the 115.5 MHz ^{11}B n.m.r. spectroscopy.

3.3.2(c) In dichloromethane.

The set-up was the same as that described in sect. 3.3.2(b) except that the solvent dichloromethane was used. The current was very low and the total current corresponded to less than one-half electron oxidation. The 80 MHz n.m.r. spectrum indicated starting material (90%) as a major component and traces of decomposition products.

3.3.3 Electrochemical Oxidation of $[N(PPh_3)_2][B_3H_7(NCS)]$ in 1,3-dioxalane.

The set-up was the same as that described in sect. 3.3.2(b) except that $[N(PPh_3)_2][B_3H_7(NCS)]$ (0.127g, 0.2 mmol) was used. A potential of +1.3 V was applied to the working electrode. The current rose to a maximum of 3 mA and fell to 0.3 mA after the passage of 17.5 C (corresponding to 0.9 e^- of that theoretically calculated for 1 e^-). The colourless anolyte was evaporated under vacuum to dryness and examined by 115.5 MHz ^{11}B and 360 MHz ^{1}H n.m.r. spectroscopy.

3.3.4 Anodic Dissolution of Copper in Solutions of $[N(PPh_3)_2][B_3H_6(Cl)_2]$.

3.3.4(a) In acetonitrile.

$[N(PPh_3)_2][B_3H_6(Cl)_2]$ (0.162g, 0.25 mmol) was dissolved in acetonitrile (15 cm^3) in the anodic compartment of the cell. The cathodic compartment contained a solution of $[NBu^n_4][BF_4]$ (0.1 mol dm^{-3}) in acetonitrile (15 cm^3). The working electrode was Cu foil and the secondary electrode was Pt foil. The reference electrode was $Ag/AgNO_3$ (0.1 mol dm^3) in acetonitrile. A potential of $-0.3 \longrightarrow +0.3$ V was applied to working electrode and stopped after 1 e^- electrolysis. The weight loss of Cu electrode was 0.0155g [c.f. theoretically 0.0159g for $Cu \longrightarrow Cu(I)$]. The colourless anolyte changed to pale yellow rapidly on being evaporated under vacuum to dryness. The pale yellow solid changed to brown on standing. The product was examined by 115.5 MHz ^{11}B and 360 MHz ^1H n.m.r. spectroscopy.

3.3.4(b) In 1,3-dioxalane.

The conditions were the same as those described in sect. 3.3.4(a) except that the solvent 1,3-dioxalane was used and the reference electrode was $Ag/[N(PPh_3)_2]Cl$ (0.1 mol dm^{-3}) in 1,3-dioxalane. A potential of +0.3 V was applied to the working electrode and the maximum current was 9 mA and fell to 3 mA after the passage 24.3 C. The weight loss of Cu electrode was 0.0165g [c.f. theoretically 0.0159g for $Cu \longrightarrow Cu(I)$]. Gas evolution

was observed in both compartments and a dark brown precipitate formed in the anodic compartment during electrolysis. The anolyte was evaporated under vacuum to dryness yielding a dark brown solid which was monitored by 115.5 MHz ^{11}B n.m.r. spectroscopy.

3.3.4(c) In benzonitrile.

The conditions were the same as those described in sect. 3.3.4(a) except that the solvent benzonitrile was used and the reference electrode was Ag/$[N(PPh_3)_2]Cl$ (0.1 mol dm^{-3}) in benzonitrile. A potential of 0.0 $\longrightarrow$ +0.22 V was applied to the working electrode to maintain current at ca. 10 mA. A white precipitate formed in the colourless solution during electrolysis. After the passage of 24.7 C, the weight loss of Cu electrode was 0.0167g [c.f. theoretically 0.0159g for $Cu \longrightarrow Cu(I)$]. The anolyte was evaporated under vacuum to dryness yielding a yellowish precipitate which changed to a green solution on monitoring by 115.5 MHz ^{11}B n.m.r. spectroscopy.

3.3.5 Anodic Dissolution of Copper in Solutions of $[N(PPh_3)_2][B_3H_6(Cl)(NCS)]$.

3.3.5(a) In acetonitrile.

(i) Without PPh_3.

The set-up was the same as that described in sect. 3.3.4(a) except that $[N(PPh_3)_2][B_3H_6(Cl)(NCS)]$ (0.167g, 0.25 mmol) was used. A potential of -0.4 $\longrightarrow$

-0.18 V was applied to the working electrode and the current was 2-3 mA. After the passage of 24.22 C, the weight loss of Cu electrode was 0.0178g [c.f. theoretically 0.0159g for $Cu \longrightarrow Cu(I)$]. A small amount of black precpitate formed in the colourless anolyte. The electrolyte in the cathodic compartment changed to a green solution. The anolyte was evaporated to dryness under vacuum and was monitored by 80.2 MHz ^{11}B n.m.r. spectroscopy.

(ii) With PPh_3.

This was carried out in a similar manner, except that two equivalent of PPh_3 was added. The white product was monitored by 80.2 MHz ^{11}B n.m.r. spectroscopy.

3.3.5(b) In 1,3-dioxalane.

The set-up was the same as that described in 3.3.4(b) except that $[N(PPh_3)_2][B_3H_6(Cl)(NCS)]$ (0.134g, 0.2 mmol) was used. A potential of $0.0 \longrightarrow +1.0$ V was applied to the working electrode and the maximum current was 3 mA. After the passage of 19.3 C (ca. 5.5 hr.), the current fell to 0.8 mA. There was no significant weight loss of Cu electrode. A small amount of white precipitate formed in the yellowish anolyte which was taken to dryness under vacuum and was examined by 115.5 MHz ^{11}B n.m.r. spectroscopy.

3.3.6 Anodic Dissolution of Nickel in Acetonitrile Solution of $[N(PPh_3)_2][B_3H_6(Cl)(NCS)]$.

$[N(PPh_3)_2][B_3H_6(Cl)(NCS)]$ (0.268g, 0.4 mmol) and PPh_3 (0.2099g, 0.8 mmol) were dissolved in acetonitrile (15 cm^3) and placed in the anodic compartment of the cell. The cathodic compartment contained a solution of $[NBu^n_4][BF_4]$ (0.1 mol dm^{-3}) in acetonitrile (15 cm^3). The working electrode was a coil of nickel wire and the secondary electrode was Pt foil. The reference elctrode was $Ag/AgNO_3$ (0.1 mol dm^{-3}) in acetonitrile. A potential of -0.35 $\longrightarrow$ -0.27 V was applied to the working electrode and the current was 8 mA. After the passage of 38.9 C, the weight loss of Ni electrode was 0.0117g [c.f. theoretically 0.0117g (0.2 mmol) for Ni $\longrightarrow$ Ni(II)]. The anolyte was taken to dryness under vacuum and was examined by 80.2 MHz ^{11}B n.m.r. spectroscopy.

3.3.7 Electrochemical Synthesis of $[N(PPh_3)_2][B_3H_7(NCBH_3)]$.

$[N(PPh_3)_2][B_3H_8]$ (0.869g, 1.5 mmol) and $[N(PPh_3)_2][BH_3CN]$ (0.867, 1.5 mmol) were dissolved in acetonitrile (15 cm^3) and placed in the anodic compartment of the cell. The cathodic compartment contained solution of $[NBu^n_4][BF_4]$ (0.1 mol dm^{-3}) in acetonitrile (15 cm^3). Both working and secondary electrodes were Pt foil, the reference electrode was $Ag/AgNO_3$ (0.1 mol dm^{-3}) in acetonitrile. A potential of -0.3 V was applied to the working electrode. The current rose to

a maximum of 20 mA and fell to 4 mA after the passage of 144.8 C (1 e^- oxidation). The anolyte was evaporated to dryness yielding a white solid which was purified by chromatography over silica gel using dichloromethane as eluting solvent. The product was identified as $[N(PPh_3)_2][B_3H_7(NCBH_3)]$ by its ^{11}B n.m.r. spectroscopy.

CHAPTER 4

HIGH FIELD ^{11}B AND ^{1}H N.M.R. STUDIES OF THE OCTAHYDROTRIBORATE ANION, AND ITS MONOSUBSTITUTED AND DISUBSTITUTED DERIVATIVES.

4.1 INTRODUCTION

The ^{11}B n.m.r. spectra of monosubstituted octahydrotriborate derivatives $[B_3H_7(X)]^-$ have been reported[141]. These spectra were essentially similar to those previously reported for fluxional, neutral triborane (7) base adducts[142,143]. In general, the spectra comprised a low field (high frequency) resonance of relative area two, attributed to the unsubstituted borons, and a high field (low frequency) resonance of relative area one attributed to the substituted boron atom. Each resonance exhibited multiplet structure which resulted from coupling of the boron atoms to seven fluxional hydrogens and further coupling between ^{11}B atoms in each environment. The spectra were further complicated by partial quadrupolar relaxation. The substituents and solvents were found to affect the chemical shift of the resonances, and also the line shapes of the multiplets as a result of changes in the rate of quadrupolar relaxation.

This work has comprised studies of the ^{11}B n.m.r. spectra of disubstituted octahydrotriborate derivatives $[B_3H_6(X)(X')]^-$ and $[B_3H_7(NCO)]^-$, and the ^1H n.m.r. spectra of $[B_3H_8]^-$ and its monosubstituted and disubstituted derivatives by applying line-narrowing and specific frequency irradiation techniques.

4.2 RESULTS AND DISCUSSION

4.2.1 ^{11}B N.m.r.

(a) Disubstutited octahydrotriborate anions.

The ^{11}B n.m.r. spectra of $[B_3H_6(Cl)_2]^-$ in $CDCl_3$ and CD_3CN shown in Fig. 2.2 (Chapter 2) and Fig. 4.1 are different. In $CDCl_3$, each of the two boron environments in the ratio of 2:1 shows multiplet structure comprising seven lines of relative intensities 1:6:15:20:15:6:1 which is interpreted as coupling to six equivalent fluxional hydrogens, although the low field (high frequency) resonance of area one is less well resolved. A spectrum simulated using a computer programme is shown in Fig. 4.2(a). The parameters which gave the best fit with the experimental spectra were:-

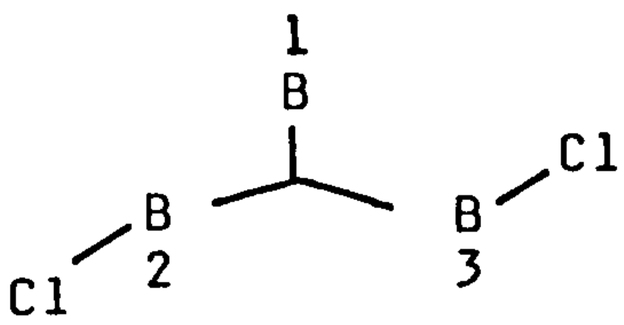

$J_{B1B2} = J_{B1B3} = J_{B2B3} \leqslant 3.0$ Hz

$J_{^{11}B-^{1}H} = 34.5$ Hz as measured from the experimental spectrum.

These parameters suggest that the ^{11}B-^{11}B coupling constant is small. In $CDCl_3$, ^{11}B-^{11}B coupling was not observed and this was attributed to the small coupling constant and line broadening resulting from quadrupolar relaxation effects. Fig. 4.2(b) shows the ^{11}B n.m.r. spectrum of $[B_3H_6(Cl)_2]^-$ in $CDCl_3$ at 323°K where the ^{11}B-^{11}B coupling is just observed. Therefore as the temperature is increased, the quadrupolar relaxation effect is reduced. However, the compound is not stable

Fig.4.1. 80.2 MHz ^{11}B n.m.r. spectrum of $[B_3H_6(Cl)_2]^-$ in CD_3CN (line-narrowed)

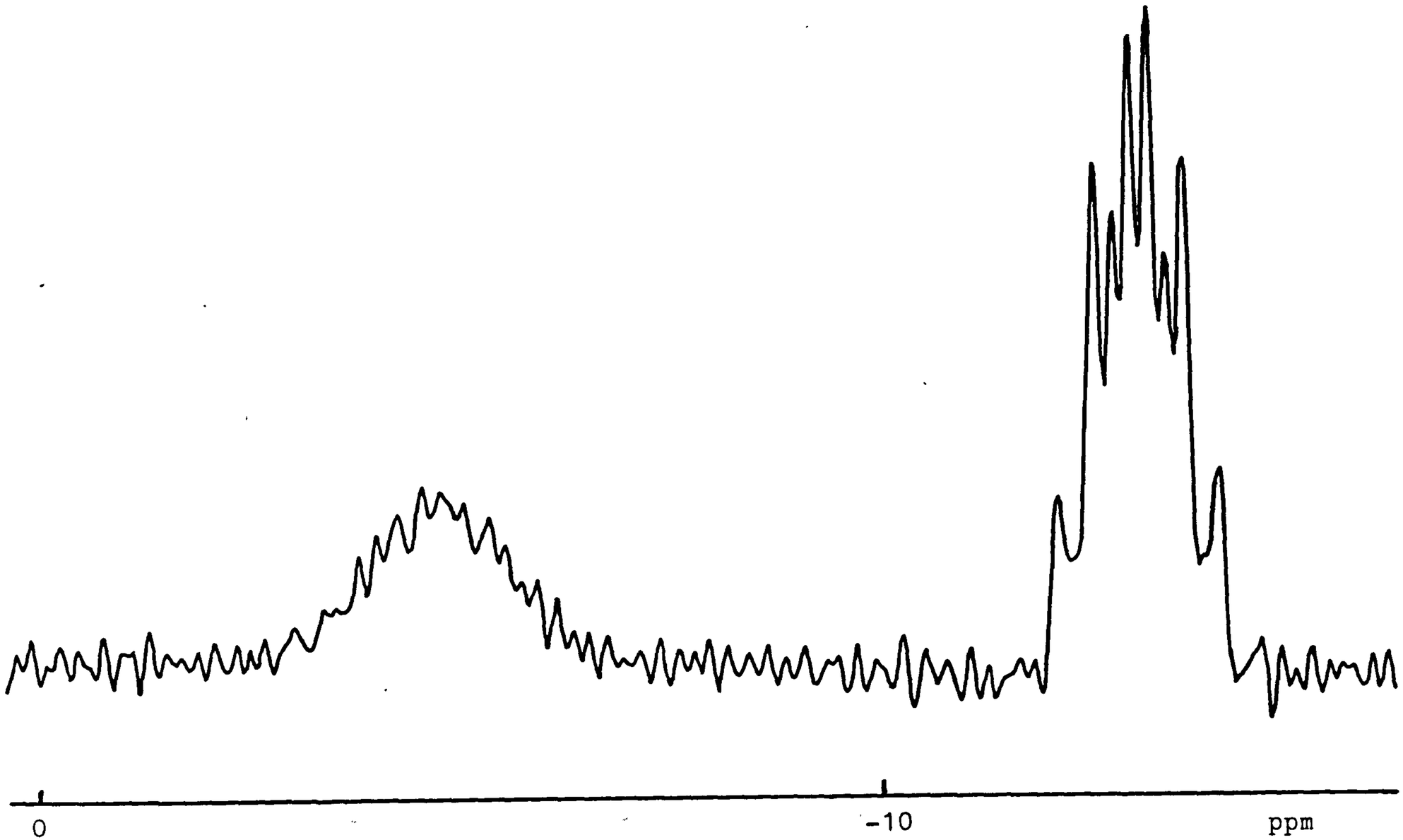

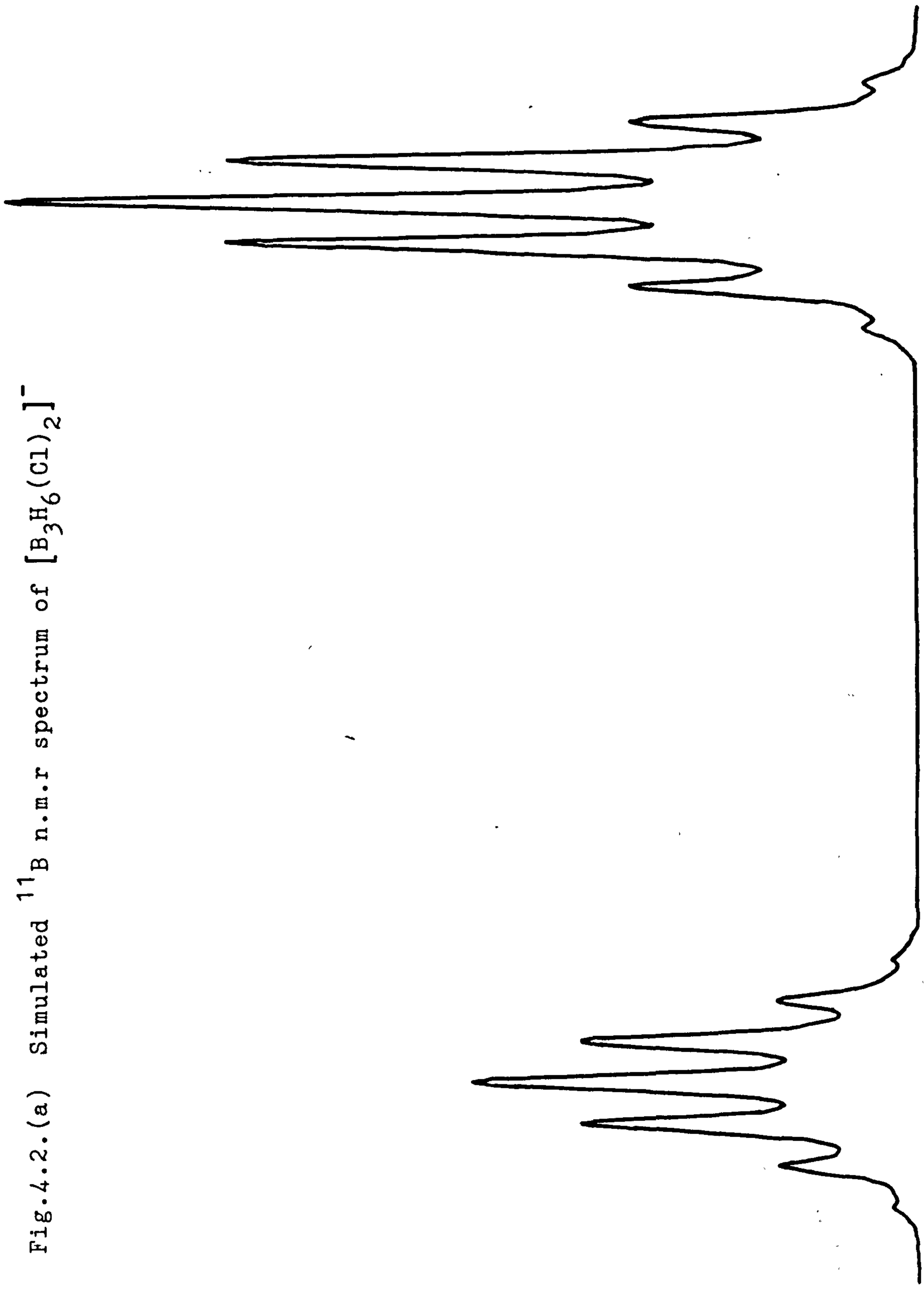

Fig.4.2.(a) Simulated ^{11}B n.m.r spectrum of $[B_3H_6(Cl)_2]^-$

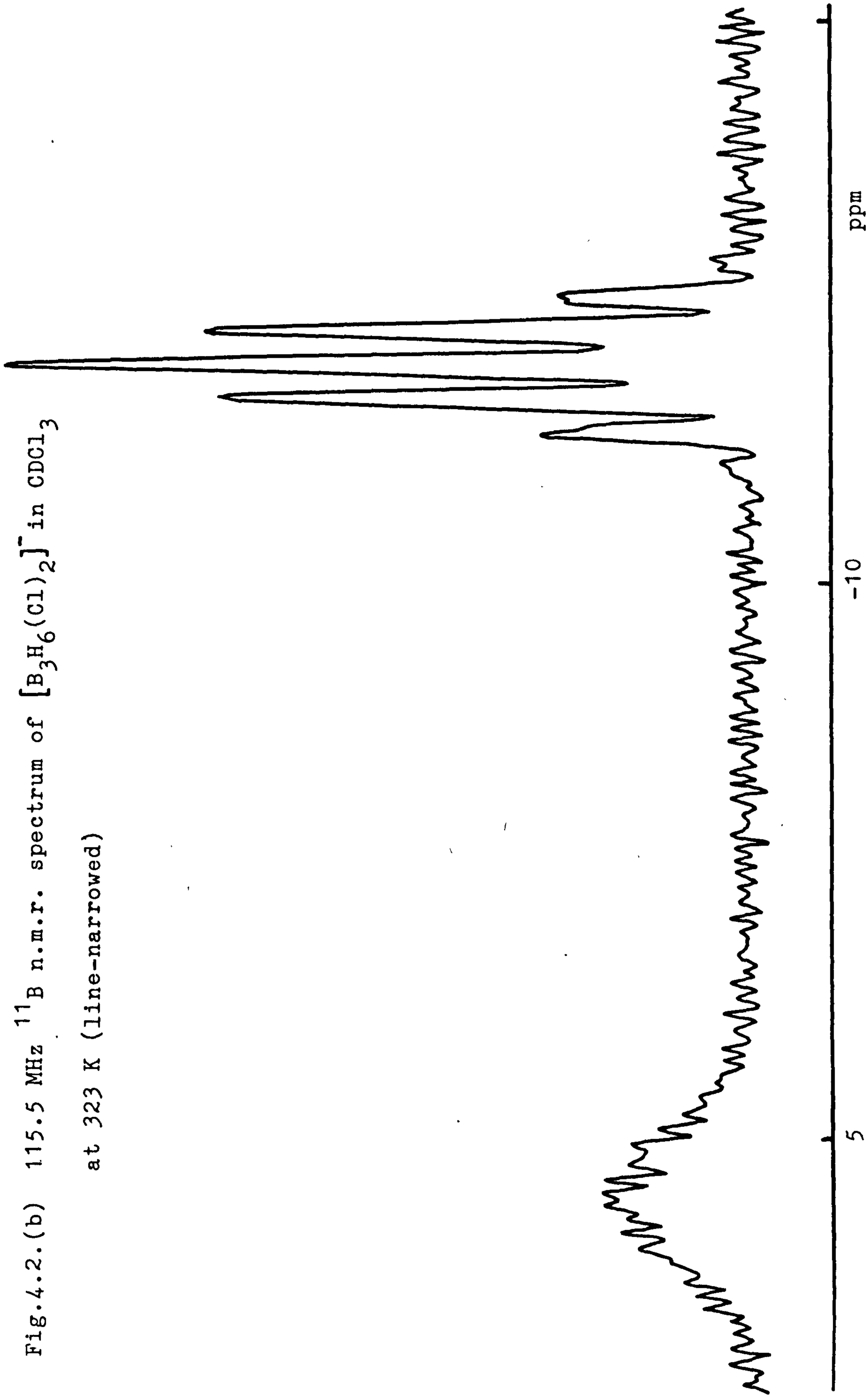

Fig.4.2.(b) 115.5 MHz ^{11}B n.m.r. spectrum of $[B_3H_6(Cl)_2]^-$ in $CDCl_3$ at 323 K (line-narrowed)

enough to operate at a higher temperature. In CD_3CN, the line-narrowed spectrum shows resolved ^{11}B-^{1}H and ^{11}B-^{11}B spin coupling which is complicated by the quadrupolar effect.

The proton decoupled ^{11}B n.m.r. spectra of $[B_3H_6(Cl)_2]^-$ in $CDCl_3$ and CD_3CN are shown in Fig. 4.3. The line-narrowed spectra failed to show well-defined ^{11}B-^{11}B coupling in $CDCl_3$, whereas in CD_3CN, some ^{11}B-^{11}B coupling was observed, although the spectra showed lines typical of partial quadrupolar relaxation. It has been shown previously that the observed line shape resulting from partial quadrupolar relaxation depend on the parameter, α, which for ^{11}B, has the relationship[141,151]

$$\alpha = \frac{5}{\pi T_1 J}$$

The separation of 16 Hz of the apparent doublet from the substituted boron atoms in the $^{11}B\{^{1}H\}$ spectrum of $[B_3H_6(Cl)_2]^-$ in CD_3CN must represent the maximum value for $J_{^{11}B-^{11}B}$. Since the observed line shape corresponded to an α-value near 5, the calculated relaxation time had a maximum value near 0.02 sec. Since more extensive collapse of the multiplet occurred in $CDCl_3$ with a line shape corresponding to an α-value closer to 20, the relaxation time in this solvent was calculated to be nearer to 0.005 sec. The observed coupling, and the more extensive multiplet collapse

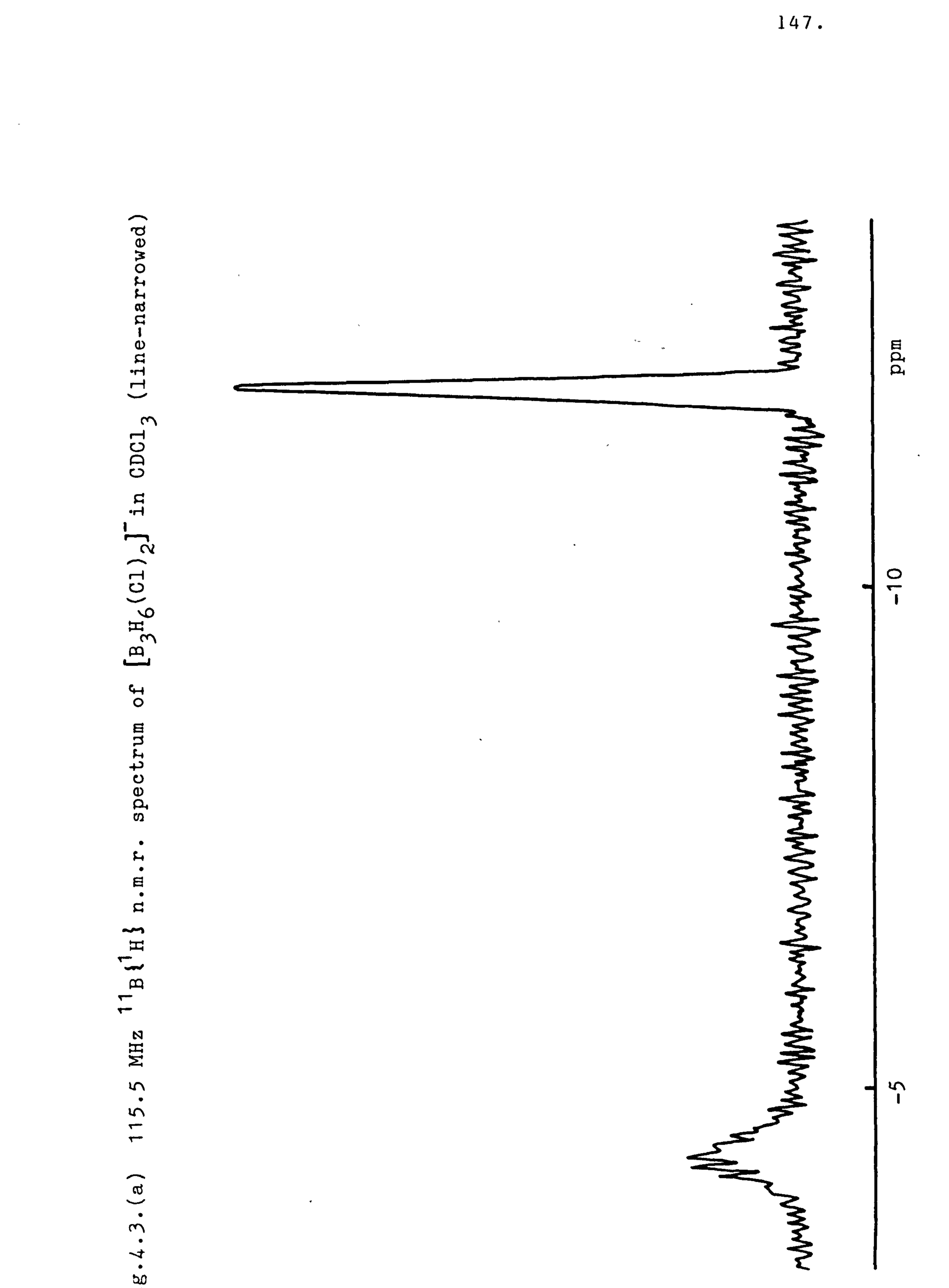

Fig.4.3.(a) 115.5 MHz $^{11}B\{^1H\}$ n.m.r. spectrum of $[B_3H_6(Cl)_2]^-$ in $CDCl_3$ (line-narrowed)

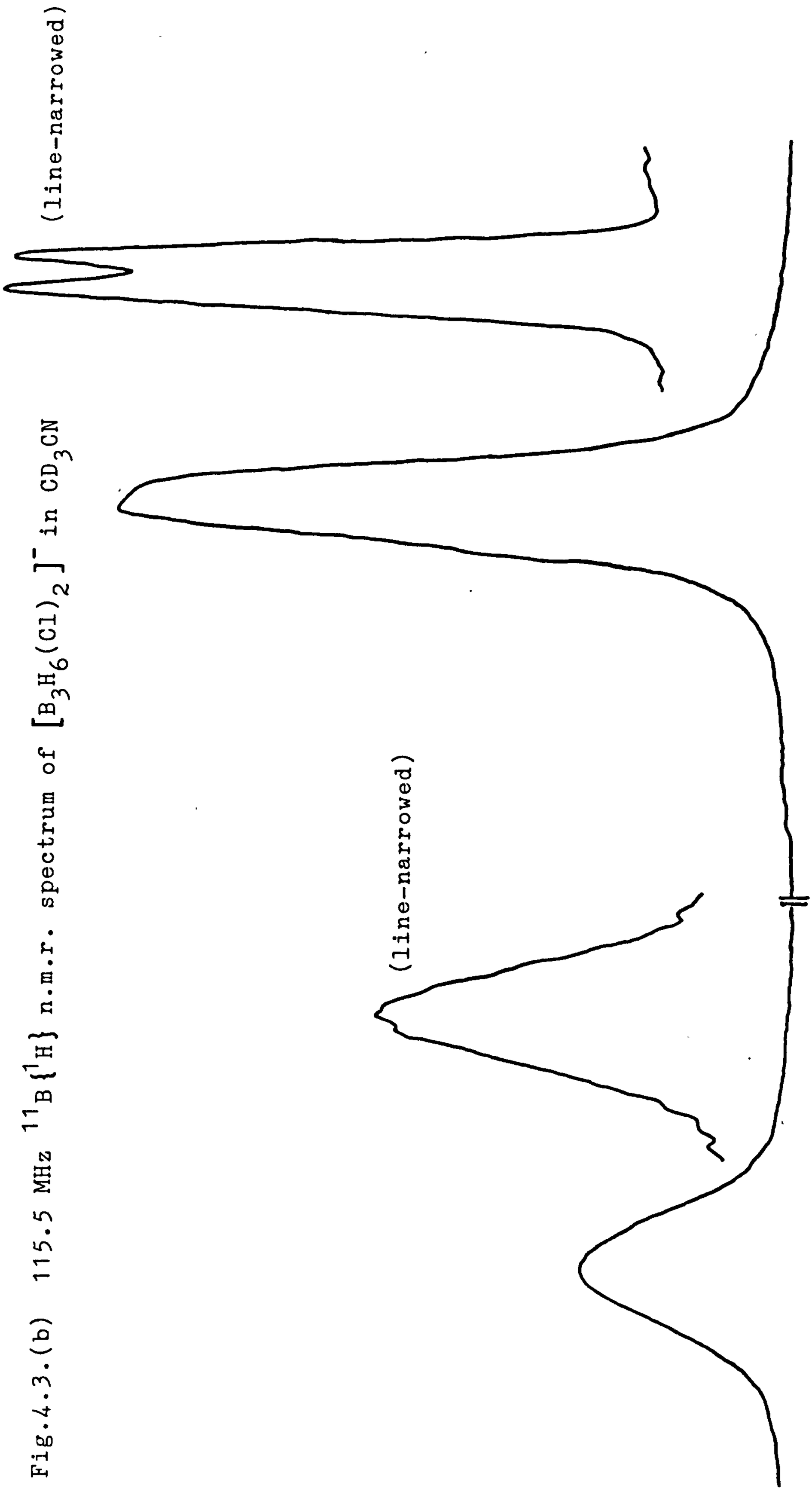

Fig.4.3.(b) 115.5 MHz $^{11}B\{^1H\}$ n.m.r. spectrum of $[B_3H_6(Cl)_2]^-$ in CD_3CN

in the lower polarity solvent are similar to effects observed earlier for $[B_3H_7(Cl)]^-$. In the earlier work, this was explained in terms of ion pairing and presumably a similar explanation applies also to the disubstituted derivatives.

The ^{11}B n.m.r. spectra in $CDCl_3$ of $[B_3H_6(Cl)(NCS)]^-$, $[\{B_3H_6(Cl)(NC)\}_2Ag]^-$ and $[B_3H_6(Cl)(NCBH_3)]^-$ each showed three unique boron chemical shifts. At ambient temperature, none of the compounds exhibited spectra in which either ^{11}B-^{11}B or ^{11}B-^{1}H couplings were resolved even with line narrowing. These are presented in Fig. 2.3 to Fig. 2.5 (Chapter 2). The $^{11}B\{^1H\}$ n.m.r. spectrum of $[B_3H_6(Cl)(NCS)]^-$ in CD_3CN is shown in Fig. 4.4. The chemical shift difference between the two unique boron resonances became less in CD_3CN than in $CDCl_3$ and the line-narrowed spectrum revealed some fine structures due to ^{11}B-^{11}B coupling.

(b) Monosubstituted octahydrotriborate anions.

The ^{11}B and $^{11}B\{^1H\}$ n.m.r. spectra of $[B_3H_7(NCO)]^-$ in $CDCl_3$ at 303°K are shown in Fig. 2.1 (Chapter 2). The ^{11}B n.m.r. spectrum exhibited a multiplet of one boron environment. The $^{11}B\{^1H\}$ n.m.r. spectrum shows only a single peak, whose width at half-height was 54 Hz, which did not resolve even with line-narrowing indicating that the difference in chemical shift of the two boron environments is very small and the ^{11}B-^{11}B coupling is also very small. The multiplet structure of the line-narrowed ^{11}B n.m.r. spectrum shown

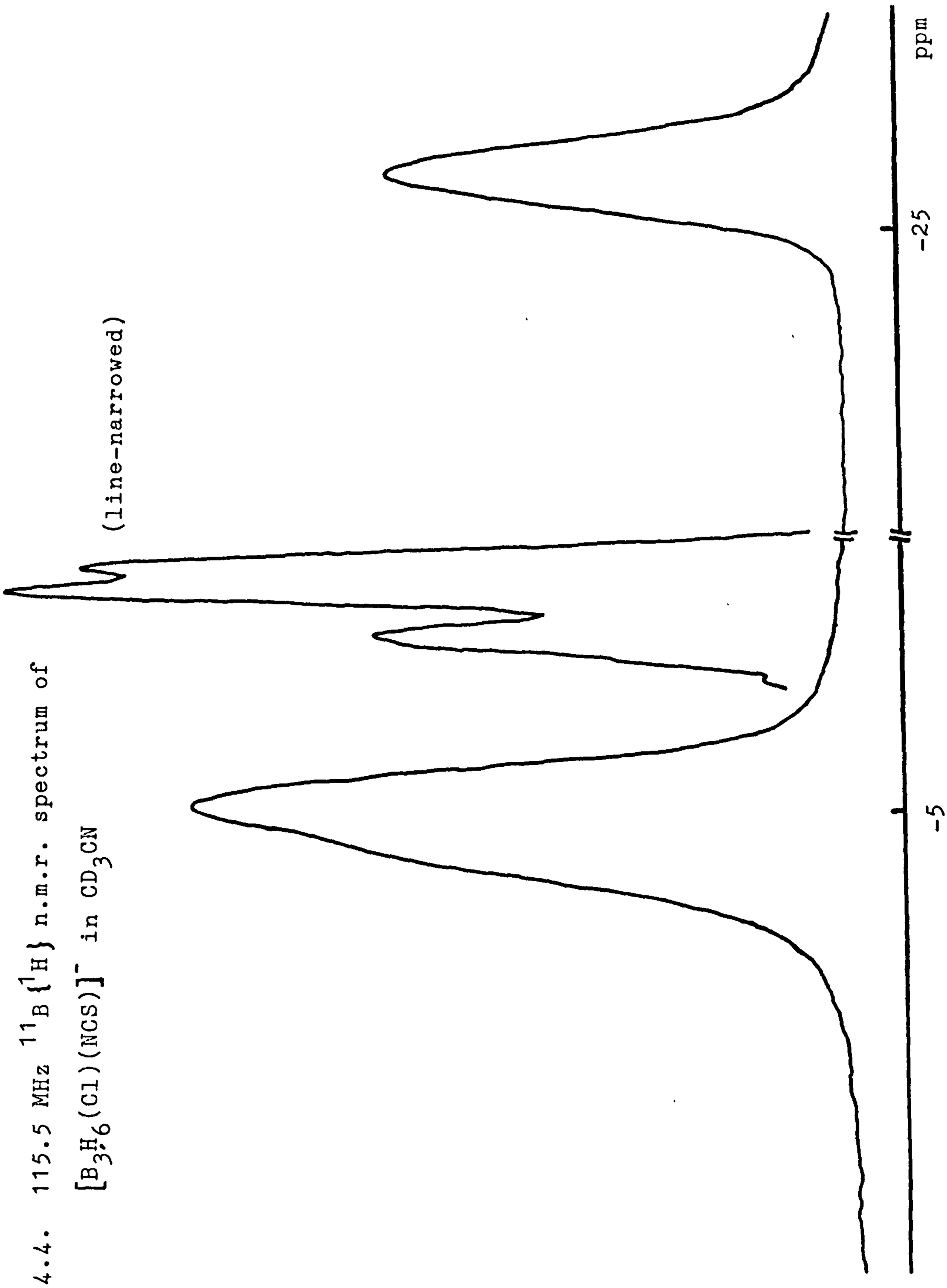

Fig.4.4.4. 115.5 MHz $^{11}B\{^1H\}$ n.m.r. spectrum of $[B_3H_6(Cl)(NCS)]^-$ in CD_3CN

in Fig. 4.5(a) indicates coupling to hydrogens with fluxional behaviour, and in which the three borons are not equivalent.

This can be better described by using a computer programme to simulate the line shapes as shown in Fig. 4.5(b). The parameters which gave the best fit with the experimental spectrum were:-

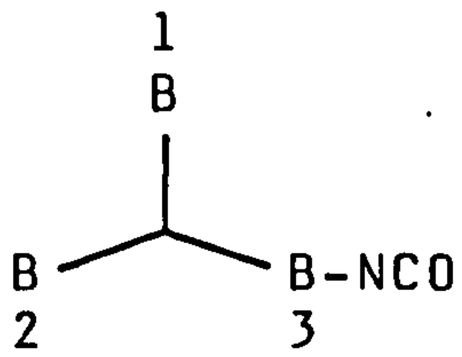

$J_{B12} = J_{B13} = J_{B23} \leqslant 3$ Hz

$J_{^{11}B-^{1}H}$ = 35.0 Hz by measuring from the experimental spectrum.

The chemical shift difference between B(3) and B(1), B(2) is 35.0 Hz and B(3) is at lower field than B(1), B(2).

When the $^{11}B\{^{1}H\}$ spectrum of $[B_3H_7(NCO)]^-$ was recorded at 323 ^{o}K (Fig. 4.6), it showed fine structure consistent with two boron environments, and corresponded with the simulated spectrum in which the substituted boron was at lower field. The structure of the line-narrowed spectrum indicated ^{11}B-^{11}B coupling with extensive quadrupolar relaxation.

The ^{11}B chemical shift data for the octahydrotriborate derivatives are presented in Table 4.1.

4.2.2 ^{1}H N.m.r.

Although the ^{11}B n.m.r. spectrum of $[B_3H_8]^-$ has been thoroughly reported[113,114,117], the correspond-

Table 4.1 ^{11}B N.m.r. Data for Octahydrotriborate Derivatives at 115.5 MHz

Substituents X	X′	B	Boron Chemical Shift(ppm) B(X)	B(X′)	Solvent
(a) Cl	Cl	-4.3	-11.9		$CDCl_3$
(b) Cl	Cl	-4.8	-11.8		$CDCl_3$
Cl	Cl	-4.0	-11.3		CD_3CN
Cl	NCS	-8.3	-4.2	-25.1	$CDCl_3$
Cl	NCS	-5.0	-4.6	-25.4	CD_3CN
(c) Cl	NC	-0.09	-3.41	-31.45	$CDCl_3$
Cl	$NCBH_3$	-2.09	-3.64	-30.5	$CDCl_3$
(b) H	NCO		-21.3	-19.8	$CDCl_3$

(a) 303°K; (b) 323 °K;

(c) In the complex $[\{B_3H_6(Cl)(NC)\}_2Ag]^-$

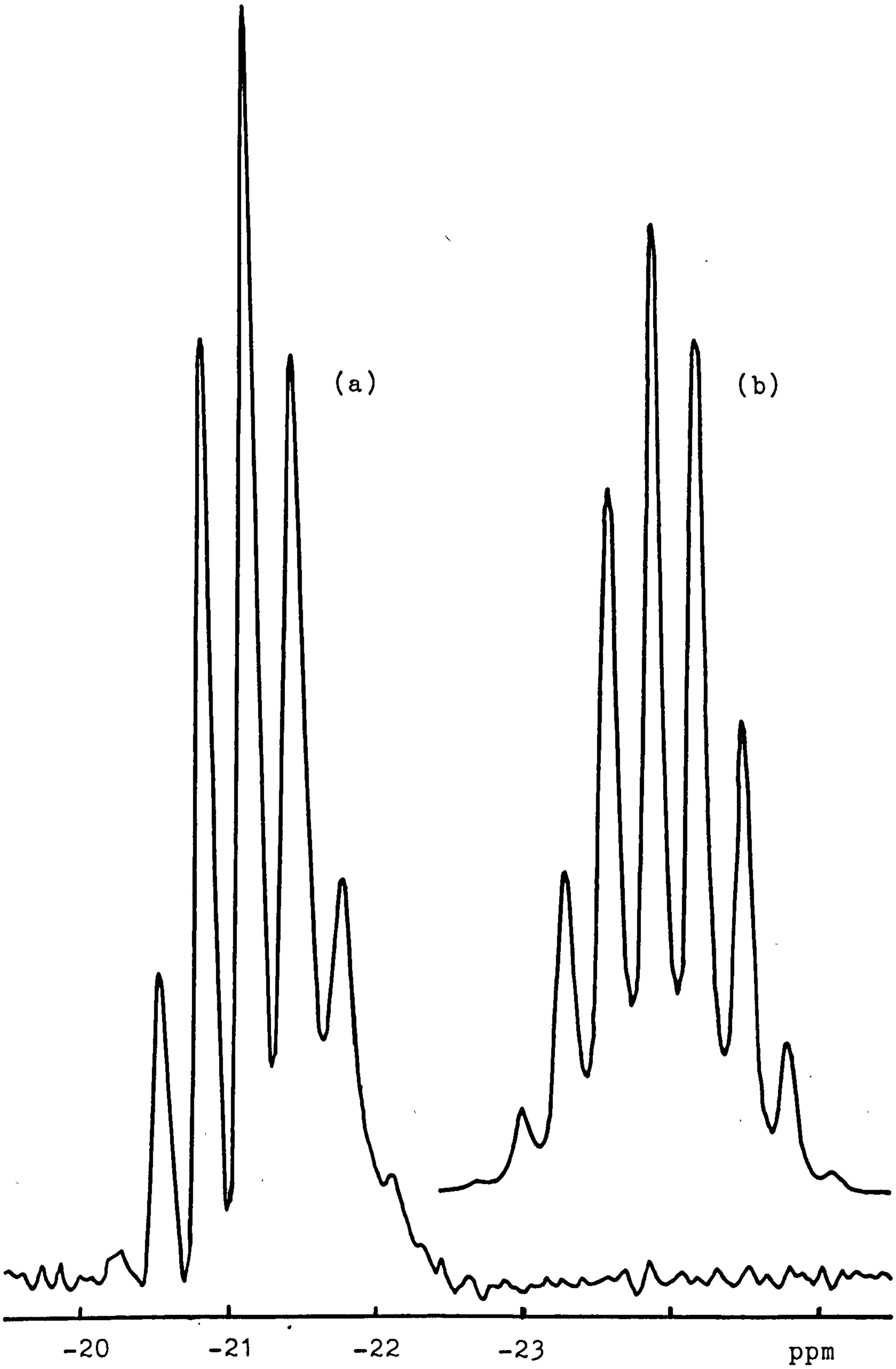

Fig.4.5. (a) Experimental (115.5 MHz) and (b) Simulated ^{11}B n.m.r. spectra of $[B_3H_7(NCO)]^-$ in $CDCl_3$ at 303 K

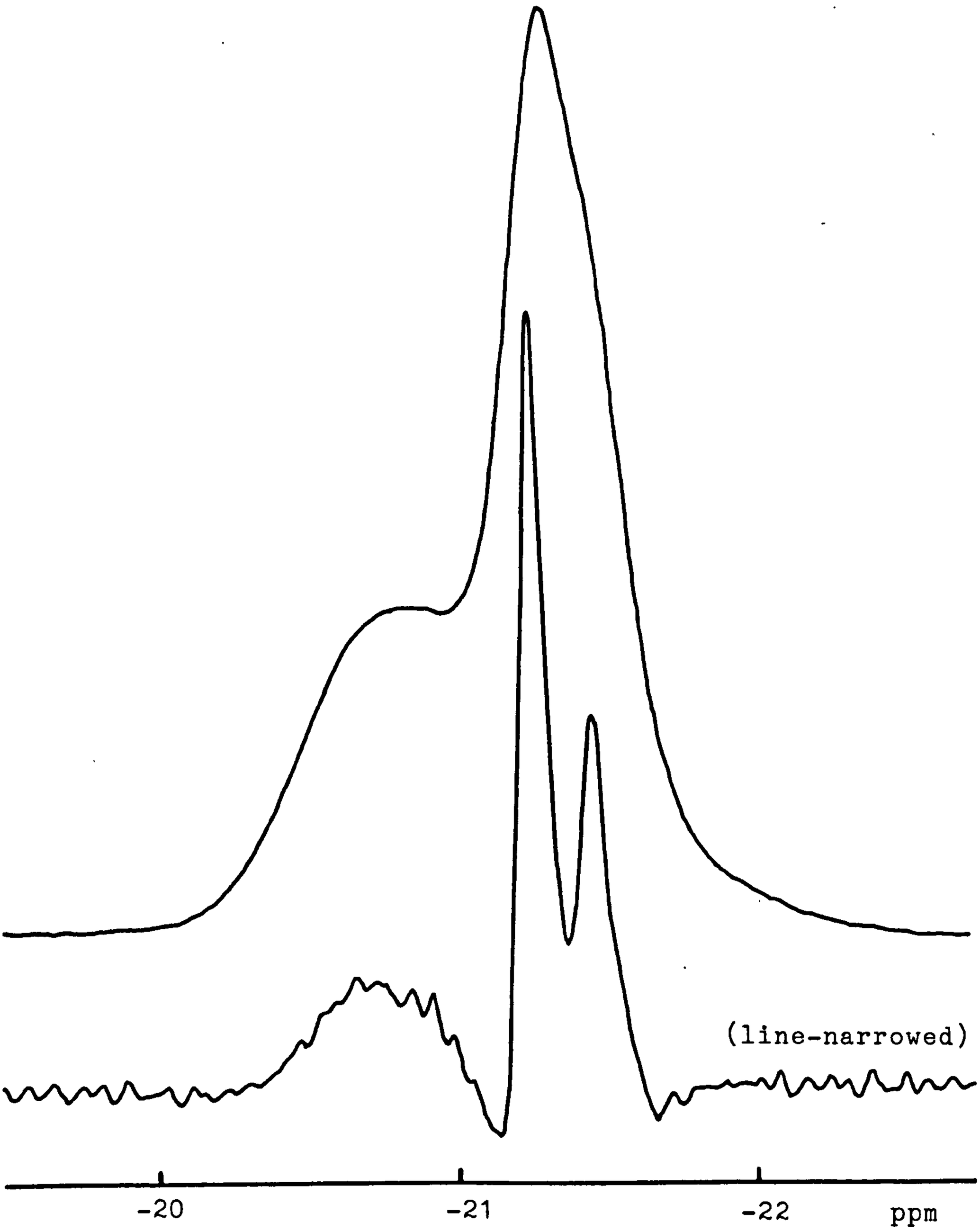

Fig.4.6. 115.5 MHz $^{11}B\{^{1}H\}$ n.m.r. spectra of $[B_3H_7(NCO)]^-$ in $CDCl_3$ at 323 K

ing ^{1}H n.m.r. spectra have been reported only as a broad resonance having some discernible fine structure arising from ^{1}H-^{11}B coupling[116,117]. It was of interest to study these to see if the factors which were proposed to influence the ^{11}B spectra also applied to the ^{1}H spectra, and also to study the ^{1}H and $^{1}H\{^{11}B\}$ spectra of the monosubstituted and disubstituted derivatives.

(a) Octahydrotriborate (-1), $[B_3H_8]^-$.

The ^{1}H n.m.r. spectrum in CD_3CN of $[B_3H_8]^-$ with line-narrowing is presented in Fig. 4.7. It can be seen that the spectrum consists of a complex multiplet at δ = 0.175 ppm which may be interpreted as arising from ^{1}H-^{11}B and ^{1}H-^{10}B couplings from various isotopic species. By considering the relative abundances of ^{11}B and ^{10}B and the probabilities of each occuring in a B_3 unit, the relative abundances of the isotopic species $^{11}B_3$, $^{11}B_2{}^{10}B$, $^{11}B{}^{10}B_2$ and $^{10}B_3$ are 64, 48, 12 and 1 respectively. In view of the small contributions from $^{11}B{}^{10}B_2$ and $^{10}B_3$, only $^{11}B_3$ and $^{11}B_2{}^{10}B$ need to be considered for the analysis of the line shape of the multiplet.

The eight equivalent hydrogens coupling to three equivalent boron nuclei of spin quantum number $^{3}/_{2}$ clearly shows a multiplet of ten lines with relative intensities close to 1:3:6:10:12:12:10:6:3:1. The measured value of $J_{^{1}H-^{11}B}$ is 32.7 Hz. Further structure, observed between these lines, correlates with eight equivalent hydrogens coupling to two equivalent boron

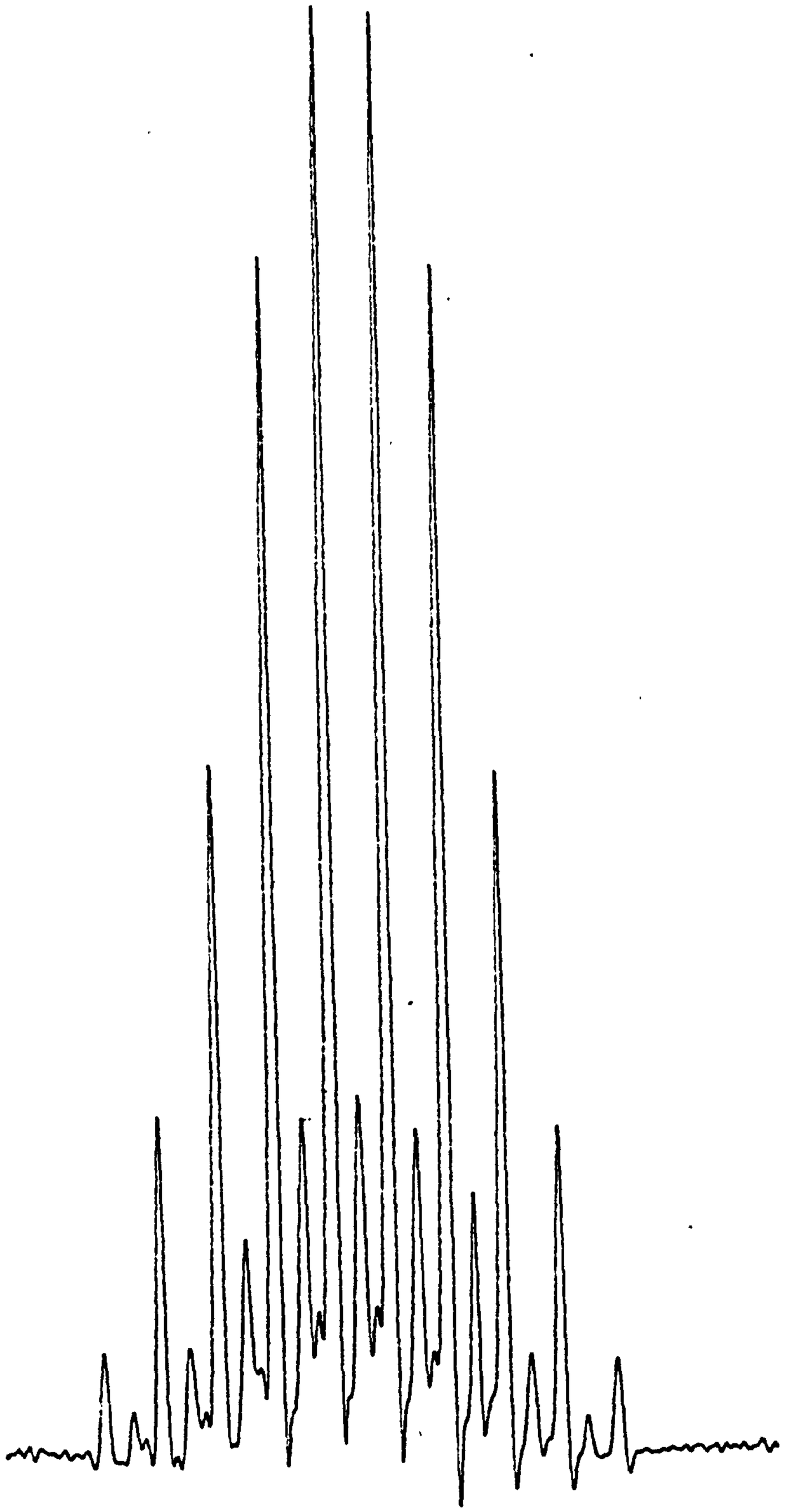

Fig.4.7. 360 MHz ^{1}H n.m.r. spectrum of $[B_3H_8]^-$ (line-narrowed).

nuclei of spin quantum number $^{3}/_{2}$ and further coupling with a boron nucleus of spin quantum number 3 giving rise to a multiplet of twenty five lines of relative intensities 1:1:1:3:3:3:6:5:5:9:7:7:10:7:7:9:5:5:6:3:3:3:1:1:1. These lines are not all observed as some lines are obscured by the more intense lines resulting from ^{1}H and $^{11}B_3$ coupling. The observed ratio of the coupling constants, $\frac{J_{(10_{BH})}}{J_{(11_{BH})}}$, is in agreement with the ratio of gyromagnetic ratios, γ, of the boron isotopes:

$$\frac{J_{(10_{BH})}}{J_{(11_{BH})}} = \frac{\gamma_{(10_B)}}{\gamma_{(11_B)}} = \frac{4.575}{13.660} = 0.335$$

(b) Monosubstituted octahydrotriborate.

The $^{1}H\{^{11}B\}$ n.m.r. spectra of $[B_3H_7(Cl)]^-$ in CD_3CN and $CDCl_3$ obtained with broad band irradiation or continuous wave specific frequency irradiation of the ^{11}B resonances are presented in Fig. 4.8 and Fig. 4.9.

In CD_3CN, the $^{1}H\{^{11}B$, broad band$\}$ spectrum showed a proton resonance of seven hydrogens at δ = 1.46 ppm. The spectrum resulting from irradiation of the unsubstituted borons B(1) and B(2) [Fig. 4.8(b)]

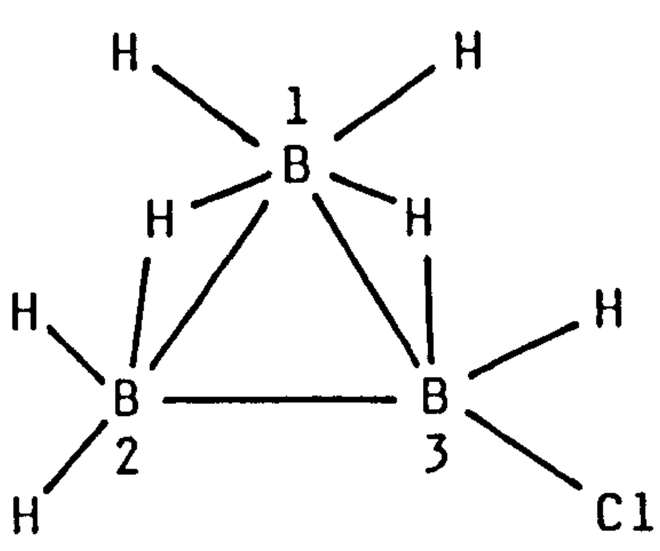

showed a coupling pattern comprising a partly relaxed 1:1:1:1 quartet which resulted from the remaining coupling of the seven equivalent hydrogens to boron atom, B(3) with a coupling

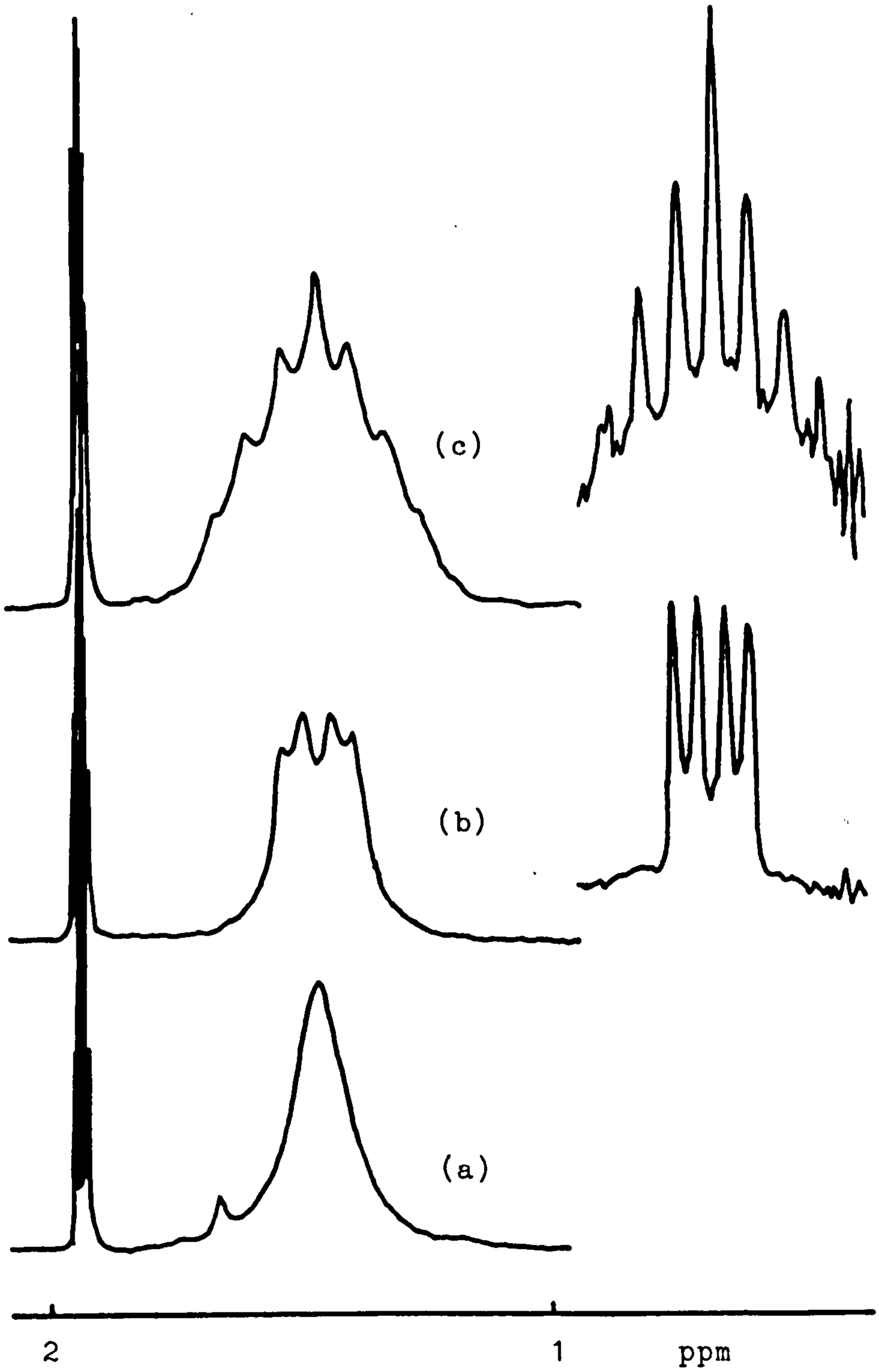

Fig.4.8. 360 MHz $^{1}H\{^{11}B\}$ n.m.r. spectra of $[B_3H_7(Cl)]^-$ in CD_3CN (a) broad band, (b) irradiation of two unsubstituted borons and (c) irradiation of the substituted boron.

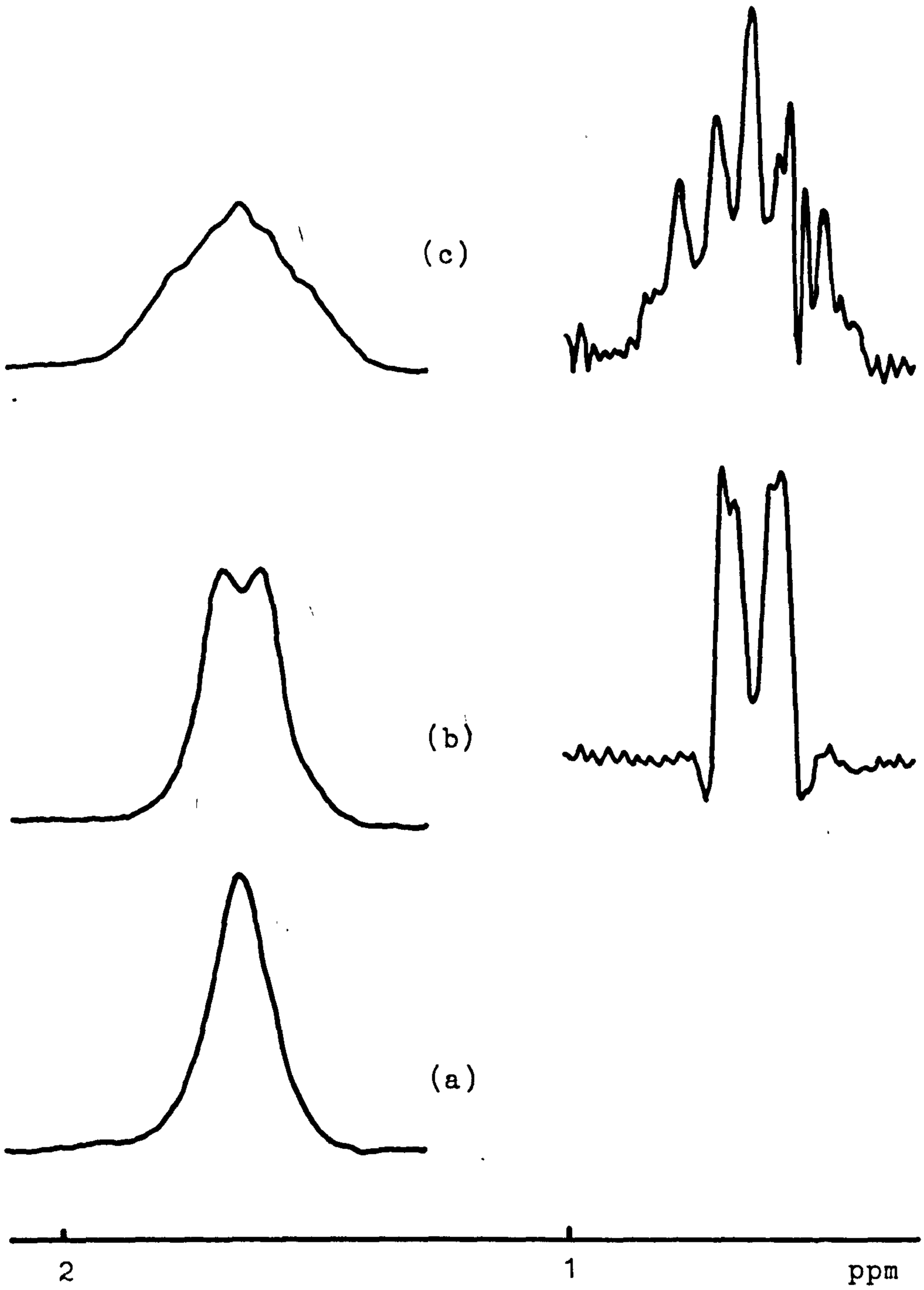

Fig.4.9. 360 MHz $^{1}H\{^{11}B\}$ n.m.r. spectra of $[B_3H_7(Cl)]^-$ in $CDCl_3$ (a) broad band, (b) irradiation of two unsubstituted borons and (c) irradiation of the substituted boron.

constant $J_{^1H-^{11}B(3)}$ of 18.0 Hz. The coupling pattern observed on irradiating substituted boron atom B(3) comprises an apparent seven line multiplet of the expected relative intensities 1:2:3:4:3:2:1 with additional fine structure probably resulting from other isotopic species of the B_3 system, together with a trace of impurity. The $J_{^1H-^{11}B(1,2)}$ measured was 25 Hz.

There are apparent discrepancies: first, between $J_{^1H-^{11}B(3)}$ of 18.0 Hz and $J_{^1H-^{11}B(1,2)}$ of 25 Hz and second, these couplings observed in the ^1H spectra and those derived from the ^{11}B spectra where $J_{^{11}B-^1H}$ is 39.0 Hz. These are discussed in sect. 4.2.3.

It should be noted that the less well resolved of $^1H-^{10}B$ coupling in $[B_3H_7(Cl)]^-$ than in $[B_3H_8]^-$ is probably due to a decrease in relative abundance of $^{11}B_2\,^{10}B$ unit. The relative abundance of $^{11}B_2{}^{10}B$ reduced from 48 in $[B_3H_8]^-$ to 32 and 16 in $[B_3H_7(Cl)]^-$ due to the substituent as shown below.

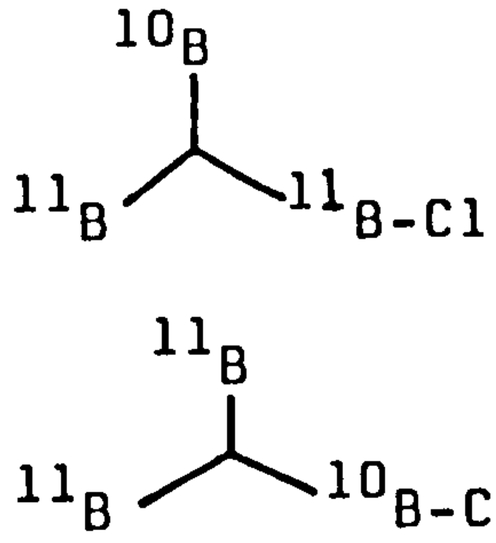

relative abundance 32

relative abundance 16

In $CDCl_3$, the $^1H\{^{11}B\}$ n.m.r. spectra showed more extensive quadrupolar relaxation. This observation is consistent with earlier work[5].

The $^{1}H\{^{11}B\}$ n.m.r. spectra of $[B_3H_7(NCS)]^-$ and $[B_3H_7(NCO)]^-$ each showed resonance of seven hydrogens (with respect to proton resonances of $[N(PPh_3)_2]^+$ counter ion at δ = 7.5 ppm) at chemical shift δ = 1.4 ppm and δ = 1.2 ppm respectively. The $^{1}H\{^{11}B\}$ n.m.r. spectra with specific frequency irradiations of the boron resonances did not show any resolvable fine structure due to ^{1}H-^{11}B coupling.

The $^{1}H\{^{11}B, noise\}$ n.m.r. spectrum of $[B_3H_7(NCBH_3)]^-$ in CD_3CN showed two resonances, that at δ = +1.5 ppm corresponded to seven hydrogens and the resonance of δ = 0.4 ppm corresponded to three hydrogens with respect to proton resonance at δ = 7.5 ppm of $[N(PPh_3)_2]^+$ containing thirty hydrogens. The $^{1}H\{^{11}B\}$ n.m.r. spectra with continuous wave specific frequency irradiation of the ^{11}B resonances presented in Fig. 4.10 are similar to those of $[B_3H_7(Cl)]^-$ but show a greater degree of quadrupolar relaxation. On irradiating the two unsubstituted boron atoms

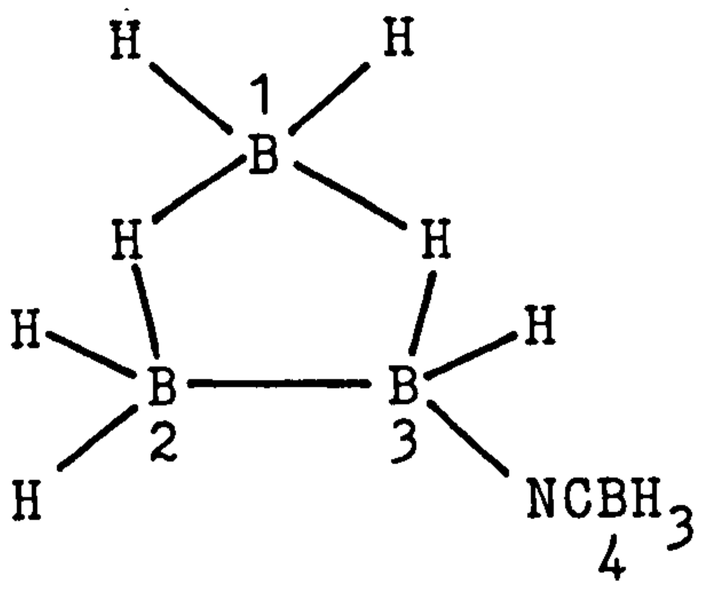

B(1) and B(2), the spectrum contained a resonance at 0.4 ppm which comprised a 1:1:1:1 quartet of area three, and which arose as a result of the three hydrogens in the H_3BCN moiety coupling with B(4).

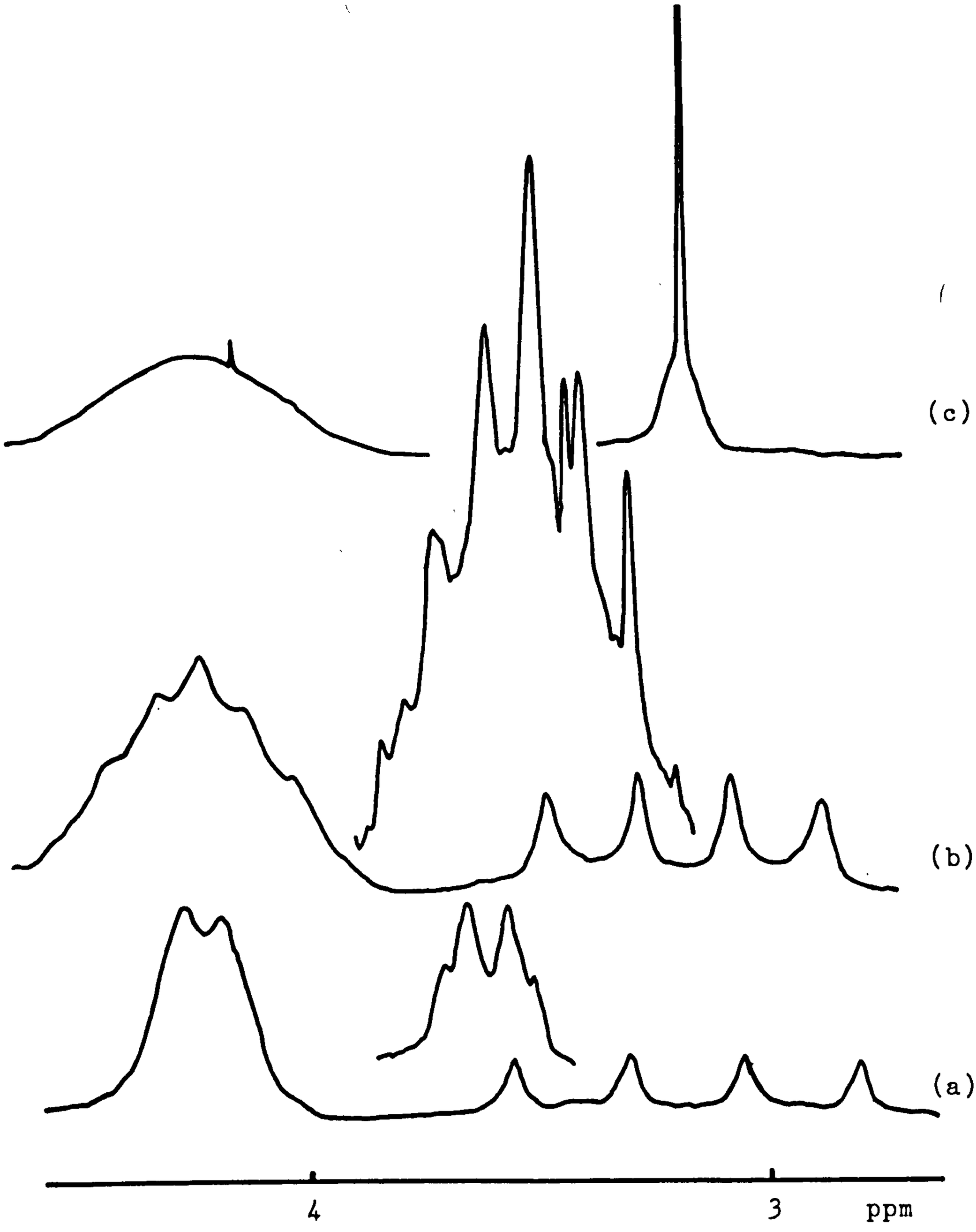

Fig.4.10. 360 MHz $^{1}H\{^{11}B\}$ n.m.r. spectra of $[B_3H_7(NCBH_3)]^-$ in CD_3CN (a) irradiation of two unsubstituted borons, (b) irradiation of the substituted boron and (c) irradiation of boron in BH_3CN

The coupling constant, $J_{^1H-^{11}B(4)}$, is 90 Hz. The resonance at 1.5 ppm of relative intensity seven which had the appearance of a partly relaxed 1:1:1:1 quartet, was assigned to seven fluxional hydrogens coupling to B(3) with $J_{^1H-^{11}B(3)}$ of 25.2 Hz. The spectrum resulting from irradiation of the substituted boron, B(3), showed a multiplet of the intensity ratio 1:2:3:4:3:2:1 expected for seven equivalent hydrogens coupling with boron atom B(1) and B(2) and with $J_{^1H-^{11}B(1,2)}$ of 36 Hz together with fine structure as discussed in $[B_3H_7(Cl)]^-$. A spike between the apparent seven lines of the multiplet was more likely resulted from impurities because it also appeared in spectrum shown in Fig. 4.10(c). On irradiating the boron in the BH_3CN moiety, the spectrum showed a sharp peak corresponding to three hydrogens in H_3BCN moiety and a broad peak of intensity corresponding to seven hydrogens without any structure due to $^1H-^{11}B$ coupling. A spike of impurities was also observed in the broad peak.

(c) Disubstituted octahydrotriborate ions.

The $^1H\{^{11}B\}$ n.m.r. spectra of $[B_3H_6(Cl)_2]^-$ in $CDCl_3$ obtained with off-resonance or continuous wave specific frequency irradiation of the ^{11}B resonances are given in Fig. 4.11. The $^1H\{^{11}B$, off resonance$\}$ spectrum showed a broad band (δ = 2.57 ppm) corresponding to six hydrogens with respect to the thirty hydrogens in the $[N(PPh_3)_2]^+$ counter-ion (δ = 7.5 ppm). The proton

spectrum resulting from irradiation of the unique unsubstituted boron atom, B(1) [Fig. 4.11(b)] shows a resonance of relative intensity of six equivalent hydrogens with fine structure corresponding to coupling to the remaining two boron atoms, B(2) and B(3). The coupling pattern was distorted from the theoretical 1:2:3:4:3:2:1, probably as a result of a quadrupolar relaxation effect. On irradiating the substituted boron atoms, B(2) and B(3), the remaining coupling of the six equivalent hydrogens with boron atom B(1) would be expected to be a 1:1:1:1 quartet. However, it is shown in Fig. 3.11(c) that the quartet has collapsed to a broad doublet with an apparent coupling constant of 65 Hz.

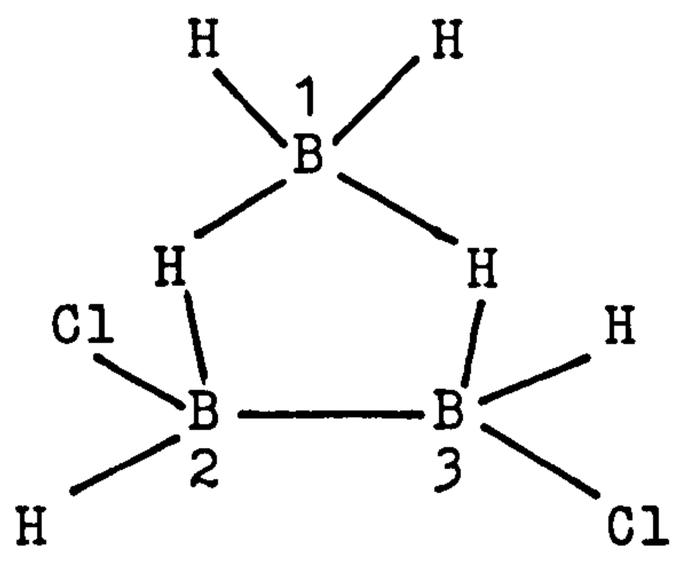

The $^{1}H\{^{11}B$, broad band$\}$ n.m.r. spectra of $[B_3H_6(Cl)(NCS)]^-$ in $CDCl_3$ at 303°K and 220°K each showed a single resonance of six hydrogens at δ = 2.30 ppm. The specific frequency irradiation at each unique boron did not reveal any structure resulting from ^{1}H-^{11}B coupling.

The $^{1}H\{^{11}B$, broad band$\}$ n.m.r. spectrum of $[N(PPh_3)_2][\{B_3H_6(Cl)(NC)\}_2Ag]$ in $CDCl_3$ showed proton resonances at δ = 7.5 ppm with relative area thirty and

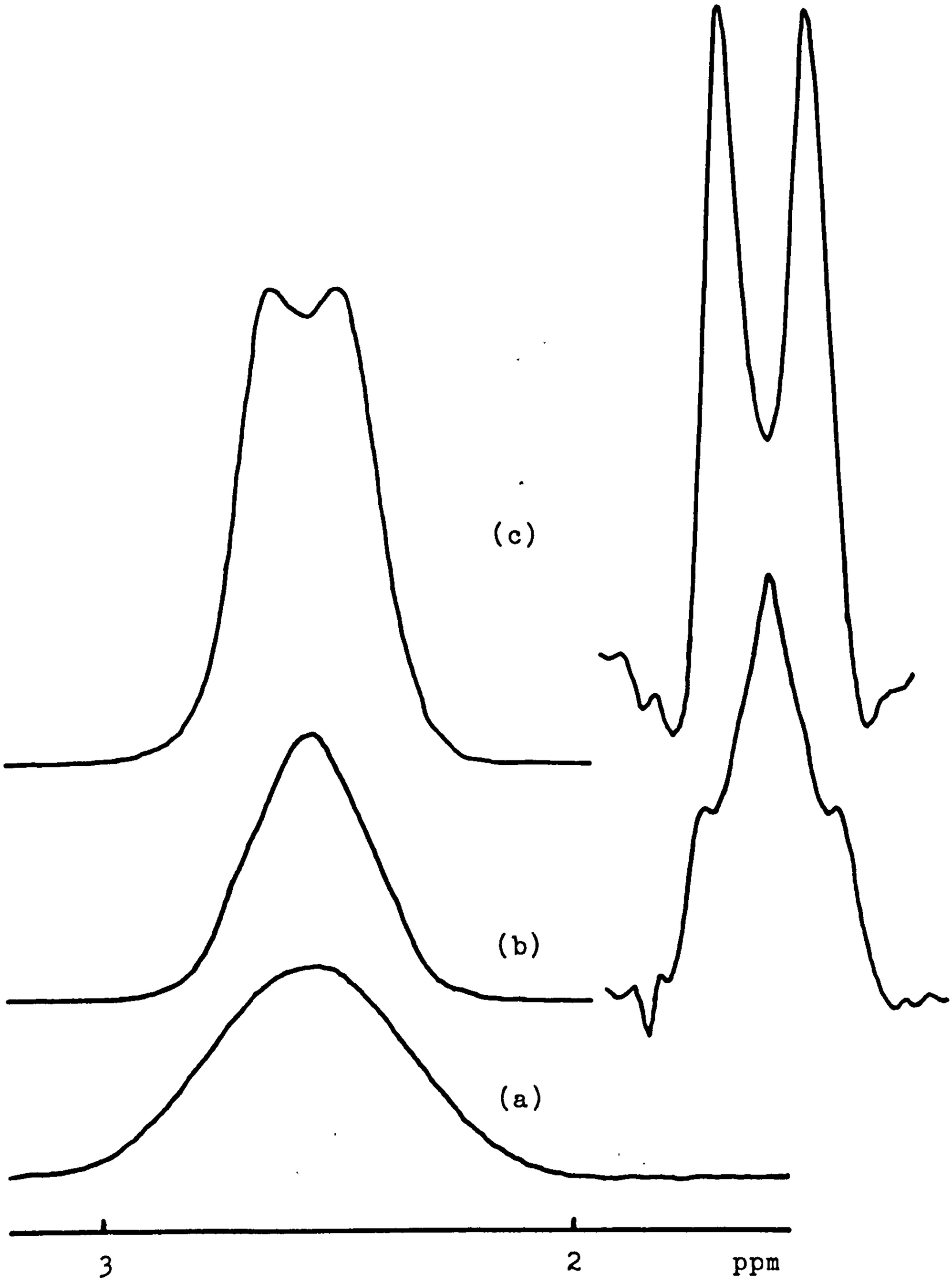

Fig.4.11. 360 MHz $^{1}H\{^{11}B\}$ n.m.r. spectra of $[B_3H_6(Cl)_2]^-$ in $CDCl_3$ (a) off-resonance, (b) irradiation of the unsubstituted boron and (c) irradiation of two substituted borons.

at δ = 2.24 ppm with relative area twelve which corresponded to the hydrogens in $[N(PPh_3)_2]^+$ and those in the $[\{B_3H_6(Cl)(NC)\}_2Ag]^-$ anion. The specific frequency irradiation at each unique boron did not show any fine structure attributable to coupling between hydrogen and boron.

The relevant ^1H n.m.r. parameters for the octahydrotriborate derivatives are presented in Table 4.2.

4.2.3 Discussion

(a) Quadrupolar relaxation.

Observation of ^{11}B n.m.r. spectra of disubstituted octahydrotriborate (-1) ions and ^1H n.m.r. spectra of the octahydrotriborate (-1) ion, and its mono- and disubstituted derivatives reveals that previously reported effects of substituents and solvent polarity on quadrupolar relaxation[141] also apply to these studies. The effect of substituents, shown in the ^1H n.m.r. spectra of $[B_3H_7(Cl)]^-$ and $[B_3H_7(NCBH_3)]^-$, is that greater quadrupolar relaxation was observed in $[B_3H_7(NCBH_3)]^-$ than in $[B_3H_7(Cl)]^-$. This is in agreement with previous studies of the ^{11}B n.m.r. spectra of these compounds. The effects of solvent polarity are demonstrated in the ^{11}B n.m.r. spectra of $[B_3H_6(Cl)_2]^-$ and the ^1H n.m.r. spectra of $[B_3H_7(Cl)]^-$ in different solvents such as CD_3CN or $CDCl_3$. The results support previous observation that greater quadrupolar relaxation was found in the less polar solvent, $CDCl_3$.

Table 4.2. ^{1}H N.m.r. Data for Octahydrotriborate Derivatives at 115.5 MHz.

Compound	(^{1}H)/ppm	$J_{^{1}H-^{11}B}$/Hz	Solvent
$[B_3H_8]^-$	+0.175	$^{1}H-^{11}B = 32.7$	CD_3CN
		$^{1}H-^{10}B = 10.96$	
$[B_3H_7(Cl)]^-$	+1.46	H-B(3) = 18.0	CD_3CN
		H-B(1,2) = 25.0	
$[B_3H_7(Cl)]^-$	+1.63		$CDCl_3$
$[B_3H_7(NCS)]^-$ (a)	+1.4		CD_3CN
$[B_3H_7(NCO)]^-$	+1.22		$CDCl_3$
$[B_3H_7(NCBH_3)]^-$	+1.5	H-B(3) = 25.2	CD_3CN
		H-B(1,2) = 36	
		H-B(4) = 90	
$[B_3H_6(Cl)_2]^-$	+2.57	H-B(1) = 65	$CDCl_3$
$[B_3H_6(Cl)(NCS)]^-$	+2.30		$CDCl_3$
$[\{B_3H_6(Cl)(NC)\}_2Ag]^-$	+2.24		$CDCl_3$

(a) at 303 and 220 °K.

In general, a comparison of the ^{11}B or ^{1}H n.m.r. spectra of $[B_3H_7(Cl)]^-$ with those of $[B_3H_6(Cl)_2]^-$ and the spectra of $[B_3H_7(NCS)]^-$ with those of $[B_3H_6(Cl)(NCS)]^-$ showed that the quadrupolar relaxation effect is greater in disubstituted derivatives than in monosubstituted derivatives. Obviously this was due to the additional substituent, Cl^-. The chlorine atom (I = $\frac{3}{2}$) possesses an electric quadrupole moment which causes fluctuating electric-field gradients and therefore possibly increases the rate of relaxation of boron or proton nuclei. Furthermore, an addition of chlorine atom to the molecule increases the size of the molecule such that the tumbling motion of the molecule in solution is reduced and the electric-field gradients around boron or proton nuclei become more effective and thus intensify quadrupolar effects.

(b) Coupling constants.

The ^{11}B-^{1}H coupling constants observed in the ^{11}B n.m.r. spectra of $[B_3H_7(X)]^-$ ($X = Cl^-$, NCS^-, $NCBH_3$, $NC^{-(a)}$) were reported[141] to be in the range of 38.0-40.0 Hz. However, in this work, the coupling constants measured from the ^{1}H n.m.r. spectra appeared to be different from one anion to another, and even in an individual anion the coupling constants resulting from protons coupling with different borons were different (Table 4.2). It can be seen that in ^{1}H n.m.r. spectra of $[B_3H_7(Cl)]^-$ and $[B_3H_7(NCBH_3)]^-$, the ^{1}H-^{11}B coupling constants observed are smaller than those observed in

---

Footnote (a) in $[\{B_3H_7(NC)\}_2Ag]^-$ complex.

^{11}B n.m.r. spectra whereas in the ^{1}H n.m.r. spectra of $[B_3H_6(Cl)_2]^-$, the ^{1}H-^{11}B coupling constant observed is larger than that observed in ^{11}B n.m.r. spectrum. The discrepancies possibly could arise as a result of several factors. (a) The data were obtained from $^{1}H\{^{11}B, C.W.\}$ spectra, in which one of the two boron resonances was irradiated with sufficient power to cause decoupling of the protons attached to that specific boron atom. It may not be possible experimentally to decouple one boron resonance without simultaneously affecting the other, and as a result, any ^{1}H-^{11}B coupling constants may be unreliable. It can be seen that the chemical shift difference between the boron resonances in $[B_3H_7(NCBH_3)]^-$ is greater than those in either $[B_3H_7(Cl)]^-$ or $[B_3H_6(Cl)_2]^-$; as a result, the discrepancies in coupling constants obtained from the ^{11}B and $^{1}H\{^{11}B\}$ n.m.r. spectra are found to be greater in $[B_3H_7(Cl)]^-$ and $[B_3H_6(Cl)_2]^-$ than in $[B_3H_7(NCBH_3)]^-$. Furthermore, the discrepancies are also found to be greater when resonance containing two equivalent boron atoms was irradiated than on irradiating that of the unique boron atom. (b) A further factor may involve the fluxional nature of the compounds. All the hydrogens are fluxional, and hence spin couple equally to all three boron atoms. The observed coupling constant must result from contribution to coupling involving all three atoms. If one or two of these are subsequently decoupled by double irradiation, then it is

likely that the observed coupling constant to the remaining (unirradiated) boron atom will be affected.

(c) Chemical shifts.

Chemical shifts are affected by several factors such as diamagnetic, paramagnetic, anisotropic and solvent effects. Many approaches have been made to account for magnitude and direction of ^{11}B chemical shifts. Good and Ritter[152] considered $\delta^{11}B$ of tri-coordinated boron compounds as the sum of σ- and π-bonding effects. The concept of Good and Ritter was extended by Nöth and Vahrenkamp[153] who included aniso-tropic effects for the various substituents, calculated from a correlation between the electronegativity of X in BX_4^- and ^{11}B chemical shifts. Thompson and Davis[154] tried to explain ^{11}B chemical shifts in terms of ligand electronegativities and anisotropic effects. Lipscomb and coworkers[155] tried to correlate and establish a theoretical basis for the ^{11}B shifts in the carba-boranes. So far there is no generally satisfactory theoretical treatment available.

The assignments for the ^{11}B n.m.r. spectra of the disubstituted octahydrotriborate anions (Table 4.1) are based on the correlation of the chemical shifts of the parent anions - monosubstituted derivatives. Fig. 4.12 presents a correlation diagram of the ^{11}B chemical shifts of octahydrotriborate (-1) ion and its mono- and disubstituted derivatives. The substituent X in $[B_3H_7(X)]^-$ splits the boron resonance in $[B_3H_8]^-$ into two

X	X′
H	H
H	F
H	Cl
H	Br
H	NCO
H	NC
H	$NCBH_3$
H	NCS
Cl	NC
Cl	$NCBH_3$
Cl	NCS

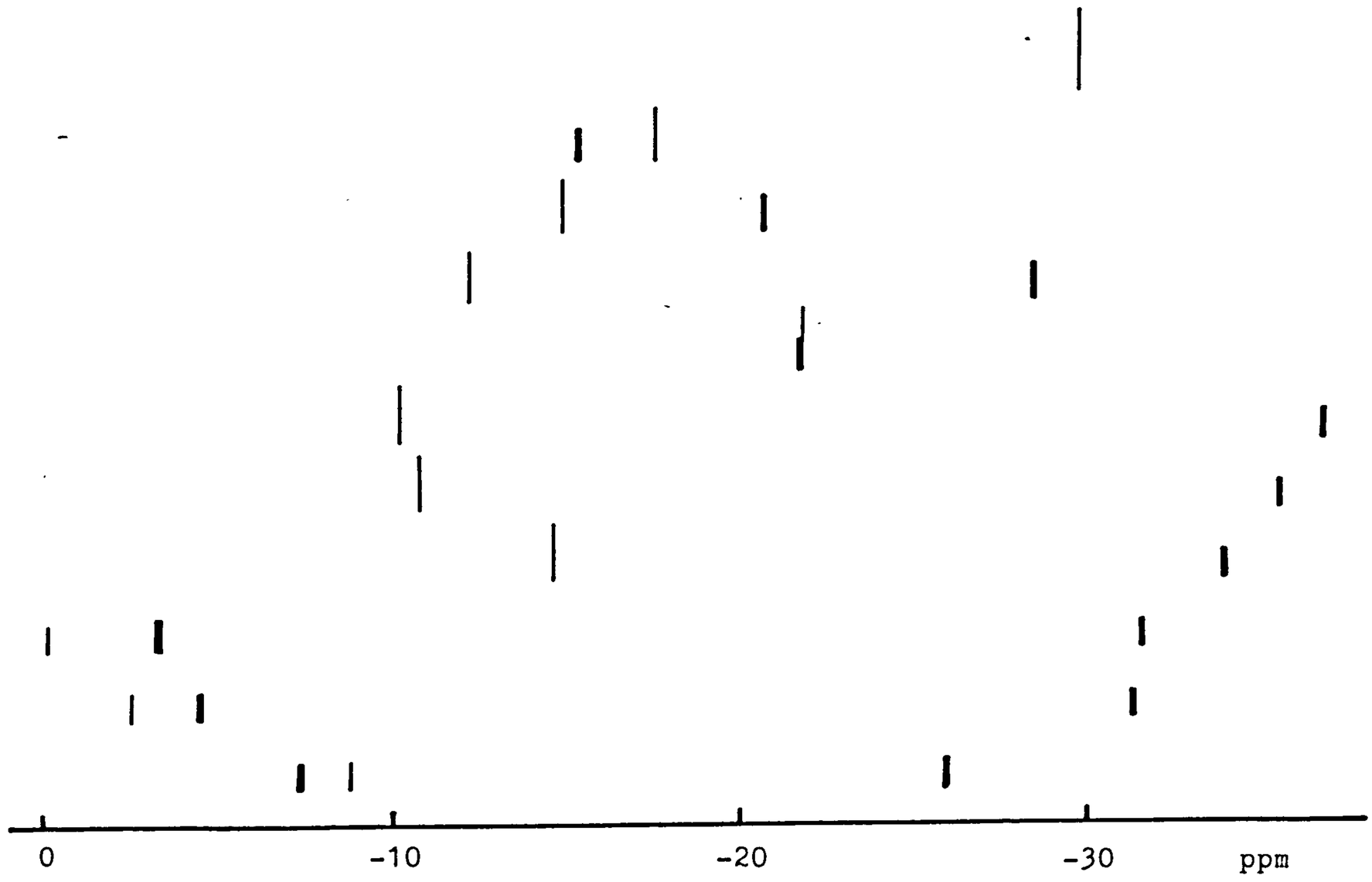

Fig.4.12. Correlation diagram of ^{11}B chemical shift of $[B_3H_6XX']^-$ anions.
The length of the line is proportional to the number of boron atoms in the resonance. The thick lines represent resonances which carry substitutents. The thin lines represent resonances which carry hydrogens.

boron resonances. In general, the high field resonance is designated to boron that carries the substituent and the low field resonance is designated to the two unsubstituted boron atoms except for the cases of $[B_3H_7(F)]^-$ and $[B_3H_7(NCO)]^-$. The chemical shifts of the substituted boron atom resonances in $[B_3H_7(X)]^-$ when X = F^-, Cl^-, Br^- agree with the order of the electronegativity $F^- > Cl^- > Br^-$. However the electronegativity effect does not account for the fact that resonances of the unsubstituted boron atoms occur at lower field than that of the substituted boron atom (except for the case of $[B_3H_7(F)]^-$). The ^{11}B chemical shifts are apparently dominated by paramagnetic shielding and anisotropic effects. In disubstituted derivatives, the effects are even more complicated to analyse qualitatively due to effects from two substituents.

4.3 EXPERIMENTAL

$[N(PPh_3)_2]^+$ salts of $[B_3H_8]^-$, $[B_3H_7(Cl)]^-$, $[B_3H_7(NCS)]^-$ and $[B_3H_7(NCBH_3)]^-$ were prepared as reported[27] and $[N(PPh_3)_2]^+$ salts of $[B_3H_6(Cl)_2]^-$, $[B_3H_6(Cl)(NCS)]^-$ and $[\{B_3H_6(Cl)(NC)\}_2Ag]^-$ were prepared as described in Chapter 2. CD_3CN and $CDCl_3$ for n.m.r. spectroscopy were used as received.

The n.m.r. techniques and the computer programme for the simulation of n.m.r. line shapes are described in Chapter 6.

CHAPTER 5

N.M.R. AND ELECTROCHEMICAL STUDIES OF $[B_{10}H_{13}(L)]^-$ ANIONS

5.1 INTRODUCTION

There have been a number of studies on the n.m.r. spectroscopic properties, and on the electrochemistry of closo-, nido-, and arachno-derivatives containing ten boron atoms. The ^{11}B n.m.r. spectra of closo-$[B_{10}H_{10}]^{2-}$, nido-$B_{10}H_{14}$, nido-$[B_{10}H_{13}]^{-}$, arachno-$[B_{10}H_{14}]^{2-}$ and arachno-$B_{10}H_{12}L_2$ are well established[156,124,125,126,157,134,132] but the spectra of arachno-$[B_{10}H_{13}L]^{-}$ ions have been poorly described[158]. Similarly, the electrochemistry of $[B_{10}H_{10}]^{2-}$, $B_{10}H_{14}$, $B_{10}H_{12}L_2$ had been studied[95,89,90,91,92], but no data has been reported on $[B_{10}H_{13}L]^{-}$. In this work, the high field ^{11}B and ^{1}H n.m.r. spectra of tetramethylammonium salts of $[B_{10}H_{13}L]^{-}$ anions have been investigated in detail and their electrochemical properties obtained from cyclic voltammetry, a.c. voltammetry and controlled potential electrolysis of $[B_{10}H_{13}(PPh_3)]^{-}$ and $[B_{10}H_{13}(SMe_2)]^{-}$ in different solvents.

5.2 RESULTS AND DISCUSSION

5.2.1 Preparations and NMR studies of $[B_{10}H_{13}L]^{-}$.

(a) $[B_{10}H_{13}(PPh_3)]^{-}$

$[N(CH_3)_4][B_{10}H_{13}(PPh_3)]$ was prepared as has been reported[54] with slight modification. $B_{10}H_{14}$ was treated with NaH in ether to give $NaB_{10}H_{13}$ which was then treated with PPh_3 to give $Na[B_{10}H_{13}(PPh_3)]$. The product was converted from the Na^+ salt to one

containing the $[N(CH_3)_4]^+$ cation. It was then recrystallized from acetonitrile-ether.

The ^{11}B n.m.r. spectrum of $[B_{10}H_{13}(PPh_3)]^-$ in CD_3CN and its $^1H\{^{11}B\}$ n.m.r. spectra with broad band and specific frequency irradiation of boron resonances are presented in Fig. 5.1 and Fig. 5.2. The ^{11}B n.m.r. spectrum consisted of six boron resonances with relative area 1:1:2:2:1:3 (see Table 5.1). The resonance at -27.1 ppm was a triplet of relative area one and the rest of boron resonances were doublets, indicating that there are nine BH groups and one BH_2 group in $[B_{10}H_{13}(PPh_3)]^-$. The $^1H\{^{11}B$, broad band$\}$ n.m.r. spectrum showed a resonance (δ = -4.21 ppm) attributable to two bridge hydrogens (with respect to the resonance of twelve hydrogens in $[N(CH_3)_4]^+$, δ = 3.08 ppm). The $^1H\{^{11}B\}$ n.m.r. spectra with specific frequency irradiation at each of the boron resonances appear to be useful in structural information. Irradiation of boron resonances at δ = -17.05 and -19.63 ppm resulted in line sharpening of the bridge hydrogens, and this indicates that these four boron atoms are related to these bridge hydrogens. They therefore must be B(5, 7, 8, 10) (structure in Fig. 5.3). Information obtained therefore suggests that $[B_{10}H_{13}(PPh_3)]^-$ is isostructural to $[B_{10}H_{14}]^{2-}$. Since the assignment of the low field doublet of relative area two in the ^{11}B n.m.r. spectrum of $[B_{10}H_{14}]^{2-}$ [134] and the doublets of relative area 1:1 in the ^{11}B n.m.r. spectra of $B_{10}H_{12}L_2$ [132] were B(2) and

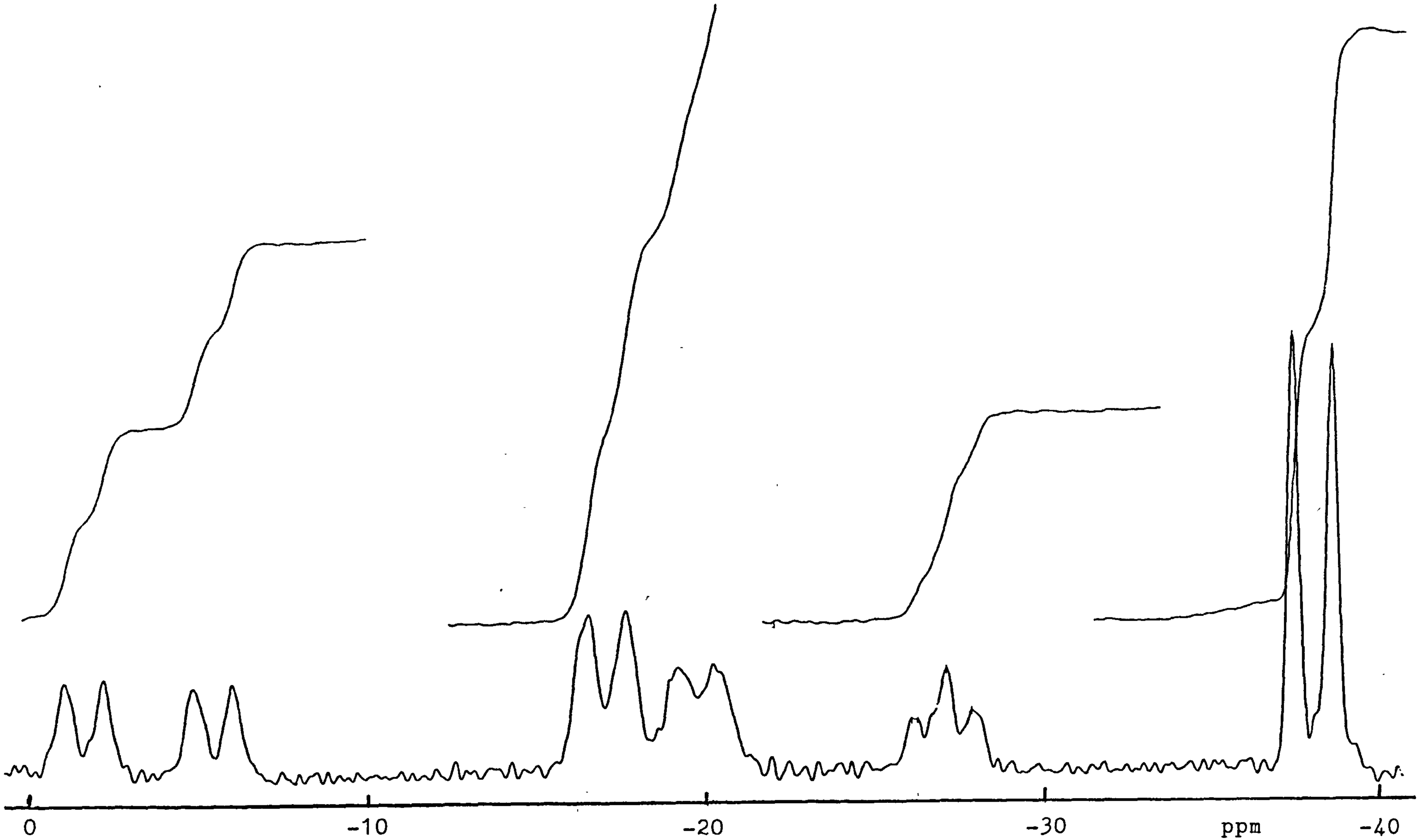

Fig.5.1. 115.5 MHz ^{11}B n.m.r. spectrum of $[B_{10}H_{13}(PPh_3)]^-$ in CD_3CN.

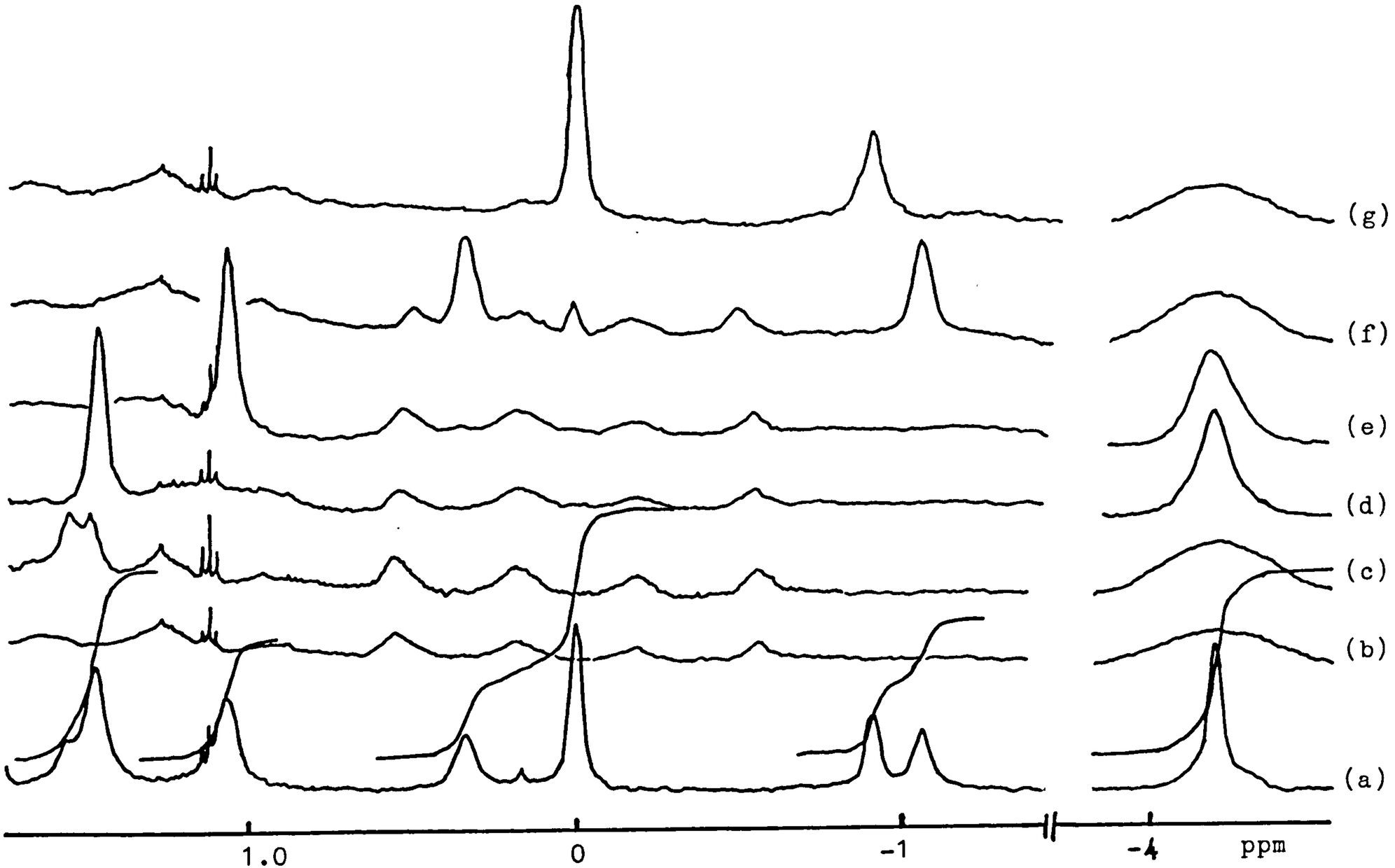

Fig.5.2. 360 MHz $^{1}H\{^{11}B\}$ n.m.r. spectra of $[B_{10}H_{13}(PPh_3)]^-$ in CD_3CN
(a) $^{1}H\{^{11}B\}$, (b) - (g) $^{1}H\{^{11}B\}$ at boron resonances from low field to high field.

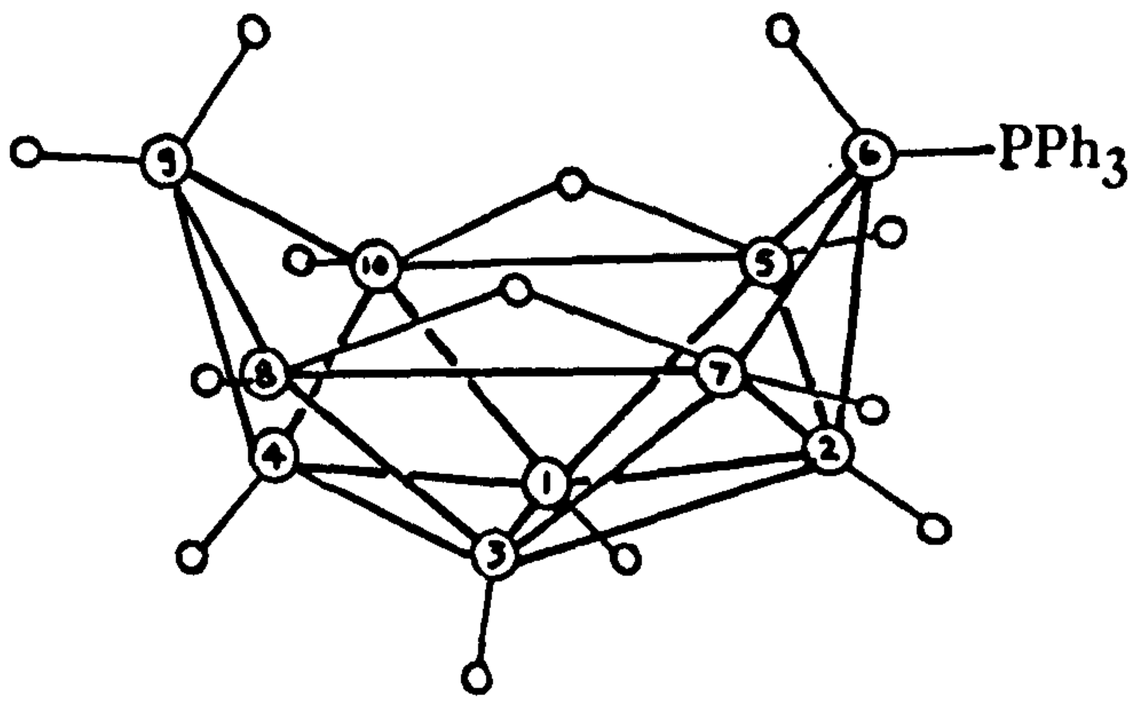

Fig.5.3. The structure of the $[B_{10}H_{13}(PPh_3)]^-$ ion.

B(4), the assignment of two low field doublets of relative area 1:1 in ^{11}B n.m.r. spectrum of $[B_{10}H_{13}(PPh_3)]^-$ may be similar. However, the $^1H\{^{11}B\}$ n.m.r. spectrum, on irradiating the boron resonance at δ = -5.37 ppm, showed ^1H-P coupling ($J_{^1H\text{-}P}$ = 24 Hz) which possibly resulted from either H(6)-P coupling or long range H(2)-P coupling. The ^{11}B n.m.r. spectra of the analogues $[B_{10}H_{13}(Py)]^-$ and $[B_{10}H_{13}(NEt_3)]^-$ were therefore examined and the results suggested that the two low field doublets were B(4) and B(2). This was confirmed by the comparison of the ^{11}B n.m.r. spectrum of $[B_{10}H_{13}(PPh_3)]^-$ with that of $[B_{10}H_{12}(PPh_3)(CH_3CN)]$ which is discussed in sect. 5.2.2(c). Table 5.1 lists respectively the relevant ^{11}B n.m.r. data for $[B_{10}H_{13}(Py)]^-$, $[B_{10}H_{13}(NEt_3)]^-$, $[B_{10}H_{13}(PPh_3)]^-$ and $[B_{10}H_{12}(PPh_3)(CH_3CN)]$ and Table 5.2 contains the ^1H n.m.r. data for $[B_{10}H_{13}(PPh_3)]^-$ and $[B_{10}H_{12}(PPh_3)(CH_3CN)]$. It should be noted that the proton of B(4) in $[B_{10}H_{13}(PPh_3)]^-$ was not observed on irradiating at that boron. It is likely that the "missing" proton was under the large peak at δ (^1H) = 2.6 ppm.

(b) $[B_{10}H_{13}(NCS)]^{2-}$.

Reactions of anhydrous KNCS with $[N(CH_3)_4]$-$[B_{10}H_{13}]$ in dimethoxyethane-dioxane did not yield $[N(CH_3)_4]_2[B_{10}H_{13}(NCS)]$ as reported[61]. Instead, a mixture of products identified by their ^{11}B n.m.r. spectra as $[B_9H_{14}]^-$ and $[B_9H_{13}(NCS)]^-$ were obtained. Attempts were also made to prepare $[NBu^n_4]_2[B_{10}H_{13}(NCS)]$

Table 5.1. 115.5 MHz ^{11}B N.m.r. Spectral Data for $[B_{10}H_{13}(L)]^-$ Compounds in CD_3CN.

Compounds	Chemical shifts of boron positions (J_{B-H}/Hz) B(4)	B(2)	B(5,7,8,10)		B(6)	B(9)	B(1,3)
$[B_{10}H_{13}(Py)]^-$	-4.2d	-5.9d	-18.0d,	-20.2d	-17.2d	-30.2t	-39.3d
	(146)	(139)	(122),	(137)	-	(107)	(134)
$[B_{10}H_{13}(NEt_3)]^-$	-6.5d	-8.6d	-19.6d	-20.7d	-15.0d	-31.6t	-40.6d
	(127)	(127)	(127)	(127)	(115)	(104)	(133)
$[B_{10}H_{13}(PPh_3)]^-$	-1.6d	-5.4d	-17.1d	-19.6d	-38.0	-27.1t	-38.0d
	(139)	(133)	(127)	(122)		(95.3)	(139)
$[B_{10}H_{12}(PPh_3)(CH_3CN)]$	-0.5d	-3.8d	-17.1d		-35.3t	-27.2d	-38.2d
	(121)	(121.3)	(106)		(106)	(101)	(116)

d = doublet; t = triplet.

Table 5.2 360 MHz ^1H N.m.r. Spectral Data for

(A) = $[B_{10}H_{13}(PPh_3)]^-$ and (B) = $[B_{10}H_{12}(PPh_3)(CH_3CN)]$

in CD_3CN

$\delta(^1H)$ Terminal/ppm		Associated boron atom	$\delta(^1H)$ Bridge/ppm		Other	
(A)	(B)		(A)	(B)	(A)	(B)
-	2.16	4	-4.21(2)	-4.34(2)	3.08 $[N(CH_3)_4]^+$	7.5 (PPh_3)
1.5	1.63	2				
1.47	1.63	5,7 or 8,10				
1.08	1.49	8,10 or 5,7				
0.34, -1.06	0.0	9				
-0.91	-0.8	6				
0.0	0.15	1,3				

by treating $[NBu^n_4][B_{10}H_{13}]$ with $[NBu^n_4][NCS]$ in dichloromethane. However, the reaction product was $[B_9H_{14}]^-$.

(c) $[B_{10}H_{13}]^-$.

The 70.6 MHz ^{11}B n.m.r. spectra of $[N(C_2H_5)_3H][B_{10}H_{13}]$ in CH_3CN had been assigned[157]. In this work, the ^{11}B and ^1H n.m.r. spectra of $[N(CH_3)_4][B_{10}H_{13}]$ were re-examined for several purposes: firstly to ensure that the starting material, $[N(CH_3)_4][B_{10}H_{13}]$, for the preparation of $[B_{10}H_{13}(NCS)]^{2-}$ was pure; secondly, for comparison with the ^{11}B and ^1H n.m.r. spectra of $[B_{10}H_{13}(SMe_2)]^-$ which is discussed in sect. 5.2.1(d); thirdly, it was not known why the 70.6 MHz n.m.r. spectrum of $[B_{10}H_{13}]^-$ in CH_3CN showed that B(1) and B(3) were nonequivalent while B(2, 4) and B(5, 7, 8, 10) were magnetically equivalent if the structure was proposed as in Fig. 5.4(a), and it was thought that the ^{11}B n.m.r. spectrum obtained at higher field strength (115.5 MHz) might improve the resolution. Furthermore the $^{11}B\{^1H\}$ n.m.r. spectra with specific frequency irradiation of boron resonances are quite informative for structural analysis, and it was hoped that the data would lead to the positions of bridge hydrogens in the structure. However, it was a disappointment to find that the improved resolution in the ^{11}B spectrum was not observed, and that the ^1H data was inconclusive. The 115.5 MHz ^{11}B n.m.r. spectrum of $[N(CH_3)_4][B_{10}H_{13}]$ in CD_3CN was similar to that reported earlier in that it

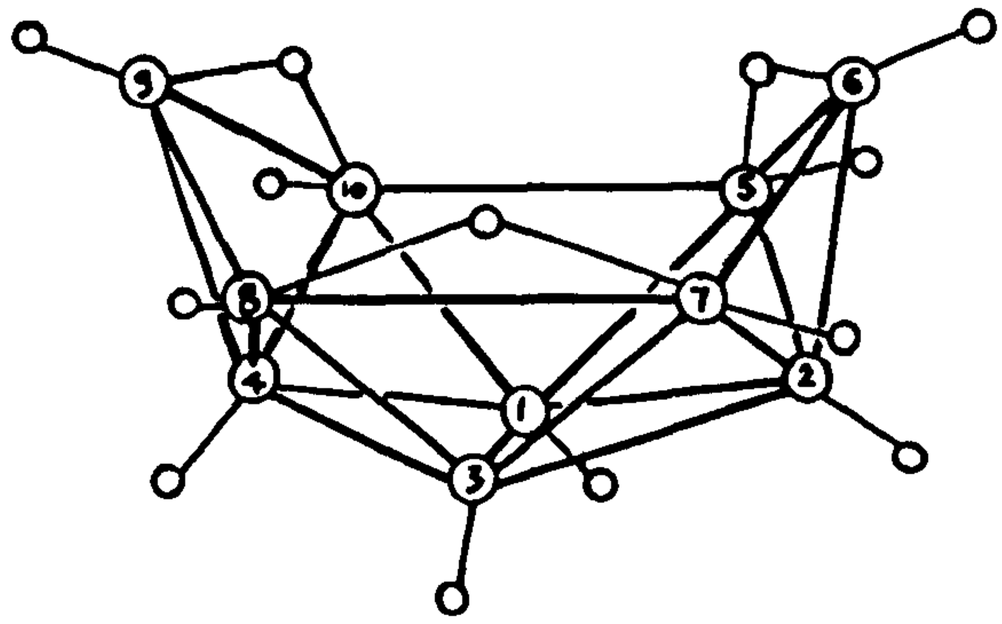

Fig.5.4(a) The proposed structure for the $[B_{10}H_{13}]^-$ ion in solution.

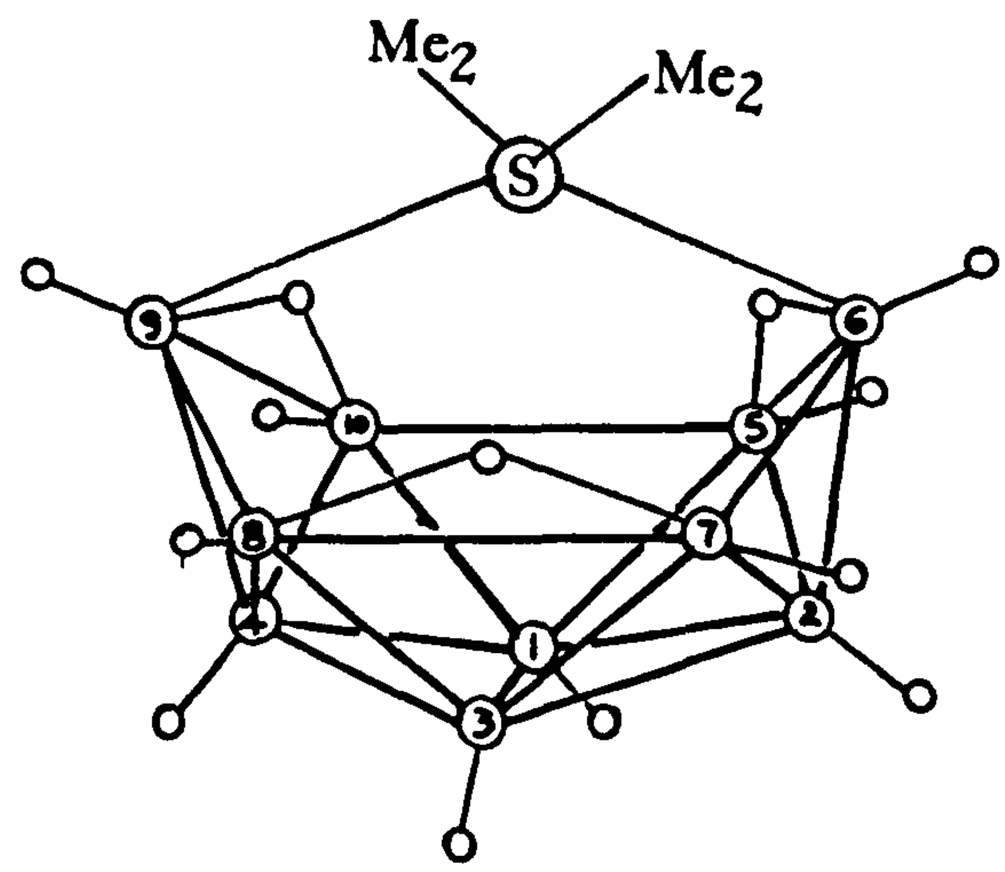

Fig.4.5(b) The possible structure for the $[B_{10}H_{13}(SMe_2)]^-$ ion in solution.

consisted of four doublets of relative area 2:1:5:2. The 360 MHz ^{1}H n.m.r. spectrum showed two distinct bridge hydrogen resonances at δ = -3.0 and -3.7 ppm with relative area 1:2, the $^{1}H\{^{11}B\}$ n.m.r. spectra with specific frequency irradiation were not structurally informative as no line-sharpening of bridge hydrogen resonances were observed to indicate the relationship between bridge hydrogens and boron atoms. The relevant ^{11}B and ^{1}H n.m.r. data of $[B_{10}H_{13}]^-$ are listed in Table 5.3 and Table 5.4 respectively.

(d) $[B_{10}H_{13}(SMe_2)]^-$.

The reaction of $B_{10}H_{14}$ with NaH in SMe_2 resulted $Na[B_{10}H_{13}(SMe_2)]$[58]. This was then treated with $[N(CH_3)_4]Cl$ in water to give $[N(CH_3)_4][B_{10}H_{13}(SMe_2)]$. The ^{11}B n.m.r. spectrum of $[N(CH_3)_4][B_{10}H_{13}(SMe_2)]$ in CD_3CN is identical to that of $Na[B_{10}H_{13}(SMe_2)]$ in D_2O and is presented in Fig. 5.5. It comprised six doublets of relative intensities 1:4:2:1:2. The $^{1}H\{^{11}B$, off-resonance$\}$ n.m.r. spectrum exhibited a bridge hydrogen resonance at δ = -3.9 ppm of relative area three with respect to the resonance of methyl groups. The $^{1}H\{^{11}B\}$ n.m.r. spectra with specific frequency irradiation did not give information about the position of bridge hydrogens and although it provided the chemical shifts of hydrogen atoms attached to boron atoms, the hydrogen of B(3 or 1) was not observed, or obscured by other signals. These ^{1}H

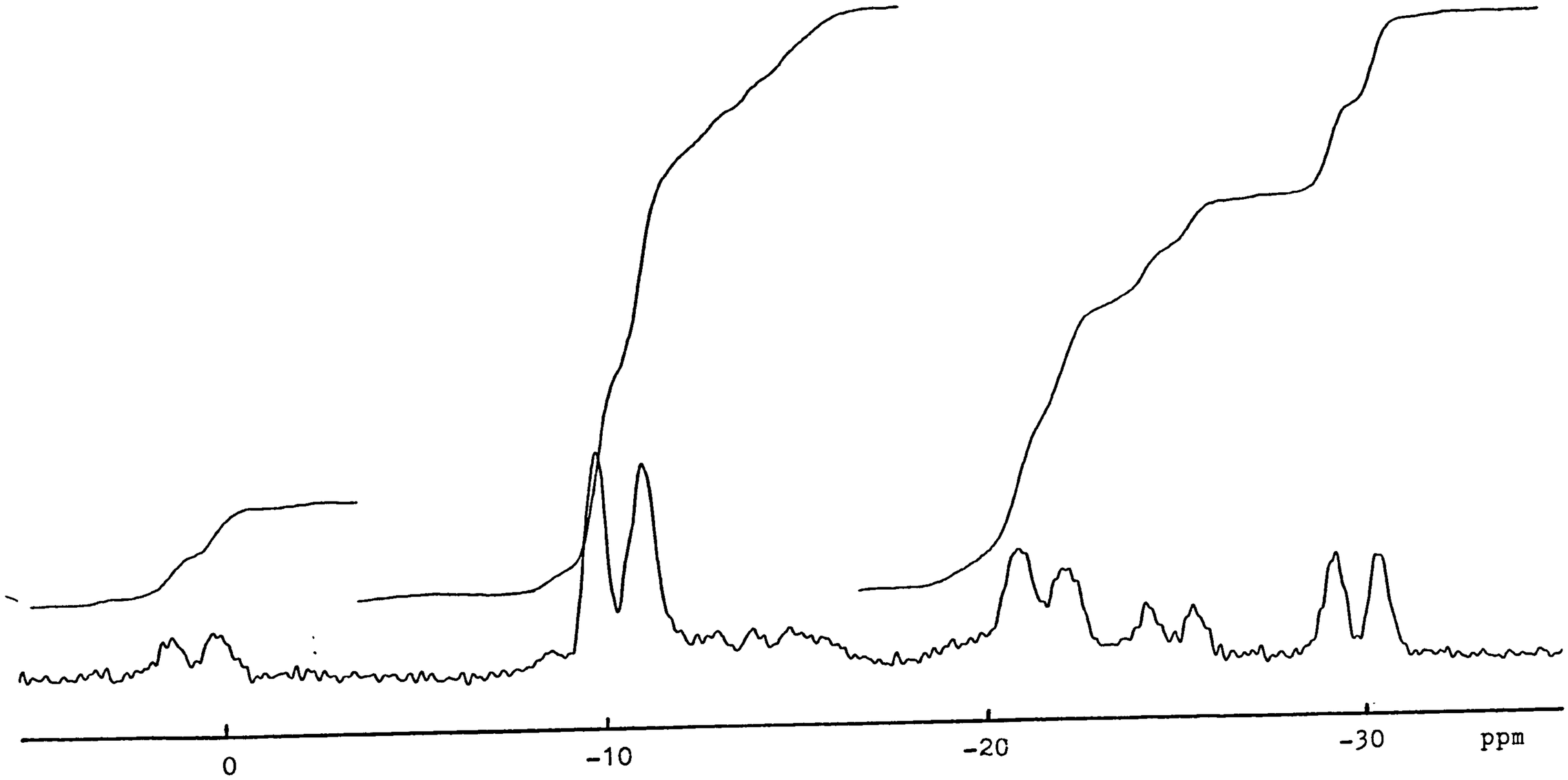

Fig.5.5. 115.5 MHz ^{11}B n.m.r. spectrum of $[B_{10}H_{13}(SMe_2)]^-$

Table 5.3 115.5 MHz ^{11}B N.m.r. Spectral Data for (A) = $[B_{10}H_{13}]^-$ and B = $[B_{10}H_{13}(SMe_2)]^-$ in CD_3CN

$\delta(^{11}B)$/ppm		$J_{(B-H)}$/Hz		Assignment
(A)	(B)	(A)	(B)	
+ 8.75	-21.45	142	151	6,9
+ 1.11	+ 0.89	128	123	1 or 3
- 3.53	-24.8	134	147	3 or 1
- 3.53	-10.34	134	132	5,7,8,10
-33.72	-29.74	141	123	2,4

Table 5.4 360 MHz ^1H N.m.r. Spectral Data for

(A) = $[B_{10}H_{13}]^-$ and (B) = $[B_{10}H_{13}(SMe_2)]^-$ in CD_3CN

$\delta(^1H)$ Terminal/ppm		Associated	δ (^1H) Bridge/ppm		Other	
(A)	(B)	boron atom	(A)	(B)	(A)	(B)
3.19	1.11	6,9	-3.0(1)	-3.9(3)	3.08	3.08
			and		$[N(CH_3)_4]^+$	$[N(CH_3)_4]^+$
2.54	2.23	1 or 3	-3.7(2)			and
2.27	-	3 or 1				(SMe_2)
2.25	1.88;1.23	5,7,8,10				
0.01	0.33	2,4				

chemical shift data are listed in Table 5.4.

The ^{11}B and ^{1}H n.m.r. spectra of $[B_{10}H_{13}(SMe_2)]^-$ are different from those of $[B_{10}H_{13}(Py)]^-$, $[B_{10}H_{13}(NEt_3)]^-$ and $[B_{10}H_{13}(PPh_3)]^-$ in that there is no triplet in the ^{11}B n.m.r. spectrum to show the existence of the BH_2 group, and the $^{1}H\{^{11}B\}$ n.m.r. spectrum on irradiating B(5, 7, 8, 10) did not exhibit line sharpening of the bridge hydrogen resonance. Therefore the structure of $[B_{10}H_{13}(SMe_2)]^-$ must be different from that shown in Fig. 5.3. A comparison of the n.m.r. spectra of $[B_{10}H_{13}(SMe_2)]^-$ with those of $[B_{10}H_{13}]^-$, shows them to be quite similar. The ^{11}B n.m.r. spectra showed similarities in chemical shift range and resonance patterns. The ^{1}H n.m.r. spectra suggested that there are three bridge hydrogens in both anions but unfortunately no information concerning the hydrogen bridge positions could be obtained. The assignment of the ^{11}B n.m.r. spectrum of $[B_{10}H_{13}(SMe_2)]^-$ is therefore based on the established assignment for $[B_{10}H_{13}]^-$ [157]. The possible structure of $[B_{10}H_{13}(SMe_2)]^-$ which agreed with the n.m.r. data is shown in Fig. 5.4(b). Addition of the SMe_2 group to the $[B_{10}H_{13}]^-$ cage by the sulphur atom bridging the B(6) and B(9) positions, maintained the symmetry of the B_{10} cage. Therefore the resonance pattern of the ^{11}B n.m.r. spectrum of $[B_{10}H_{13}(SMe_2)]^-$ is similar to that of $[B_{10}H_{13}]^-$ although the chemical shifts of B(6, 9) and B(5, 7, 8, 10) changed greatly. The resonances due to B(1) or B(3) in $[B_{10}H_{13}]^-$ and

$[B_{10}H_{13}(SMe_2)]^-$ showed unusual behaviour: firstly, as mentioned earlier, the borons are non-equivalent while B(2) and B(4) are equivalent, as are B(5, 7, 8, 10); secondly, the chemical shift of one resonance (either B(1) or B(3) changed greatly from $[B_{10}H_{13}]^-$ to $[B_{10}H_{13}(SMe_2)]^-$ while the chemical shift of the other was not significantly changed; and thirdly, the chemical shift of the proton attached to the boron which had the larger change in chemical shift failed to be detected in both anions.

5.2.2 Electrochemical Studies of $[B_{10}H_{13}(PPh_3)]^-$.

The electrochemical properties of $[B_{10}H_{13}(PPh_3)]^-$ in acetonitrile were studied using the techniques of cyclic voltammetry, a.c. voltammetry and controlled potential electrolysis. Attempts were made to prepare metallaboranes by the anodic dissolution of some reactive metals in acetonitrile solutions of $[B_{10}H_{13}(PPh_3)]^-$. The cyclic and a.c. voltammograms of $[B_{10}H_{13}(PPh_3)]^-$ in other solvents for example, 1,3-dioxalane, dichloromethane and tetramethylurea were also obtained.

(a) Cyclic and a.c. voltammetry.

(i) In acetonitrile.

Cyclic d.c. and a.c. voltammograms of $[B_{10}H_{13}(PPh_3)]^-$ at a Pt electrode in acetonitrile containing $[NBu_4^n][BF_4]$ (0.1 mol dm^{-3}) as supporting electrolyte are given in Fig. 5.6. The cyclic d.c. voltammogram showed oxidation waves at -0.4 and +0.74 V

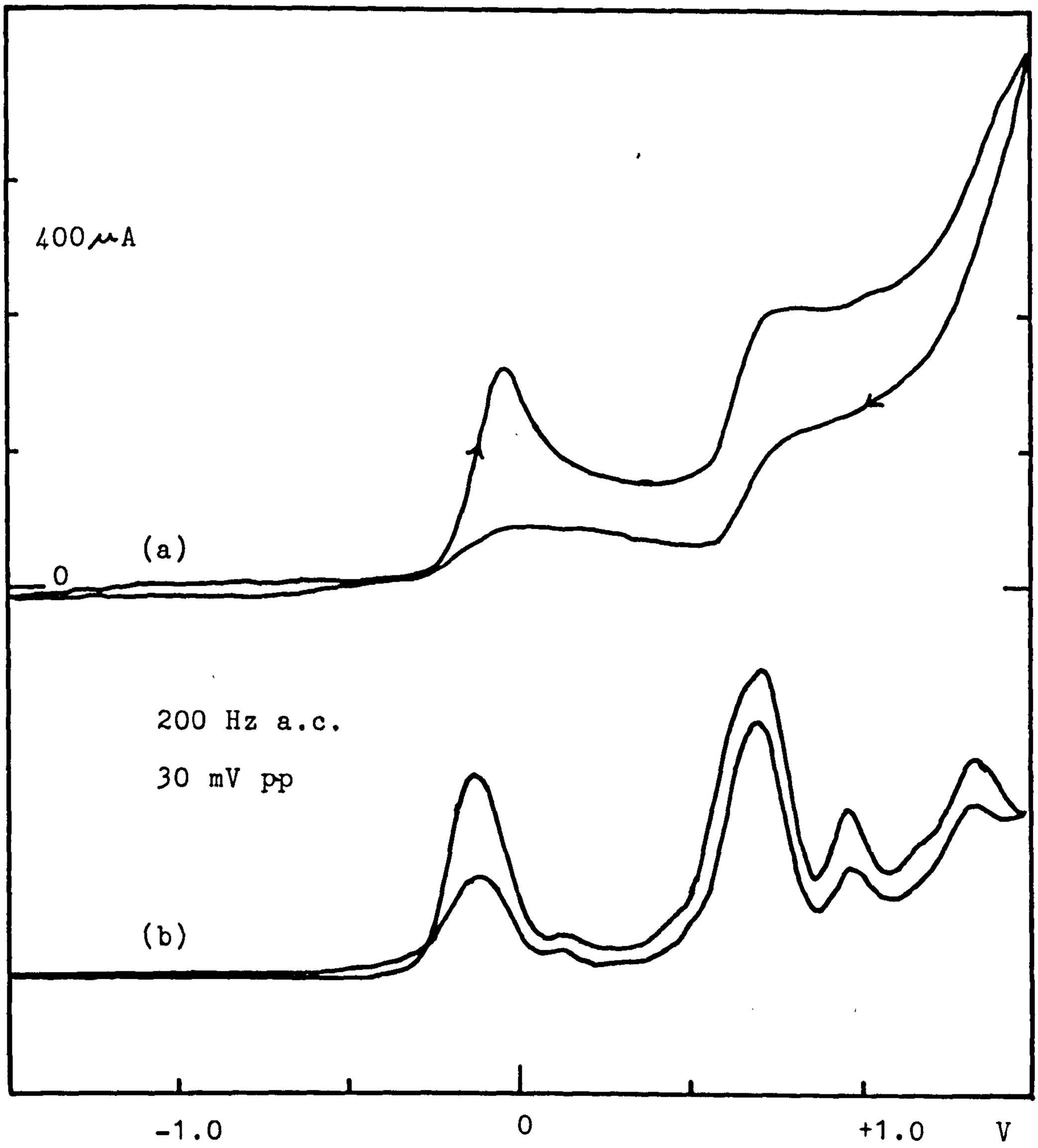

Fig.5.6. (a) Cyclic voltammogram (scan rate 0.5 VS^{-1}) and (b) A.c. voltammogram (scan rate 0.05 VS^{-1}) of $[B_{10}H_{13}(PPh_3)]^-$ in 0.1 M Bu_4NBF_4/CH_3CN

and less well defined waves at higher potentials. The cyclic a.c. voltammogram exhibited a better resolution of the electrochemical processes than the cyclic d.c. voltammogram, and revealed that the electrochemical processes were approximately reversible. The oxidation waves at -0.12, +0.72, +0.96 and +1.34 V observed on the forward scan were considered to approach electrochemical reversibility since the width at half-height of the peaks was ca. 180 mV. (expected $\leqslant$ 90 mV for a fully reversible reaction)[72]. The potentials of the waves were only slightly shifted ($\lesssim$20 mV) on the reverse scan which also is in agreement with reversibility as in, for example, the previous studies of the cyclic a.c. voltammogram of cis-$[Mo(CO)_2(DPE)_2]$ in which a separation in peak potential of approximately 15 mV in the forward and reverse scans was observed[159]. In the cyclic a.c. voltammogram on the reverse scan, the waves at -0.11, +0.70, +0.98 and +1.34 V showed decreases in peak heights which probably resulted from the slow scan rate allowing oxidised species at the electrode surface to diffuse away; however, the first oxidation wave (-0.11 V) showed a greater decrease in peak height on the reverse scan, and this must be due to chemical steps following the electrochemical step which resulted in the concentration of the oxidised species being greatly reduced at the electrode surface. In addition, there was evidence for a chemical step preceding the first electrochemical process in that the first oxidation was not present in

other solvents. Although the $[B_{10}H_{15}]^-$ species was found to be electroinactive at mercury in acetonitrile[91] there is evidence to suggest that the $[B_{10}H_{13}(PPh_3)]^-$ anion reacted with the coordinating solvent, CH_3CN, to give $[B_{10}H_{13}(PPh_3)(CH_3CN)]^-$ before the electrochemical step occurred.

Firstly, the cyclic voltammograms of $[B_{10}H_{13}(PPh_3)]^-$ at Pt in less polar solvents such as 1,3-dioxalane, dichloromethane or tetramethylurea [sect. 5.2.2(a) (ii)(iii) and (iv)] showed the first oxidation wave at 0.68, 0.70 and 0.80 V respectively. These were possibly the oxidation potentials of the $[B_{10}H_{13}(PPh_3)]^-$ anion in each solvent, whereas the voltammograms of $[B_{10}H_{13}(PPh_3)]^-$ in acetonitrile exhibited a lower oxidation potential at -0.4 V which probably resulted from oxidation of a less stable species, e.g. $[B_{10}H_{13}(PPh_3)(CH_3CN)]^-$. The second oxidation wave at 0.74 V probably resulted from further oxidation of the oxidation product, $[B_{10}H_{12}(PPh_3)(CH_3CN)]$. This product was isolated from the controlled potential electrolysis [sect. 5.2.2(c)] at a Pt electrode of $[B_{10}H_{13}(PPh_3)]^-$ in acetonitrile at potentials between -0.4 V to 0.0 V. This involved overall a one-electron oxidation.

Secondly, the $[B_{10}H_{13}(PPh_3)]^-$ anion was slowly oxidised to give $[B_{10}H_{12}(PPh_3)(CH_3CN)]$ on prolonged standing in air for several months, and the oxidation could possibly take place via $[B_{10}H_{13}(PPh_3)(CH_3CN)]^-$ which arose from recrystallisation of $[N(CH_3)_4][B_{10}H_{13}(PPh_3)]$

from acetonitrile-ether. The analysis of $[N(CH_3)_4][B_{10}H_{13}(PPh_3)]$ after recrystallisation from acetonitrile-ether corresponds best to $[N(CH_3)_4][B_{10}H_{13}(PPh_3)].\frac{1}{2}CH_3CN$ although the data for C were significantly low. These processes can be summarised as follows:

$$[B_{10}H_{13}(PPh_3)]^- + CH_3CN \longrightarrow [B_{10}H_{13}(PPh_3)(CH_3CN)]^- \quad (5.1)$$

$$[B_{10}H_{13}(PPh_3)(CH_3CN)]^- \rightleftharpoons [B_{10}H_{13}(PPh_3)(CH_3CN)]^{\cdot} + e^- \quad (5.2)$$

$$[B_{10}H_{13}(PPh_3)(CH_3CN)]^{\cdot} \longrightarrow [B_{10}H_{12}(PPh_3)(CH_3CN)] + H^{\cdot} \quad (5.3)$$

$$[B_{10}H_{12}(PPh_3)(CH_3CN)] \rightleftharpoons [B_{10}H_{12}(PPh_3)(CH_3CN)]^{+\cdot} + e^- \quad (5.4)$$

Equations (5.1) to (5.3) described first oxidation step, the product of which underwent the second oxidation step described in equation (5.4).

(ii) In 1,3-dioxalane.

The cyclic d.c. voltammogram of $[B_{10}H_{13}(PPh_3)]^-$ at platinum in 1,3-dioxalane containing $[NBu_4^n][BF_4]$ (0.1 mol dm^{-3}) as supporting electrolyte between the cathodic and anodic limits of -1.5 V and +1.5 V is shown in Fig. 5.7. Oxidation waves near +0.68 V and +0.84 V and

reduction waves near 0.0 V and -0.7 V were observed. When the anodic potential limit was decreased, the reduction wave near 0.0 V was smaller until at the limit of +1.0 V, the decreased current of the reduction wave gave rise to a better resolution in the electrochemical process of the second oxidation wave (at 0.84 V). The second oxidation wave was then found to be reversible (Fig. 5.8). When the cathodic potential limit was adjusted to more positive than the reduction wave at -0.7 V, the second oxidation wave (0.84 V) was less pronounced indicating that the electrochemical oxidation process at this potential was associated with the reductant produced at -0.7 V. The electrode processes of $[B_{10}H_{13}(PPh_3)]^-$ in 1,3-dioxalane are complex; furthermore, controlled potential electrolysis had not been studied due to the poor solubility of $[N(CH_3)_4]$-$[B_{10}H_{13}(PPh_3)]$ in 1,3-dioxalane. As a result, detailed electrochemical mechanisms are not proposed. However, the electrode processes in 1,3-dioxalane must be different from those in acetonitrile since the voltammograms are different.

(iii) In dichloromethane.

Cyclic voltammograms of $[B_{10}H_{13}(PPh_3)]^-$ at a Pt electrode in dichloromethane containing $[NBu_4^n][BF_4]$ (0.1 mol dm^{-3}) as supporting electrolyte are shown in Fig. 5.9. Fig. 5.9(a) and Fig. 5.9(b) showed the trace of the first scan and traces of three cycles after the first scan respectively. The oxidation wave near +0.9 V

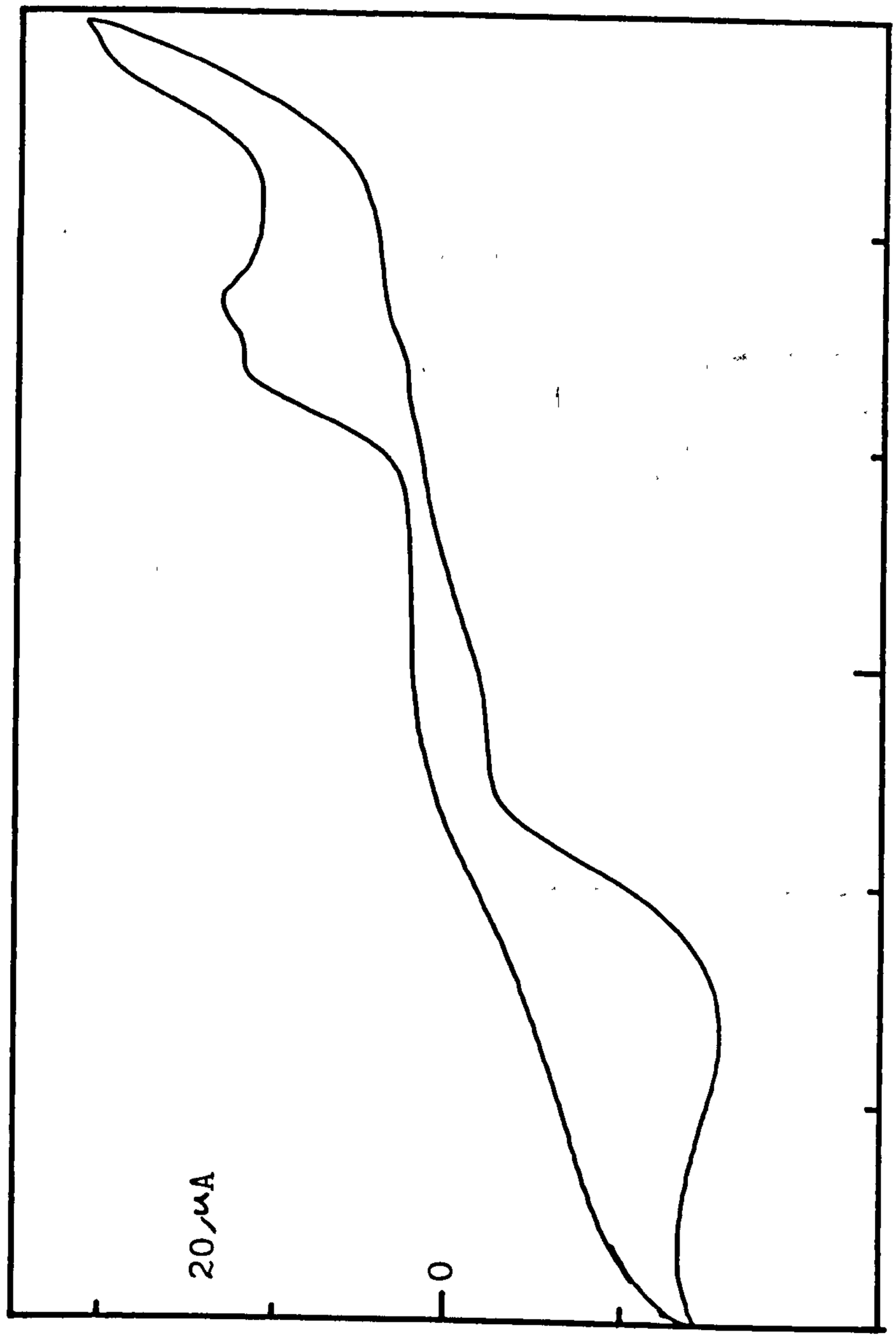

Fig.5.7. Cyclic voltammogram (scan rate 0.5 VS^{-1}) of $[B_{10}H_{13}(PPh_3)]^-$ in 0.1 M Bu_4NBF_4/1,3-dioxalane.

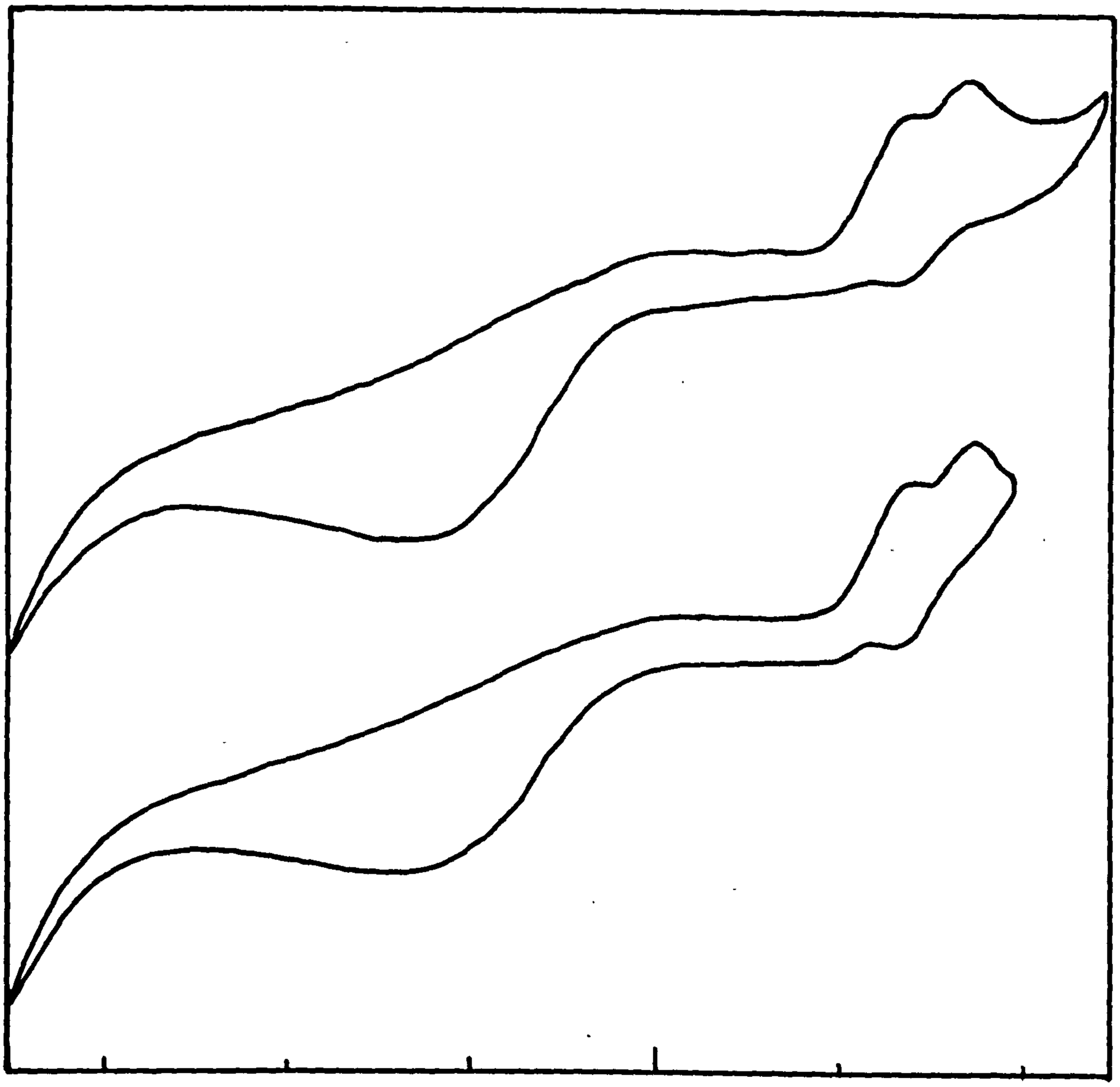

Fig.5.8. Cyclic voltammograms (scan rate 0.5 VS^{-1}) of $[B_{10}H_{13}(PPh_3)]^-$ in 0.1 M Bu_4NBF_4/1,3-dioxalane.

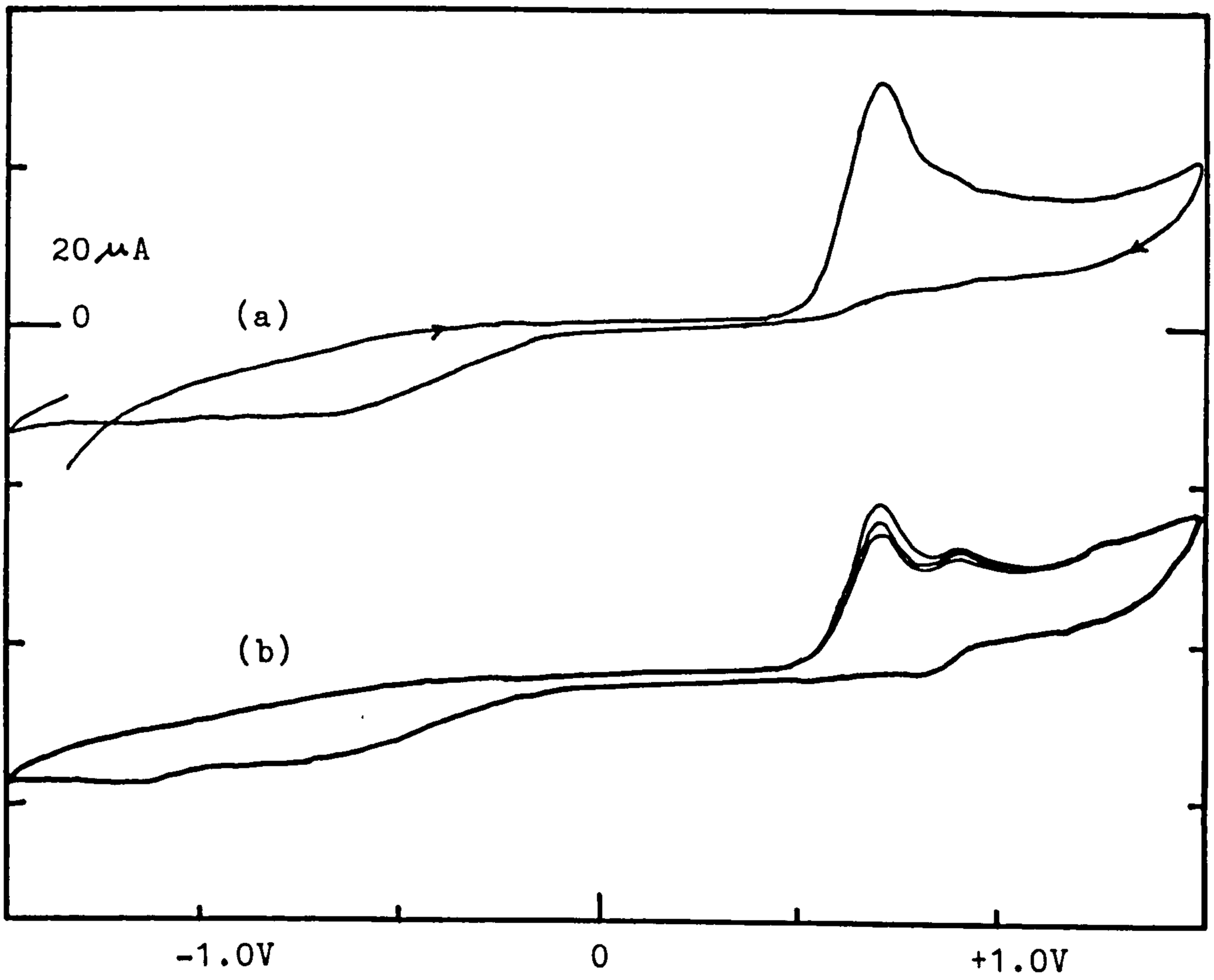

Fig.5.9. Cyclic voltammograms (scan rate 0.5 VS^{-1}) of $[B_{10}H_{13}(PPh_3)]^-$ in 0.1 M Bu_4NBF_4/CH_2Cl_2

(a) First trace and (b) Second, third and fourth traces.

shown in Fig. 5.9(b) was not observed on the first scan indicating that the species being oxidised must have resulted from the oxidation of a slow chemical reaction product arising from the first oxidation at the potential 0.7 V. Changes of either anodic or cathodic potential limits did not alter the oxidation or reduction waves. The voltammograms showed that the electrode processes of $[B_{10}H_{13}(PPh_3)]^-$ in dichloromethane are again different from those in acetonitrile or 1,3-dioxalane.

(iv) In tetramethylurea.

Cyclic and a.c. voltammograms of $[B_{10}H_{13}(PPh_3)]^-$ at a Pt electrode in tetramethylurea containing $[NBu_4^n][BF_4]$ (0.1 mol dm^{-3}) as supporting electrolyte are given in Fig. 5.10. Oxidation waves at 0.80 V and 1.24 V and reduction waves at 0.2 V and -0.32 V in the cyclic voltammograms corresponded to oxidation waves at 0.84 V and 1.28 V and a reduction wave at 0.2 V in the a.c. voltammogram. When the cathodic potential limit was adjusted to a less negative potential, the oxidation waves were not affected. However, when the anodic potential limit was lowered from 1.5 V to 1.0 V, the reduction waves were less pronounced. These indicated that the first oxidation wave at 0.80 V must have resulted from oxidation of $[B_{10}H_{13}(PPh_3)]^-$; The unstable oxidised species formed probably then underwent a chemical step to produce a more stable species, which, in turn, was oxidised at 1.24 V. The oxidation product at 1.24 V probably underwent further chemical steps to produce

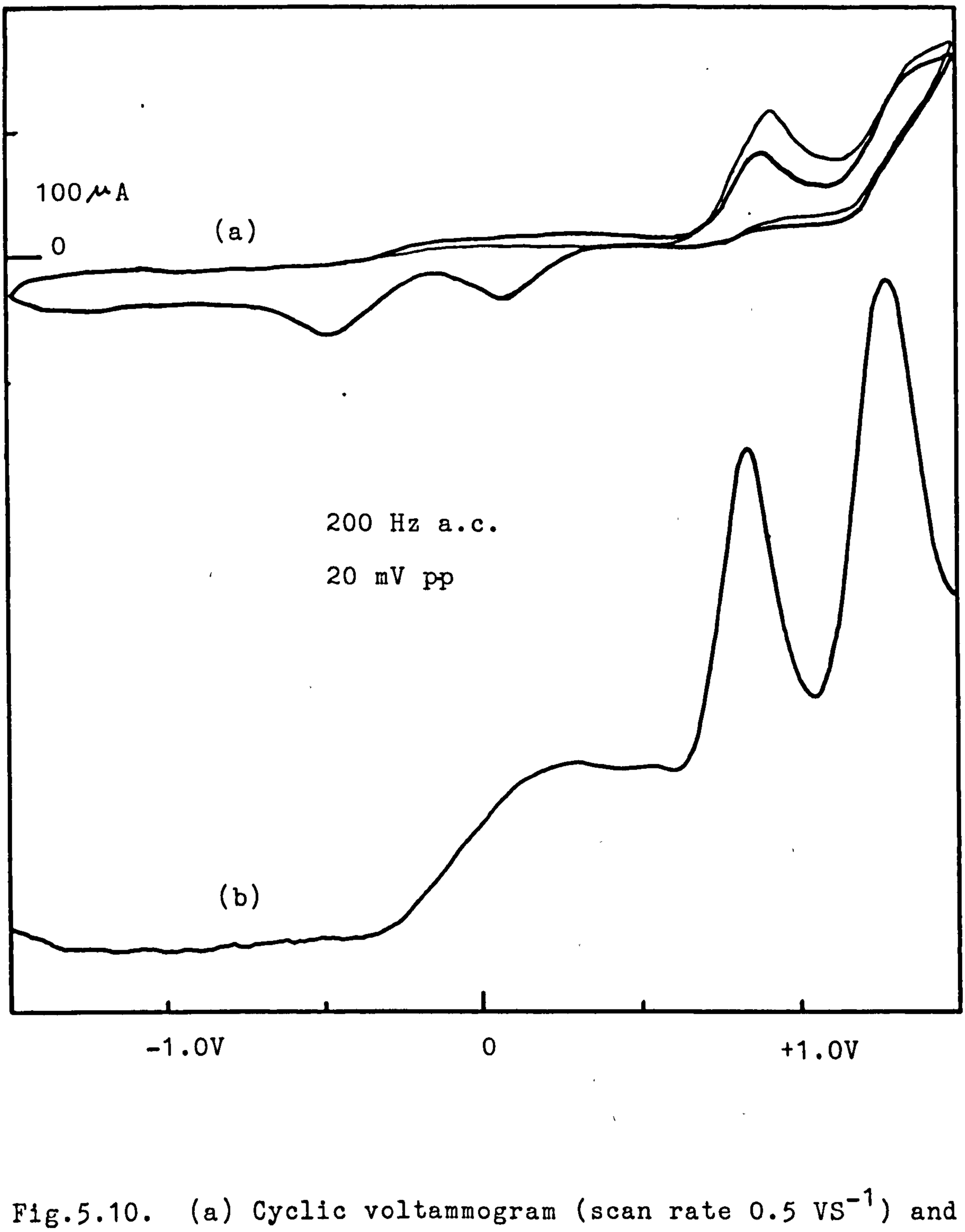

Fig.5.10. (a) Cyclic voltammogram (scan rate 0.5 VS^{-1}) and (b) A.c. voltammogram (scan rate 0.05 VS^{-1}) of $[B_{10}H_{13}(PPh_3)]^-$ in 0.1 M Bu_4NBF_4/TMU.

products which were reduced at 0.2 V and -0.32 V. Apparently, the electrochemical processes taking place in tetramethylurea are again different from those in acetonitrile, 1,3-dioxalane or dichloromethane.

(b) Anodic behaviour of transition metal.

The anodic behaviour of transition metals in acetonitrile solution of $[B_{10}H_{13}(PPh_3)]^-$ was evaluated in order to find out which metals were suitable as anodes for the electrochemical preparation of metalla-borane complexes. The behaviour could be categorised in three types as described in Chapter 3, sect. 3.2.2.

Type (a) are metals which are themselves inert but allow anodic oxidation of the anion. These are Pt (-0.16 V), Pd (-0.2 V) and V (+0.1).

Type (b) are metals which are inert, yielding no products from either anodic dissolution or anodic oxidation of the anions. These are Ti, Nb, Zr, W, Ta, Au.

Type (c) are metals which undergo anodic dissolution. These are Cu (-0.6 V), Co (-0.3 V), Ni (-0.2 V), Fe (-0.4 V), Zn (-0.5 V), Cd (-0.4 V).

(c) Controlled potential electrolysis.

Exhaustive electrolysis at platinum of an acetonitrile solution of $[B_{10}H_{13}(PPh_3)]^-$ was carried out at potentials between -0.24 $\rightarrow$ 0.0 V and overall one-electron oxidation was involved. The product, characterized by analysis of its ^{11}B and ^{1}H n.m.r. spectra, was $[B_{10}H_{12}(PPh_3)(CH_3CN)]$. The ^{11}B n.m.r. spectrum of

$[B_{10}H_{12}(PPh_3)(CH_3CN)]$ shown in Fig. 5.11 consisted of five doublets of relative intensities 1:1:4:1:2 and a triplet of intensity one which resulted from B-H and B-P couplings. The $^{11}B\{^1H\}$ n.m.r. spectrum confirmed the existence of the B-P coupling (J_{B-P}=120 Hz). The assignment of the ^{11}B n.m.r. spectrum of $[B_{10}H_{12}(PPh_3)(CH_3CN)]$ is listed in Table 5.1 and is similar to that of $[B_{10}H_{13}(PPh_3)]^-$. Therefore it is isostructural with $[B_{10}H_{14}]^{2-}$. The triplet due to the BH_2 group at B(9) of $[B_{10}H_{13}(PPh_3)]^-$ (Fig. 5.3) was replaced by a doublet due to substitution of CH_3CN at the B(9) position to give $[B_{10}H_{12}(PPh_3)(CH_3CN)]$. The B(5, 7) and B(8, 10) positions became magnetically equivalent, the B(6) and B(1, 3) positions were resolved, and therefore coupling of B(6) to phosphorous of nuclear spin ½ was observed in $[B_{10}H_{12}(PPh_3)(CH_3CN)]$. This confirmed the assignment of the ^{11}B n.m.r. data of $[B_{10}H_{13}(PPh_3)]^-$ where the doublet of B(1,3) was superimposed on the triplet of B(6) and therefore B-P coupling was not observed. The $^1H\{^{11}B\}$ n.m.r. spectra with specific frequency irradiation of the boron resonances of $[B_{10}H_{12}(PPh_3)(CH_3CN)]$ is presented in Fig. 5.12. They appeared to be similar to those of $[B_{10}H_{13}(PPh_3)]^-$ in that irradiation of the B(5, 7, 8, 10) resonances resulted in line sharpening of the two bridge hydrogen resonances, and on irradiating B(2) resonance, long range H(2)-P coupling of J_{H-P} = 24 Hz was observed. The large peak at δ = 2.25 ppm was thought to be due to water; when it was removed by subtracting

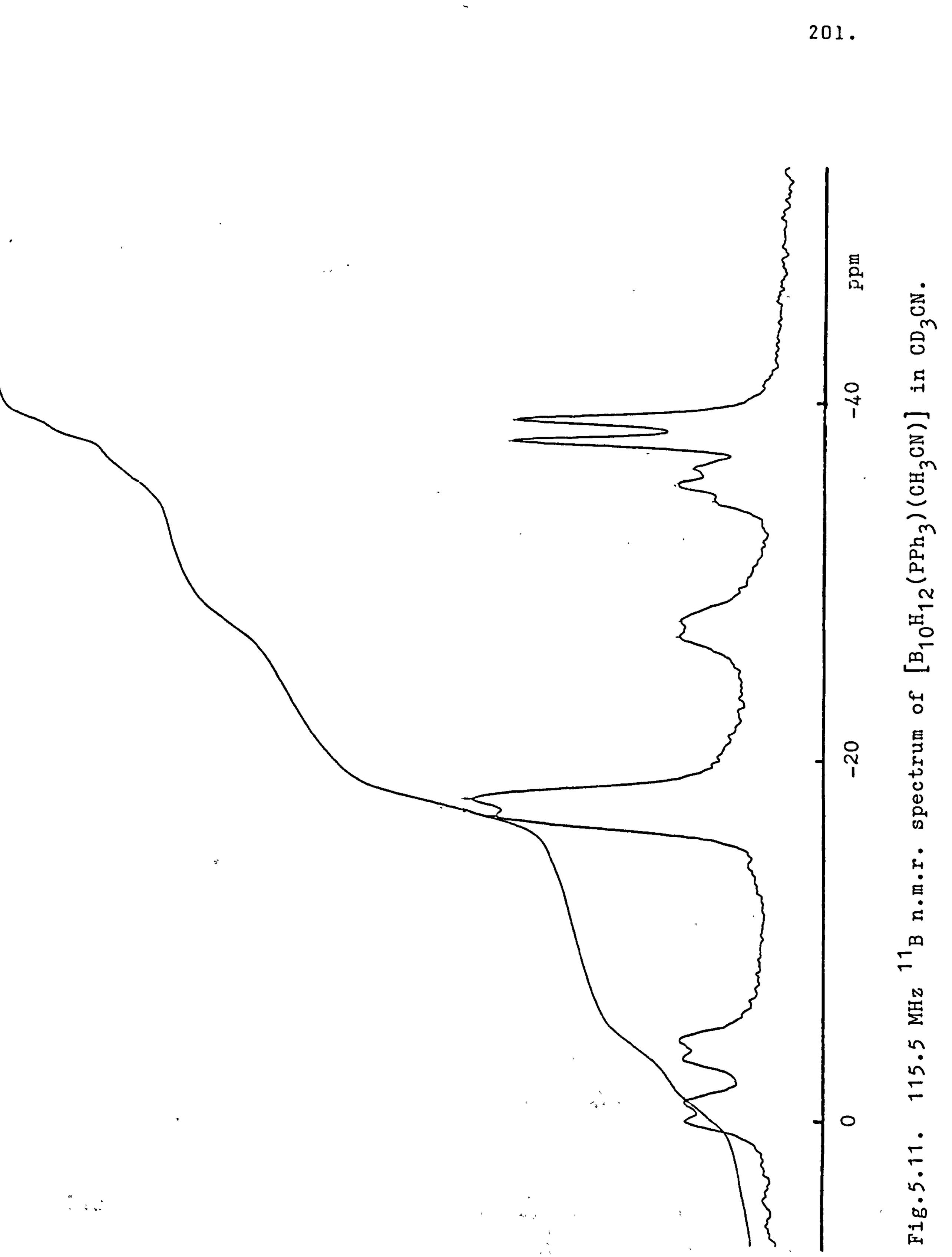

Fig.5.11. 115.5 MHz ^{11}B n.m.r. spectrum of $[B_{10}H_{12}(PPh_3)(CH_3CN)]$ in CD_3CN.

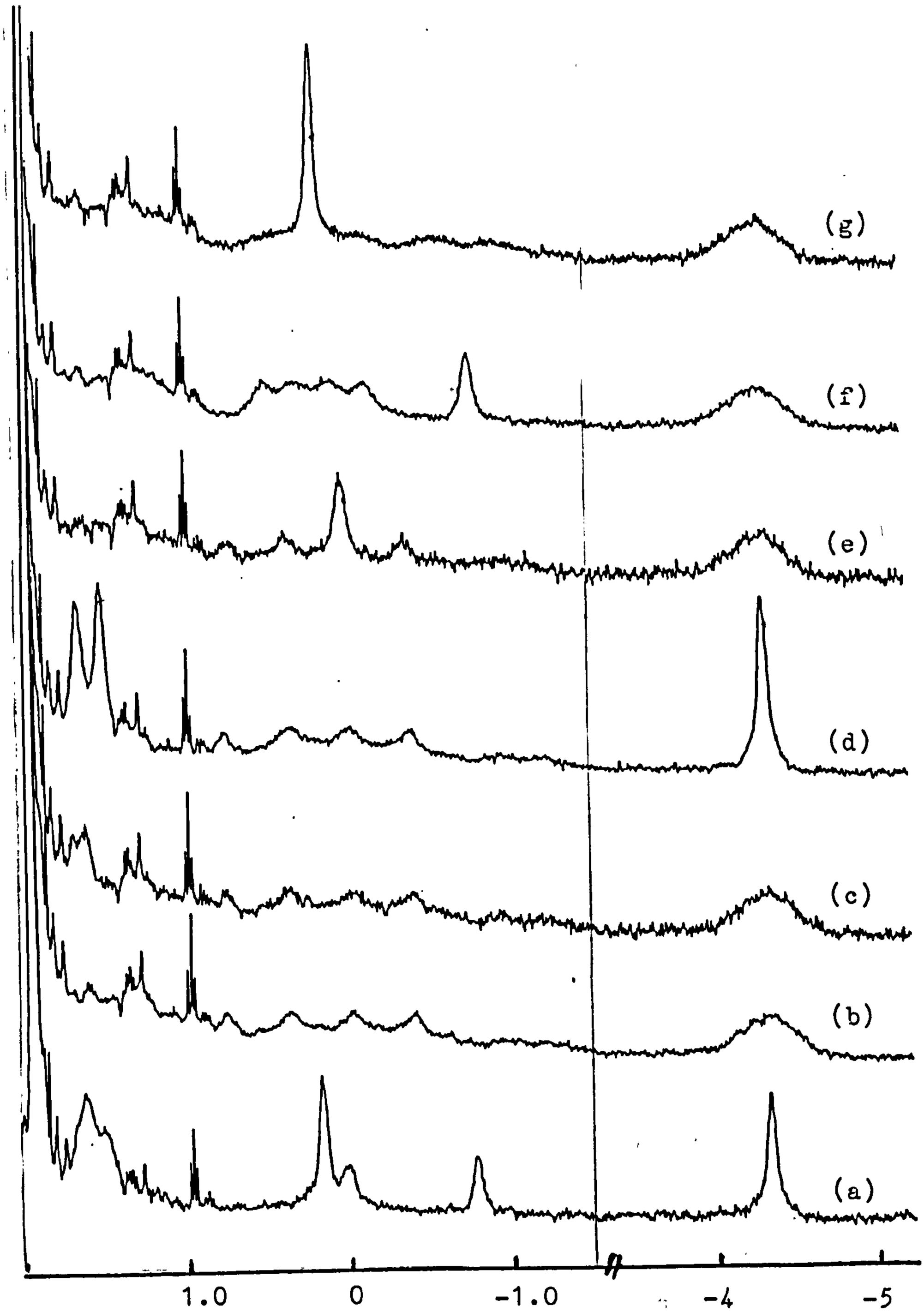

Fig.5.12. 360 MHz $^{1}H\{^{11}B\}$ n.m.r. spectra of $[B_{10}H_{12}(PPh_3)(CH_3CN)]$ in CD_3CN. (a) $^{1}H\{^{11}B\}$, (b) - (g) $^{1}H\{^{11}B\}$ at boron resonances from low field to high field.

the off-resonant signal, the proton resonance of B(4) was revealed at δ = 2.16 ppm rather than at δ = 2.25 ppm. Peaks at δ = 1.98 ppm and 7.5 ppm were due to CD_2HCN and PPh_3 respectively. A peak at δ = 4.73 ppm was probably associated with the boron resonance at δ = 20 ppm.

The electrolysis of an acetonitrile solution of $[B_{10}H_{13}(PPh_3)]^-$ at a copper anode proceeded at potentials between -0.6 V $\longrightarrow$ -0.2 V. The weight loss of the copper anode was consistent with copper entering the solution as Cu(I). The 80.24 MHz ^{11}B n.m.r. spectrum of the product was similar to that of $[B_{10}H_{13}(PPh_3)]^-$ except that the triplet due to BH_2 group of the B(9) position had shifted from -28.6 ppm to -30.7 ppm. This could possibly have resulted from a weak interaction between hydrogens of BH_2 and Cu(I). However the interaction was not strong enough to form the $\{[B_{10}H_{13}(PPh_3)]Cu(CH_3CN)_2\}$ complex. A similar experiment was carried out with the addition of two equivalents of PPh_3 to the anode compartment. The product obtained appeared to have a similar n.m.r. spectrum.

The eletrolysis of an acetonitrile solution of $[B_{10}H_{13}(PPh_3)]^-$ at a nickel anode proceeded at a potential of -0.4 V. The weight loss of the nickel anode was less than that required for Ni $\rightarrow$ Ni(II). Therefore either Ni(III) formed or else oxidation of the anion occurred. It had been shown[20] that Ni(III) and Ni(IV) species could be formed by anodic oxidation of nickel metal in hydrogen fluoride solutions at high potentials

(10-35 V). Therefore, it is likely that nickel entered the solution as Ni(II) and the anion was oxidised at the Ni anode as well as by Ni(II). The product identified by its ^{11}B n.m.r. spectrum was $[B_{10}H_{12}(PPh_3(CH_3CN)]$.

The electrolysis of an acetonitrile solution of $[B_{10}H_{13}(PPh_3)]^-$ at a zinc anode proceeded at potentials between -0.3 V $\longrightarrow$ -0.17 V. The weight loss of the zinc anode was consistent with zinc entering the solution as Zn(II). The product identified by its ^{11}B n.m.r. spectrum was $[B_{10}H_{12}(PPh_3)(CH_3CN)]$. The $[B_{10}H_{13}(PPh_3)]^-$ anion was probably oxidised by Zn(II). A similar experiment was carried out with the addition of two equivalents of PPh_3, the products characterized by their ^{11}B n.m.r. spectrum were $[B_{10}H_{12}(PPh_3)(CH_3CN)]$ and a little of $[B_{10}H_{13}(PPh_3)]^-$.

5.2.3 Chemical Oxidation of $[B_{10}H_{13}(PPh_3)]^-$.

Electrochemical studies of $[B_{10}H_{13}(PPh_3)]^-$ have shown that the BH_2 group at the B(9) position was readily oxidised. Anodic dissolution of Cu, Ni or Zn in acetonitrile solutions of $[B_{10}H_{13}(PPh_3)]^-$ did not give the desired metallaborane complexes, but instead, the anion was oxidised at the Ni anode and by Ni(II) and Zn(II) generated electrochemically to give $[B_{10}H_{12}(PPh_3)(CH_3CN)]$, or showed a weak interaction between BH_2 group and the electrochemically generated Cu(I). The chemical oxidation of $[B_{10}H_{13}(PPh_3)]^-$ was therefore studied for comparison.

(a) The reaction of $[B_{10}H_{13}(PPh_3)]^-$ with $CuCl.H_2O$.

The reaction of $[B_{10}H_{13}(PPh_3)]^-$ with $CuCl.H_2O$ with the addition of PPh_3 in acetonitrile yielded a mixture of $[B_{10}H_{13}(PPh_3)]^-$ and $[B_{10}H_{12}(PPh_3)(CH_3CN)]$(ca.1:1 ratio in 7 hr. of stirring). Therefore Cu(I) slowly oxidised $[B_{10}H_{13}(PPh_3)]^-$

(b) The reaction of $[B_{10}H_{13}(PPh_3)]^-$ with $NiSO_4.6H_2O$.

The reaction of $[B_{10}H_{13}(PPh_3)]^-$ with $NiSO_4.6H_2O$ in acetonitrile showed that $[B_{10}H_{13}(PPh_3)]^-$ was not oxidised by Ni(II) within 20 hr. This could possibly be due to the solvent effect in that Ni(II) was coordinated with H_2O.

(c) The reaction of $[B_{10}H_{13}(PPh_3)]^-$ with Hg_2Cl_2.

Reactions of Hg_2X_2 with $[B_3H_8]^-$ or $[B_9H_{12}]^-$ had previously given rise to $[B_3H_7(X)]^-$ or $[B_9H_{11}(X)]^-$, $[B_9H_{10}(X)_2]^-$, and $B_{18}H_{22}$ respectively[27,160]. It was therefore anticipated that $[B_{10}H_{13}(PPh_3)]^-$ with Hg_2Cl_2 might lead to $[B_{10}H_{12}(Cl)(PPh_3)]^-$ or substituted higher boranes. This did not occur, and instead, $[B_{10}H_{12}(PPh_3)(CH_3CN)]$or $B_9H_{13}[PPh_3]$ were obtained when these reactions were carried out in acetonitrile or dichloromethane respectively. The 115.5 MHz ^{11}B n.m.r. spectrum of $B_9H_{13}[PPh_3]$ in $CDCl_3$ is shown in Fig. 5.13. It comprised two broad doublets with relative intensities of 1:2 which assigned to B(7) and B(6,8), three doublets of relative intensities 1:2:2 which assigned to B(1), B(5, 9) and B(2, 3) and a triplet resulted from B-H and B-P coupling of relative intensity one which assigned to

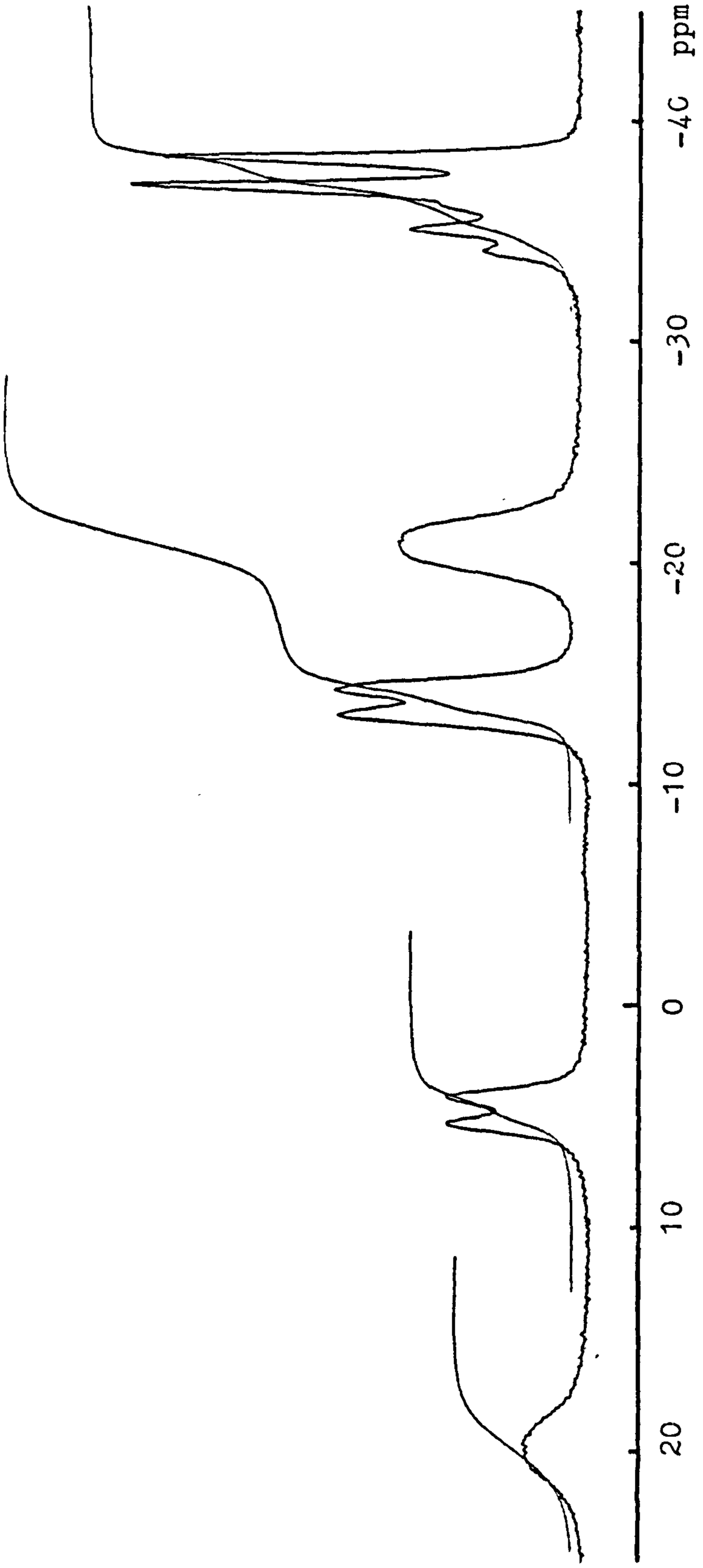

Fig.5.13. 115.5 MHz ^{11}B n.m.r. spectrum of $B_9H_{13}[PPh_3]$ in $CDCl_3$.

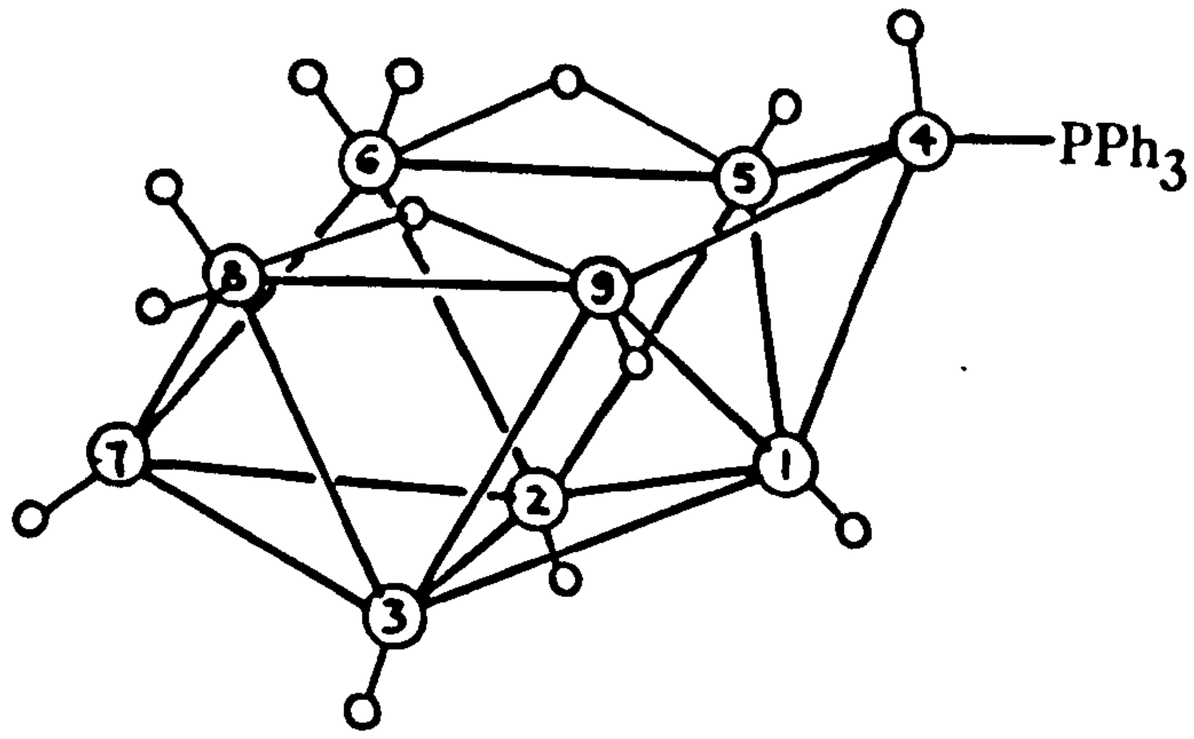

Fig.5.14. The structure of $B_9H_{13}[PPh_3]$

B(4) attached to PPh_3. These assignments are based on the well established results for $B_9H_{13}L$[140,161] [L = CO, CH_3CN, SMe_2, SEt_2 . The structure of $B_9H_{13}[PPh_3]$ shown in Fig. 5.14 is derived from the crystal structure of B_9H_{13} $[CH_3CN]$[162]. The ^1H n.m.r. spectrum of $B_9H_{13}[PPh_3]$ supported the ^{11}B n.m.r. data and is consistent with the ^1H n.m.r. data for $B_9H_{13}L$. It contained a resonance attributable to two bridge hydrogens at a chemical shift of -3.09 ppm and the resonance of the bridge hydrogens was sharpened on irradiating B(5, 9), and to a lesser extent on irradiating B(6, 8). This implied that these borons were associated with the bridge hydrogens. The ^{11}B and ^1H n.m.r. spectral data for $B_9H_{13}[PPh_3]$ are listed in Table 5.5.

(d) The reaction of $[B_{10}H_{13}(PPh_3)]^-$ with HCl.

Reactions of $[B_{10}H_{13}(PPh_3)]^-$ with HCl in dichloromethane led to $B_9H_{13}[PPh_3]$ in lower yield than that obtained with Hg_2Cl_2. It had previously been shown that[54] reaction of $[B_{10}H_{13}(X)]^-$ with HCl in acetonitrile or diethyl sulfide yielded $[B_{10}H_{12}(X)(CH_3CN)]$ or $[B_{10}H_{12}(X)(SEt_2)]$ respectively whereas treatment of $[B_{10}H_{13}(X)]^-$ with aqueous acid solutions resulted in $B_9H_{13}X$. The reaction products are therefore dependent on solvent.

Table 5.5 ^{11}B and ^{1}H N.m.r. Spectral Data for $B_9H_{13}[PPh_3]$

$\delta^{11}B$/ppm	J_{B-H}/Hz	$\delta^{1}H$ Terminal/ppm	$\delta^{1}H$ Bridge/ppm	Assignment
+19.8 b	-	4.17	-3.09(2)	7
+ 4.8 d	145	2.76		1
-13.7 d	139	1.91		5,9
-20.8 b	-	2.04,0.23		6,8
-35.1 t	J_{B-P}= 120	0.03		4
-37.6 d	147	0.47		2,3

b = broad; d = doublet; t = triplet

5.2.4 Electrochemical Studies of $[B_{10}H_{13}(SMe_2)]^-$.

(a) Cyclic and a.c. voltammetry.

(i) In acetonitrile.

Cyclic and a.c. voltammograms of $[B_{10}H_{13}(SMe_2)]^-$ at a Pt electrode in acetonitrile containing $[NBu_4^n][BF_4]$ (0.1 mol dm^{-3}) as supporting electrolyte are shown in Fig. 5.15. The cyclic voltammogram showed oxidation waves near 0.28 V, 0.44 V, 0.62 V, 0.86 V and 1.2 V and reduction waves near -0.6 V and -1.1 V. The a.c. voltammogram showed oxidation waves at 0.28 V, 0.59 V, 0.9 V and 1.3 V but reduction waves were not well defined. When the anodic potential limit was decreased (Fig. 5.16), the reduction waves were less pronounced; however, the remaining oxidation waves were not affected which indicated that the reduction waves resulted from the oxidised species which were produced at higher potentials. When the cathodic potential limit was adjusted from -1.7 V to -1.1 V, the oxidation wave at 0.44 V was not observed which indicated that the species being oxidised at 0.44 V resulted from the species reduced near -1.3 V. When the cathodic potential limit was adjusted to 0.0 V, the oxidation wave near 0.28 V was not observed which implied that the species oxidised at 0.28 V was associated with species reduced near -0.6 V. These voltammograms are shown in Fig. 5.17. It is now quite certain that the first oxidation potential of $[B_{10}H_{13}(SMe_2)]^-$ is near 0.62 V. The controlled potential electrolysis of $[B_{10}H_{13}(SMe_2)]^-$ proceeded at 0.6 V

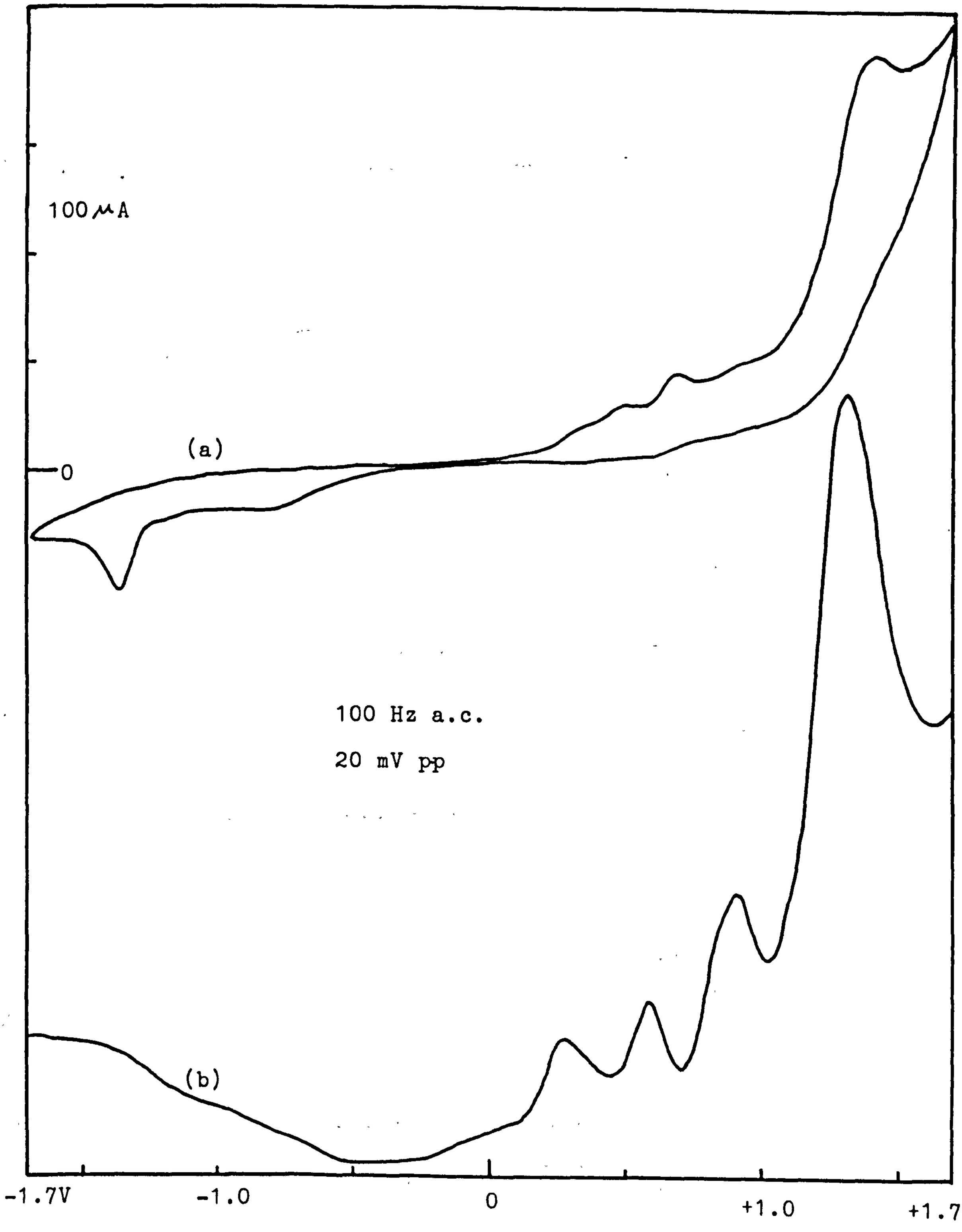

Fig.5.15. (a) Cyclic voltammogram (scan rate 0.5 VS^{-1}) and (b) A.c. voltammogram (scan rate 0.05 VS^{-1}) of $[B_{10}H_{13}(SMe_2)]^-$ in 0.1 M Bu_4NBF_4/CH_3CN.

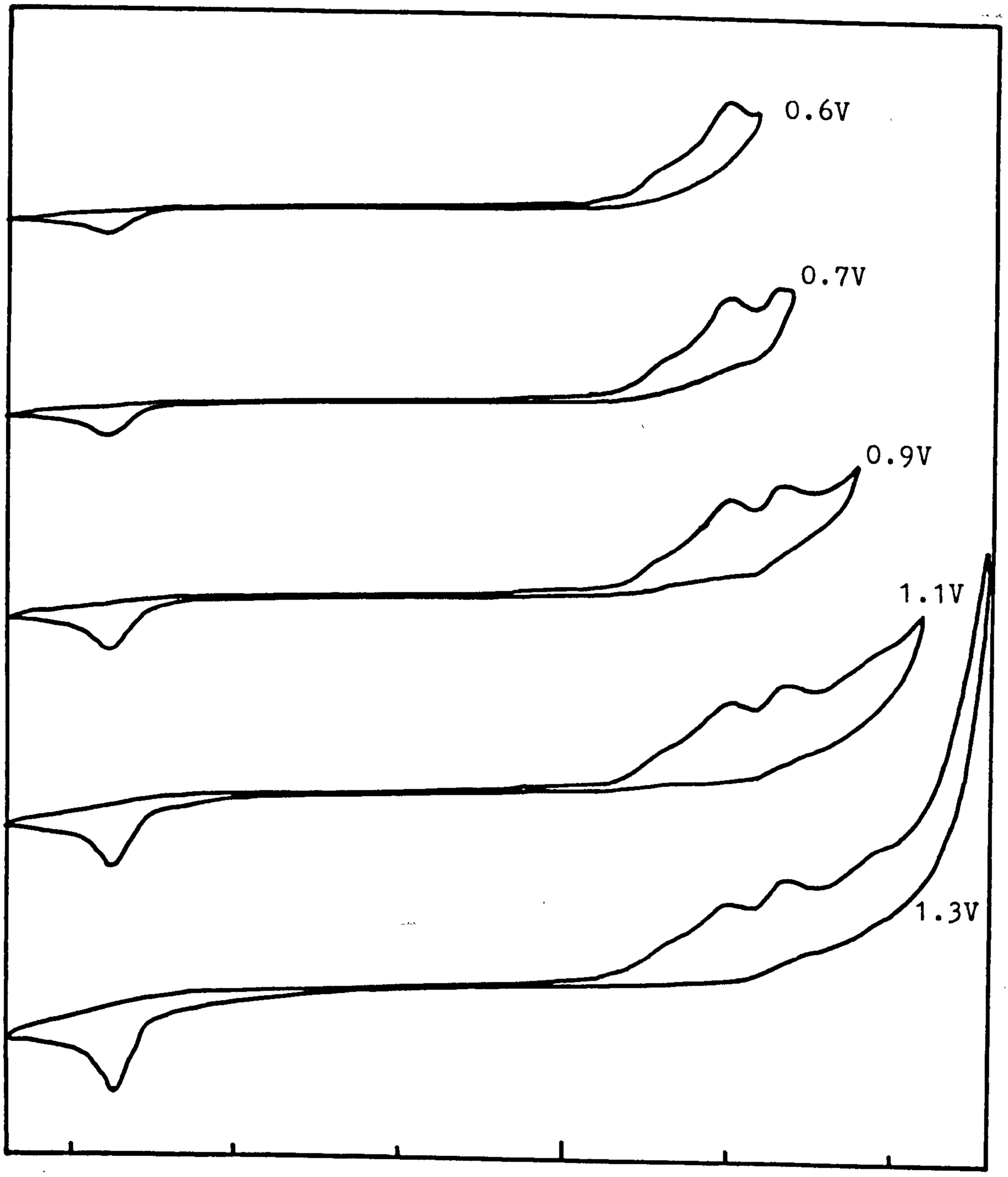

Fig.5.16. Cyclic voltammograms (scan rate 0.5 VS^{-1}) of $[B_{10}H_{13}(SMe_2)]^-$ in 0.1 M Bu_4NBF_4/CH_3CN.

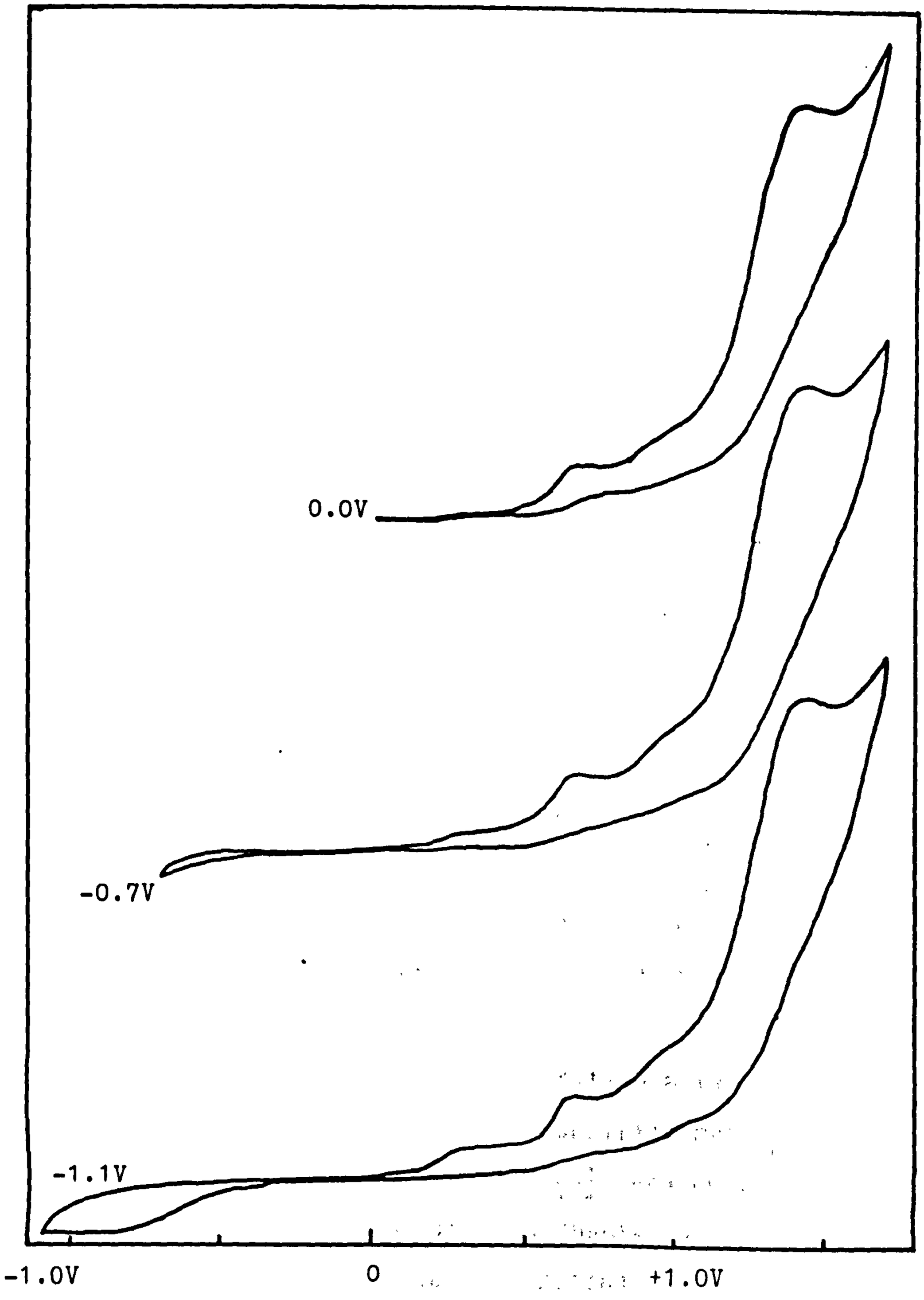

Fig.5.17. Cyclic voltammograms (scan rate 0.5 VS^{-1}) of $[B_{10}H_{13}(SMe_2)]^-$ in 0.1 M Bu_4NBF_4/CH_3CN.

[sect. 5.2.3(c)]. It was not complicated by the oxidation steps which had been observed near 0.28 V and 0.44 V since the small waves at 0.28 and 0.44 V resulted from oxidation of species produced by the reduction wave at -1.3 V. This, in turn, was related to oxidations occuring at potentials above 1.0 V. The oxidation wave near 0.44 V was possibly due to unstable reduced species, since it was not observed in the a.c. voltammogram as a result of the slow scan rate.

(ii) In 1,3-dioxalane.

Cyclic and a.c. voltammograms of $[B_{10}H_{13}(SMe_2)]^-$ at a Pt electrode in 1,3-dioxalane containing $[NBu_4^n][BF_4]$ (0.1 mol dm^{-3}) as supporting electrolyte are given in Fig. 5.18. The cyclic voltammogram showed an oxidation wave near 1.2 V and a reduction wave near -0.7 V. The a.c. voltammogram was better resolved and showed three oxidation waves at 0.72 V, 1.1 V and 1.4 V, and a reduction wave near -0.6 V. The voltammograms of $[B_{10}H_{13}(SMe_2)]^-$ in 1,3-dioxalane are different from those in acetonitrile. and therefore the electrode processes would be expected to be different.

(b) Anodic behaviour of transition metals.

The anodic behaviour of transition metals in an acetonitrile solution of $[B_{10}H_{13}(SMe_2)]^-$ was characterized in three types as described in Chapter 3, sect. 3.2.2 and in this Chapter, sect. 5.2.2(b).

Type (a) are those metals which gave rise to anion oxidation, e.g. Pt (0.4 V), Pd (0.1, 0.6 and 1.0 V), V(0.0V).

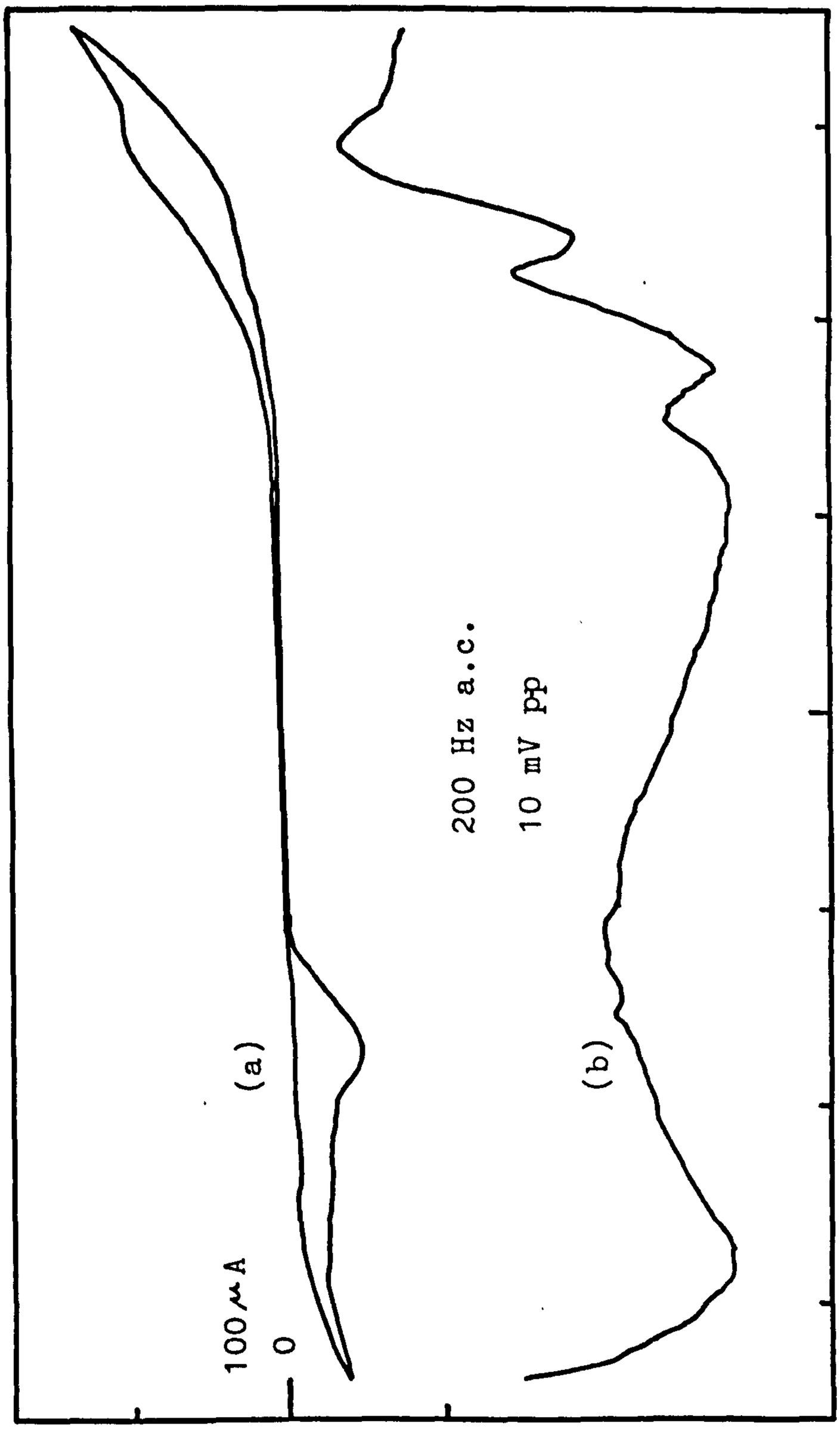

Fig.5.18. (a) Cyclic voltammogram (scan rate 0.5 VS^{-1}) and
(b) A.c. voltammogram (scan rate 0.05 VS^{-1}) of
$[B_{10}H_{13}(SMe_2)]^-$ in 0.1 M Bu_4NBF_4/1,3-dioxalane.

Type (b) are those metals which were essentially inert, e.g. Ta, Ti, W, Zr, Mo, Nb.

Type (c) are those metals which underwent anodic dissolution, e.g. Cu (-0.5 V), Co (-0.3 V), Ni (-0.1 V), Cd (-0.8 V), Zn (-0.4 V).

(c) Controlled potential electrolysis.

Exhaustive electrolysis at platinum of an acetonitrile solution of $[B_{10}H_{13}(SMe_2)]^-$ proceeded at potentials between 0.3 → 0.6 V and involved overall one-electron oxidation. The products identified by their ^{11}B and $^{11}B\{^1H\}$ n.m.r. spectra shown in Fig. 5.19 consisted of $B_9H_{13}[CH_3CN]$ (doublets of chemical shifts 17.6, 5.5, -14.0 -20.1, -26.8, -38.3 ppm with relative intensities 1:1:2:2:1:2)[140] as a minor component, a major component whose 115.5 MHz ^{11}B n.m.r. spectrum consisted of three doublets of relative intensities 2:2:1 at δ = 12.6, 1.1, -33.9 ppm which is similar to that of $B_{10}H_{14}$ in CD_3CN[126] whose 86.6 MHz ^{11}B n.m.r. spectrum consisted of three doublets of relative intensities 4:4:2 at δ = 11.2, -0.90, -35.3 ppm and borane or borate (δ = 20.6, 20.9 ppm).

The controlled potential electrolysis of an acetonitrile solution of $[B_{10}H_{13}(SMe_2)]^-$ at a copper anode proceeded at a potential of -0.4 V. The anode weight loss corresponding to copper entering the solution as Cu(I). The ^{11}B and $^{11}B\{^1H\}$ n.m.r. spectra of the crude products are given in Fig. 5.20. The products identified by their ^{11}B and $^{11}B\{^1H\}$ n.m.r. spectra contained $[B_9H_{14}]^-$ (doublets of chemical shifts -6.8, -19.2,

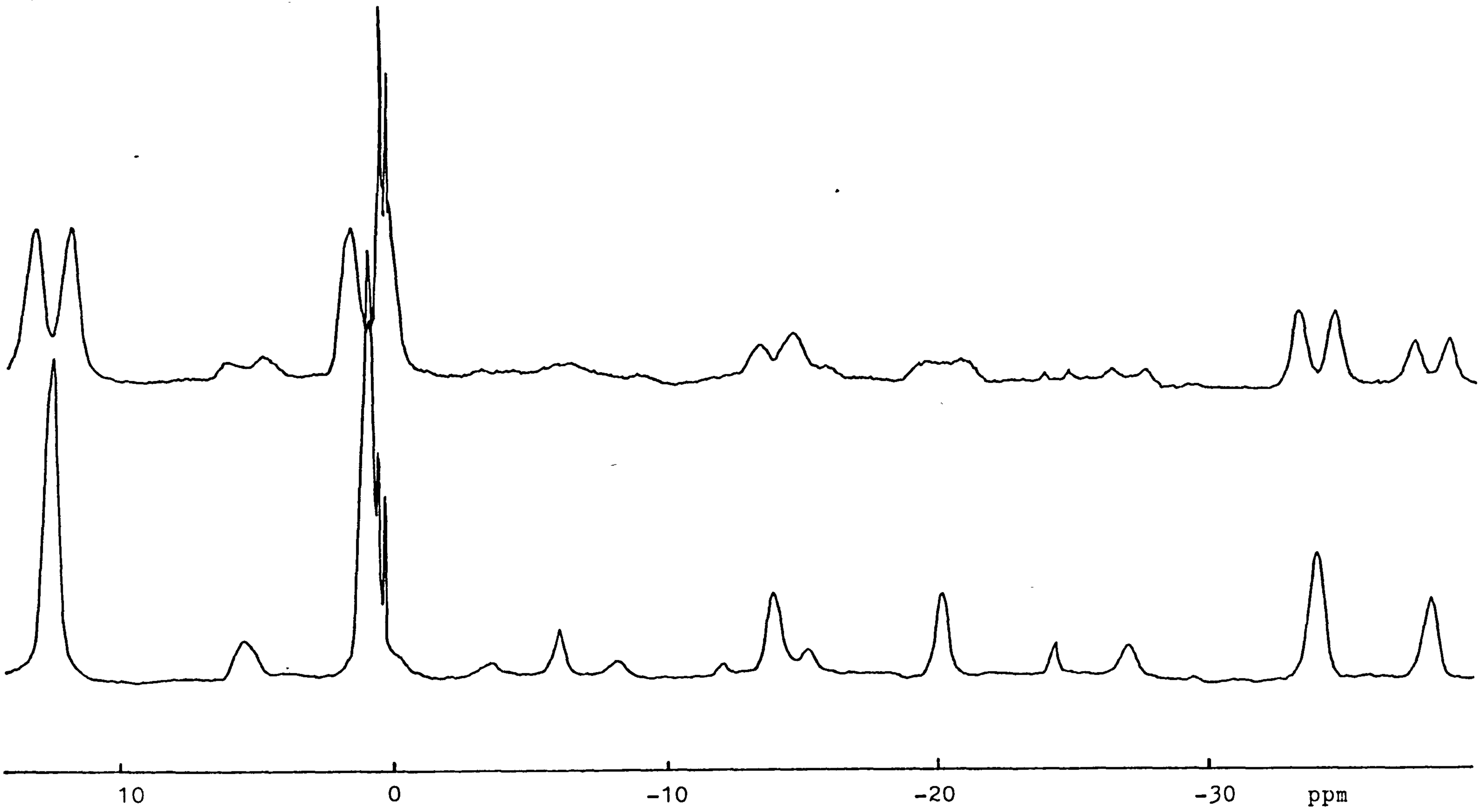

Fig.5.19. 115.5 MHz ^{11}B and $^{11}B\{^1H\}$ n.m.r. spectra of electrolysis product of $[B_{10}H_{13}(SMe_2)]^-$ at Pt in acetonitrile.

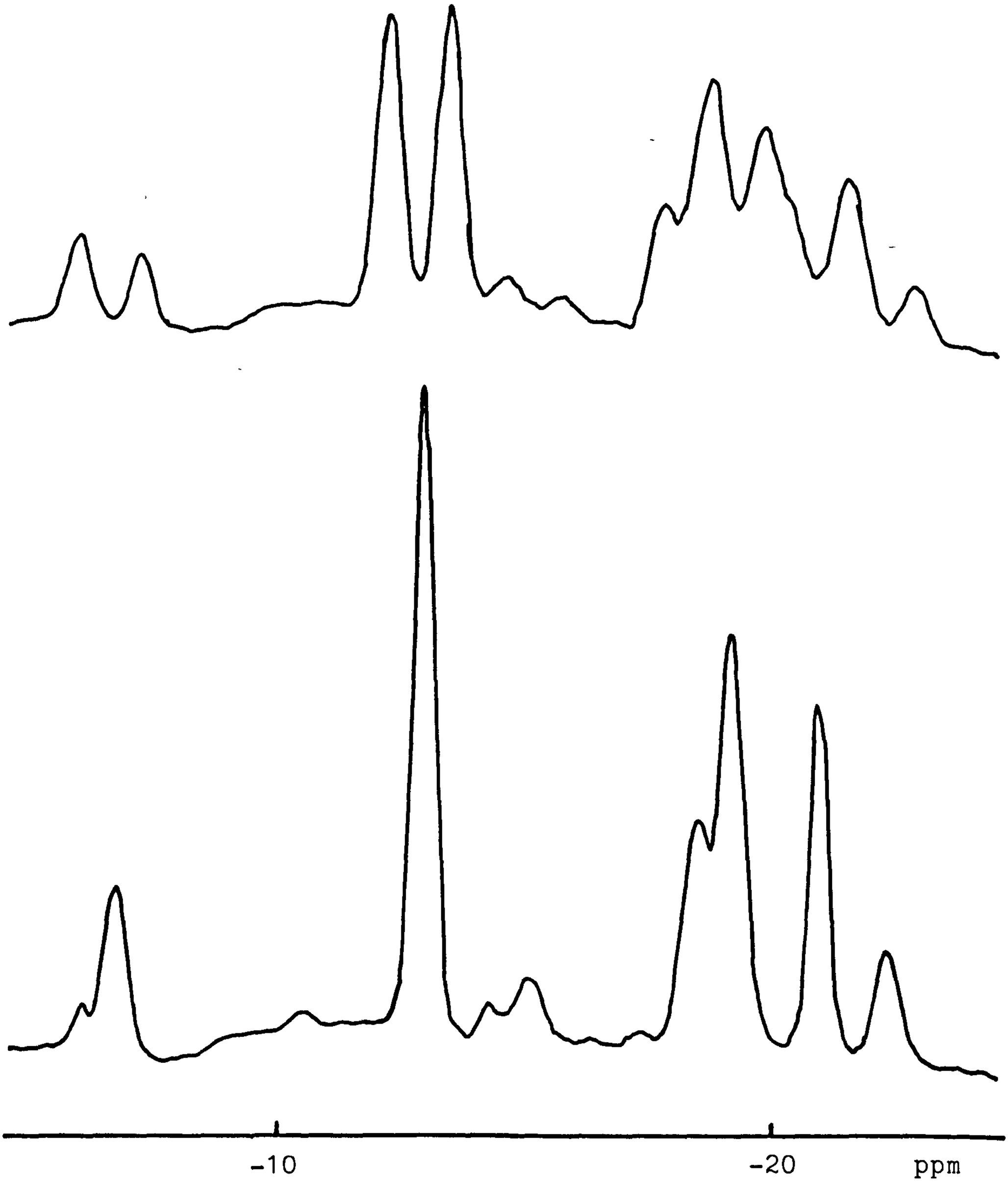

Fig.5.20. 115.5 MHz ^{11}B and $^{11}B\{^{1}H\}$ n.m.r. spectra of electrolysis product of $[B_{10}H_{13}(SMe_2)]^-$ at Cu in acetonitrile.

-22.4 ppm with relative intensities 3:3:3)[140] and possibly $[B_{10}H_{15}]^-$ (doublets of chemical shifts -13.01, -18.5, -19.2, -22.3 ppm with relative intensities 4:2:2:2) which was identified by comparison with the ^{11}B and $^{11}B\{^1H\}$ n.m.r. spectra of $Na[B_{10}H_{15}]$ in monoglyme and by the comparison of the correlation diagram of the 70.6 MHz ^{11}B n.m.r. spectra of $B_{10}H_{14}$, $[B_{10}H_{13}]^-$, $[B_{10}H_{15}]^-$ and $[B_{10}H_{14}]^{2-}$ ($BF_3.OEt_2$)[163] with the 115.5 MHz ^{11}B n.m.r. spectral data of $B_{10}H_{14}$, $[B_{10}H_{13}]^-$, $[B_{10}H_{13}L]^-$, and $[B_{10}H_{15}]^-$ obtained in CD_3CN.

5.2.5 Conclusion.

X-ray diffraction studies of $B_9H_{13}[CH_3CN]$[162], $[B_9H_{14}]^-$ [164] and ^{11}B and ^1H n.m.r. studies of $[B_9H_{14}]^-$ [164(b), 165] $[B_9H_{13}L]^n$ [140] (n = 0, -1) had shown that the formal replacement of a ligand, L, by H^- need not always yield the analogous structure, whereas the structures of $[B_{10}H_{14}]^{2-}$ and $B_{10}H_{12}L_2$ had been shown to be isostructural[134]. The ^{11}B and ^1H n.m.r. studies of $[B_{10}H_{13}L]^-$ derivatives revealed that $[B_{10}H_{13}(PPh_3)]^-$, $[B_{10}H_{13}(Py)]^-$ and $[B_{10}H_{13}(NEt_3)]^-$ are also isostructural to $[B_{10}H_{14}]^{2-}$ and $B_{10}H_{12}L_2$, whereas $[B_{10}H_{13}(SMe_2)]^-$ appeared to be structurally similar to $[B_{10}H_{13}]^-$.

The cyclic and a.c. voltammetric studies of $[B_{10}H_{13}(PPh_3)]^-$ and $[B_{10}H_{13}(SMe_2)]^-$ revealed that these anions underwent different electrode processes. The electrode processes of $[B_{10}H_{13}(PPh_3)]^-$ were simpler than those of $[B_{10}H_{13}(SMe_2)]^-$ and were confirmed by the

controlled potential electrolysis at platinum in acetonitrile, where one electron oxidation was involved in both anions. The electrochemical oxidation of $[B_{10}H_{13}(PPh_3)]^-$ led to $[B_{10}H_{12}(PPh_3)(CH_3CN)]$ whereas that of $[B_{10}H_{13}(SMe_2)]^-$ yielded $B_9H_{13}[CH_3CN]$ and a major component which possibly was $B_{10}H_{14}$.

The cyclic and a.c. voltammograms of $[B_{10}H_{13}(PPh_3)]^-$ at a Pt electrode in various solvents such as acetonitrile, 1,3-dioxalane, dichloromethane and tetramethylurea were different, which implied that the electrode processes were different for each solvent. The controlled potential electrolysis of $[B_{10}H_{13}(PPh_3)]^-$ was carried out in acetonitrile but not in other solvents due to poor solubilities of $[N(CH_3)_4][B_{10}H_{13}(PPh_3)]$. Since the reaction products of the reactions between $[B_{10}H_{13}(PPh_3)]^-$ and HCl or Hg_2Cl_2 were solvent dependent, it is likely that the electrochemical oxidation of $[B_{10}H_{13}(PPh_3)]^-$ in different solvents also yielded different products. The limitation of the solubilities may be overcome by changing the cations of the salts from $[N(CH_3)_4]^+$ to $[NBu_4^n]^+$ or $[N(PPh_3)_2]^+$.

5.3 EXPERIMENTAL

5.3.1 General.

$B_{10}H_{14}$ was purchased from Callery Chemical Company and was purified by sublimation before use. $[N(CH_3)_4][B_{10}H_{13}(PPh_3)]$ was prepared as reported[54] except that it was recrystallized from acetonitrile-ether.

$[N(CH_3)_4][B_{10}H_{13}(SMe_2)]$ and $[N(CH_3)_4][B_{10}H_{13}]$ were prepared as published[58,47]. All other reagents and CD_3CN, $CDCl_3$, or D_2O for n.m.r. spectroscopy were used as received.

The details of all electrochemical equipment, cell design and reagents and solvents for electrochemistry are described in Chapter 6.

5.3.2 Electrochemical Oxidation of $[N(CH_3)_4][B_{10}H_{13}(PPh_3)]$

$[N(CH_3)_4][B_{10}H_{13}(PPh_3)]$ (0.0918 g, 0.2 mmol) was dissolved in CH_3CN (15 ml) and placed in the anodic compartment of the cell. The cathodic compartment contained a solution of $[NBu^n_4][BF_4]$(0.1 mol dm^{-3}) in acetonitrile (15 cm^3). Both working and secondary electrodes were Pt foil, and the reference electrode was $Ag/AgNO_3$ (0.1 mol dm^{-3}) in acetonitrile. A potential of -0.24→ 0.0 V was applied to the working electrode. The current was 6 mA and fell to 0.1 mA after the passage of 15.8 C (corresponding to 0.82 times that calculated for 1 e^-). The colourless anolyte was evaporated under vacuum to dryness and the solid products were monitored by ^{11}B and ^1H n.m.r. spectroscopy.

5.3.3 Electrochemical Oxidation of $[N(CH_3)_4][B_{10}H_{13}(SMe_2)]$

The conditions were similar to those described in sect. 5.3.2 except that $[N(CH_3)_4][B_{10}H_{13}(SMe_2)]$ (0.0388 g, 0.15 mmol) was used. A potential of 0.3⟶ 0.6 V was applied to the working electrode. The current

rose to a maximum of 16 mA and fell to 0.2 mA after the passage of 14.76 C (corresponding to 1.02 times that calculated for 1 e^- oxidation). The anolyte was evaporated under vacuum to dryness and examined by ^{11}B n.m.r. spectroscopy.

5.3.4 Anodic Dissolution of Copper in acetonitrile solution of $[N(CH_3)_4][B_{10}H_{13}(PPh_3)]$.

(a) Without PPh_3 added.

$[N(CH_3)_4][B_{10}H_{13}(PPh_3)]$ (0.1148 g, 0.25 mmol) was dissolved in acetonitrile (20 cm^3) and placed in the anodic compartment of the cell. The cathodic compartment contained solution of $[NBu^n_4][BF_4]$ (0.1 mol dm^{-3}) in acetonitrile (20 cm^3). The working electrode was Cu foil and the secondary electrode was Pt foil. The reference electrode was $Ag/AgNO_3$ (0.1 mol dm^{-3}) in acetonitrile. A potential of -0.6 $\rightarrow$ -0.2 V was applied to the working electrode and stopped after the passage of 24.125 C (corresponding to 1 e^-). The weight loss of Cu electrode was 0.0161 g [c.f. theoretically 0.0159 g for Cu $\rightarrow$ Cu(I)]. The clear brown-yellow anolyte was evaporated to dryness and examined by ^{11}B n.m.r. spectroscopy.

(b) With PPh_3 added.

The conditions were similar to those described in sect. 5.3.4(a) except that PPh_3 (0.1312 g, 0.5 mmol) was added. The weight loss of Cu electrode was 0.0159 g [c.f. theoretically 0.0159 g for Cu $\rightarrow$ Cu (I)]. The

yellow anolyte with some white precipitate was evaporated under vacuum to dryness and examined by ^{11}B n.m.r. spectroscopy.

5.3.5 Anodic Dissolution of Copper in Acetonitrile Solution of $[N(CH_3)_4][B_{10}H_{13}(SMe_2)]$.

The conditions were similar to those described in sect. 5.3.4(a) except that $[N(CH_3)_4][B_{10}H_{13}(SMe_2)]$ (0.0388 g, 0.15 mmol) was used. A potential of -0.4 V was applied to the working electrode and stopped after the passage of 24.13 C. The weight loss of Cu electrode was 0.110 g [c.f. theoretically 0.0095 g for Cu→ Cu(I)]. The anolyte was evaporated under vacuum to dryness and examined by ^{11}B n.m.r. spectroscopy.

5.3.6 Anodic Dissolution of Nickel in acetonitrile solution of $[N(CH_3)_4][B_{10}H_{13}(PPh_3)]$.

The set-up was the same as that described in sect. 5.3.4(a) except that the working electrode was a coil of nickel wire. A potential of -0.4 V was applied to the working electrode and stopped after the passage of 24.24 C. The weight loss of Ni electrode was 0.0046 g (0.078 mmol). The anolyte initially turned green but changed to brown during the electrolysis (ca. 1 hr.). The anolyte was evaporated under vacuum to dryness and examined by ^{11}B n.m.r. spectroscopy.

5.3.7 Anodic Dissolution of Zinc in Acetonitrile Solution of $[N(CH_3)_4][B_{10}H_{13}(PPh_3)]$.

(a) Without PPh_3 added.

$[N(CH_3)_4][B_{10}H_{13}(PPh_3)]$(0.0689 g, 0.15 mmol) was dissolved in acetonitrile (15 cm^3) and placed in the anodic compartment of the cell. The cathodic compartment contained solution of $[NBu_4^n][BF_4]$(0.1 mol dm^{-3}) in acetonitrile (15 cm^3). The working electrode was a piece of Zn wire and the secondary electrode was Pt foil. The reference electrode was $Ag/AgNO_3$ (0.1 mol dm^{-3}) in acetonitrile. A potential of -0.3 $\longrightarrow$ -0.17 V was applied to the working electrode and was stopped after the passage of 14.47 C (ca. 6.5 hr). The weight loss of Zn electrode was 0.0049 g [c.f. theoretically 0.0049 g for $Zn \longrightarrow Zn(II)$]. The anolyte was evaporated under vacuum to dryness and examined by ^{11}B n.m.r. spectroscopy.

(b) With PPh_3 added.

The set-up was the same as that described in 5.3.7(a) except that PPh_3 (0.0787 g, 0.30 mmol) was added. A potential of -0.6 $\longrightarrow$ -0.5 V was applied to the working electrode and stopped after the passage of 14.47 C. The weight loss of Zn electrode was 0.0051 g [c.f. theoretically 0.0049 g for $Zn \longrightarrow Zn(II)$]. The anolyte was evaporated under vacuum to dryness and examined by ^{11}B n.m.r. spectroscopy.

5.3.8 Reaction of $[N(CH_3)_4][B_{10}H_{13}(PPh_3)]$ with $CuCl.H_2O$.

About 15 cm^3 of dried, degassed CH_3CN was

condensed onto the solid reagents $[N(CH_3)_4][B_{10}H_{13}(PPh_3)]$ (0.0689 g, 0.15 mmol), PPh_3 (0.0787 g, 0.3 mmol) and $CuCl.H_2O$ (0.0287 g, 0.15 mmol). The mixture was stirred for 7 hr. and the solvent removed under vacuum. The product was examined by ^{11}B n.m.r. spectroscopy.

5.3.9 Reaction of $[N(CH_3)_4][B_{10}H_{13}(PPh_3)]$ with $NiSO_4.6H_2O$.

About 15 cm^3 of dried, degassed CH_3CN was condensed onto the solid reagents $[N(CH_3)_4][B_{10}H_{13}(PPh_3)]$ (0.0689 g, 0.15 mmol) and $NiSO_4.6H_2O$ (0.021 g, 0.05 mmol). The mixture was stirred for 19 hr. and then the solvent was removed. The product was examined by ^{11}B n.m.r. spectroscopy.

5.3.10 Reaction of $[N(CH_3)_4][B_{10}H_{13}(PPh_3)]$ with Hg_2Cl_2.

(a) In dichloromethane.

About 20 cm^3 of dried, degassed CH_2Cl_2 was condensed onto the solid reagents $[N(CH_3)_4][B_{10}H_{13}(PPh_3)]$ (0.30 g, 0.66 mmol) and Hg_2Cl_2 (0.156 g, 0.33 mmol). The mixture was stirred for ca 3 hr. After filtering, the filtrate was evaporated under vacuum to dryness. This was purified by chromatography on silica gel using CH_2Cl_2 as eluting solvent. The product identified by its ^{11}B and ^1H n.m.r. spectra was $B_9H_{13}[PPh_3]$ (Found C, 55.36; H, 7.19; P, 7.21% $B_9C_{18}H_{28}P$ requires C, 57.99; H, 7.57; P, 8.3%).

(b) In acetonitrile.

The experiment conditions were similar to

that described in 5.3.10(a) except that acetonitrile was used as a solvent. The crude product was monitored by ^{11}B n.m.r. and was identified as $[B_{10}H_{12}(PPh_3)(CH_3CN)]$.

5.3.11 Reaction of $[N(CH_3)_4][B_{10}H_{13}(PPh_3)]$ with HCl.

In a 100 cm^3 flask fitted with a stopcock adaptor was placed $[N(CH_3)_4][B_{10}H_{13}(PPh_3)]$ (0.1377 g, 0.3 mmol) and 15 cm^3 of dried, degassed CH_2Cl_2 was condensed in under vacuum. Gaseous HCl (0.3 mmol) was introduced. The mixture was warmed to ca. 20°C and stirred for 15 min. Solvent was removed under vacuum and the product was examined by ^{11}B n.m.r. spectroscopy.

CHAPTER 6

EXPERIMENTAL TECHNIQUES

6.1 EXPERIMENTAL TECHNIQUES

6.1.1 General

All the reactions were carried out under vacuum or in a nitrogen atmosphere. No rigorous attention was paid to maintain anaerobic or anhydrous conditions during the subsequent handling of the products which were reasonable air-stable in the solid state. Less stable products were either stored in the mother liquid on recrystallization or freshly prepared as required.

6.1.2 Vacuum Line and Glove Box

Standard vacuum line, inert atmosphere and glove-box techniques were employed and these have been described elsewhere[166].

6.1.3 Solvents

Most solvents were dried and purified before use.

Dichloromethane and 1,2-dichloroethane	Stored over CaH_2 and distilled from CaH_2 before use.
Diethylether	Bulk dried over Na and was distilled from Na/-benzophenone before use.
Glyme or 1,2-dimethoxyethane	Bulk dried over CaH_2 and was distilled from CaH_2 before use.
n-hexane	Bulk dried over Na and

	distilled before use.
Tetrahydrofuran	Bulk dried over CaH_2 and distilled before use.
Acetonitrile	For non-electrochemical use (Fisons S.L.R. Grade) stored over CaH_2 and distilled before use.

6.1.4 Chromatographic Techniques

Column chromatography was carried out by using silica gel [M.F.C. 100-200 mesh (Hopkin and Williams)]. The size of the column depended on the quantity of the compounds required to be separated and the R_f values of the components. In general, for 3 g. of compound to be separated, 150-200 g. of silica gel in a column of dimensions ca. 25 cm x 20 cm^2 were used. The eluent from the columns was collected in fractions which were monitored by thin layer chromatography (t.l.c.). The t.l.c. plates were made in the laboratory as required from silica gel [Kieselgel 60 G (Merck)]. Solvents for chromatography were reagent grade and were used without further purification. Separations were carried out on the open bench.

6.2 SPECTROSCOPIC TECHNIQUES

6.2.1 Infrared Spectroscopy

The infrared spectra of the various compounds were obtained as mulls in nujol or hexachloro-1,3-

butadiene between KBr plates on a Perkin-Elmer 457 Grating Infrared Spectrometer.

6.2.2 Nuclear Magnetic Resonance Spectroscopy

The n.m.r. spectra were recorded on Brüker WH250 and WH360 spectrometers (^{1}H, 250 MHz and 360 MHz; ^{11}B, 80.2 MHz and 115.5 MHz). Lock was achieved by the use of a deuterated solvent. Chemical shifts are quoted as being negative to high field of the reference standards which were tetramethylsilane for ^{1}H n.m.r. and $BF_3.OEt_2$ for ^{11}B n.m.r. A few spectra of the earlier work were obtained on a Jeol-PS-100-PET-100 spectrometer generally operating on external lock. All spectra were recorded at ambient temperature (25-30°C) unless otherwise stated.

6.2.3 Computer Program for the Simulation of N.M.R. Line Shapes

N.m.r. spectral line shapes were simulated using the U.E.A. - N.M.R. BASIC program.

6.3 ELECTROCHEMICAL TECHNIQUES

6.3.1 Equipment

Cyclic and A.C. voltammetry were carried out using a Model 363, E.G. and G. Princeton Applied Research potentiostat, a Hi-Tek Instruments Ltd. waveform generator model PPR1, and home constructed A.C. generator, phase sensitive detector, and amplifier

system. Voltammograms were recorded on a Bryans 25000 X-Y recorder.

Controlled-potential electrolysis experiments were carried out using a Hi-Tek Instruments Ltd. DT2101 potentiostat, and a Gated Digital Integrator and D.V.M. recorded the total current passed. The current was also monitored on a Servoscribe Chart Recorder measuring the voltage drop across a Decade resistance box in series with the cell.

6.3.2 Cell Design

(a) Cyclic voltammetry and a.c. voltammetry.

Undivided cells were used for voltammetry. The working electrode was the metal wire under examination and it was mounted in glass tubing or coated in Teflon so as to expose only the cross section area to the solution. The secondary electrode was a piece of platinum wire mounted in glass tubing. The reference electrodes were $Ag/AgNO_3$ (0.1 mol dm^{-3}) in acetonitrile but $Ag/[N(PPh_3)_2]Cl$ (0.1 mol dm^{-3}) in 1,3-dioxalane, benzonitrile, dichloromethane and tetramethylurea. The reference solution was contained in a capillary tube and was separated from the solution under examination by a porous ceramic sinter. The reference electrode was mounted close to the working electrode and its potential was found to be +0.366 $\pm$ 0.005 V from the S.C.E. (for acetonitrile solution). A stream of nitrogen was usually blown over the solution under examination.

(b) Controlled potential Electrolysis.

Two-compartment cells separated by Nafion 427 cation exchange membrane were used for electrolysis. The membrane was usually exchanged to the cation form appropriate for the cation of the compound studied by soaking in a solution of a salt containing that cation. The working electrode was the metal under examination and the reference electrode was as described in sect. 6.3.2(a). Both electrodes were mounted close to each other in the anode compartment. The secondary electrode was platinum foil and was placed in the cathodic compartment. The anolyte was stirred magnetically and a stream of nitrogen was flushed over both compartments. The current flow in the cell was improved by large surface area of electrodes, proper position of electrodes and the stirring speed.

6.3.3 Metals, Solvents and Reagents

The metal wires were the purest grade obtained from Koch-Light: Co, Cu, Zn, Ni (better than 99.997%), Pd (99.99%), Ta, Ti, W (99.9%), Nb, Zr (99.5%), and goodfellow metals: V (99.8%) and Fisons : Pt (99.9%).

Acetonitrile for electrochemistry, Fisons H.P.L.C. (Far U.V. Grade) was used without further purification. Dichloromethane, 1,3-dioxalane, benzonitrile and tetramethylurea were stored over CaH_2 and distilled before use.

The supporting electrolyte used was $[NBu^n_4][BF_4]$

throughout the work. Solutions were prepared in solvent under study (0.1 mol dm^{-3}) and their purities were monitored by cyclic voltammetry at a Pt electrode prior to each experiment.

REFERENCES

REFERENCES

1. A. Stock, "The Hydrides of Silicon and Boron", Cornell University Press, 1933.

2. (a) R.T. Holzmann, R.L. Hughes, I.C. Smith, and E.W. Lawless, "Production of the Boranes and Related Research", Academic Press, New York, 1967, pp.116-124.

   (b) R.W. parry and M.K. Walter, Prep. Inorg. React., 1968, 5, 92.

3. R.T. Holzmann, R.L. Hughes, I.C. Smith, and E.W. Lawless, "Production of the Boranes and Related Research", Academic Press, New York, 1967, Chapters V and VI.

4. H.C. Longuet-Higgins, J. Chim. Phys., 1949, 46, 268.

5. W.H. Eberhardt, B. Crawford, and W.N. Lipscomb, J. Chem. Phys., 1954, 22, 989.

6. R.E. Dickerson and W.N. Lipscomb, J. Chem. Phys., 1957, 27, 212.

7. W.N. Lipscomb, "Boron Hydrides", Benjamin, New York, 1963.

8. I.R. Epstein and W.N. Lipscomb, Inorg. Chem., 1971, 10, 1921.

9. (a) K. Wade, "Electron Deficient Compounds", Nelson, London, 1971.

   (b) K. Wade, Chem. Commun., 1971, 792.

   (c) K. Wade, Adv. Inorg. Chem. Radiochem., 1976,18,1.

10. R.W. Rudolph, Acc. Chem. Res., 1976, 9, 446.

11. (a) American Chemical Society, "The Nomenclature of Boron Compounds", Inorg. Chem., 1968, 7, 1945.

    (b) International Union of Pure and Applied Chemistry. "Nomenclature of inorg. Boron Compounds", Pure Appl. Chem., 1972, 30, 638.

12. (a) J.B. Casey, W.J. Evans, and W.H. Warren, Inorg. Chem., 1981, 20, 1333.

    (b) J.B. Casey, W.J. Evans, and W.H. Warren, Inorg. Chem., 1981, 20, 3556.

12. (c) J.B. Casey, W.J. Evans and W.H. Warren, Inorg. Chem., 1983, 22, 2228.

(d) J.B. Casey, W.J. Evans and W.H. Warren, Inorg. Chem., 1983, 22, 2236.

13. (a) R. Schaeffer and F. Tebbe, J. Am. Chem.Soc. 1962, 84, 3974.

(b) D.F. Gaines and R. Schaeffer, Inorg. Chem., 1964, 3, 438.

(c) J. Dobson, D.F. Gaines and R. Schaeffer, J. Am. Chem. Soc., 1965, 87., 4072.

14. (a) I.A. Ellis, D.F. Gaines, and R. Schaeffer, J. Am. Chem. Soc., 1963, 85., 3885.

(b) H.C. Miller, N.E. Miller, and E.L. Muetterties, J. Am. Chem. Soc., 1963, 85,3885

(c) H.C. Miller, N.E. Miller and E.L. Muetterties Inorg. Chem., 1964, 3, 1456.

15. (a) S.J. Lippard and D.A. Ucko, Inorg. Chem., 1968, 7, 1051.

(b) F. Klanberg, E.L. Muetterties, and L.J. Guggenberger, Inorg. Chem., 1968, 7, 2272.

16. (a) W.V. Hough, L.J. Edwards, and A.D. McElroy, J. Am. Chem. Soc., 1956, 78, 689.

(b) W.V. Hough, L.J. Edwards, and A.D. McElroy, J. Am. Chem. Soc., 1958, 80, 1828.

17. G. Kodama and R.W. Parry, J. Am. Chem. Soc., 1960, 82, 6250.

18. B.M. Graybill, J.K. Ruff, and M.F. Hawthorne, J. Am. Chem. Soc., 1961, 83, 2669.

19. R.B. Cruikshank, W.V. Hough, M.D. Marshall, and A.D. McElroy, Callery Chemical Company Final Report No. NOw 60-0168-C, 1962. (Cited as reference 404 in Holzmann et al., "Production of the Boranes and Related Research" , Academic Press , New York, 1967).

20. K.C. Nainan and G.E. Ryschkewitsch, Inorg. Nucl. Chem. Lett., 1970, 6, 765.

21. D. Gaines, R. Schaeffer and F. Tebbe, Inorg. Chem., 1963, 2, 526.

22. H.C. Miller and E.L. Muetterties, Inorg. Synth., 1967, 10, 81.

23. W.J. Dewkett, M. Grace, and H. Beall, J. Inorg. Nucl. Chem., 1971, 33, 1279.

24. (a) G.E. Ryschkewitsch and V.A. Miller, J. Am. Chem. Soc., 1975, 97, 6258.

(b) G.E. Ryschkewitsch and V.A. Miller, Inorg. Synth., 1974, 15, 118.

25. V.D. Aftandilian, H.C. Miller, and E.L. Muetterties, J. Am. Chem. Soc., 1961, 83, 2471.

26. W.L. Jolly, J.W. Reed, and F.T. Wang, Inorg. Chem., 1979, 18, 377.

27. G.B. Jacobsen and J.H. Morris, Inorg. Chim. Acta, 1982, 59, 207.

28. M. Arunchaiya, J.H. Morris, S.J. Andrews, D.A. Welch, and A.J. Welch, J. Chem. Soc., Dalton Trans., 1984 (in press).

29. D.G. Meina, unpublished work.

30. B.F. Spielvogel, Ph.D. Dissertation, University of Michigan, 1963. Diss. Abstr., 1964, 24, 4985.

31. P.J. Dolan, J.H. Kindsvater, and D.G. Peters, Inorg. Chem., 1976, 15, 2170.

32. A. Drummond and J.H. Morris, Inorg. Chim. Acta , 1978, 24, 191.

33. J. Borlin and D.F. Gaines, J. Am. Chem. Soc., 1972, 95, 1367.

34. (a) R.N. Grimes, "Carboranes", Academic Press, New York, 1970.

(b) G.B. Dunks and M.F. Hawthorne, Acc. Chem. Res., 1973, 6, 124.

35. M.F. Hawthorne and G.B. Dunks, Science, 1972, 178, 462.

36. M.F. Hawthorne, Adv. Inorg. Chem. Radiochem., 1963, 5, 307.

37. W. De Acetis and S.I. Trotz, U.S. Patent, 1956, 2, 983, 581; Chem. Abstr., 1962, 56, 2154e.

38. M. Hillman, D.J. Mangold, and J.H. Norman, J. Inorg. Nucl. Chem., 1962, 24, 1565.

39. J.A. Neff, U.S. patent, 1961, 2,989, 374; Chem. Abst., 1961, 55, 23592i.

40. J.P. Faust and N.C. Goodspeed, U.S. Patent, 1961, 2,987, 377; Chem. Abstr., 1961, 55, 23593a.

41. (a) G.B. Dunks and K.P. Ordonez, J. Am. Chem. Soc., 1978, 100, 2555.

(b) G.B. Dunks, K. Barker, E. Hedaya, C. Hefner, K:P. Ordonez, and P. Remec, Inorg. Chem., 1981, 20, 1692.

42. M.A. Toft, J.B. Leach, F.L. Himpsl, and S.G. Shore, Inorg. Chem., 1982, 21, 1952.

43. L.E. Benjamin, S.F. Stafiej, and E.A. Tackacs, J. Am. Chem. Soc., 1963, 85, 2674.

44. (a) V.T. Brice, H.D. Johnson, II, D.L. Denton, and S.G. Shore, Inorg. Chem., 1972, 11, 1135.

(b) C.G. Savory and M.G.H. Wallbridge, J. Chem. Soc. Dalton Trans., 1973, 179.

(c) D.L. Denton, W.R. Clayton, M. Mangion, S.G. Shore, and E.A. Meyers, Inorg. Chem., 1976, 15, 541.

45. R.A. Geanangel, H.D. Johnson, II, and S.G. Shore, Inorg. Chem., 1971, 10, 2363.

46. (a) G.A. Guter and G.W. Schaeffer, J. Am. Chem. Soc. 1956, 78, 3546.

(b) W.V. Hough, L.J. Edwards, andA.D. McElroy, Chemical Company under contract No. NOa(s) 52-1024-TR-168. (Cited as reference 297 in Holzmann et al. (33, p.263).

(c) H.E. Messner and A.E. Weber, Callery Chemical Company under Contract No. Noa(s) 52-1024-TR-190. (Cited as reference 308 in Holzmann et al. (33, p.267).

47. M.F. Hawthorne, A.R. Pitochelli, R.D. Strahm, and J.J. Miller, J. Am. Chem. Soc., 1960, 82, 1825.

48. R.W. Parry and L.J. Edwards, J. Am. Chem. Soc., 1959, 81, 3554.

49. (a) M.F. Hawthorne and J.J. Miller, J. Am. Chem. Soc., 1958, 80, 754.

(b) J.J. miller and M.F. Hawthorne, J. Am. Chem. Soc.,1959, 81, 4501.

49. (c) I. Shapiro, M. Lustig, and R. Williams, J. Am. Chem. Soc., 1959, 81, 4998.

50. W.V. Hough and L.J. Edwards, Abstr. Pap., 133rd Meet., Am. Chem. Soc., San Francisco, 1958, p.28L.

51. B. Siegel, J.L. Mack, J.U. Lowe, Jr., and J. Gallagham, J. Am. Chem. Soc., 1958, 80, 4523.

52. (a) P.H. Wilkes and J.C. Carter, J. Am. Chem. Soc, 1966, 88, 3441.

(b) E. Amberger and P. Leidel, J. Organometal. Chem., 1969, 18, 345.

(c) N.N. Greenwood and D.N. Sharrocks, J. Chem. Soc. A, 1969, 2334.

53. S.J. Fitch and A.W. Laubengayer, J. Am. Chem. Soc., 1958, 80, 5911.

54. B.M. Graybill, A.R. Pitochelli and M.F. Hawthorne, Inorg. Chem., 1962, 1, 622.

55. R. Schaeffer, J. Am. Chem. Soc., 1957, 79, 1006.

56. M.F. Hawthorne and A.R. Pitochelli, J. Am. Chem. Soc., 1958, 80, 6685.

57. (a) M.F. Hawthorne and A.R. Pitochelli, J. Am. Chem. Soc., 1959, 81, 5519.

(b) V.D. Aftandilian, U.S. Patent, 1960, 2961444.

58. W.H. Knoth and E.L. Muetterties, J. Inorg. Nucl. Chem., 1961, 20, 66.

59. (a) R.J. Pace, J. Williams, and R.L. Williams, J. Chem. Soc., 1961, 2196.

(b) R.J. Polak and T.L. Heying, J. Org. Chem., 1962, 27, 1483.

(c) H. Schroeder, J.R. Reiner, and T.L. Heying, Inorg. Chem., 1962, 1, 618.

60. M.F. Hawthorne and P.A. Wegner, Inorg. Chem., 1964, 3, 774.

61. E.L. Muetterties and W.H. Knoth, Inorg. Chem., 1965, 4, 1498.

62. E.L. Muetterties and F. Klanberg, Inorg. Chem., 1966, 5, 315.

63. J. Williams, R.L. Williams and J.C. Wright, J. Chem. Soc., London, 1963, 5816.

64. (a) R.H. Toeniskoetter, Ph.D. Thesis, St. Louis University, Missouri, 1958, Diss. Abstr., 1959, 20, 879.

(b) R.H. Toeniskoetter, G.W. Schaeffer, E.C. Evers, R.E. Hughes, and C.E. Bagley, Abst. 234th Meet. Amer. Chem. Soc., Chicago, 1958, p.N23.

65. E.L. Muetterties, Inorg. Chem., 1963, 2, 647.

66. M.F. Hawthorne and R.L. Pilling, Inorg. Synth., 1967, 9, 16.

67. M.F. Hawthorne, R.L. Pilling and R.N. Grimes, J. Am. Chem. Soc., 1964, 86, 5338.

68. E.L. Meutterties and V.D. Aftandilian, Inorg. Chem., 1962, 1, 731.

69. V.D. Aftandilian, U.S. patent, 1961, 3, 013, 041; Chem. Abstr., 1962, 57, 8197e.

70. H. Schroeder, Inorg. Chem., 1963, 2, 390.

71. B. Stibr, J. Plesek, and S. Hĕrmánek, Collect. Czech. Chem. Commun., 1972, 37, 2696.

72. A.J. Bard and L.R. Faulkner, "Electrochemical Methods Fundamental and Applications", John Wiley & Sons, New York, 1980.

73. W.H. Schechter, U.S. patent, 1962, 3,033,766.

74. H.R. Hoektra, U.S. Atomic Energy Commission Report, A.E.C.D., 1949, 2144.

75. R.K. Birdwhistell, H.E. Ulmer, and L.L. Quill, U.S. patent, 1959, 2, 876, 176.

76. W.H. Schechter, R.M. Adams, and G.F. Huff, Brit. Patent, 1960, 826, 558.

77. L.A. Melcher, I.A. Boening, and K. Niedenzu, Inorg. Chem., 1973, 12, 487.

78. R.L. Pecsok, J. Am. Chem. Soc., 1953, 75, 2862.

79. M.E. Indig and R.N. Snyder, J. Electrochem. Soc., 1962, 109, 1104.

80. (a) J.A. Gardiner and J.W. Collat, Inorg. Chem., 1965, 4,1208.

80. (b) J.A. Gardiner, Diss. Abst., 1965, 25, 6945.

81. J.P. Elder and A. Hickling, A. Trans. Faraday Soc., 1962, 58, 1852.

82. J.P. Elder, Electrochim. Acta, 1962, 7, 417.

83. J.H. Morris and D. Reed, J. Chem. Res., 1980, (S) 282; (M) 3567.

84. A. Drummond, J.F. Kay, J.H. Morris and D. Reed, J. Chem. Soc., Dalton Trans., 1980, 284.

85. J.H. Morris and D. Reed, J. Chem. Res., 1980, 378; (M) 4522.

86. P.J. Dolan, J.H. Kindsvater, and D.G. Peters, Inorg. Chem., 1976, 15, 2170.

87. B.G. Cooksey, J.D. Gorham, J.H. Morris, and L. Kane, J. Chem. Soc., Dalton Trans., 1978, 141.

88. G.B. Jacobsen, Ph.D. thesis, University of Strathclyde, 1982.

89. E.B. Rupp, D.E. Smith, and D.F. Shriver, J. Am. Chem. Soc., 1967, 89, 5562.

90. D.E. Smith, E.B. Rupp, and D.F. Shriver, J. Am. Chem. Soc., 1967, 89, 5568.

91. J.Q. Chambers, A.D. Norman, M.R. Bickell and S.H. Cadle, J. Am. Chem. Soc., 1968, 90, 6056.

92. J.H. Morris and D. Reed, J. Chem. Res., 1980, (S) 380.

93. (a) F. Klanberg, D.R. Eaton, L.J. Guggenberger, and E.L. Muetterties, Inorg. Chem., 1967, 6, 1271.

(b) E.L. Muetterties, J.H. Balthis, Y.T. Chia , W.H. Knoth, and H.C. Miller, Inorg. Chem., 1964, 3, 444.

(c) F. Klanberg and E.L. Muetterties, Inorg. Chem., 1966, 5, 1955.

(d) E.L. Muetterties and W.H. Knoth, "Polyhedral Boranes", Marcel Dekker: New York, 1968, 103.

94. W.H. Knoth, H.C. Miller, J.C. Gauer, J.H. Balthis, Y.T. Chia, and E.L. Muetterties, Inorg. Chem., 1964, 3, 159.

95. R.L. Middaugh and F. Farha, J. Am. Chem. Soc., 1966, 88, 4147.

96. A. Kaczmarczyk, R.D. Dobrott, and W.N. Lipscomb, Proc. Natl. Acad. Sci. U.S.A., 1962, 48, 729.

97. A.R. Pitochelli, W.N. Lipscomb and M.F. Hawthorne, J. Am. Chem. Soc., 1962, 84, 3026.

98. M.F. Hawthorne, R.L. Pilling, P.F. Stokely, and P.M. Garret, J. Am. Chem. Soc., 1963, 85, 3704.

99. B.L. Chamberland and E.L. Muetterties, Inorg. Chem., 1964, 3, 1450.

100. M.F. Hawthorne, R.L. Pilling and P.F. Stokely, J. Am. Chem. Soc., 1965, 87, 1893.

101. R.J. Wiersema and R.L. Middaugh, J. Am. Chem. Soc., 1967, 89, 5078.

102. R.J. Wiersema and Middaugh, Inorg. Chem., 1969, 8, 2074.

103. R.A. Ogg, J. Chem. Phys., 1954, 22, 1933.

104. J.N. Schoolery, Discuss. Faraday Soc., 1955, 19, 215.

105. G.R. Eaton and W.N. Lipscomb, "NMR Studies of Boron Hydrides and Related Compounds", p.558 and references cited therein. Benjamin, New York, 1969.

106. G.R. Eaton and W.N. Lipscomb, "NMR Studies of Boron Hydrides and Related Compounds", p.546. Benjamin, New York, 1969.

107. H. Nöth and B. Wrackmeyer, "Nuclear Magnetic Resonance Spectroscopy of Boron Compounds", Springer-Verlag Berlin Heidelberg New York, 1978.

108. (a) J.W. Akitt, J. Magn. Res., 1970, 3, 411.

(b) J. Bacon, R.J. Gillespie and J.W. Quail, Can. J. Chem., 1963, 41, 3036.

109. (a) H. Beall and C.H. Bushweller, Chem. Rev., 1973, 73, 465.

(b) J.C. Lockhart, "Redistribution reactions", Academic, New York, 1970.

110. W. McFarlane, B. Wrackmeyer and H. Nöth, Chem. Ber., 1975, 108, 3811.

111. (a) D.F. Gaines, R. Schaeffer, and F. Tebbe, J. Phys. Chem., 1963, 67, 1937.

(b) D.F. Gaines, Inorg. Chem., 1963, 2, 523.

112. T.C. Farrar, R.B. Johannesen, and T.D. Coyle, J. Chem. Phys., 1968, 49, 281.

113. W.D. Phillips, H.C. Miller, and E.L. Muetterties, J. Am. Chem. Soc., 1959, 81, 4496.

114. W.N. Lipscomb, Adv. Inorg. Chem. Radiochem., 1959, 1, 117.

115. C.R. Peters and C.E. Nordman, J. Am. Chem. Soc., 1960, 82, 5758.

116. H. Beall, C.H. Bushweller, W.J. Dewkett, and M. Grace, J. Am. Chem. Soc., 1970, 92, 3484.

117. D. Marynick and T. Onak, J. Chem. Soc., A, 1970, 1160.

118. C.H. Bushweller, H. Beall, M. Grace, W.J. Dewkett, and H.S. Bilofsky, J. Am. Chem. Soc., 1971, 93, 2145.

119. S.J. Lippard and K.M. Melmed, Inorg. Chem., 1969, 8 2755.

120. F. Klanberg and L.J. Guggenberger, Chem. Commun., 1967, 1293.

121. L.J. Guggenberger, Inorg. Chem., 1970, 9, 367.

122. J.N. Schoolery, Discuss. Faraday Soc., 1955, 19, 215.

123. (a) E.B. Moore, R.E. Dickerson, and W.N. Lipscomb, J. Chem. Phys., 1957, 27, 209.

(b) J.S. Kasper, C.M. Lucht, and D. Harker, Acta Crystallogr., 1950, 3, 436.

(c) A. Tippe and W.C. Hamilton, Inorg. Chem., 1969, 8, 464.

124. R.L. Pilling, F.N. Tebbe, M.F. hawthorne, and E.A. Pier, Proc. Chem. Soc., London, 1964, 402.

125. P.C. Keller, D. Maclean, and R.O. Schaeffer, Chem. Commun., 1965, 204.

126. D.F. Gaines, C.K. Nelson, J.C. Kung, J.H. Morris and D. Reed, submitted to J. Magn. Reson.

127. D. Reed, J. Chem. Res., 1984 (in press).

128. W.C. Hutton, R. Grimes, and T.L. Venable, J. Am. Chem. Soc., 1982, 104, 4716.

129. G.M. Bodner and L.G. Sneddon, Inorg. Chem., 1970, 9 1421.

130. R.L. Williams, N.N. Greenwood, and J.H. Morris, Spectrochim. Acta, 1965, 21, 1579.

131. E.L. Muetterties, Inorg. Chem., 1963, 2, 647.

132. D.E. Hyatt, F.R. Scholer, and L.J. Todd, Inorg. Chem., 1967, 6, 630.

133. W.N. Lipscomb, "Boron Hydrides", Benjamin, New York, 1963, p.183.

134. W.N. Lipscomb, R.J. Wiersema, and M.F. Hawthorne, Inorg. Chem., 1972, 11, 651.

135. D.S. Kendall and W.N. Lipscomb, Inorg. Chem., 1973, 12, 546.

136. S.J. Andrews and A.J. Welch, to be published.

137. R.F. Borch, M.D. Bernstein, and H. Dupont Durst, J. Am. Chem. Soc., 1971, 93, 2897.

138. A.R. Dodds and G. Kodama, Inorg. Chem., 1977, 16, 3353.

139. M.A. Nelson and G. Kodama, Inorg. Chem., 1979, 18, 3276.

140. G.B. Jacobsen and J.H. Morris, J. Chem. Soc., Dalton Trans., 1984, 415.

141. G.B. Jacobsen, J.H. Morris and D. Reed, J. Chem. Res., 1983, (S) 42; (M) 401.

142. G. Kodama, Inorg. Chem., 1975, 14, 452.

143. A.R. Dodds and G. Kodama, Inorg. Chem., 1976, 15, 741.

144. V.L. Bishop and G. Kodama, Inorg. Chem., 1981, 20, 2724.

145. S.J. Andrews, A.J. Welch, G.B. Jacobsen and J.H. Morris, J. Chem. Soc., Chem. Commun., 1983, 749.

146. S.J. Andrews and A.J. Welch, Inorg. Chim. Acta, 1984 (in press).

147. J.D. Glore, J.W. Rathke and R. Schaeffer, Inorg. Chem., 1973, 12, 2175.

148. C.E. Nordman and C. Reimann, J. Am. Chem. Soc., 1959, 81, 3583.

149. (a) H. Adkins and G.M. Whitman, J. Am. Chem. Soc., 1942, 64, 150.

(b) A. Dornow, I. Kühlke, and F. Baxmann, Chem. Ber., 1949, 82, 254.

150. A. Drummond and J.H. Morris, Inorg. Chim. Acta, 1977, 24, 191.

151. (a) M. Suzuki and R. Kubo, Mol. Phys. 1964, 7, 201.

(b) M. Kubo, M. Watanabe, T. Totani and M. Ohtsuru, Mol. Phys., 1968, 14, 367.

152. C.D. Good and D.M. Ritter, J. Am. Chem. Soc., 1962, 84, 1162.

153. H. Nöth and H. Vahrenkamp, Chem. Ber., 1966, 99, 1049.

154. R.J. Thompson and J.C. Davis, Inorg. Chem., 1965, 4, 1464.

155. (a) H.A. Beall and W.N. Lipscomb, Inorg.Chem., 1967, 6, 874.

(b) J.A. Potenza, W.N. Lipscomb, G.D. Vickers, and H. Schroeder, J. Am. Chem. Soc., 1966, 88, 628.

(c) F.P. Boer, R.A. Hegstrom, M.D. Newton, J.A. Potenza, and W.N. Lipscomb, J. Am. Chem. Soc., 1966, 88, 5340.

156. E.L. Muetterties, J.H. Balthis, Y.T. Chia, W.H. Knoth, and H.C. Miller, Inorg. Chem., 1964, 3, 444.

157. A.R. Siedle, G.M. Bodner and L.J. Todd, J. Inorg. Nucl. Chem., 1971, 33, 3671.

158. W.H. Knoth and E.L. Muetterties, J. Inorg. Nucl. Chem., 1961, 20, 66.

159. A.M. Bond, J. Electroanal. Chem., 1974, 50, 285.

160. C.K. Nelson (Ph.D. thesis), Diss. Abstr., 1983, 48 2549.

161. R. Schaeffer and E. Walter, Inorg.Chem., 1973, 12, 2209.

162. F.E. Wang, P.G. Simpson and W.N. Lipscomb, J. Chem. Phys., 1961, 35, 1335.

163. R.R. Rietz, A.R. Siedle, R.O. Schaeffer and L.J. Todd, Inorg. Chem., 1973, 12, 2100.

164. (a) N.N. Greenwood, J.A. McGinnety, and J.O. Owen, J. Chem. Soc., Dalton Trans., 1972, 1963.

(b) N.N. Greenwood, H.J. Gysling, J.A. McGinnety, and J.O. Owen, Chem. Commun., 1970, 505.

165. P.C. Keller, Inorg. Chem., 1970, 9, 75.

166. D.F. Shriver, "The Manipulation of Air-Sensitive Compounds", McGraw-Hill, New York, 1969.